AD-A084 448 UNIVERSITY COLL OF NORTH WALES BANGOR F/G 11/9
A STUDY OF THE NATURE AND ORIGINS OF PYROELECTRICITY AND PIEZOE--ETC(U)
JAN 80 D K DAS-GUPTA DA-ERO-77-G-088
UNCLASSIFIED NL

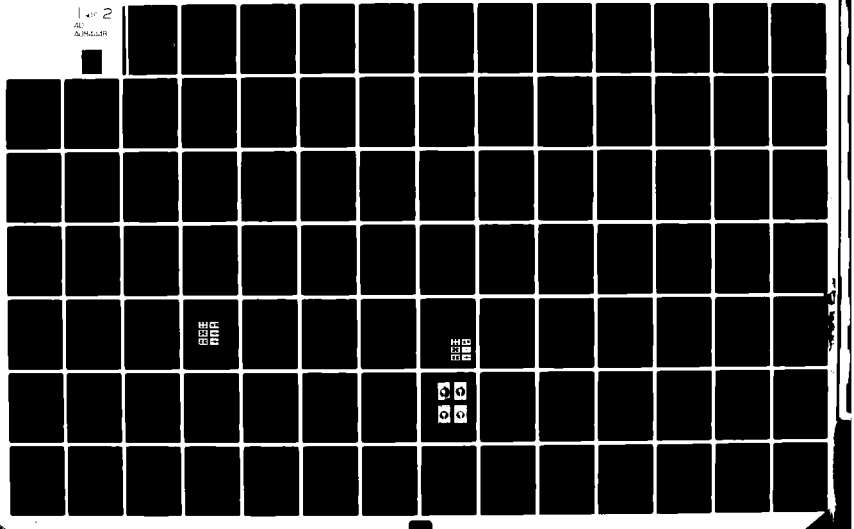

(12) LEVEL II

AD

(6) A STUDY OF THE NATURE AND ORIGINS OF PYROELECTRICITY AND PIEZOELECTRICITY IN POLYVINYLIDENEFLUORIDE AND ITS CO-POLYMERS.

(9) Final Technical Report. Feb 78 - Oct 79

by

(10) Dr D. K. Das-Gupta

(11) Jan 80 (12) 16 p

United States Army

RESEARCH AND STANDARDIZATION GROUP (EUROPE)

London England

(15) (G) CONTRACT NUMBER DA-ERO-77-G-088

✓DA-ERO-78-G-[illegible]

University College of North Wales, Dean Street, Bangor, Gwynedd LL57 1UT, G.B.

Approved for public release; distribution unlimited.

387224

UNCLASSIFIED

SECURITY CLASSIFICATION OF THIS PAGE (When Data Entered)

REPORT DOCUMENTATION PAGE	READ INSTRUCTIONS BEFORE COMPLETING FORM
1. REPORT NUMBER	2. GOVT ACCESSION NO. AD-A084 448 / 3. RECIPIENT'S CATALOG NUMBER
4. TITLE (and Subtitle) A Study of the Nature and Origins of Pyroelectricity and Piezoelectricity in Polyvinylidenefluoride and its Co-Polymers	5. TYPE OF REPORT & PERIOD COVERED Final Report Feb 78 - Oct 79 / 6. PERFORMING ORG. REPORT NUMBER
7. AUTHOR(s) Dr. D.K. Das-Gupta	8. CONTRACT OR GRANT NUMBER(s) DAERO-78-G-004
9. PERFORMING ORGANIZATION NAME AND ADDRESS University College of North Wales Dean Street Bangor, Gwynedd LL57 1UT, U.K.	10. PROGRAM ELEMENT, PROJECT, TASK AREA & WORK UNIT NUMBERS 6.11.02A 1T1611
11. CONTROLLING OFFICE NAME AND ADDRESS US Army Research & Standardization Group (Europe) Box 65 FPO NY 09510	12. REPORT DATE January 1980 / 13. NUMBER OF PAGES 157
14. MONITORING AGENCY NAME & ADDRESS(if different from Controlling Office)	15. SECURITY CLASS. (of this report) Unclassified / 15a. DECLASSIFICATION/DOWNGRADING SCHEDULE

16. DISTRIBUTION STATEMENT (of this Report)

Approved for Public Release - Distribution Unlimited

17. DISTRIBUTION STATEMENT (of the abstract entered in Block 20, if different from Report)

18. SUPPLEMENTARY NOTES

19. KEY WORDS (Continue on reverse side if necessary and identify by block number)

Organic Compound; Structure; Pyroelectric Effect; Piezoelectric Effect; Fluorides; Transients; Polyvinyls; Films; Structural Models; Mathematical Models; Radiations; Electric Current; Thickness.

20. ABSTRACT (Continue on reverse side if necessary and identify by block number)

The results of these experiments indicate that at least a large part of the polarization in PVF_2 after poling is due to dipole orientation in the crystalline regions. There is ample evidence to show that crystallites are aligned by the poling field and remain in or close to this new angular position when the field is removed. Ageing experiments indicate that they do not return to their original positions even after annealing at high temperature.

DD FORM 1 JAN 73 1473 EDITION OF 1 NOV 65 IS OBSOLETE

UNCLASSIFIED

SECURITY CLASSIFICATION OF THIS PAGE (When Data Entered)

20. Contd.

It is possible that space charges are also present in the film. However, the distribution of space charges in the bulk of the material after poling is not of importance as regards permanent polarization. It has been possible to achieve a stable value of d_{31} as high as $40pCN^{-1}$.

1. Summary

It is well established that significant piezoelectric and pyroelectric behaviour may be induced in Polyvinylidene fluoride (PVF_2) and its copolymer with Tetrafluorethylene (VF_2/TFE) after suitable stretching and poling at an elevated temperature with a high d.c. field for an extended period of time.

However, at the start of this work, there was no definitive knowledge about the exact role played by the stretching and the poling processes with regard to the origins of piezo- and pyroelectricity in this polymer (PVF_2).

Therefore, this research programme was begun with the intention of establishing unambiguously the origins of high field polarization in PVF_2. By investigating the effects of the stretching and the poling processes independently and simultaneously by studies of structural and electrical properties, it has been shown that the observed microscopic and macroscopic changes are related and that by optimising the treatments, thermal, mechanical and electrical, the maximum possible coefficients of piezo- and pyroelectricity could be obtained.

List of Keywords

Organic Compound; Structure; Pyroelectric Effect; Piezoelectric Effect; Fluorides; Transients; Polyvinyls; Films; Structural Models; Mathematical Models; Radiations; Electric Current; Thickness.

LIST OF CONTENTS

LIST OF ILLUSTRATIONS

LIST OF TABLES

EXPERIMENTAL FINDINGS

2. Structure and Morphology of Films

2.1 Unstretched Films

50μm thick rolls of PVF_2 from the Kureha Chemical Co. Ltd. of Japan were studied by infra-red spectroscopy and by X-ray diffraction in both transmission and reflection modes and were found to have a crystallinity of 52% at room temperature. A method due to Gal'perin[1] (see 1st Annual Report) was used to determine the crystallinity. Furthermore, the crystalline content was found to be entirely of the Form 2 type of crystallites (see 1st Annual Report) and changes in lattice dimension and crystallinity on thermal cycling between 20 and 100°C were found to be reversible.

The samples appeared to be isotropic in the plane of the film from a study by three different methods, which are as follows:

(i) Laué diffraction rings were complete circles with the same intensity all the way around[2].

(ii) the birefringence value ($n_x - n_y$) was negligible (see publications A and B).

(iii) there was no change in the polarised infra-red spectrum by rotating the sample through various angles[2].

The spherulitic nature of the polymer was demonstrated by the production of a four-leafed clover pattern by small angle light scattering through crossed polaroids (see publications A and B). By measuring the angle at which maximum intensity occured, the average radius of a spherulite was estimated to be approximately 3μm.

2.2 Stretched Films

Films were stretched under oil up to four times their original length at temperatures from 60° up to 140°C and were clamped at constant length for 15 hours at 120°C to prevent subsequent shrinkage. The thickness of the film after stretching was found to have decreased roughly in proportion to the reciprocal of the square root of the stretch ratio.

Further samples were stretched by the British Post Office at their Martlesham Research Centre at 60°C up to 7 times their original length in such a way that the thickness remained constant, i.e. the film width decreased on stretching. The U.S. Army Materials Research Centre at Watertown also provided stretched and heat-treated films for our investigation.

The results of stretching were:-

(i) At lower temperatures (i.e. 60°C) of stretching, a conversion of Form 2 crystallites into Form 1 crystallites is achieved with a lower stretch ratio. The conversion is complete at 5:1; however, a significant portion of Form 2 constants remain after stretching to 5:1 at 140°C.

(ii) A change of chain confirmation from TGTG' occurs to a nearly planar zig-zag form.

(iii) A preferential orientation of the crystallites occurs and the c-axis is aligned parallel to the stretch direction. The degree of preferential orientation increases as the stretch ratio and temperature are increased. No evidence was found to suggest any significant alignment in the amorphous phase.

(iv) An increase in the crystalline disorder, or a decrease in the average crystallite size was indicated by an increase in the half-width of diffraction peaks.

(v) Deformation of the spherulites from spheres into ellipsoids occurs at relatively low stretch ratios. Further deformation occurs as the stretch ratio is increased to 200% and the light scattering technique cannot detect the presence of spherulites beyond this stretch ratio.

These results are described in publication A, B, C, 1st Annual Report and reference 9.

3. Structural Changes after Corona Charging

3.1 Form 1 Films

After corona charging, the structure was investigated using wide angle X-ray diffraction. Fig. 1 shows the X-ray diffraction peak (110)+(200) of a Form 1 sample before and after corona charging at 20°C. It is clear that the peak intensity is significantly increased and that the background intensity (due to amorphous scattering for example) is noticeably decreased.

In Fig. 2 is shown the increase in intensity of the (110)+(200) peak as a function of the applied surface potential corona charging. It may be observed that a saturation level of about 1.35 times the unpoled peak intensity is reached at fields of $4 \times 10^8 Vm^{-1}$. This saturation level may be achieved with a lower applied field at a higher charging temperature[2].

A simple model of crystallite orientation in units of 60° developed by Kepler and Anderson[3] predicts that the intensity of this diffraction peak should increase with poling, but that the saturation level should be 1.2 times that of the unpoled level. It is possible that the additional increases in the intensity of diffraction observed in the present case and not predicted by theory, may be due to an increase in crystallinity. This may occur due to a removal by the field of defects introduced into the lattice on stretching, as proposed by Takahashi et al[4], and such a conception may be supported by the observed decreases in the half-widths of the diffraction peak profiles with increasing field as shown in Fig. 3.

These results are discussed in publication C.

3.2 Form 2 Films

Only the 50μm thick films were found to be completely in the Form 2 structure and it was found, for these films, that breakdown occured at fields $>3 \times 10^8 Vm^{-1}$. This is probably due to thin films having higher breakdown strength than thick films[5], rather than to the Form 2 having a lower breakdown strength than the Form 1.

However, extremely significant structural changes were observed by X-ray diffraction after corona charging due to the creation of a new crystalline form, originated by a rotation of alternate chains through $+90^{o}$ and -90^{o} to produce polar unit cells with their polar axes aligned in the direction of the field.

Experimental results and discussion are given in the 1st Annual Report and in Publications A and C.

3.3 Mixed Form 1 and Form 2 Films

Kureha 9, 16 and 25μm thick films were all biaxially oriented and contained both Form 1 and Form 2 crystallites, although the quantities of each in the different films were different. Also, films stretched uniaxially to fairly low extensions or at high temperatures contain significant amounts of both crystal forms.

X-ray diffraction studies after corona charging of such samples not only confirm the formation of a new crystalline form at the expense of the Form 2 crystallites (see Publication D) but also show that both the Form 2 and the new polar variation were converted to the Form 1 at the highest fields (see Publications E and F).

It may be reported that such structural modifications are accompanied by changes in chain conformation, which may be characterised by infra-red spectroscopy. It is not possible to detect new bands associated with an intermediate form between Form 1 and Form 2, but the reduction in the intensities of bands associated with the Form 2 structure, i.e. TGTG' chains, and the increase in Form 1 (zig-zag) bands confirm that such a change does occur. This may be observed in Fig. 4, which shows the infra-red spectrum of a 25μm thick sample before and after corona charging with a high field ($4 \times 10^{8} Vm^{-1}$).

The greatest changes occur for the bands at 510, 530, 615, 762, 795 and $975cm^{-1}$. The variationsof these absorptions with applied corona voltage are shown in Figs. 5 and 6. It may be observed that the $510cm^{-1}$ band, which is associated with the CF_2 bend of the Form 1 zig-zag chain, is the only one which increases in intensity. Although all the Form 2 band levels are reduced by the highest fields, the behaviour of each with field is different and only the reductions in the intensities of the $795cm^{-1}$ band and of the $530cm^{-1}$ band resemble the changes observed by X-ray diffraction. It is possible that only the CH_2 rock and the CF_2 bend are sensitive to the subtle change in crystallographic symmetry associated with the formation of a polar Form 2.

4. Piezoelectricity in Poled PVF_2

4.1 Form 1 Films

At a constant charging temperature and time, the piezoelectric coefficient of a highly stretched film (Form 1) was found to increase in a roughly linear manner with increasing applied field until a saturation level is approached.

d_{31} vs. voltage curves do not go through the origin but rather d_{31} is negligible until a certain temperature-dependent threshold field value is reached. At a poling temperature of 100°C this threshold field is $\bar{<}10^7 Vm^{-1}$.

On cooling back to ambient temperature in the presence of the applied field, the piezoelectric coefficient was found to increase by >10% at 120° compared to when the field is removed at the poling temperature, as shown in Figure 7. Other examples of the effects of the poling parameters on the piezoelectricity are given in the 1st Annual Report.

For a stretched film it was found that the piezoelectric response to stress applied at an angle θ° to the stretch direction, roughly obeyed the equation:

$$d = d_{31}\cos^2\theta + d_{32}\sin^2\theta$$

as shown in Fig. 8.

The ratio $d_{31}:d_{32}$ increases with increasing stretch ratio, as did the value of d_{31} for standard poling conditions, although saturation was found to occur at about 5:1 stretch ratio. These results are shown in Publication C.

It was found that a maximum value of about $36pcN^{-1}$ could be obtained for d_{31} from samples which had been stretched by 7:1 at 60°C and corona charged to a field of $3x10^8 Vm^{-1}$. However, if the samples were heat-treated to prevent subsequent shrinkage, then dielectric breakdown prevented the application of fields in excess of $2x10^8 Vm^{-1}$ with the result that a maximum value of $20pcN^{-1}$ was obtained.

In all cases, it was found that the poling rate was a function of both the poling temperature and of the applied field, which suggests that a particular energy barrier must be overcome in order to pole a sample completely. This would support a theory of crystallite orientation through some specific angle being the mechanism of poling.

4.2 Mixed Form 1 and Form 2 Films

The poling characteristics of Kureha films have been widely reported and this work has been concentrated on comparing increases in piezoelectricity with concomitant changes in structure and orientation of dipoles. (See Publications B, C, E, N and O.) Fig. 9 summarises this work by showing the effect of applied field on various structural and electrical parameters for a 25μm thick PVF_2 film. In addition, it has been shown that d_{31} increases linearly with temperature up to about 60°C and then non-linearly up to ∿100°C (see Publication F). The behaviour of d_{31} with temperature was found to be similar for Form 1, Form 2 and mixed Form 1 and Form 2 samples.

4.3 Form 2 Films

The major observation on the poling of Form 2 films is that a large threshold field must be applied before any piezoelectric activity may be observed. This threshold is temperature dependent as shown in Fig. 10 but the values of field are significantly greater than those for a Form 1 film. These data may again be compared to corresponding changes in structure, as in 1st Annual Report and Publication C which give further experimental results on the piezoelectricity of Form 2 films.

4.4 Effects of Other Poling Parameters

Neither the polarity of corona charging nor the type of metallisation employed (evaporated gold or aluminium and silver paint) have been found to have any effect on the magnitude of the piezoelectric coefficients measured (see 1st Annual Report). Furthermore, a comparison of samples poled by corona charging at various temperatures and fields with others poled in the conventional (metal-polymer-metal sandwich configuration) way, shows that there are no fundamental differences between the methods other than that higher fields may be employed by corona charging (see Fig. 11).

4.5 Ageing of Piezoelectricity

A comparison of the stability of the piezoelectricity and of the structural modifications introduced into PVF_2 samples by corona charging may be seen in Publication G, where it is shown that over one half of the initial piezoelectricity is preserved after annealing at temperatures of up to 140°C.

It has further been shown that the temperature of charging does not affect the decay in d_{31} since the average decay for samples poled at -40°C and those poled at +100°C is the same when the samples were subsequently kept at 100°C (see Fig. 12). This would suggest a single ageing process.

Further, small electrical fields, neither a.c. nor d.c. (of either polarity with respect to the original charging field) appear to affect the rate of decay of polarization, as shown in Fig. 13 where the average decays of poled films exposed to the fields at 100°C are not dissimilar to those of unexposed poled films.

It was established that the chemical medium in which the films are kept has little effect on the rate of decay of piezoelectricity by the comparison of samples immersed in distilled water and in sea-water, both at 60°C (see Fig. 14).

Generally, for films poled under a variety of conditions and stored under ambient conditions, the rate of decay of d_{31} was found to be logarithmic, as shown in Fig. 15, and 70% of the initial activity remained even after a period of over one year.

5. Pyroelectricity

5.1 The Direct Method

Early pyroelectric results for both conventionally poled and corona charged films of PVF_2 were presented in publications H and I. This work supported previous observations by other workers[6], though it was shown that the truly reversible pyroelectric current is stable beyond 100°C and that the pyroelectric coefficient increases linearly up to ~70°C and then super-linearly beyond that temperature.

It has also been discovered that the pyroelectricity may be enhanced by corona charging and by stretching of the films. During the first thermal cycle after room temperature corona charging of a mixed Form 1 and Form 2 film, a peak is observed between 40 and 50°C with an activation energy of about 1.2eV, and the magnitude of the peak is nearly linearly related to the charging voltage.

The pyroelectric coefficient, p, vs. T curves of all the crystal forms of poled PVF_2 have the same shape which does not depend on the degree of poling. Furthermore, the similarities between the curves and those for d_{31} vs. T suggest that the origins of piezoelectricity and pyroelectricity are similar in this polymer. These results appear in Publication F.

5.2 The Dynamic Method

The dynamic response of poled PVF_2 to a pulse of radiation (laser beam) can be separated into the super position of two decaying exponentials governed by the thermal and the electrical time constants of the linkage and the measurement circuit[7] respectively. Also the magnitude of the current peak, I_p, was found to be directly proportional to both the pyroelectric coefficient measured at 28°C (by the direct method) and to the piezoelectric coefficient d_{31} of similarly poled samples. These results[10] are presented in full in publication J.

6. Non-Uniformity of Poling

6.1 Piezoelectric Measurements

Results of experiments involving the poling of thin films of PVF_2 in a stack indicate that considerable non-uniformity of poling exists across the stack thickness. For three films poled in series it was found that the film closest to the positive electrode during poling was in each case the most piezoelectric. In Table 1 are the results for samples poled for 5 minutes with a field of $4 \times 10^7 Vm^{-1}$, sample thickness being 9μm. In this case, i.e. conventional poling, the non-uniformity decreases as the degree of poling increases. However, when a similar experiment was performed at room temperature using the corona charging technique, the results were significantly different, as shown in Table 2. Although non-uniformity still exists, it is less than in the conventional poling case and also the trends are opposite, i.e. non-uniformity increases with increasing poling, and the centre sample has the highest activity.

Clearly, the two poling methods must be establishing different field distributions within the stack. In the case of conventional poling, electrode or interfacial polarization may build up at the discontinuities so that space charge effects may cause field perturbations. On the other hand, the corona charging procedure may drive ions into the surface exposed to the corona and alter the field in that way. Further work is necessary to clarify the above observations.

6.2 Structural Non-Uniformity of Poling

It has been shown that the crystalline structures of PVF_2 films originally containing both the Form 1 and the Form 2 crystallites are significantly altered by the corona charging procedure, and also that the reduction in the intensities of certain infra-red absorption bands, such as that at $795cm^{-1}$ band, may provide a convenient means of monitoring the degree of poling (see Fig. 9).

The infra-red absorption or optical density as conventionally measured through the thickness of the film may identify the structure in the bulk of the film. The use of the Attenuated Total Reflection (ATR) infra-red spectroscopy method allows the examination of the surface extending up to 2 to 3μm of the film. In the present work, the $795cm^{-1}$ band has been selected for A.T.R.

analysis and it has been found that, as a result of corona charging, with a positive corona, great differences exist between the changes in the bulk and those at the two surfaces, as shown in Fig. 16. Both positive and negative corona produce similar changes in the bulk but the surface changes are slightly different as Fig. 17 shows for the negative corona case. However, it is clear that in both cases the changes at the corona surfaces (and, therefore, the field experienced at those surfaces) are much less pronounced than those in the bulk[8].

Such results further indicate that homocharge injection (in the form of ions from the air) must occur at the unelectroded top surface of the sample during corona charging and the presence of the charge layer causes a reduction in the field level close to the surface and an enhancement of the field in the sample bulk.

6.3 Pyroelectric Non-Uniformity

Applying the dynamic pyroelectric method (publication J) to reversible samples which had been corona charged with positive ions at room temperature, it was found that the peak intensity, I_p, obtained by illuminating the side of the sample which had been earthed during the charging, was greater than that obtained by illuminating the corona side. However, for a conventionally poled sample, it was found that $I_p^+ > I_p^-$ but by a smaller margin. Since it can be assumed that the radiation is absorbed at the near electrode, then these results are in agreement with the other results on non-uniform poling.

These results are presented in Publication K.

7. Current Measurements

7.1 Transient Charging and Discharging Currents

It is generally accepted that the absorption current in an insulating material, on the application or removal of a step voltage, may be attributed to the following mechanisms of polarization in the bulk: (i) electrode polarization; (ii) dipole orientation; (iii) charge storage leading to trapped space charge effects; (iv) tunnelling of charge from the electrodes to empty traps; (v) hopping of charge carriers through localized states. The exact nature of absorption currents may be identified from a study of dependence of charging and discharging currents on parameters such as electric field, sample thickness, electrode materials, temperature, time and the relation between the charging and discharging currents. Complete results of this study in the present work are given in the first annual report, publication M, references 11 and 12, and some additional information is also available in reference 2. A summary of absorption current results[11] is given in Table 3.

Below 273K it was found that the charging and discharging currents were mirror images at all fields employed in this work $\leq 4 \times 10^7 Vm^{-1}$. Thus, ruling out space charge mechanism in this temperature and field range. Above room temperature, the current transients are no longer mirror images and the charging current was observed to reach a peak in longer times ($\gtrsim 10^3$s) after the application of a step field ($\sim 10^7 Vm^{-1}$) before decaying to a quasi-steady state value at times $\gtrsim 10^5$s. Such a behaviour may be attributed to a slow drift of charge carriers and bulk space charge release

without actually limiting the current injection. Figure 18 shows the time dependence of the charging currents at 50°C, the range of field being $5x10^4$ - $2x10^7 Vm^{-1}$. The field dependence of charging and discharging currents at constant times at 40°C are shown in figure 19, from which it may be observed that, for fields 10^4 to $10^7 Vm^{-1}$, transient currents are mirror images of each other even at this temperature up to a field of $\sim 10^6 Vm^{-1}$ at shorter times with unity gradient (dI/dE). However, there is a progressive departure from this mirror image behaviour of the current transients at longer times and higher fields, probably due to the onset and predominance of the conduction current component over the displacement current.

The absorption currents in PVF_2 were also observed to be independent of sample thickness and electrode materials. Thus space charge mechanism may again be ruled out as responsible for limiting the injection of charge carriers significantly from the electrodes. It may be noted that, should there be an oxide layer between the electrode material and the polymer (interface states), then there will be two interfaces, one between the metal (electrode material) and the oxide and the other between the oxide and the polymer. The interface between the oxide and the polymer is more important from the standpoint of electrical properties, because any charged traps at or near the oxide-polymer interface will affect the barrier height far more than a charged trap at or near the metal-oxide interface, which will have virtually no effect on the electrical properties of the contact. The barrier height, in such a case ('modified Bardeen barrier') is determined largely by the properties of the oxide layer. Although this may possibly explain the observed electrode (material) independence of the current transients, electrode polarization mechanism, however, predicts that n=0.5 initially, followed by n>1 in the expression

$$I(t) = A(T)t^{-n}$$

where I is the absorption current, A is a weakly temperature dependent parameter and other symbols have their usual meaning. The observed n-values in the present work (see Table 3) would thus eliminate the mechanisms of electrode polarization and charge injection forming trapped space charge as being responsible for the nature of absorption currents in PVF_2. The observed peak in the charging transients must then be due to a shuffling and drifting of bulk space charge in the virgin material under the influence of externally impressed field and temperature. This space charge density at all times before a steady state conduction is reached must exceed that of the injected carrier density; otherwise a truly injection limited space charge limited current behaviour would have been observed.

The tunnelling model assumes a presence of empty traps lying in the band gap of the insulator. On application of a step voltage, electrons tunnel from an electrode into the empty trap sites. The model predicts the current to be inversely in proportion to the sample thickness and reasonably independent of the temperature. The observed behaviour of absorption currents would reject the tunnelling mechanism to be responsible on both counts.

The temperature behaviour of the isochronal (at constant times) discharge current (figure 22) show two distinct peaks at $\sim -40°C$ and 60°C. These may correspond to the α_a - relaxation process close to the glass transition

temperature, Tg, at $\sim -50^{o}C$ in the amorphous phase and the α_i process due to interfacial polarization or the release of trapped charges, as observed in the T.S.C. experiment, respectively (see publication F, for example).

The discharge current does not increase linearly with increasing charging field at high temperatures. This may be explained either by an onset of a permanent polarization in the bulk (i.e., an alignment of dipoles and their stability in their own internal field) or a field cleaning of bulk space charges at suitably high fields. The time and temperature dependence of the transient currents may be described by the interfacial polarization process at low fields ($<10^{7}Vm^{-1}$) which may be related to the α_i-process. At fields $>10^{7}Vm^{-1}$ the field dependence of isochronal charging current becomes super-linear (see figure 19) which is in disagreement with the interfacial polarization model. This could, however, be explained by a carrier hopping process which may at longer times produce a quasi-steady state conduction.

7.2 Quasi-Steady-State Conduction

At no time did the absorption current reach a true steady state within the experimental range of time ($t_{max} \sim 10^{5}s$) temperature($T_{max} \sim 405K$) and field($E_{max} \sim 4x10^{7}Vm^{-1}$). For low fields the quasi-steady state current I_s was reached after a time which was observed to be temperature dependent (figure 20). Assuming an Arrheneius type of thermal activation process, a plot of $I_s(t)/\frac{1}{T}$ yields an activation energy of leV. At higher temperatures and fields, it became difficult to find even a quasi-steady state level due to drifting space charges (or ions) through the sample.

Many calculations have been made to determine the band structure of polymers but little is known about their electronic structure. However, it seems to be agreed that large energy gaps exist between the filled and empty states with ill-defined band edges due to the presence of localised states. The impurities which are likely to exist in polymeric materials could not account for any appreciable electronic carrier generation and conduction currents are most likely due to injected carriers in general. However, the mechanism of ionic conduction, particularly at high temperature, should also be seriously considered.

It appears that no single conduction mechanism may be attributed to the observed results in the entire ranges of temperature and field in the present work. A linear relationship of the I-V characteristics is obeyed up to a field $\sim 10^{6}Vm^{-1}$ beyond which a square law relationship may describe the current-voltage relationship with the present data. However, it should be pointed out, that the space charge model requires not only a superlinear dependence of the current with the voltage, but also a thickness dependence ($I \alpha \frac{V^2}{d^3}$, where d is the sample thickness) which was not observed in the present work. Furthermore, assuming a space charge model, the calculated charge carrier mobility was observed to be linearly related to the external field (see Figure 21). The thermal activation energy, which was calculated to be leV at $10^{5}Vm^{-1}$), was also observed to be field dependent. Thus the I-V characteristics may not be supported by the simple space charge theory which assumes that trap energies are unaffected by the field. The observations of linear dependence of mobility values with fields and the reduction of activation energies with fields may, however, be explained by a field-induced hopping process. In view of the above arguments,

the analysis of steady state conduction measurements in PVF_2 by Takahashi et al[13], who proposed a Richardson-Schottky model, should be treated with caution. It is suggested that further work is necessary to investigate the mechanism of steady state electrical conduction in PVF_2.

8. Conclusions

The results of these experiments indicate that at least a large part of the polarization in PVF_2 after poling is due to dipole orientation in the crystalline regions. There is ample evidence to show that crystallites are aligned by the poling field and remain in or close to this new angular position when the field is removed. Ageing experiments indicate that they do not return to their original positions even after annealing at high temperatures.

Films of nonpolar Form 2 PVF_2 may be made to exhibit considerable piezo- and pyroelectric response by high field ($\sim 3 \times 10^8 Vm^{-1}$) poling at room temperature. This has been shown to be due to a change of crystallographic symmetry of the Form 2 unit cell (F.g. 23) with C_{2v} space group into an 'intermediate' polar form (Fig. 24). It has been suggested[14] that this 'intermediate' structural form may be produced by a co-operative rotation of the alternative chains through 180° about the -C-C- axis without producing a change in the unit cell (Form 2) dimensions, but with rotations of the crystallite a- and b-axis through 180°. This is equivalent to a rotation of all the Form 2 chains by 90°, but with alternate chains rotating in opposite directions to provide a stable state. At still higher fields ($>3 \times 10^8 Vm^{-1}$) there is a progressive conversion of the 'intermediate' polar Form 2 crystallites into a polar Form 1 structure (Fig. 25) with a zig-zag molecular conformation. On the other hand, on uniaxial stretching of the polymer, there is a direct conversion of the Form 2 crystallites into Form 1 structure with randomly oriented dipole moments. On subsequent poling the dipoles align, of course, at a particular angle with the direction of poling field. The dominant mechanism of piezo- and pyro-electricity in this polymer remains, however, of dipolar nature, originating in the crystalline phase (see reference 15 and publication A).

The induced polarization is remarkably stable even after annealing the poled specimens at temperatures much higher than T_p (poling temperature). This would suggest that the dipoles remain aligned in their high internal fields which must be significantly greater than kT even at 100°C.

It is possible that space charges are also present in the film. However, the distribution of space charges in the bulk of the material after poling is not of importance as regards permanent polarization. Such space charges may be removed by thermal cleaning without significant decrease in the piezoelectric and reversible pyroelectric responses. A presence of space charges at low to moderate fields may provide a non-uniform bulk polarization. Such non-uniformity, however, is progressively removed with increasing poling fields.

It has been possible to achieve a stable value of d_{31} as high as $40 pCN^{-1}$. The highest magnitude of the pyroelectric coefficient was observed to be $\sim 2.7 nC/cm^2\ ^oC$ at 20°C[2].

9. Acknowledgements

The research reported herein has been sponsored in part by the United States Army through its Research and Standardization Group (Europe). It is also a pleasure to express our gratitude to Dr. G. T. Davis of the National Bureau of Standards, Washington D.C., for invaluable discussions. I am also pleased to express my appreciation for the substantial help of Drs. R. S. Brockley and K. Doughty, and Messrs. J.S. Duffy, P.C. Grandidge, G.C. McCauley and D.B. Shier, without which the progress of this project would have been impossible.

10. Literature cited

1. Ye L. Gal'perin, B.P. Kosmynin & V.K. Smirnov, Polymer Sc. USSR 12 2144 (1970).
2. K. Doughty, PhD Thesis, UCNW Bangor (1979).
3. R.G. Kepler & R.A. Anderson, J.Appl.Phys., 49 4918 (1978).
4. N. Takahashi & A. Odajima, Rep.Prog.Polym.Phys.(Japan) Vol.XXII 151 (1979).
5. F.M. Clark, "Insulating Materials for Design & Practice", John Wiley (1962).
6. G. Pfister & M.A. Abkowitz, J.Appl.Phys. 45 1001 (1974)
7. M. Simhony & A. Shaulov, J.Appl. Phys., 42 3741 (1971).
8. K. Doughty & P. Pantelis, J. Mats. Sci. (To be published 1980).
9. P.C. Grandidge, M.Sc. Thesis, University of Wales (1979).
10. G.C. McCauley, M.Sc. Thesis, University of Wales (1979).
11. R.S. Brockley, Ph.D. Thesis, University of Wales (1979).
12. D.B. Shier, Ph.D. Thesis, to be submitted (University of Wales)
13. K. Takahashi, H. Lee, R.E. Saloman & M.M. Labes, J.Appl.Phys. 48 11 (1977).
14. G.T. Davis, J.E. McKinney, M.G. Broadhurst & S.C. Roth, J.Appl.Phys. 49 4998 (1978).
15. R.J. Shuford, A.F. Wild, J.J. Rica & G.R. Thomas, Polym. Eng. Sci. 16(1) 25 (1976).

11. Publications

A. D.K. Das-Gupta, K.Doughty and D.B. Shier, "A study of structural and electrical properties of stretched polyvinylidene fluoride films", J. Electrostatics 7 267 (1979).

B. D.K. Das-Gupta and D.B. Shier, "Small Angle Light Scattering from uniaxially stretched polyvinylidene fluoride", J.Appl.Phys. 49 5685 (1978).

C. D.K. Das-Gupta & K.Doughty, "Piezoelectricity in uniaxially stretched and corona poled polyvinylidene fluoride", J.Phys.D. 13 95 1980.

D. D.K. Das-Gupta & K. Doughty, "Changes in X-ray diffraction patterns of polyvinylidene fluoride due to corona charging", Appl.Phys.Lett. 31 585 (1977).

E. D.K.Das-Gupta & K. Doughty, "Corona charging and the piezoelectric effect in polyvinylidene fluoride", J.Appl.Phys. 49 4601 (1978).

F. D.K. Das-Gupta & K. Doughty, "Piezo- and pyroelectricity in corona poled polyvinylidene fluoride", J.Phys.D. 11 2415 (1978).

G. D.K. Das-Gupta & K. Doughty, "Ageing of corona charged polyvinylidene fluoride", Proc. IEEE Insulation Conf. Philadelphia (June 1978).

H. D.K. DaslGupta & K. Doughty, "On the nature of poling by corona charging and the pyroelectric effect in PVF_2", IEEE Trans. IAS IA-14 448 (1978).

I. D.K. Das-Gupta & J.S. Duffy, "Pyroelectricity in polyvinylidene fluoride", J.Appl.Phys. 50 561 (1979).

J. D.K. Das-Gupta & K. Doughty, "Pyroelectric transient
idene fluoride", J.Appl.Phys. 51 (To be published 1980).

11. Publications (cont.)

K. D.K. Das-Gupta & K. Doughty, "A study of the pyroelectric behaviour of polyvinylidene fluoride", Conference on Electrical Insulation and Dielectric Phenomena, p.456 (1979).

L. D.K. Das-Gupta & K. Doughty, "Thermal Ageing Effects in corona charged polyvinylidene fluoride', Conference on Electrical Insulation and Dielectric Phenomena (1978).

M. D.K. Das-Gupta & R.S. Brockley, "On origins of high field polarization in polyvinylidene fluoride", Conference on Electrical Insulation and Dielectric Phenomena (1977).

N. D.K. Das-Gupta & K. Doughty, "On the nature of piezoelectric effect in corona charged polyvinylidene fluoride", European Polymer Symposium, Pisa, Italy (1978).

O. D.K. Das-Gupta & K. Doughty, "On the nature and mechanism of piezo- and pyroelectricity in polyvinylidene fluoride", Charge Storage, Charge Transport and Electrostatics, Ed. Wada, Perlman & Kakodo, Elsevier pp.153-157 (1979).

Fig. 1.

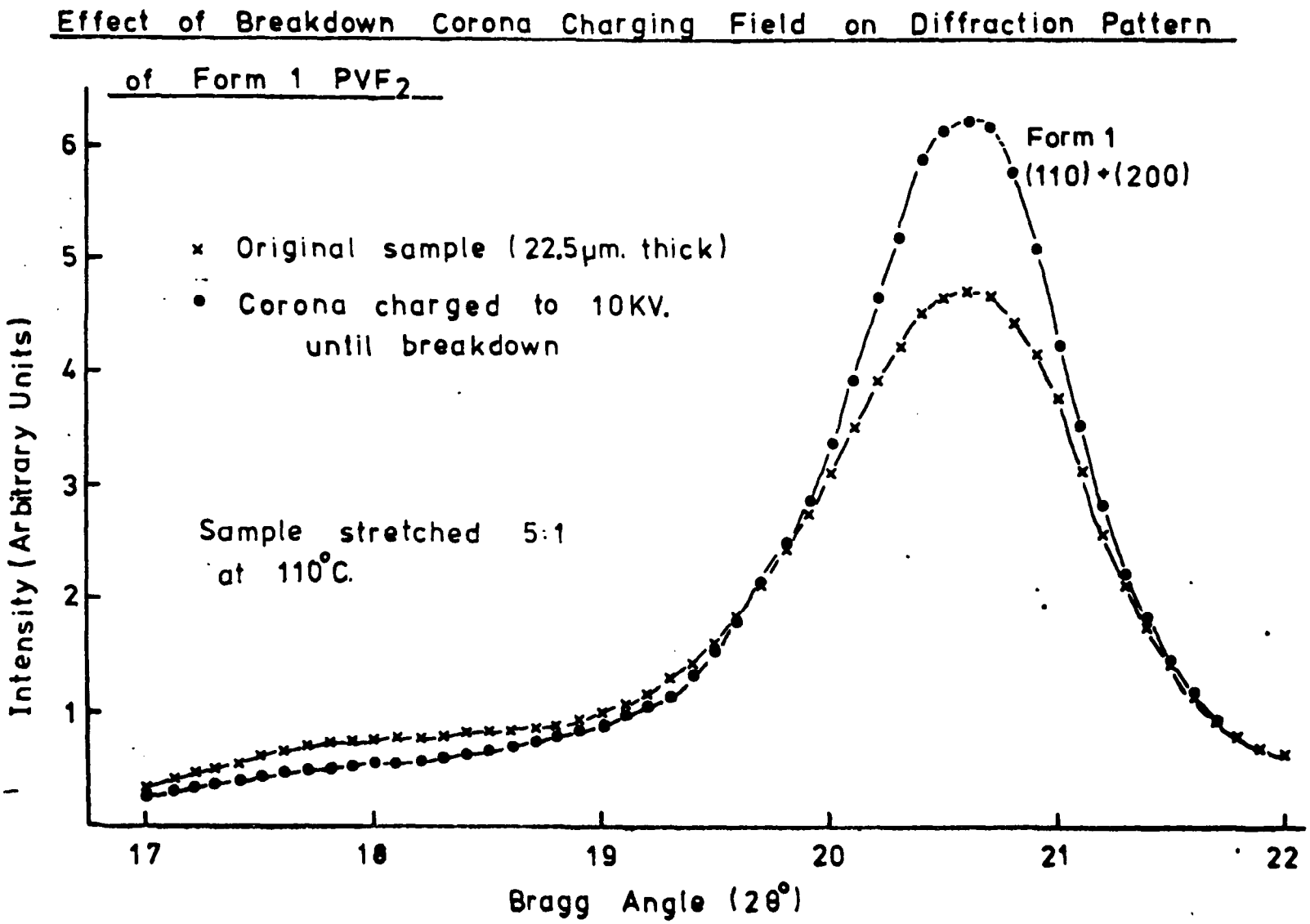
Effect of Breakdown Corona Charging Field on Diffraction Pattern of Form 1 PVF_2
Form 1
(110) + (200)
× Original sample (22.5μm. thick)
• Corona charged to 10KV. until breakdown
Sample stretched 5:1 at 110°C.
Intensity (Arbitrary Units)
1
2
3
4
5
6
17
18
19
20
21
22
Bragg Angle (2θ°)

Fig. 2.

Variation in Form 1 (110) + (200) Peak Intensity with Charging Voltage up to Breakdown for Sample Completely in Form 1

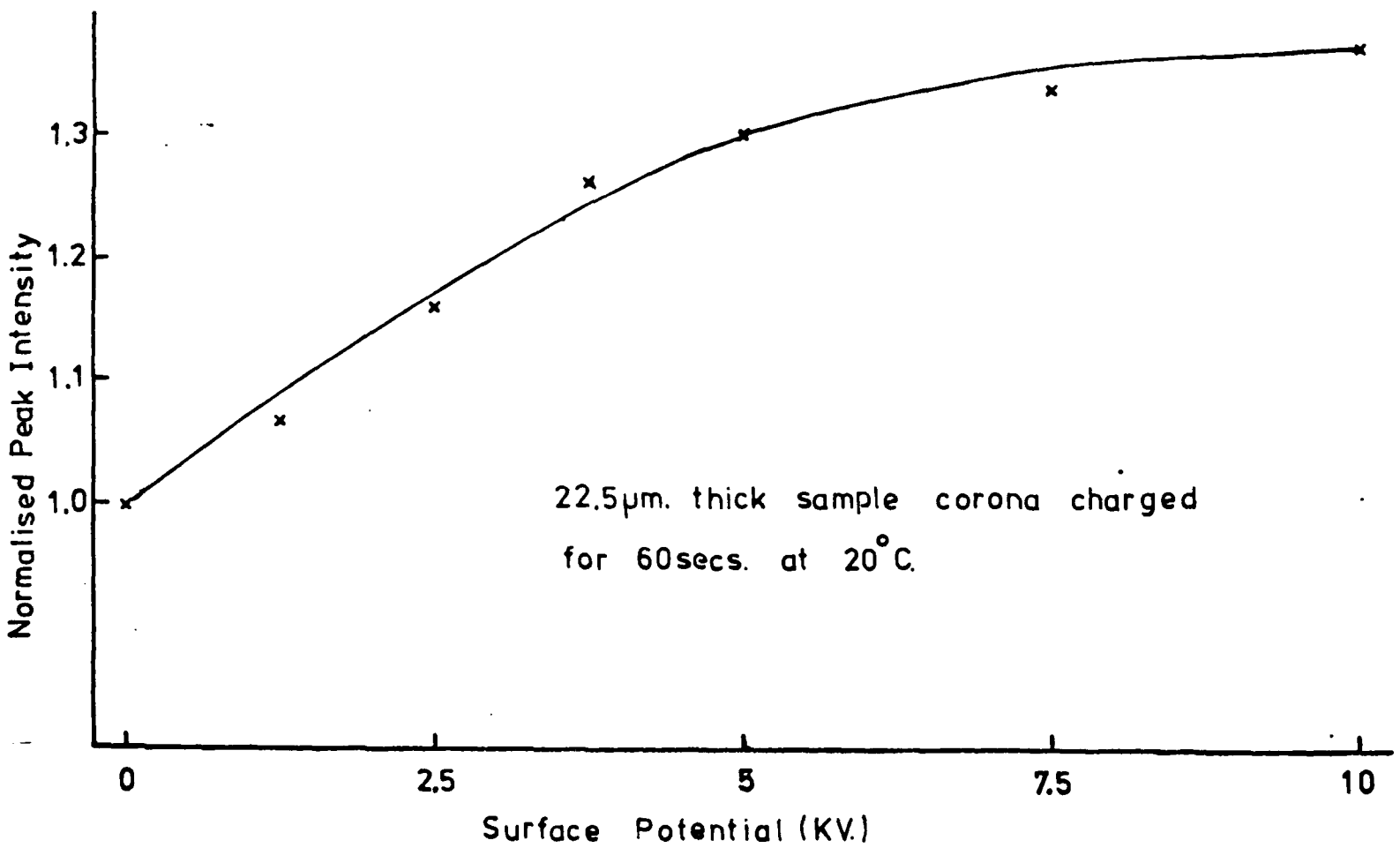

Fig. 3. Variation in Form 1 (110)+(200) Diffraction Peak Profile with Potential

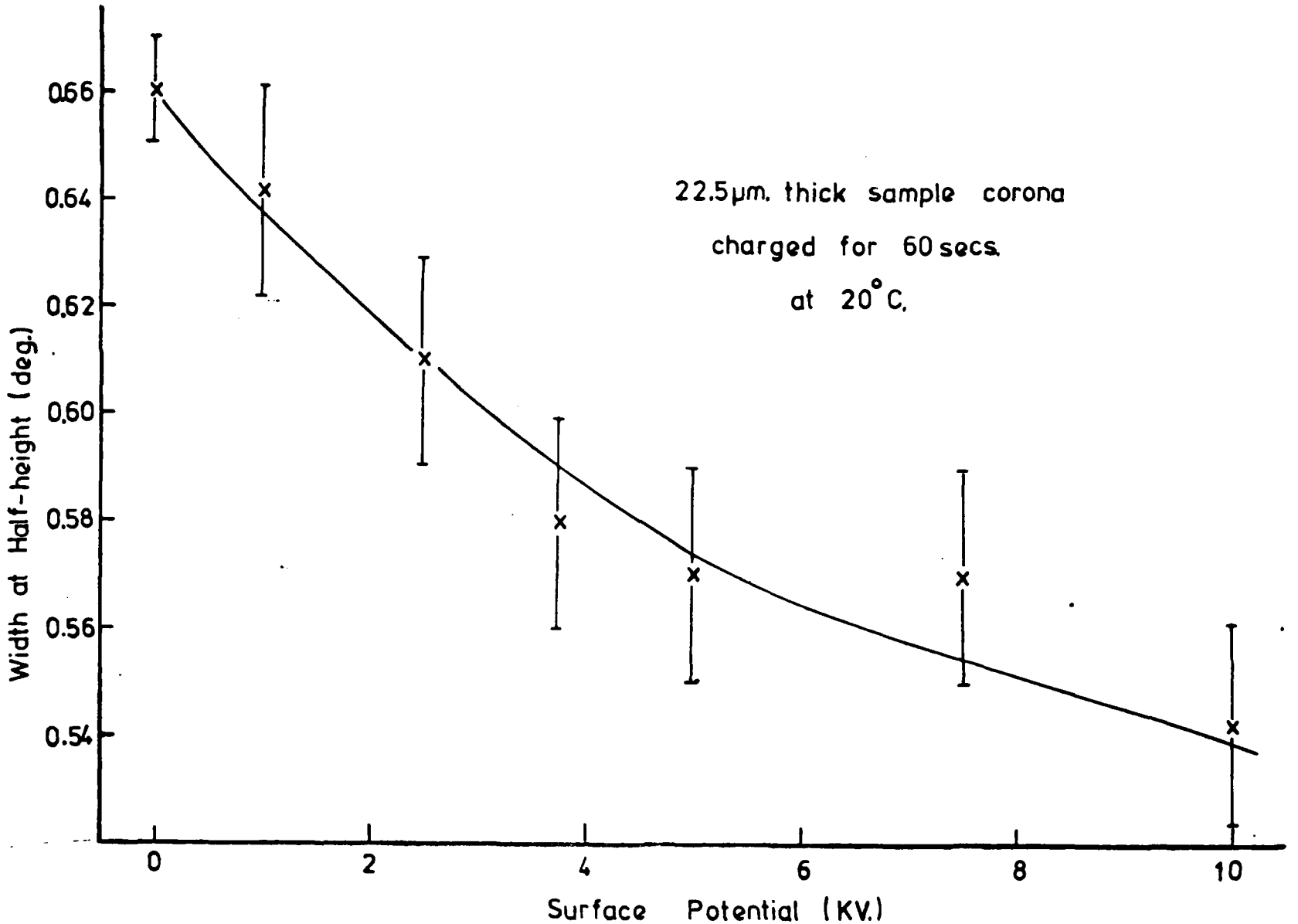

Fig. 4.

Changes in I.R. Spectrum of 25μm. Sample Due to Corona Charging to 10KV. for 1min. at 20°C.

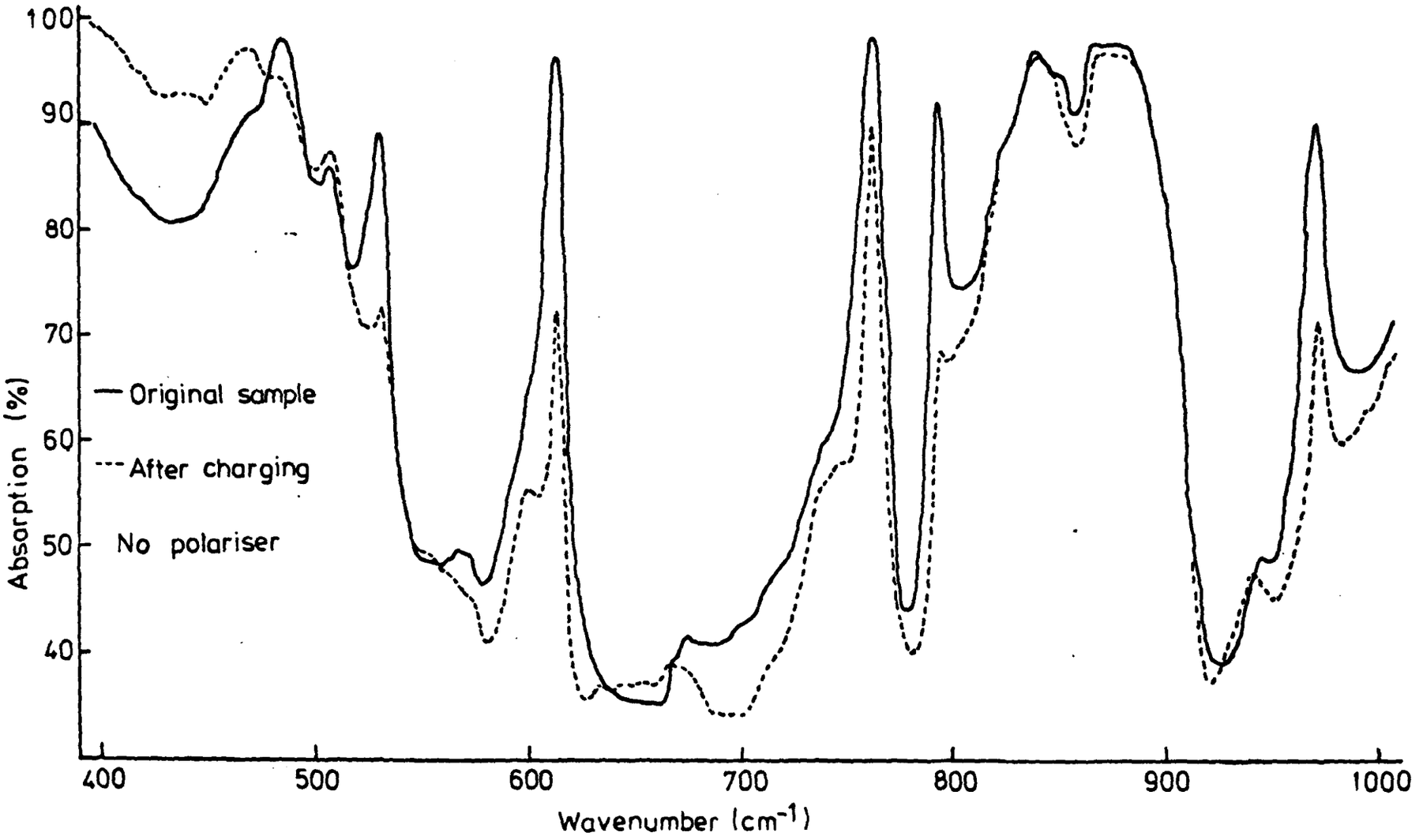

Fig. 5.

Changes in I.R. Absorption Peaks at $510cm^{-1}$, $795cm^{-1}$ and $975cm^{-1}$ with Applied Voltage for 25μm. Kureha Sample Corona Charged at 20°C. for 1min.

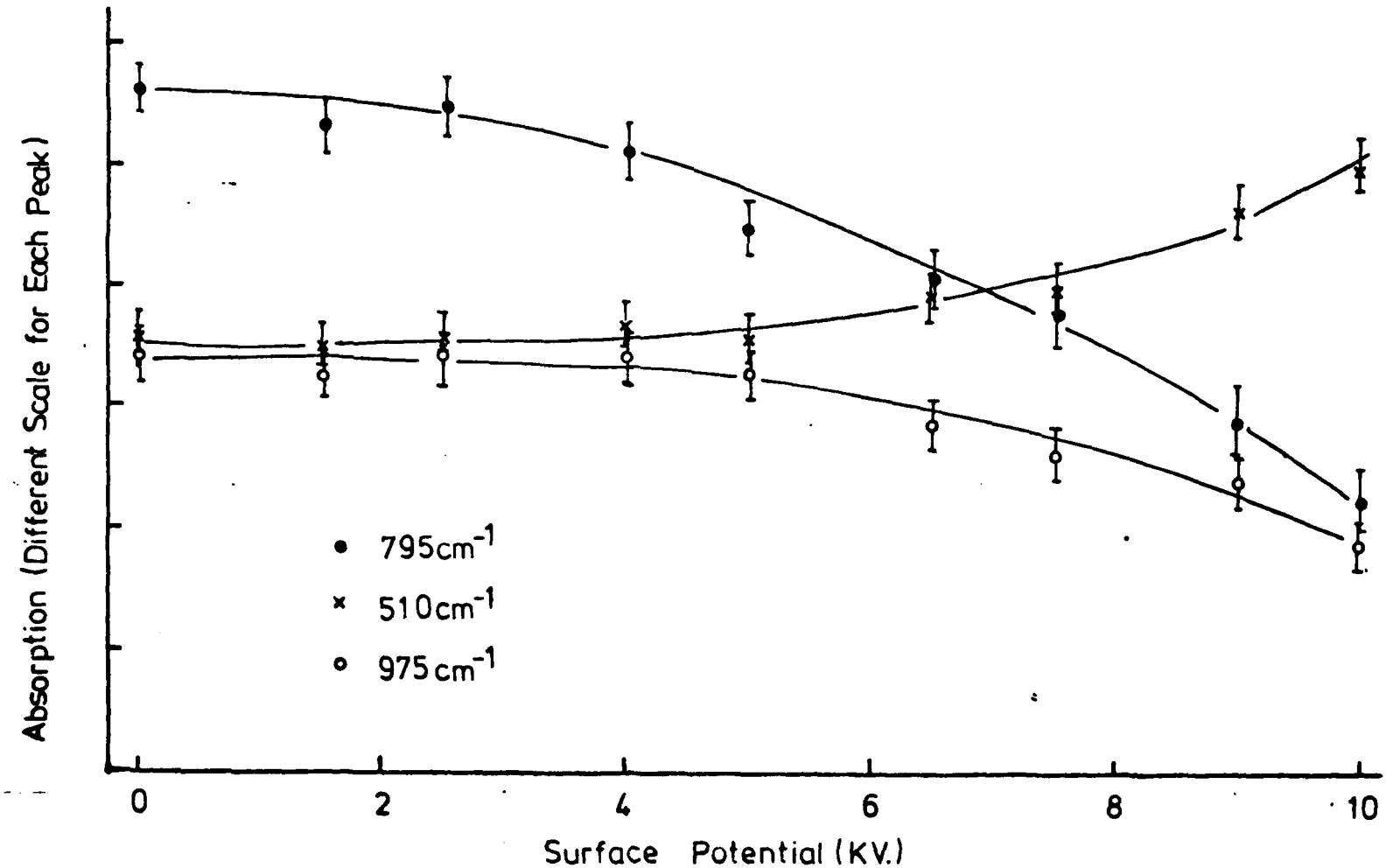

Fig. 6.

Changes in IR. Absorption Peaks at 530cm^{-1}, 615cm^{-1} and 762cm^{-1} with Applied Voltage for 25μm. Kureha Sample Corona Charged at 20°C for 1min.

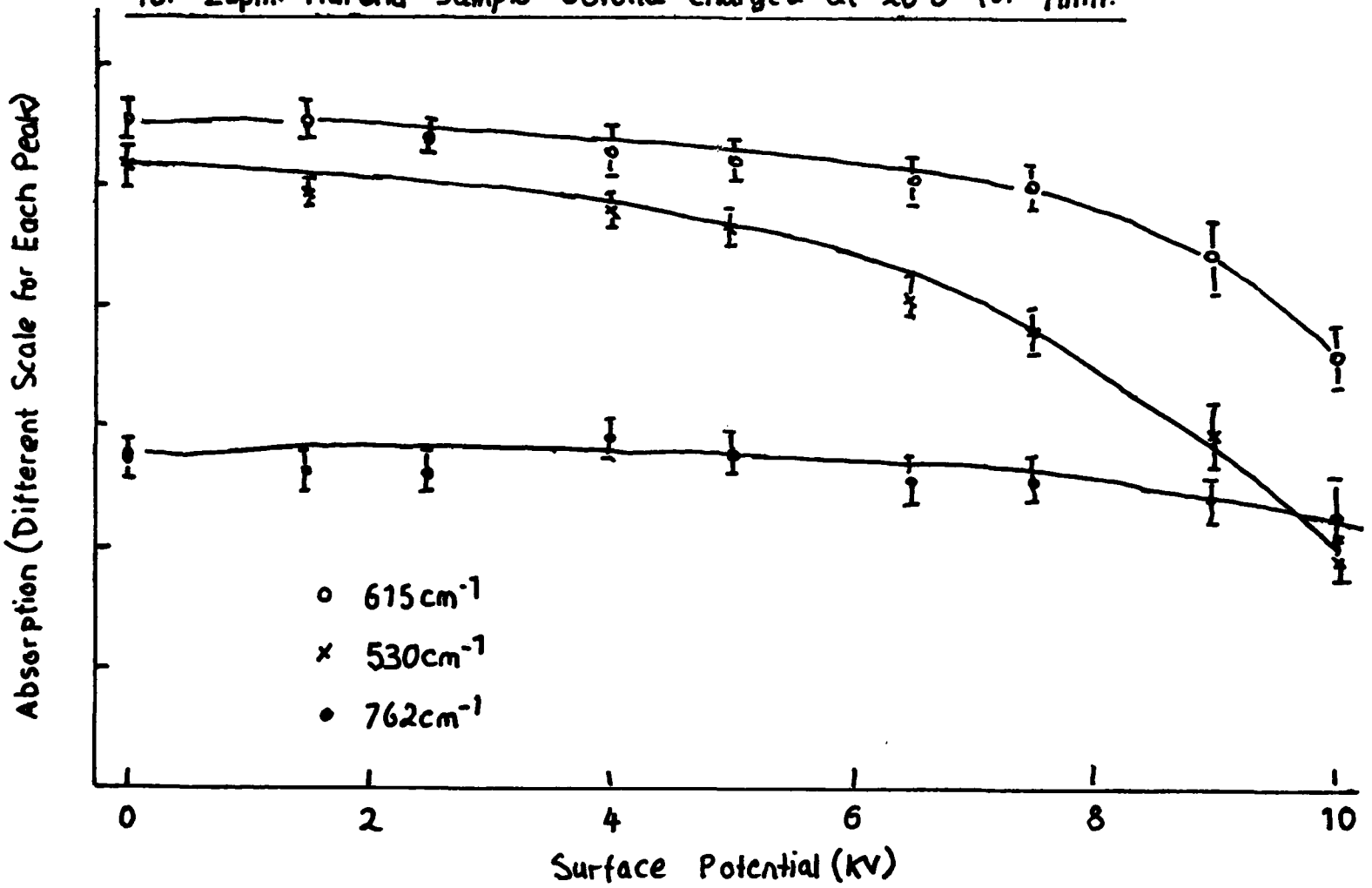

Fig. 7:

Piezoelectric Activity v Poling Temperature to show the effect of cooling in the presence of the Applied Field for a typical sample. (24 hrs after poling)

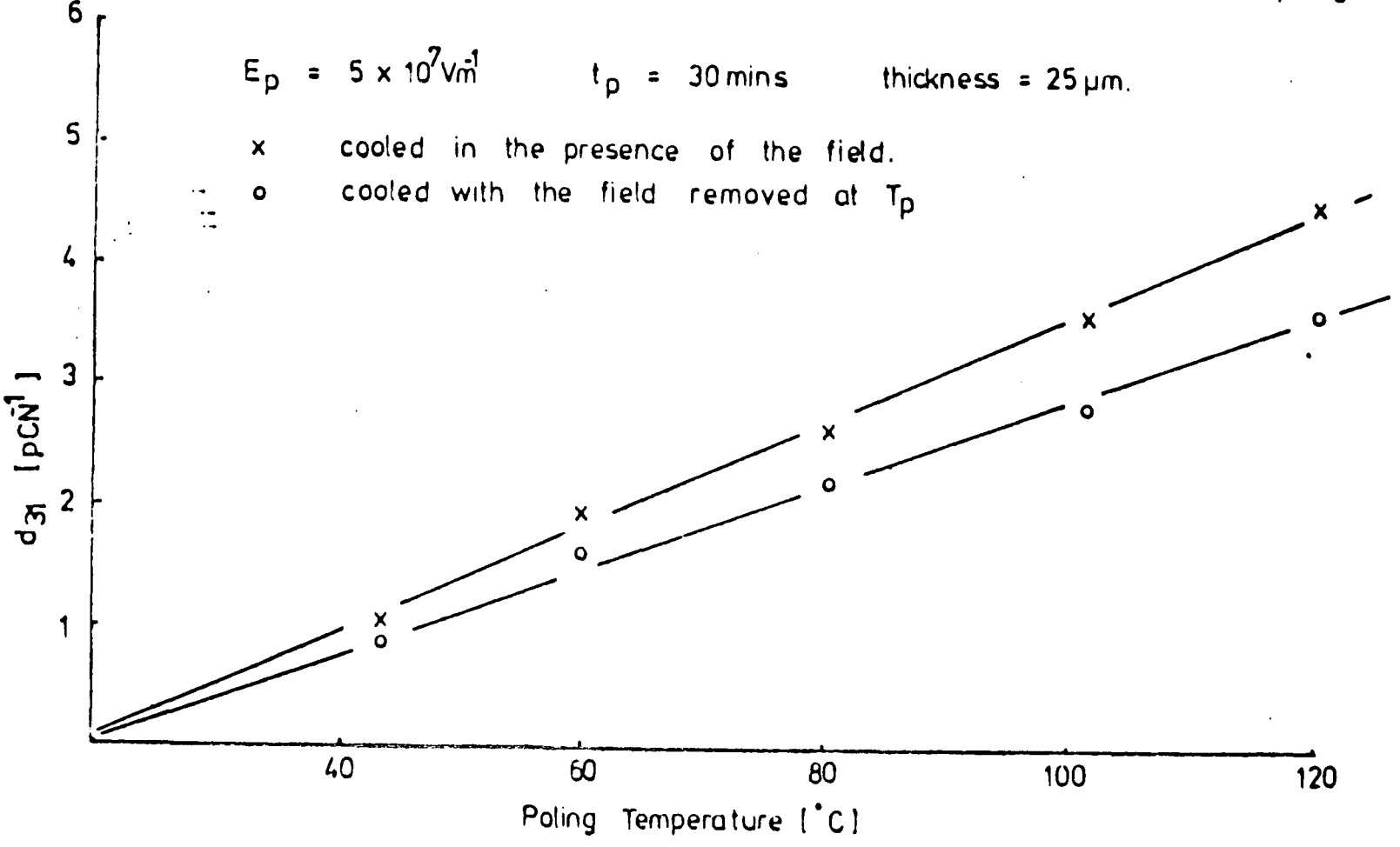

Fig. 8.

Piezoelectric Response for Uniaxially Stretched Samples at Various Angles to the Stretch Direction

Standard weight = 200 gms.

Standard capacitance = 5×10^{-7} F.

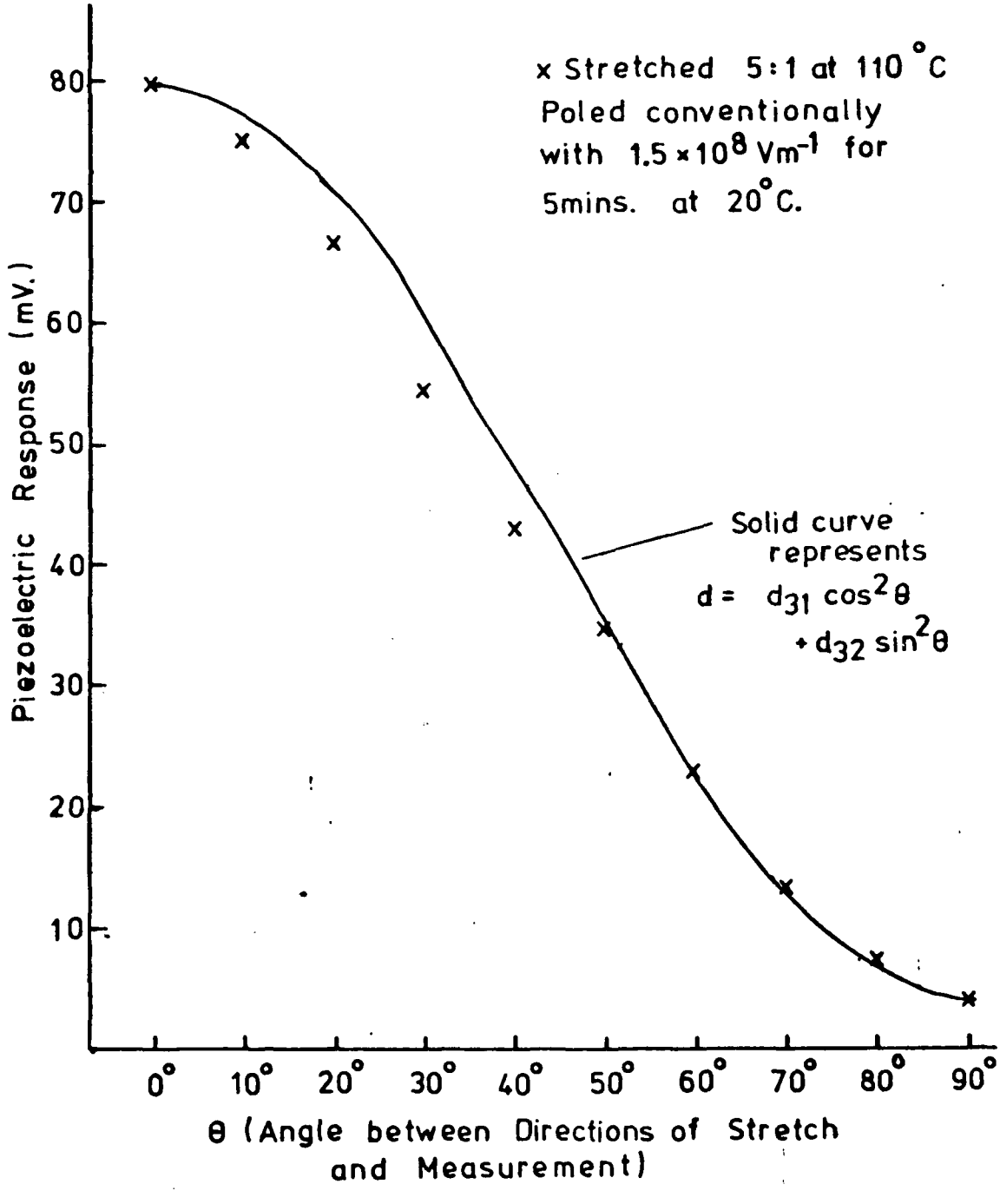

Fig. 9. Effect of Room Temperature Corona Charging on Various Parameters for 25μm. Thick Biaxially Stretched PVF_2

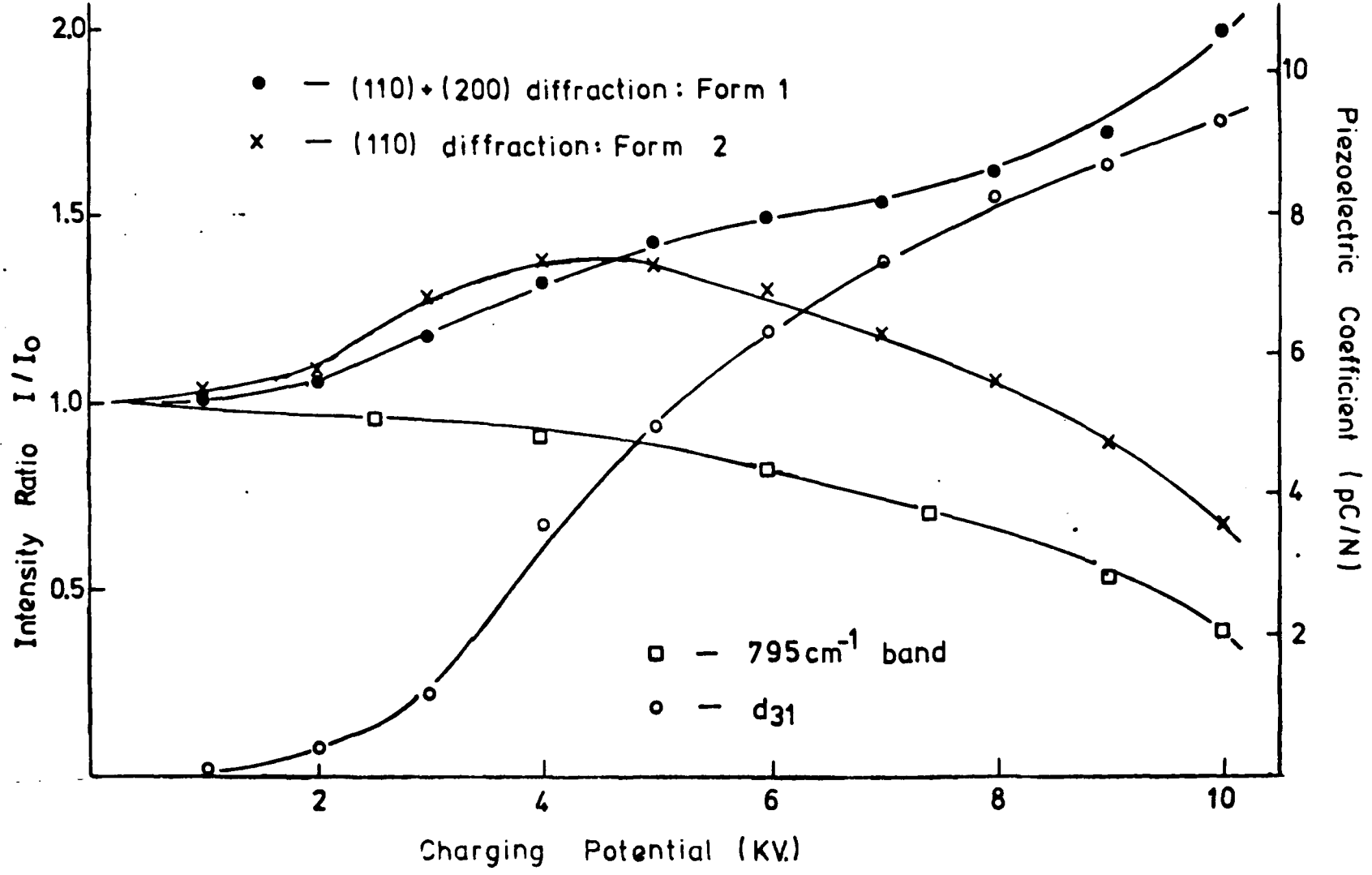

Fig. 10.

Piezoelectric Activity of Form 2 PVF_2 (50μm. thick) Corona Charged to Show the Existence of a Temperature-Dependent Threshold Voltage for Poling

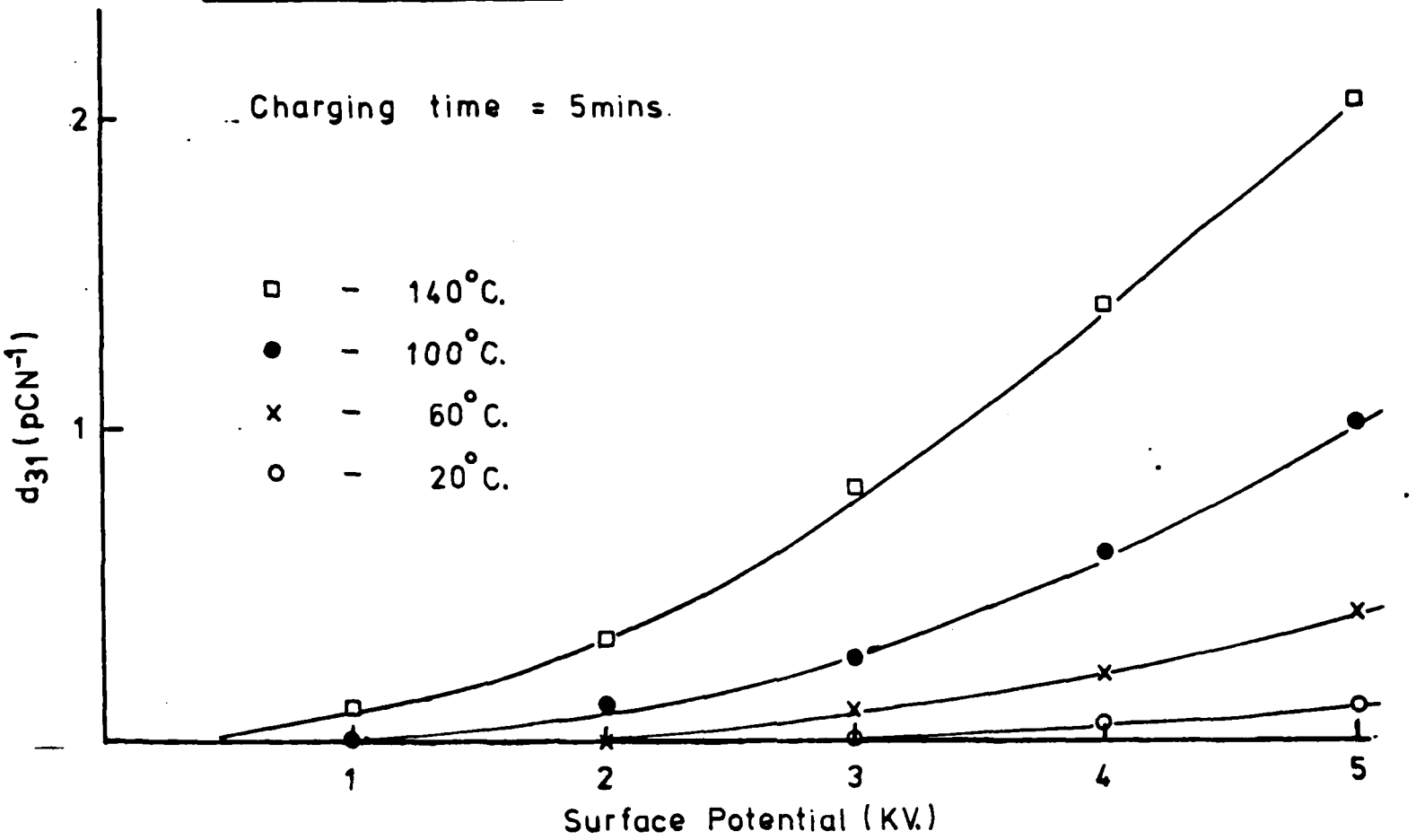

Fig. 11. Comparison of the Piezoelectric Activity v Poling Voltage for Corona Poled and Conventionally Poled samples. 25um thick samples with Aluminium Electrodes

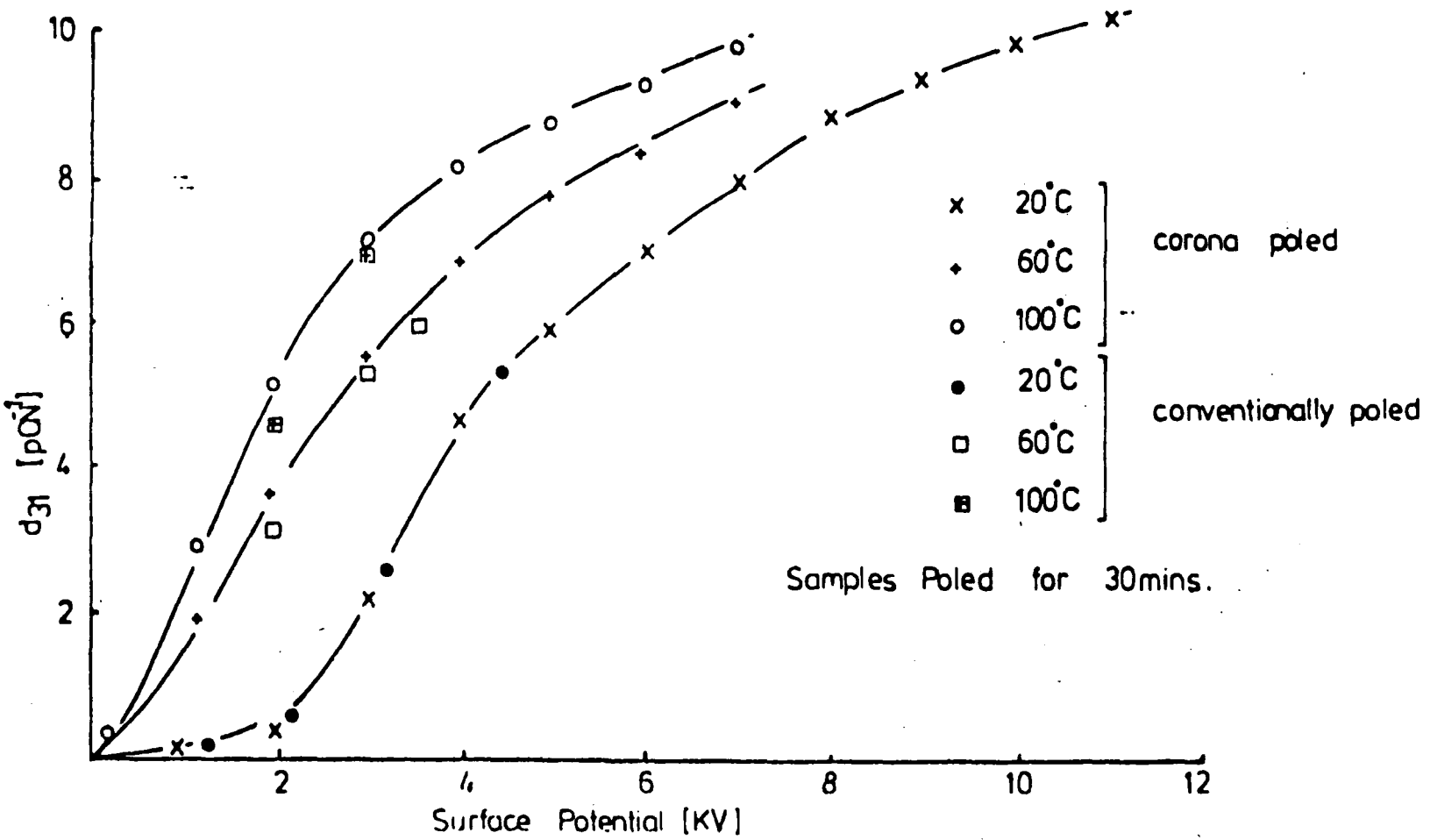

Fig. 12.

Effect of Charging Temperature on the Stability of d_{31} after Annealing at 100°C. for 15hours. Corona charging at various potentials for 5mins. 25 and 50μm. thick Kureha samples.

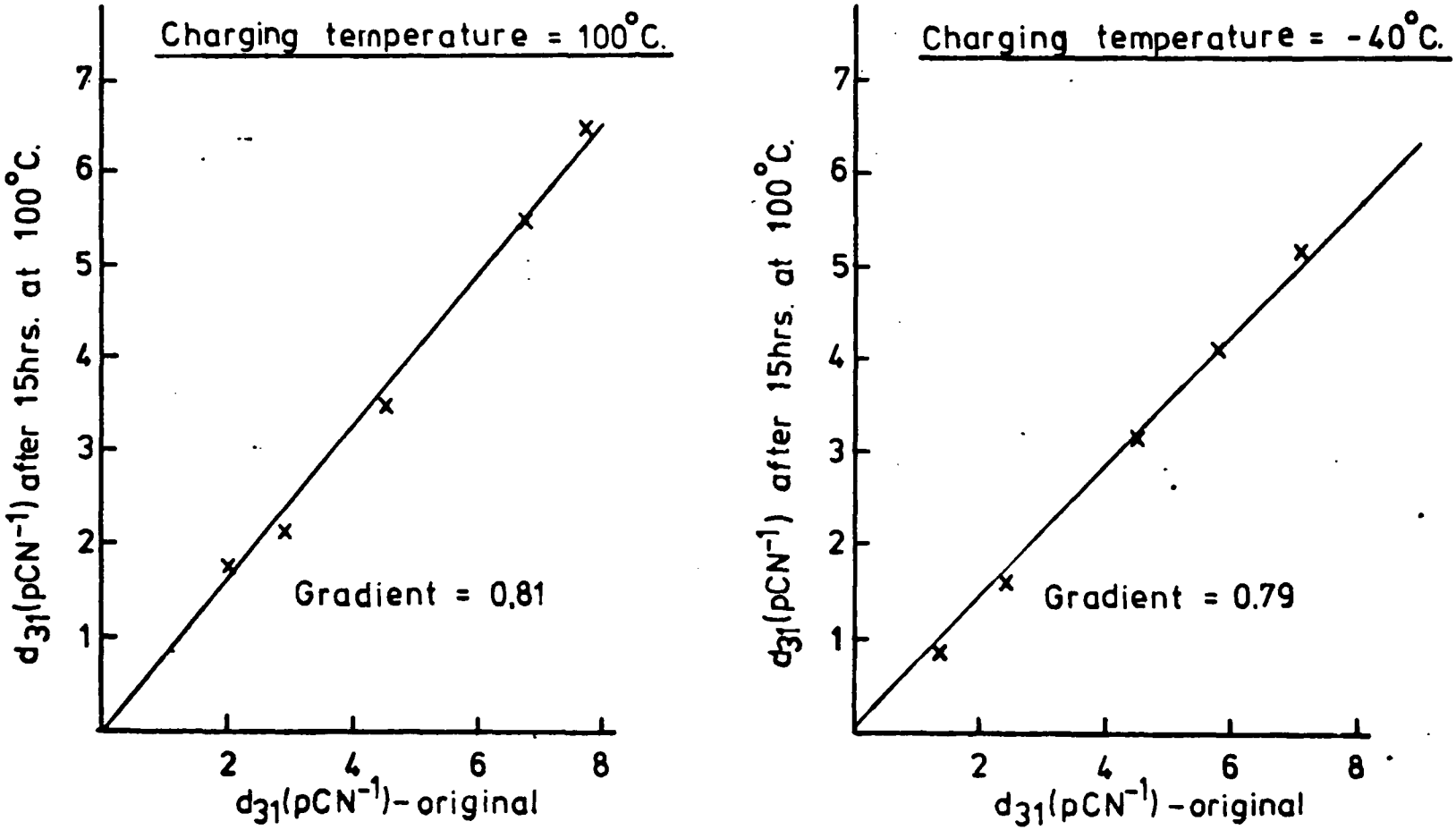

Fig. 13.

Effect on d_{31} of Conditioning at 100°C. for 15hrs. in the presence of (a) a D.C Voltage and (b) an A.C. Voltage. 25μm. thick Kureha samples corona charged at 20°C. for 5mins.

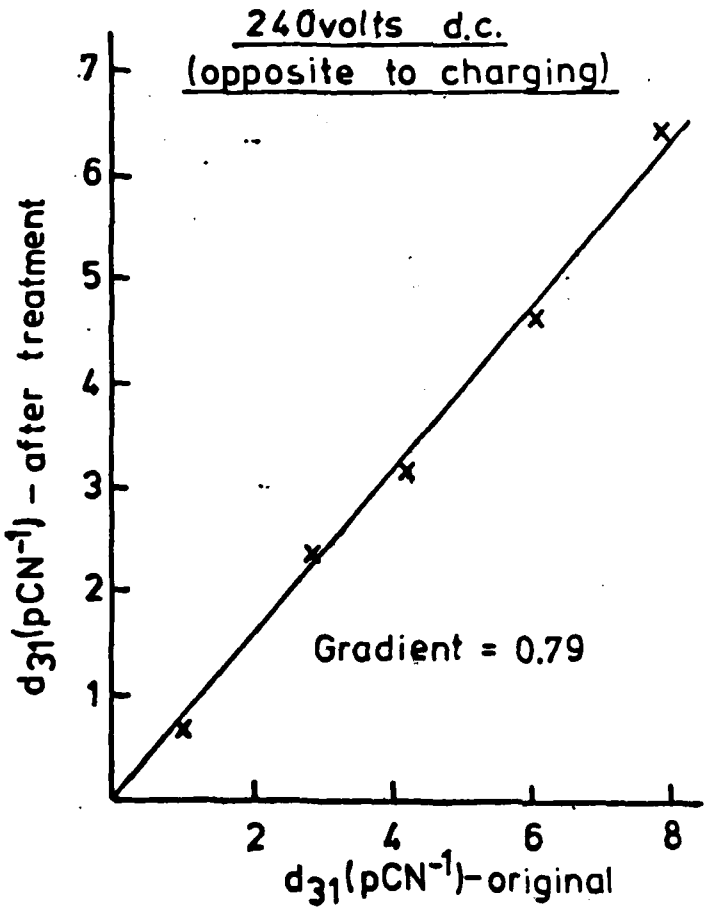

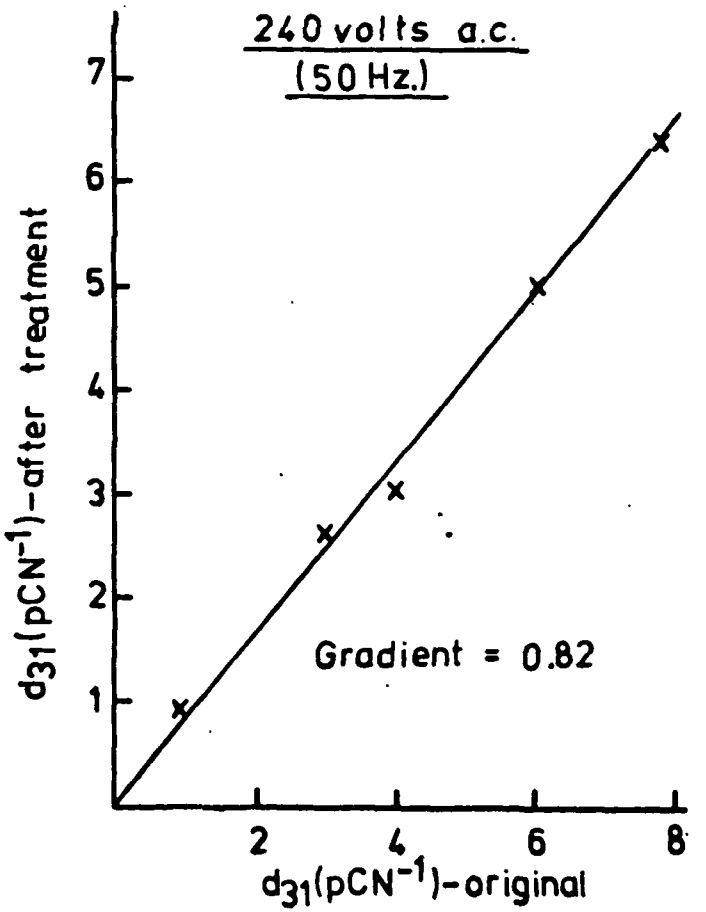

Fig. 14.

Effect on d_{31} of Conditioning at 60°C. for 15 hours in (a) Sea-water and (b) Distilled Water. 25 and 50μm. thick Kureha samples corona charged to various surface potentials at 20°C. for 5mins.

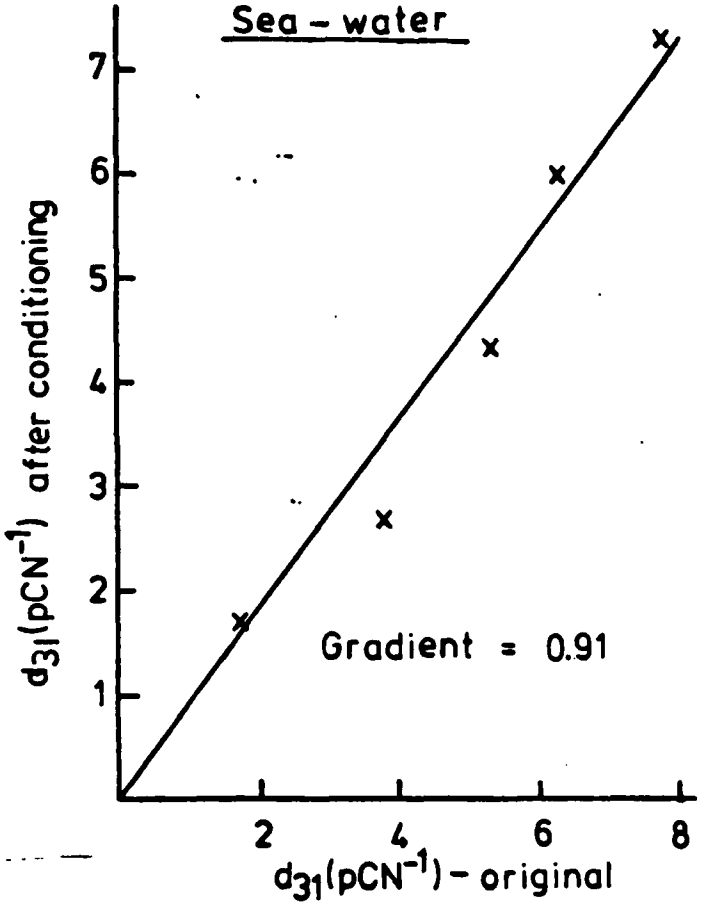

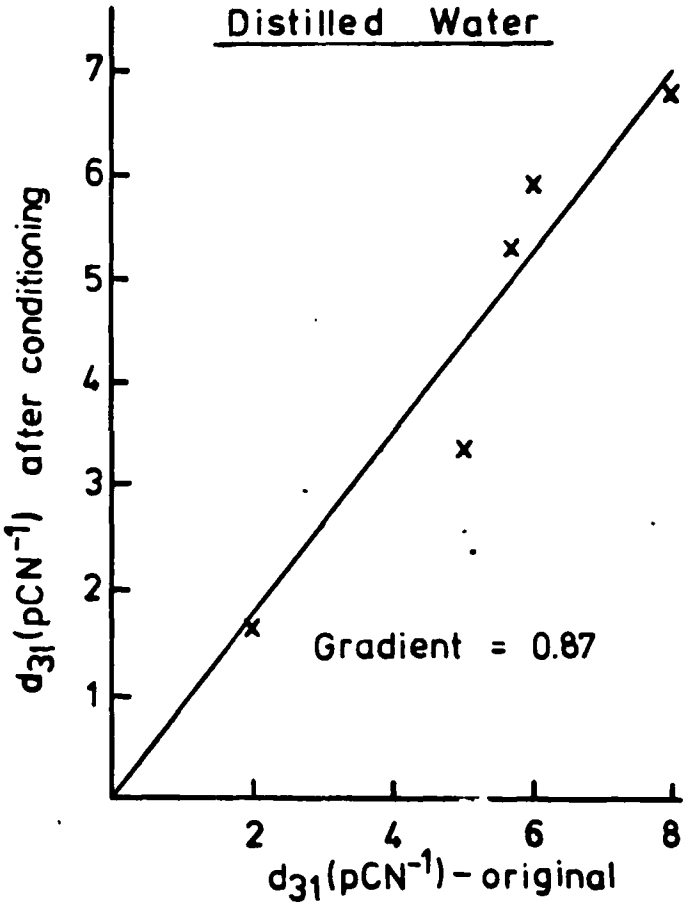

Fig. 15.

Normalised d_{31} v ageing time for sample of PVF_2 film poled under various conditions. 25μm sample

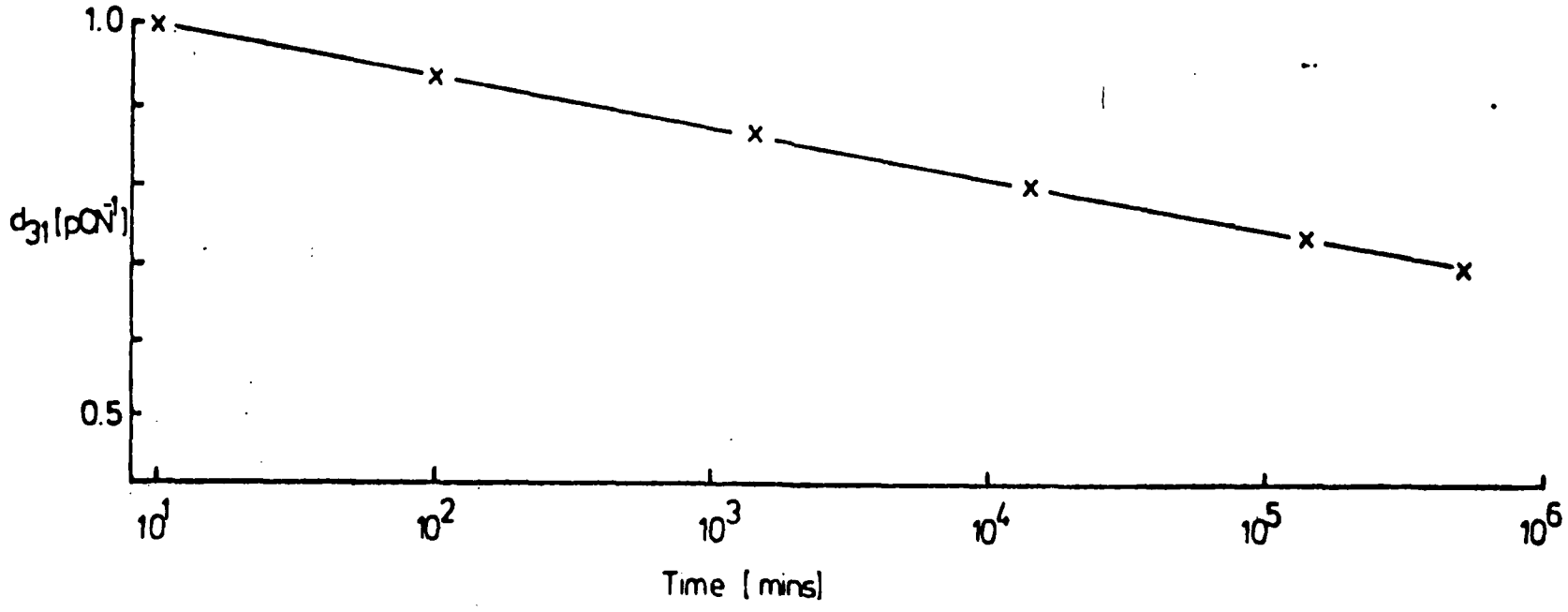

Fig. 16. Comparison of Bulk and Surface Changes in I.R. Absorption Band at 795cm^{-1} with Charging Voltage for Positive Corona

Charging for 5mins. at 20°C.

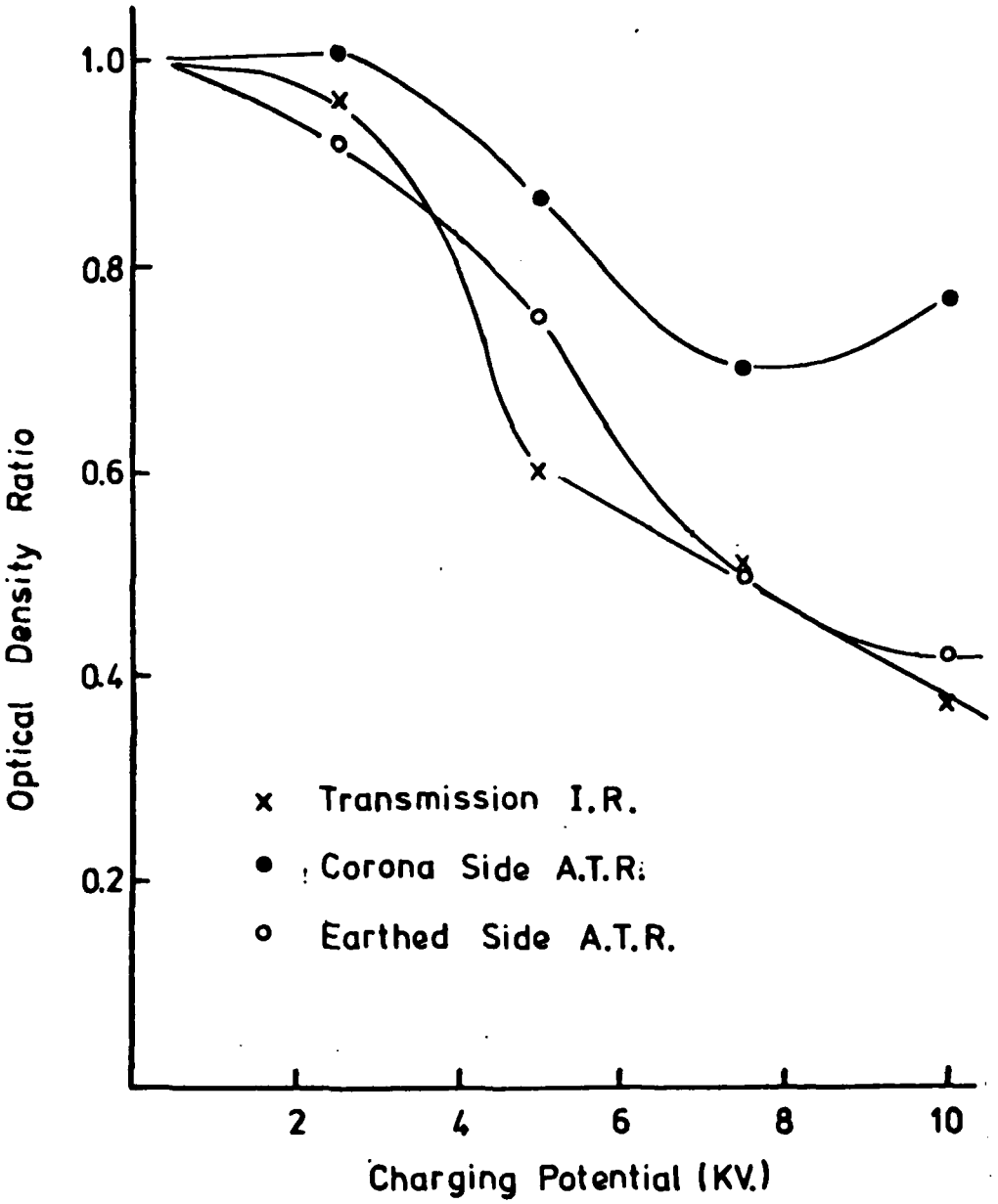

Fig. 17. Comparison of Bulk and Surface Changes in I.R. Absorption Band at 795cm^{-1} with Charging Voltage for Negative Corona

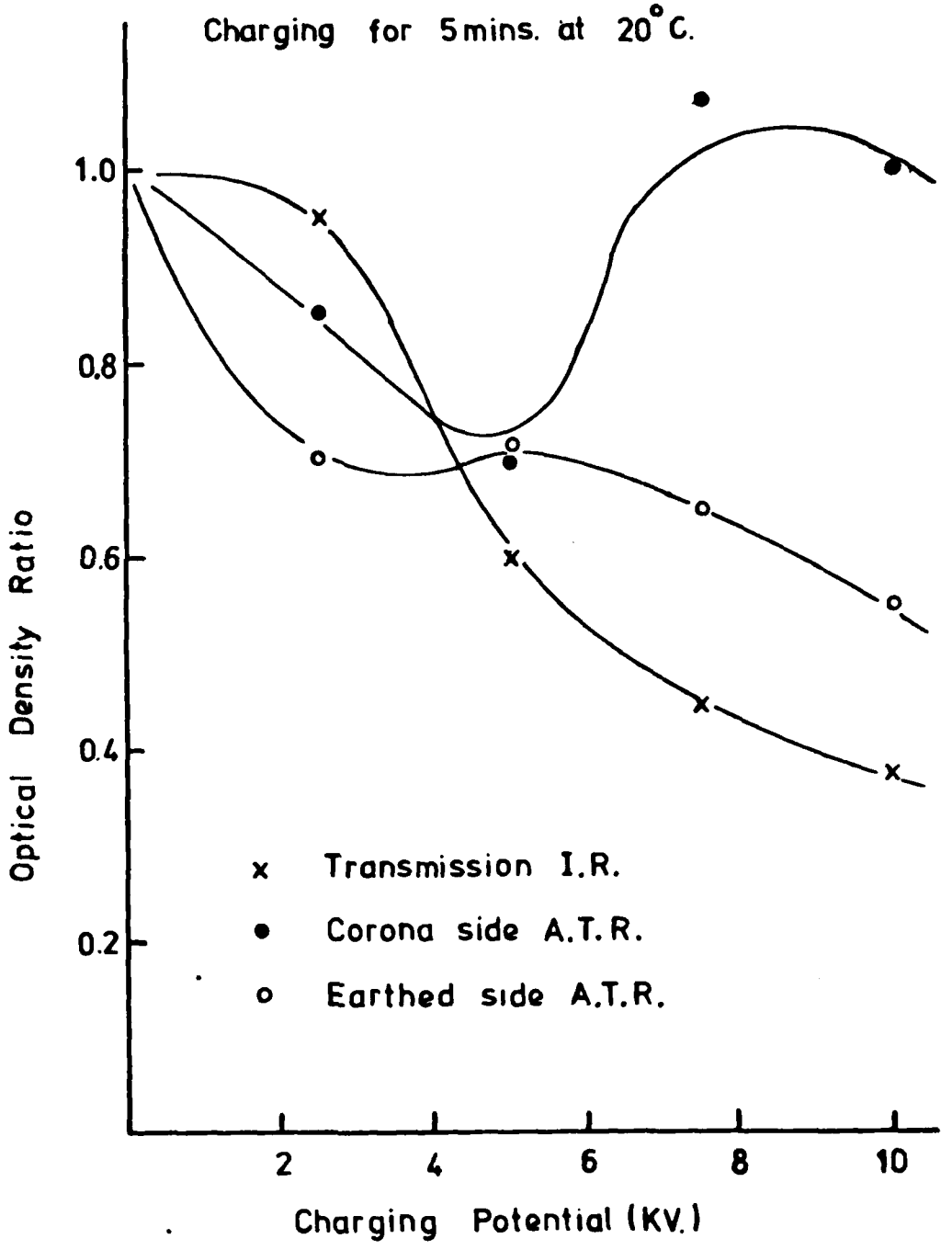

Fig. 18.

Time dependence of the charging currents for different applied potentials at 50°C.

25μm sample with aluminium electrodes.

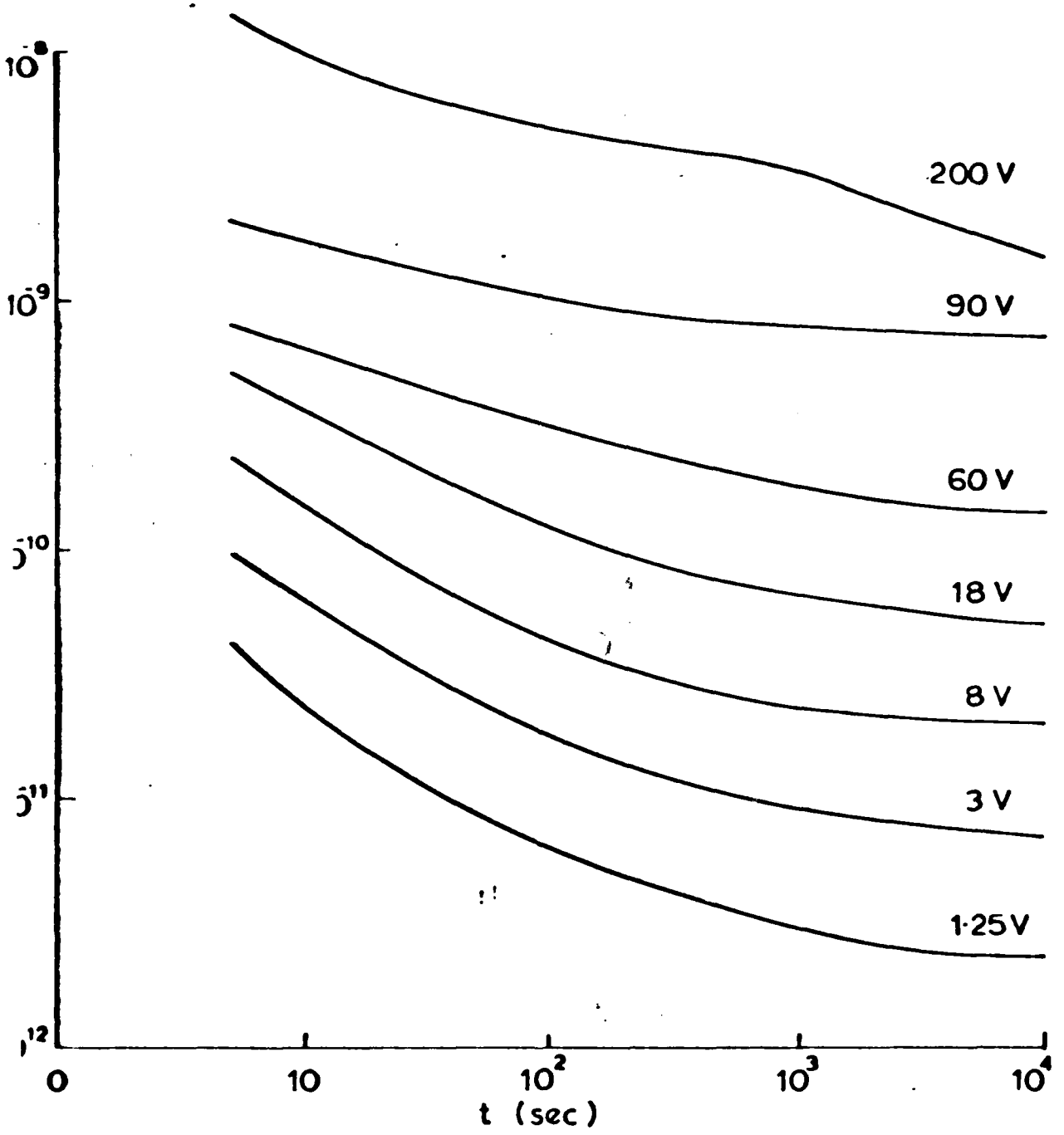

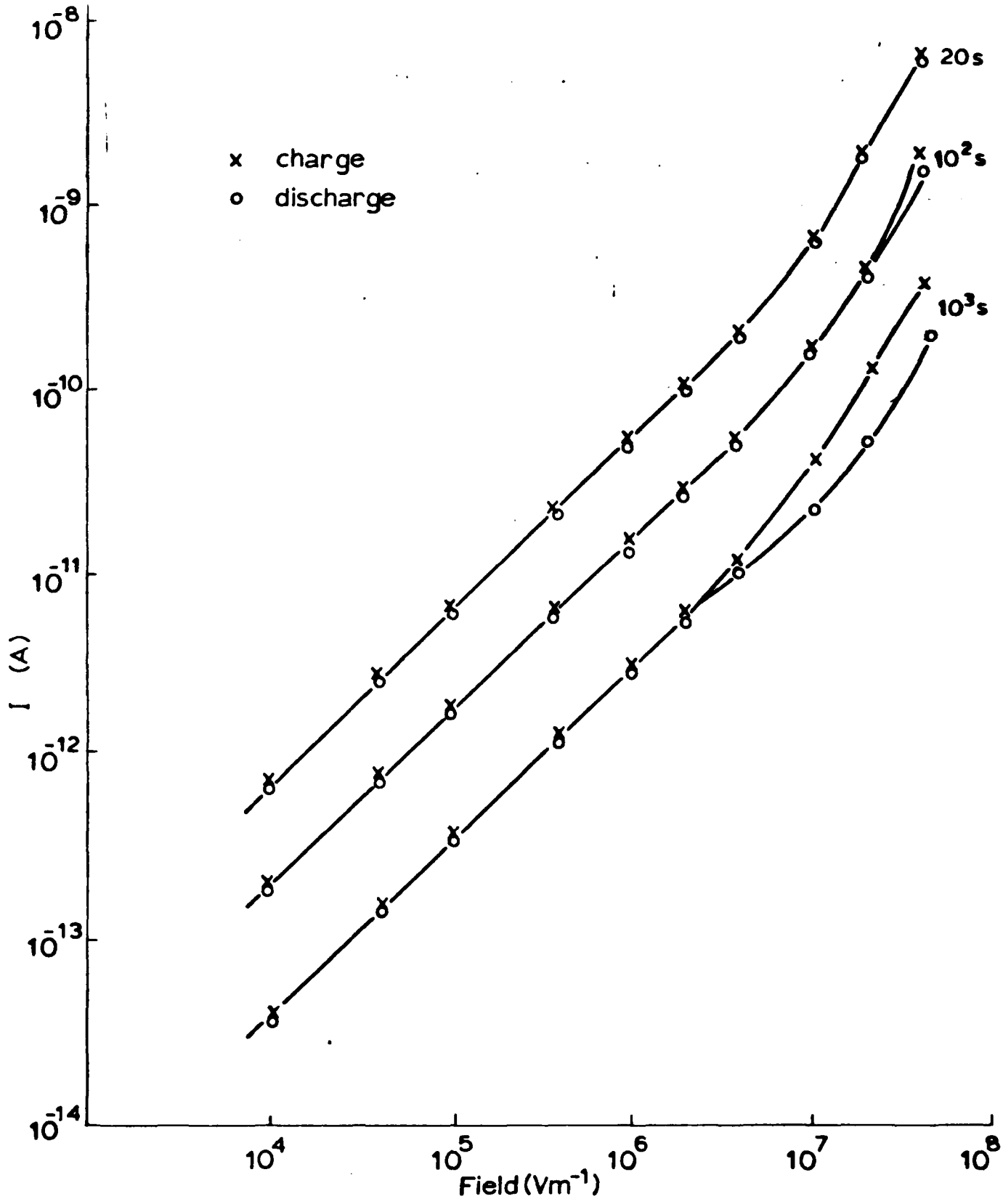

Fig. 19. Field dependence of the isochronal charging and discharging currents for a 25 μm sample with gold electrodes, at 313K.

Fig. 20.

Time dependence of the low field conduction current.

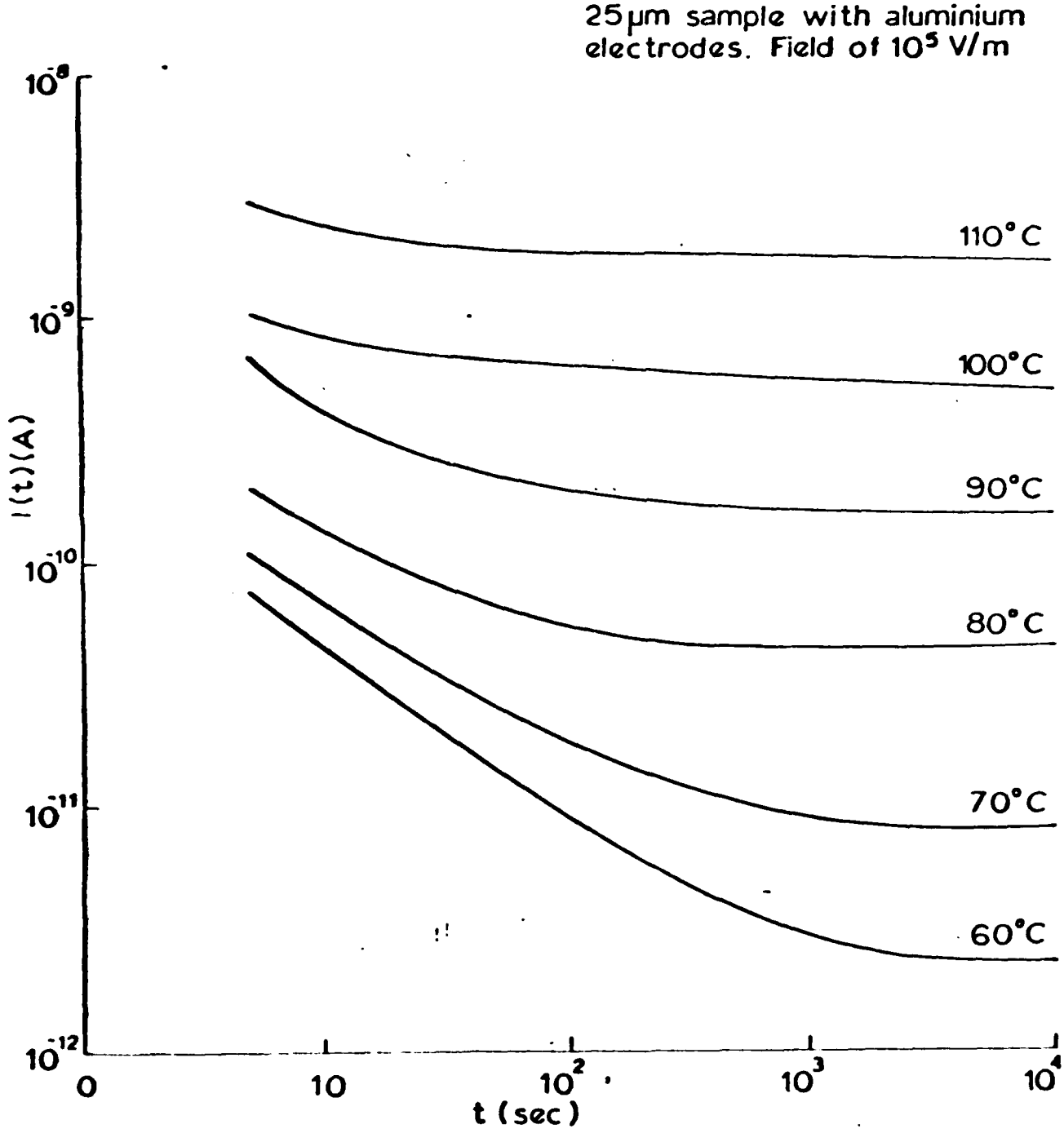

Fig. 21.
Effective Electron Mobilities in PVF_2 at 50 °C.
50 µm thick with gold electrodes

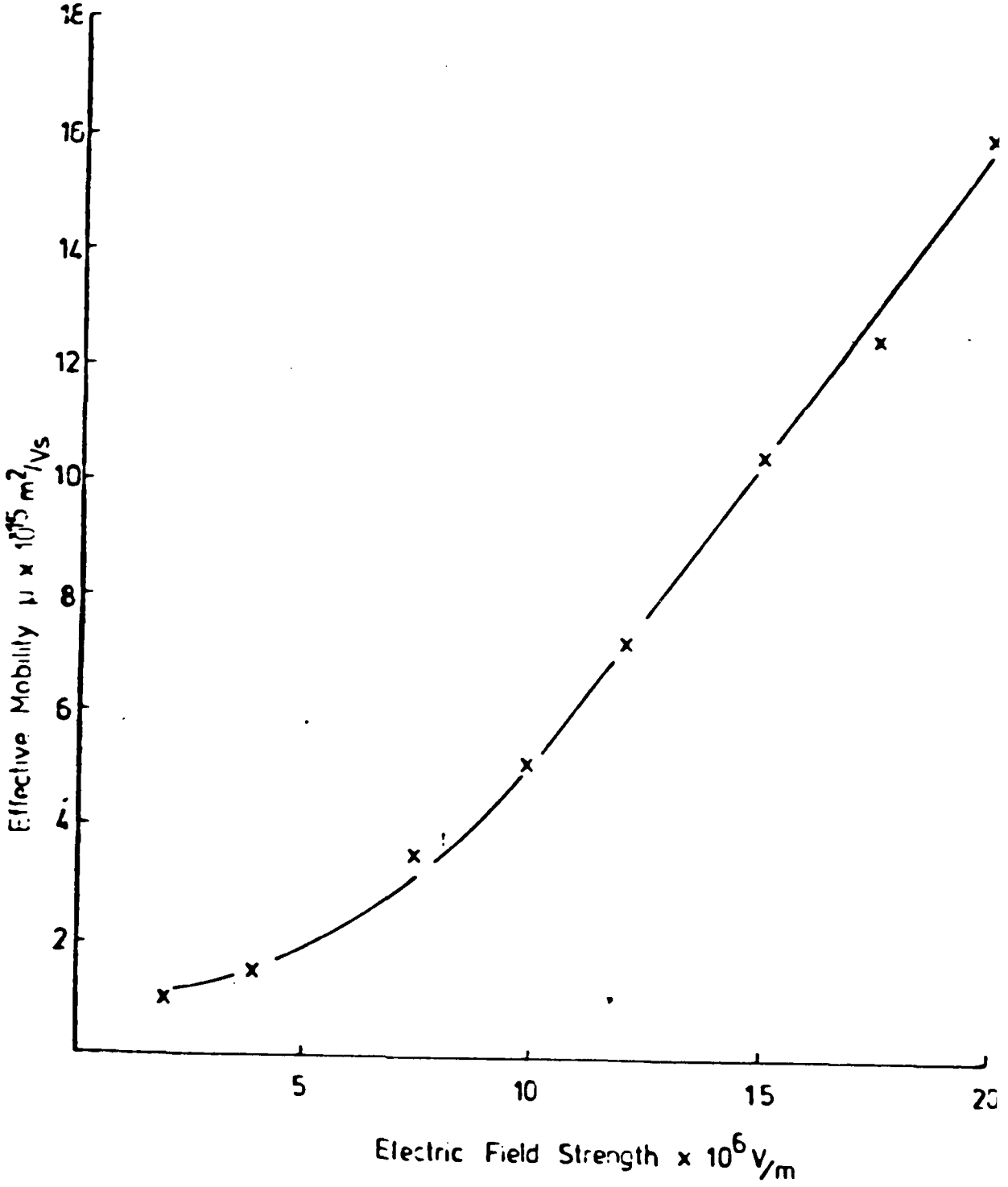

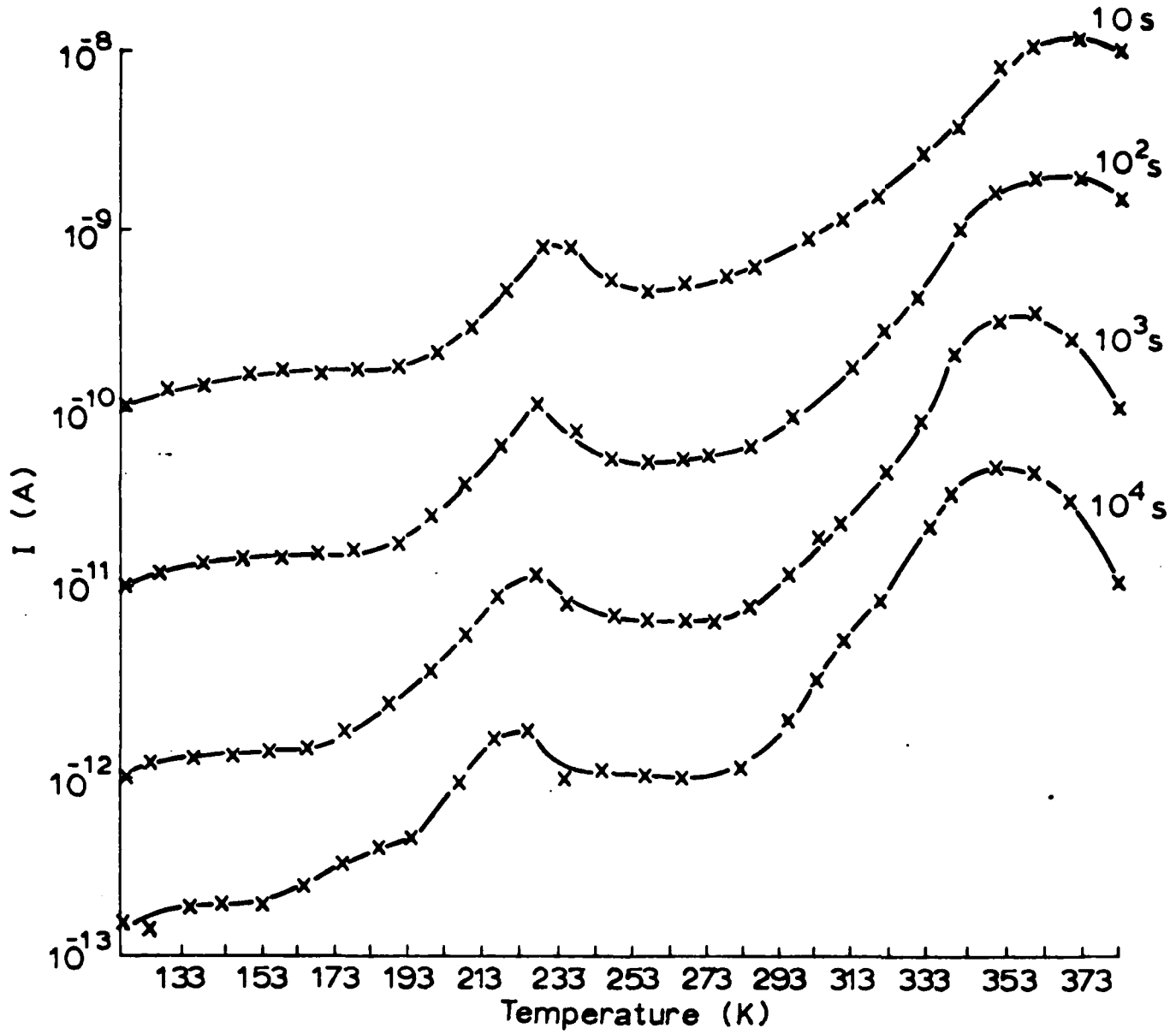

Fig. 22. Temperature dependence of the isochronal discharge currents (at prescribed times) field of $2 \times 10^7 Vm^{-1}$ 25 μm sample with gold electrodes

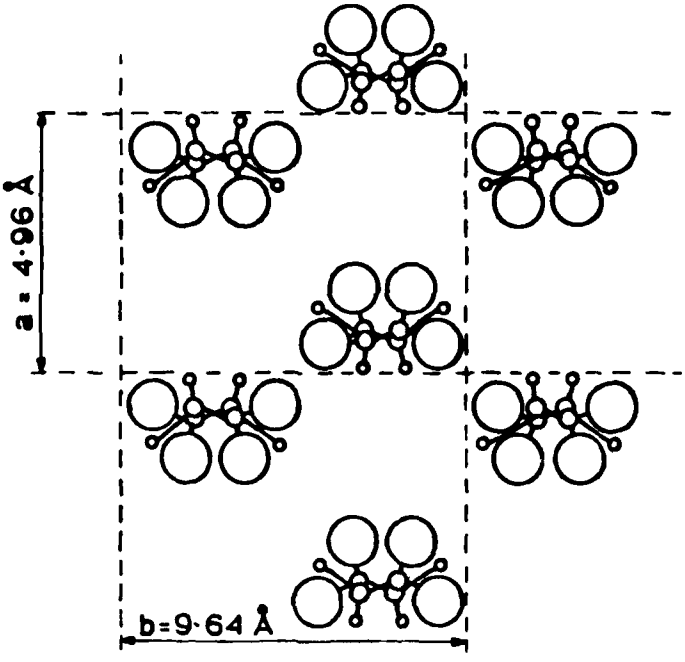

Fig. 23. Form II PVF_2 viewed along c-axis(along main chains)

○ = F : O = C : o = H :

Fig. 24. Suggested intermediate form after corona charging.

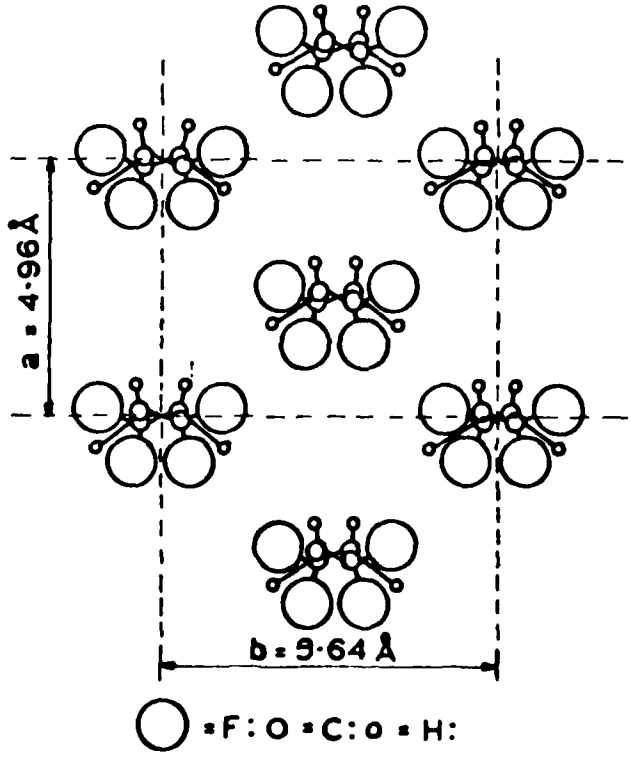

Fig. 25. Form I PVF_2 viewed along c-axis (along main chains)

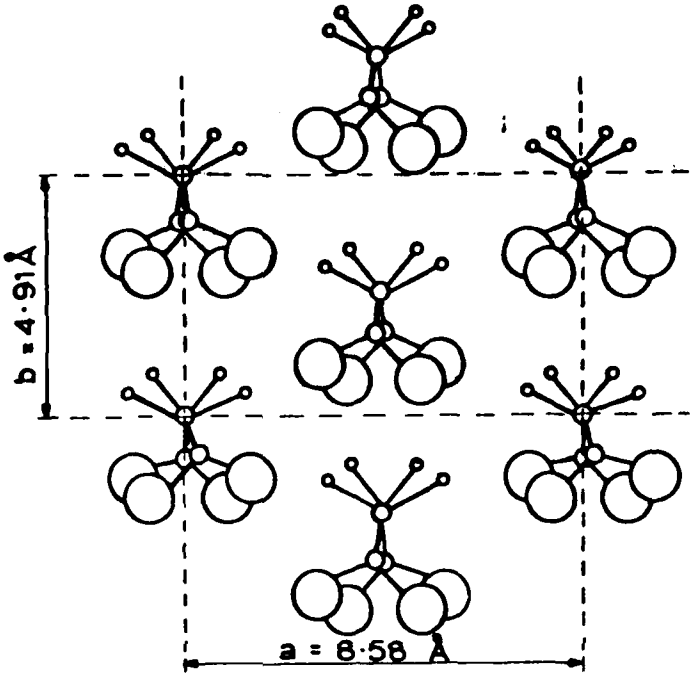

Table 1 : AN ILLUSTRATION OF NON-UNIFORMITY IN d_{31} WITH STACKED FILMS (CONVENTIONAL POLING)

Poling Temperature	Piezoelectric Coefficient d_{31}		
(^{o}C)	Sample 1 (+ve)	Sample 2	Sample 3 (-ve)
50	0.9	0.2	0.5
50	1.2	0.3	1.0
70	1.8	1.0	1.2
70	2.1	0.8	1.9
100	3.4	2.6	2.4
100	3.0	2.1	2.1

Table 2 : AN ILLUSTRATION OF NON-UNIFORMITY IN d_{31} WITH STACKED FILMS (CORONA POLING)

Surface Potential (KV)	Corona Polarity	Piezoelectric Coefficient d_{31}		
		No. 1 (corona)	No. 2	No. 3 (earth)
7	+ve	2	2	1.9
7	-ve	2.1	2.2	2.0
12	+ve	4.8	6.1	5.1
12	-ve	4.5	6.3	5.4

Table 3 : Summary of Absorption Current results.

Temperature Range (K)	Field Dependence of the Isochronal Current.	Temperature Dependence	Relationship between charging and discharging transients.	Time Dependence $I \propto t^{-n}$	Electrode Material Dependence	Thickness Dependence of the Isochronal current at constant field.
90 - 275	Proportional to E^v, where $v \approx 1$ for $E < 10^7$V/m and where $v > 1$ for $E > 10^7$V/m.	Thermally Activated	Mirror Images	$n \approx 1$	No detectable dependence	No detectable dependence
275 - 293	Proportional to E^v, where $v \approx 1$ for $E < 10^7$V/m and where $v > 1$ for $E > 10^7$V/m	Thermally Activated	Mirror Images only at shorter times and low fields.	$n < 1$	No detectable dependence	No detectable dependence

PUBLICATION A.

Journal of Electrostatics, 7 (1979) 267–282

A STUDY OF STRUCTURAL AND ELECTRICAL PROPERTIES OF STRETCHED POLYVINYLIDENE FLUORIDE FILMS

D. K. DAS-GUPTA, K. DOUGHTY and D. B. SHIER
School of Electronic Engineering Science, University College of North Wales, Dean Street, Bangor, Gwynedd, LL57 1UT (UNITED KINGDOM)

ABSTRACT

X-ray diffraction profiles and piezoelectric strain coefficient d_{31} of 50μm thick polyvinylidene fluoride (PVF_2) films, originally containing non-polar Form 2 type crystallites, have been studied after (i) corona poling (ii) uniaxial stretching and (iii) uniaxial stretching and corona poling. The results suggest that piezoelectricity in this material is of dipolar origin. Furthermore a study of the changes in birefringence and small angle light scattering (SALS) patterns have also been made in the present work. The results indicate that the major contribution to the observed orientation on uniaxial stretching originates from the crystalline region of the polymer.

1. INTRODUCTION

Polyvinylidene fluoride (PVF_2) can be made to exhibit piezo- and pyroelectric responses significantly greater than those of other polymers after suitable poling. The conventional poling procedure is to subject the polymer to a very high electrical stress at an elevated temperature for an extended period of time and then to reduce the temperature of the specimen to $\sim 20^{\circ}C$ (i.e. room temperature) without removing the external field. PVF_2 may exist at least in two stable polymorphs. In Form 1 (β-form) polar structure, the molecules have a planar zig-zag conformation and the orthorhombic unit cell with two polymer chains has the space group $Cm2m(C_{2V}^{14})$, the lattice constants being a = 8.58Å, b = 4.91Å and c (i.e. chain axis) = 2.56Å (Fig. 1), (ref. 1, 2). In the Form 1 structure the dipole moments of the monomer units ($-CH_2-CF_2-$) are all aligned parallel to each other, the magnitude of the dipole moment for each monomer unit being 7.0×10^{-30} C-m (ref. 3). Assuming a rigid dipolar model the spontaneous polarization of a single crystal of the Form 1 type PVF_2 will be 0.13 $C\text{-}m^{-2}$ (ref. 4) and it will exhibit piezoelectricity without any external poling. Form 2 crystallites (α-form) have a space group $P_{21}/C(C_{2h}^{5})$ with a primitive monoclinic unit cell structure with the lattice

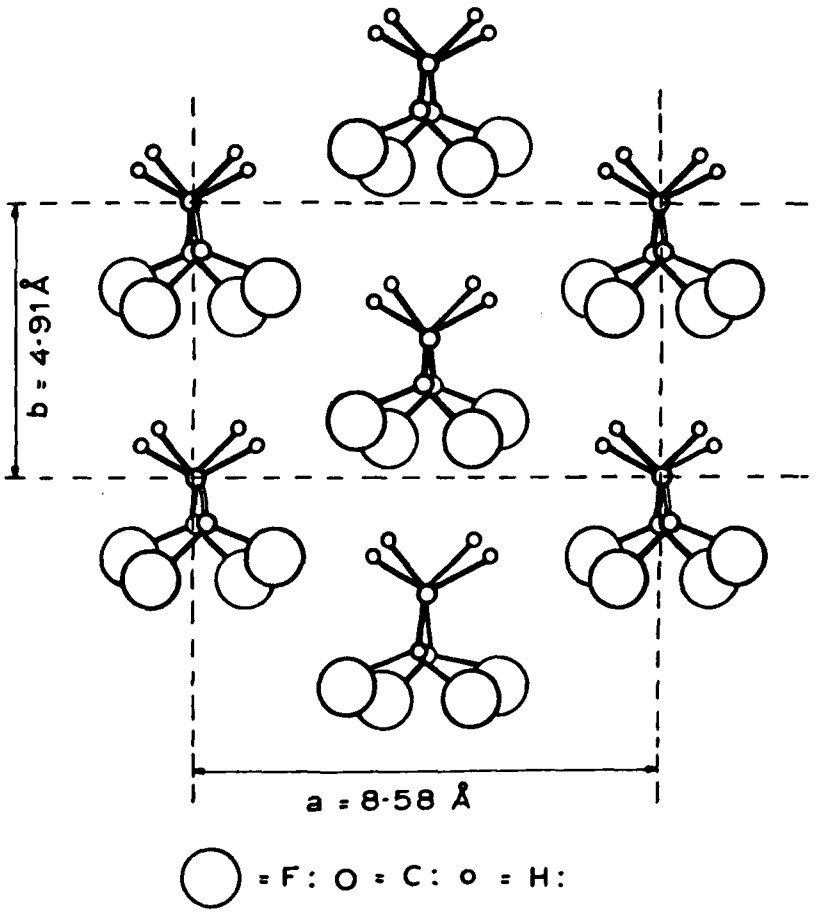

Fig. 1. Form 1 PVF_2 viewed along c-axis (along main chains).

parameters (see Fig. 2) a = 4.96Å, b = 9.64Å, c = 4.62Å and β = 90° (ref. 2). Although each molecular chain with T-G-T-G' conformation of the Form 2 structure has a dipole moment normal to the chain axis, however, the adjacent chains pack with their dipoles in an anti-polar array. As a result, the unit cell of Form 2 structure has no nett dipole moment along the b-axis. Thus PVF_2 films of Form 2

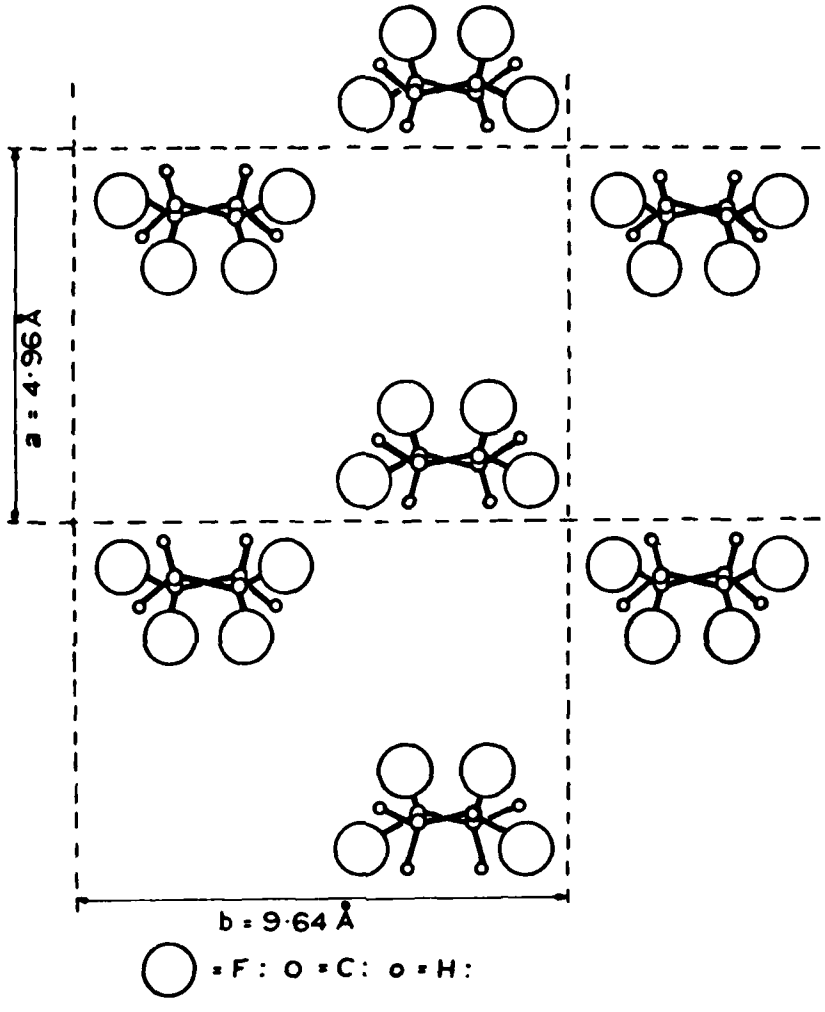

Fig. 2. Form 2 PVF_2 viewed along c-axis (along main chains).

structure may not be expected to be piezoelectric. The Form 2 crystallites may be transformed into Form 1 type crystallites on uniaxial stretching of PVF_2 films at a temperature ~60°C. However, the piezoelectric response of such stretched films will be negligible without subsequent poling. A conversion from Form 2 into Form 1

type of crystallites has also been reported with corona charging of PVF_2 films originally containing both the forms (ref. 5, 6). Murayama et al (ref. 7) show that in PVF_2 films containing both forms of crystallites, the piezoelectric response increases with increasing Form 1 content. Wada and Hayakawa (ref. 4) suggest that the piezo- and pyroelectricity in PVF_2 may be due to one of the following mechanisms, (i) strain and temperature dependence of spontaneous polarization (i.e. a dipolar model) and (ii) heterogeneity and embedded charges in the bulk of the polymer. Due to the symmetry properties of the point group mm2 for the uniaxially stretched and poled PVF_2 films the non-zero tensor elements of the piezoelectric strain coefficients (ref. 8) are $+d_{15}$, $+d_{24}$, $+d_{31}$, $+d_{32}$ and $-d_{33}$, where the first and second subscripts refer to the direction coordinates of polarization and stress respectively. It may be noted that Ohigashi (ref. 9) has shown that a large piezoelectric strain coefficient d_{33} may be obtained by poling PVF_2 films containing mostly the nonpolar Form 2 crystallites. This observation apparently suggests that the dipolar orientation may not be the origin of piezoelectricity in PVF_2. On the other hand, the observations of the hysteresis loop with the piezo- and pyroelectric coefficients in PVF_2 under the d.c. bias fields (refs. 10-13) with reproducible residual polarization (refs. 4, 14) would tend to favour the dipolar model. There is thus, as yet, no definitive knowledge of the nature and origin of piezo- and pyroelectricity in PVF_2.

Present work reports the results of a study of structural changes and the behaviour of the piezoelectric strain coefficient d_{31} on (i) drawing, (ii) poling (conventional and corona charging), and (iii) drawing and corona charging PVF_2 films, originally containing mostly Form 2 crystallites. X-ray diffraction method and observations of changes in birefringence and Small Angle Light Scattering (SALS) patterns were used for structural studies in this work. All measurements were carried out with 50μm thick films of PVF_2 which were kindly provided by Kureha Chemical Industries Company Limited of Japan.

2. EXPERIMENTAL

PVF_2 films were uniaxially stretched at 60°C and subsequently annealed at 120°C to prevent shrinkage. Aluminium electrodes were then vacuum deposited on one surface of the samples. The metallised surface was earthed and positive corona charges were deposited on the non-metallised surface of the polymer from a corona point which was connected to a stabilised EHT supply, the surface potential being monitored by a Field-Mill type electrostatic voltmeter. A micromesh control grid, connected to a separate EHT supply and maintained at 3KV potential below that of the corona point was introduced between the non-metallised polymer surface and the corona point to obtain a uniform charging. The potential at the surface of the polymer was observed to reach the desired values, in all cases, in a time not exceeding 10 seconds. After completion of poling the non-metallised surface of the polymer was earthed temporarily.

X-ray diffraction patterns were obtained using a step-scanning technique with Ni-filtered Cu-Kα radiation of wavelength 1.54Å and a Philips X-ray diffractometer (Model PW1050). The evaporated aluminium electrodes on one of the surfaces of the polymer was used as an internal standard and the uncertainty in the observed value of 2θ-position, where θ is the Bragg angle, was less than 0.1°. X-ray diffraction patterns were obtained for (i) uncharged PVF_2 films, (ii) after (positive) corona charging at different surface potentials, up to a maximum of 15KV, (iii) with increasing stretch ratios, not exceeding 180% and (iv) with stretched and corona charged specimens.

A second aluminium electrode was then evaporated on the other surface of the poled samples following the diffraction measurement. The electrodes of each sample were then short circuited again for fifteen hours. The piezoelectric strain coefficient d_{31} was subsequently obtained by measuring the open circuit voltage developed across a standard mica capacitor, which was connected in parallel with the specimen, using a conventional static method of releasing a fixed weight. A standard weight, attached to the specimen, was released by using an electro-pneumatic solenoidal valve. The open circuit voltage developed by the piezoelectric charge was monitored with a Tektronix Storage Oscilloscope (Model 549 with 1A7 amplifier).

A He-Ne laser beam was employed for studying changes in birefringence and SALS (small angle light scattering) patterns as a function of stretch ratio. The total birefringence Δ was determined by the Senarmont method (ref. 15) which utilises an analyser quarter wave plate between crossed polarizers in the H_v mode. The laser beam was spatially cleaned (see Fig. 3) by locating a small pinhole of 6μm diameter

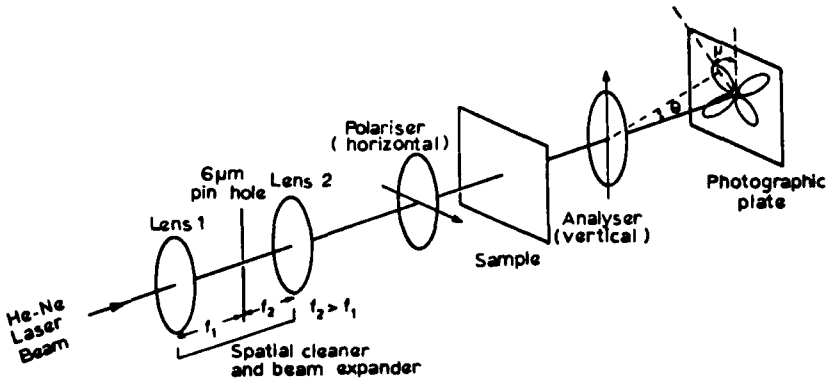

Fig. 3. The experimental arrangement to obtain light scattering patterns in the H_v mode (cross polarizers).

at the focal plane of a bi-convex lens. Using a second bi-convex lens of a suitable focal length, a collimated beam of 6mm diameter was then obtained. The experimental arrangement for obtaining the SALS pattern was similar to that of Stein and Rhodes (ref. 16) and is shown schematically in Fig. 3.

3. RESULTS

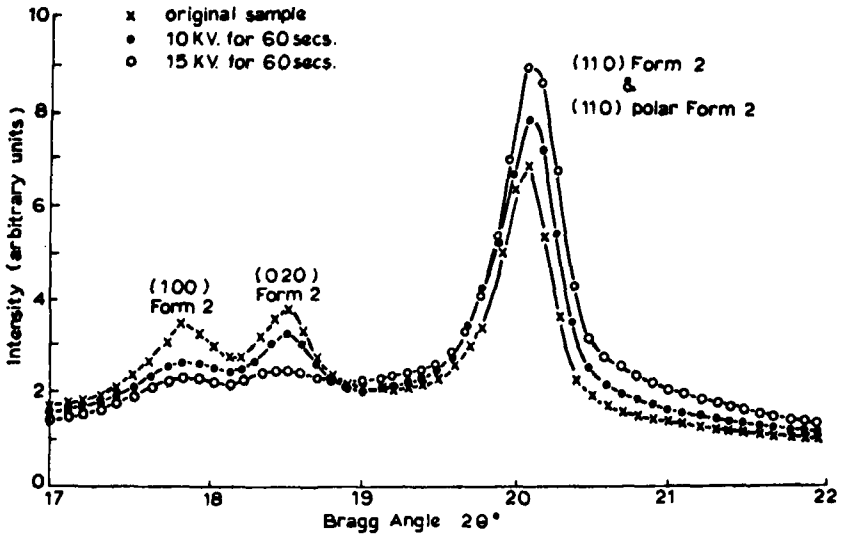

Fig. 4. X-ray diffraction patterns of (50μm) PVF_2 poled at 20°C (unstretched).

Figure 4 shows a typical set of X-ray diffraction profiles of the corona charged (i.e. poled) polymer at surface potentials of 10 and 15KV. A diffraction pattern of the unpoled polymer is also superimposed in Fig. 4 for the sake of comparison. Fig. 5 shows the behaviour of the piezoelectric strain coefficient d_{31} with the poling field (corona poling). The diffraction patterns of the stretched (185% stretch ratio) and stretched and poled specimen are shown in Fig. 7. The variation of d_{31} with stretched and corona charged specimen with the stretch ratio is shown in Fig. 8. Figs. 9 and 10 show the changes in birefringence and the SALS patterns respectively with different stretch ratios.

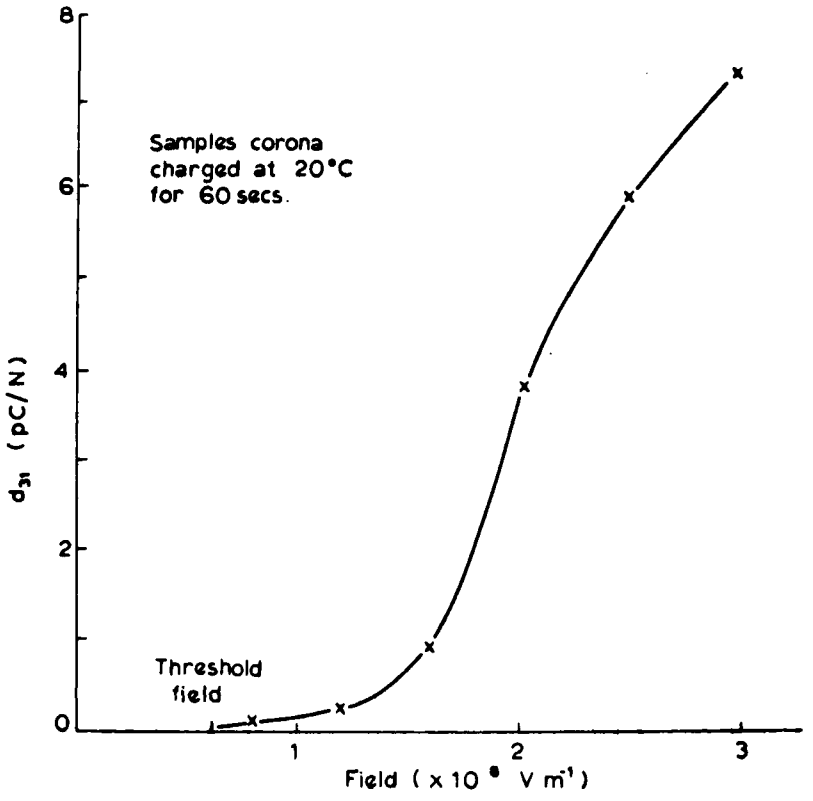

Fig. 5. Piezoelectricity as a function of field for (50μm) PVF_2 originally completely in the Form 2 type structure.

4. DISCUSSION

The diffraction profile of unstretched and unpoled PVF_2 film, containing mostly Form 2 crystallite and shown in Fig. 4, is in good agreement with Hasegawa et al (ref. 2). It may be observed from Fig. 4 that the peak values of the diffracted intensities of the Form 2 structural planes (100) and (020) become vanishingly small with corona charging. Furthermore, the peak intensity of the Form 2 (110) plane increases with the increasing poling field (Fig. 4). Das-Gupta and Doughty (ref. 7) have shown that similar changes in the diffraction patterns also occur on corona poling of PVF_2 films containing both Form 1 and Form 2 crystallites. However, it may be observed from Fig. 4 that even with the very high poling field of $3 \times 10^{8} Vm^{-1}$ (i.e., 15KV case) there is no apparent evidence of a transformation

from Form 2 (non-polar) crystallite to a polar Form 1 structure. At the same time it may be observed from Fig. 5 a very significant enhancement of the magnitude of d_{31} occurs on corona poling of PVF_2 films of Form 2 structure, reaching a value of $>7x10^{-12}CN^{-1}$ at a poling field of $3x10^{8}Vm^{-1}$. It has been stated above that using a dipolar model an antipolar unit cell of Form 2 structure may not give rise to piezoelectricity. Furthermore, the depolarization current studies in PVF_2 with respect to the variable parameters, viz. poling fields, time, temperature, electrode thickness and electrode materials indicate (ref. 18) no significant evidence of charge injection from the electrodes leading to space charge formation in the bulk of the polymer at such high fields. Therefore, in view of the observed results in Figs. 4 and 5, a structural transformation of the non-polar form to an intermediate polar form without any alteration of the lattice dimensions of the Form 2 structure must occur on corona poling in PVF_2 films, originally containing mostly Form 2 crystallites. Such a conversion to an intermediate polar form but stillmaintaining the T-G-T-G' conformation of the molecular chain may occur on poling by only a rotation of the alternate molecular chains about c-axis through 180^{o}, which is illustrated in Fig. 6. The stability of this intermediate polar form, which is in agreement with Das-Gupta and Doughty (ref. 17) with the lattice dimensions of the Form 2 unit cell structure would not violate the conditions required for the minimum potential energy (ref. 19, 20). Such a model will also explain the observed reduction of the reflection-diffraction patterns of the Form 2 (100) and (020) planes. Davis et al (ref. 20) also add that at still higher fields $\sim 5x10^{8}Vm^{-1}$ a conformational change may occur in which the intermediate polar Form 2 crystallites are finally converted to the polar zig-zag type Form 1 crystallites. This is also in agreement with Das-Gupta and Doughty (ref. 17).

On uniaxial stretching (180% stretched ratio) as expected, a molecular conformational change occurs in the polymer, giving rise to a Form 1 type of structure which may be evidenced in Fig. 7 by the (i) presence of the dominant (110)/(200) composite peak and (ii) the absence of the Former Form 2 (110) peak. On corona charging of the stretched film the composite (110)/(200) peak of the Form 1 type structure was observed to be further enhanded (Fig. 7). Even after such a conformational change due to uniaxial stretching, the magnitude of d_{31} of unpoled specimens was found to be insignificant in comparison with that of stretched and poled specimens for which a value as high as $\sim 15x10^{-12}CN^{-1}$ (see Fig. 8) was observed at 180% stretch ratio and with a poling (corona charge) field of $2x10^{8}Vm^{-1}$. This may be attributed to the fact that although the process of uniaxial stretching results in an orientation of the c-axis of the crystalline region parallel to the stretch direction, however, due to the orthorhombic symmetry of the unit cell, the rotation of the unit cell axes can be accomplished in six possible variations (i.e., 60^{o} increments) without disruption of the polymer morphology (ref. 21). Hence the uniaxial stretching produces only a conformational

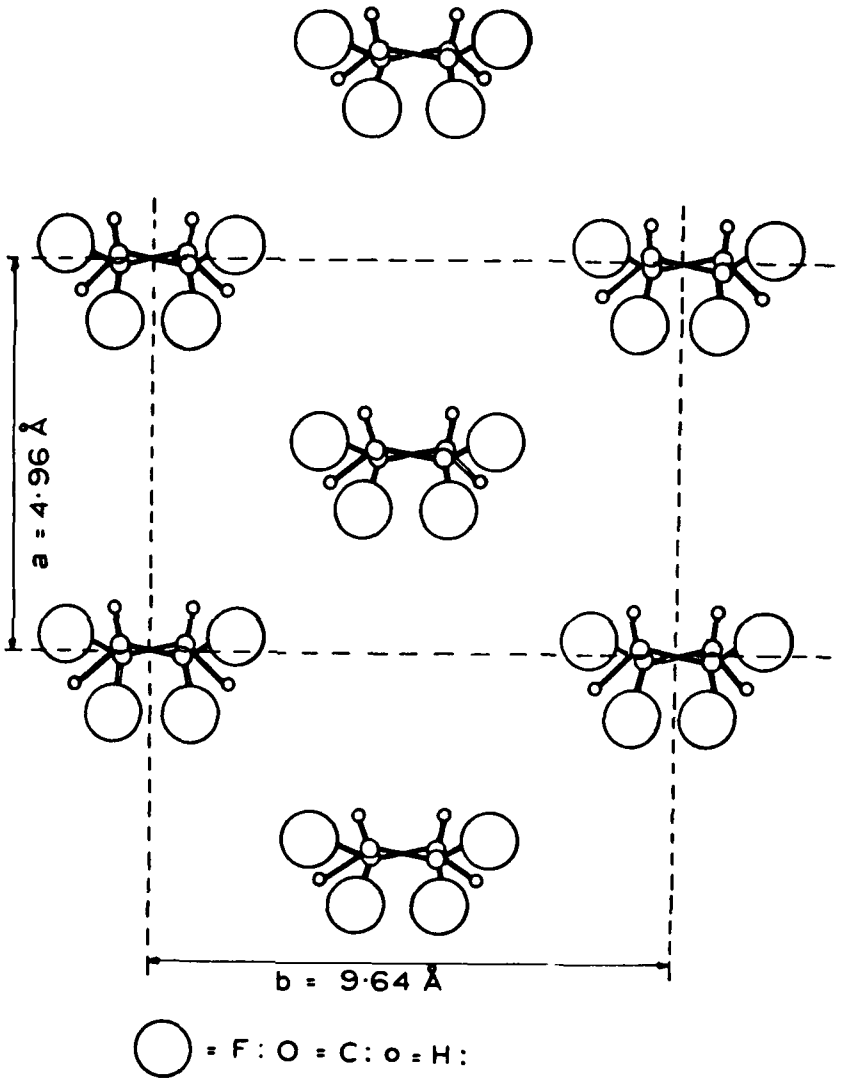

Fig. 6. Suggested intermediate form after corona charging.

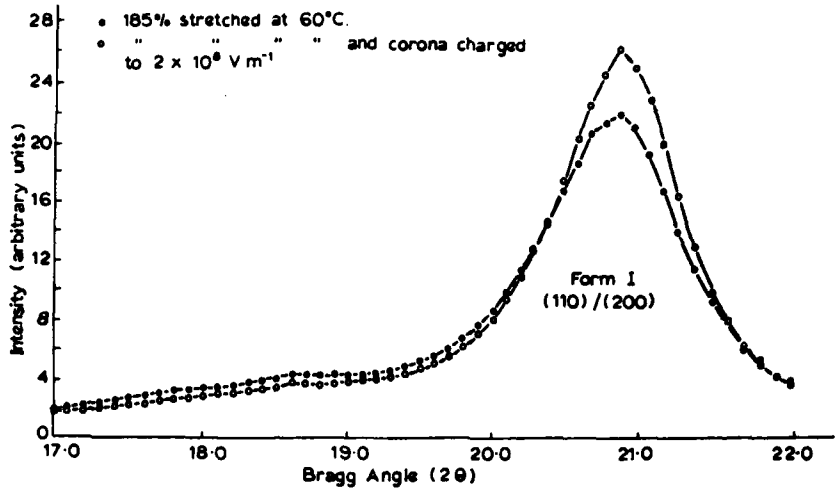

Fig. 7. X-ray diffraction patterns of (50μm) PVF_2 stretched and corona charged.

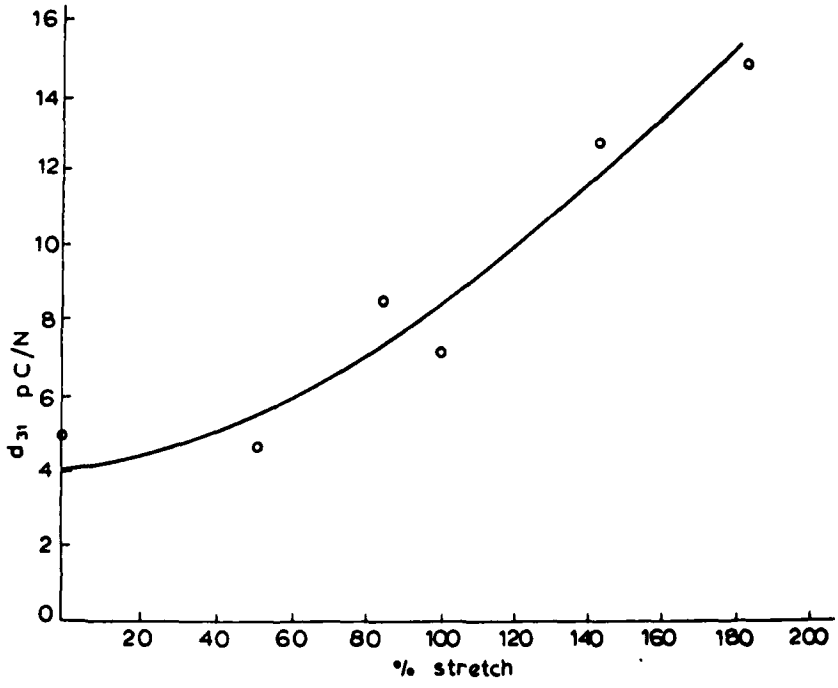

Fig. 8. Piezoelectric strain coefficient d_{31}, of corona charged ($2x10^8 Vm^{-1}$) PVF_2 with different stretch ratios.

change from Form 2 type of crystallites to Form 1 type in which the crystallites are oriented at random rotational angles about the c-axis, giving no nett dipole moment. The dipole moments can, however, be oriented at an angle with respect to the electric field during the poling process. It should also be pointed out that a significantly higher value of d_{31} may be obtained by corona charging an uniaxially stretched sample than by corona charging an unstretched sample, e.g.

d_{31} (180% stretch and $2\times10^{8}Vm^{-1}$ corona field) = $15\times10^{-12}CN^{-1}$

d_{31} ($3\times10^{8}Vm^{-1}$ corona field) = $7\times10^{-12}CN^{-1}$

In view of the changes in the X-ray diffraction pattern of the unstretched sample with corona charging (Fig. 4) and, in particular, the differences from the diffraction pattern of the stretched samples (Fig. 7), it may be suggested that the induced piezoelectricity in the unstretched film (Form 2 crystallites) after corona charging at fields up to $3\times10^{8}V/m$ is due to a new polar crystalline form. This may be produced by a cooperative rotation of alternate polymer chains about the c-axis which produces a stable polar form whilst maintaining the T-G-T-G' molecular conformation and the lattice parameters of the Form 2 crystallites. At fields higher than $3\times10^{8}Vm^{-1}$ there is a progressive conversion of the Form 2 crystallites into the Form 1 type of structure with the zig-zag molecular conformation (ref. 17, 20). On the other hand, on uniaxial stretching of the polymer there is a direct conversion of the crystallites from the Form 2 structure to that of Form 1 with randomly oriented dipole moments. On subsequent poling the dipoles align, of course, at a particular angle with the direction of the poling field. The dominant mechanism of piezoelectricity in this polymer remains, however, of dipolar origin.

In the discussion so far, it has been assumed that the dipolar orientations only in the crystalline region contribute to piezoelectricity in PVF_2. It has been suggested (ref. 22) that a dipolar alignment may be strongly influenced by the segmental motions in the amorphous regions in a semicrystalline polymer such as PVF_2. Generally, crystalline polymers are volume filled with spherulites consisting of branched crystalline lamellae of folded chain crystals propagating from their centres (ref. 23). The amorphous regions reside within these spherulites in the interlamellar areas. Such polymers deform on elongation when the spherulites change from the spherical into ellipsoidal shapes. This results in a change in the interlamellar spacing which leads to orientation of the amorphous material between the lamellae. Now, the birefringence of a semicrystalline polymer provides useful information of the preferred overall orientation of the crystallites in both the crystalline and amorphous regions. The birefringence change occurring in an anisotropic polymer upon elongation may be separated into crystalline and amorphous contributions using the following equation (ref. 24),

$$\Delta = X_{c,v}\Delta_c + (1 - X_{c,v})\,\Delta_a + \Delta_f \qquad \ldots\ldots \quad (1)$$

where $X_{c,v}$ is the volume fraction of crystalline polymer and Δ the total birefringence change; the subscripts c, a and f refer to crystalline, amorphous and the form birefringence respectively. The magnitude of Δ_f is usually small enough to be ignored. Δ_c and Δ_a may also be expressed in terms of orientation functions of the crystallites (ref. 24) which may be determined either by appropriate X-ray measurements or by small angle light scattering (SALS) analysis (ref. 16, 25-27). Thus, by combining the results of the birefringence and light scattering analysis, the respective contributions of the crystalline and amorphous phases to the total birefringence can be determined. The results of the birefringence measurements on elongation up to a stretch ratio 350%, shown in Fig. 9, are in good agreement

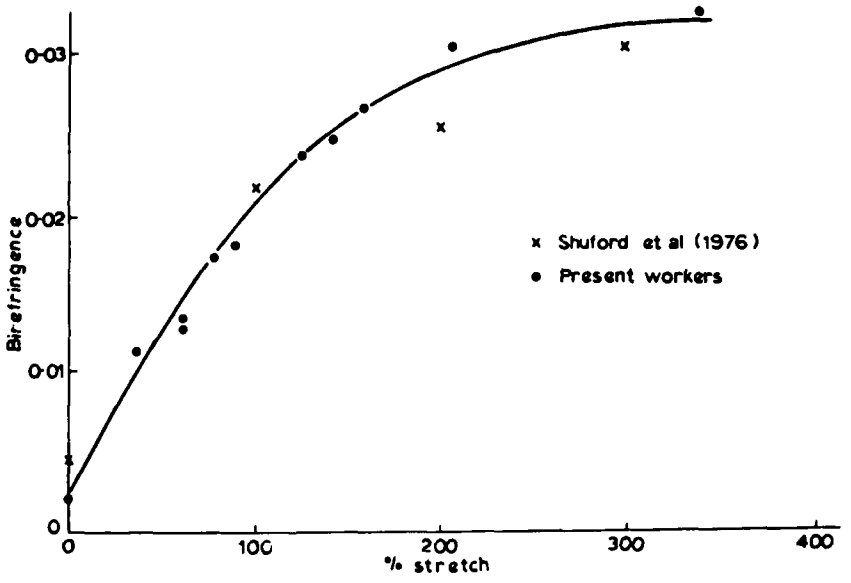

Fig. 9. Birefringence of PVF_2 with different stretch ratios.

with those of Shuford et al (ref. 28), who attribute the observed increases in the birefringence upon elongation, primarily to the changes in the degree of the preferred orientation of the crystalline phase. They (ref. 28) further argue that, as the elongation of the film is increased, the degree of orientation in the crystalline region and the corresponding changes in the observed birefringence reach

saturation values. The latter argument is supported by their observations with the sonic modulus (ref. 28) in stretched PVF_2 films. Hence the major contribution in the observed birefringence can be attributed to the orientation towards the stretch direction of the crystalline regions of PVF_2.

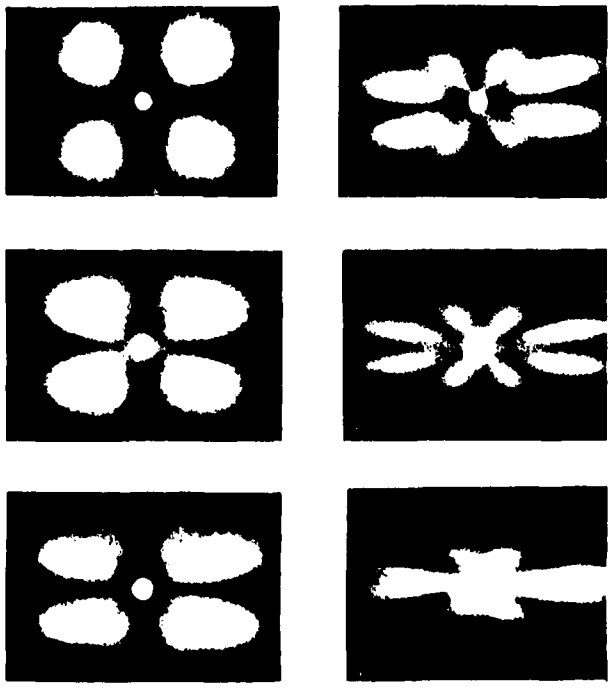

Fig. 10. Small Angle Light Scattering Patterns (SALS) of PVF_2 with different stretch ratios. a, b, c, d, e and f represent no stretch, 10%, 30%, 60%, 95% and 140% stretch ratios respectively.

Fig. 10 reveals the nature and mechanism of the orientation along the distortion in which spherulitic distortion may play a major part. Fig. 10(a) shows a typical H_v scattering pattern, prior to stretching with approximately 7^o scattering angle at the maximum lobe intensity. This type of four-lobe patterns, obtained with crossed polarizers, have been attributed to spherulite anisotropy (ref. 16). The size of the spherulite may be calculated from such a four-lobe scattering pattern of undeformed spherulite using the following expression (ref. 16):

$$4\pi \frac{R_o}{\lambda} \sin \frac{\theta_m}{2} = 4.1 \quad \ldots\ldots \quad (2)$$

where R_o is the spherulite radius, λ the wavelength of the incident radiation, θ_m the angle for which the intensity of scattering is maximum. The magnitudes of λ and θ_m both refer to measurements within the same scattering medium. Using equation (1) the radius of the Form 2 spherulite in 50μm thick PVF_2 film, employed in the present work, was found to be ∿3μm. Following the quantitative investigations of spherulitic deformation upon stretching (ref. 29-32) Nomura et al (ref. 33, 34) propose that with increasing elongation there is a predominant increase in the preferential alignment of crystal c-axis along the chain direction which results in a movement of the original four leaf pattern to the equatorial (horizontal) zone and simultaneously extending to meridional direction (vertical zone) due to lamellar untwisting. As a consequence an eight leaf pattern is progressively formed. Fig. 1o (b-f) show a good qualitative agreement of the present SALS results with Nomura et al (ref. 33, 34). However, it may be observed (Fig. 10) that the scattering pattern changes into an eight-lobe type over a relatively small range of draw ratio (0-60%), which may not be satisfactorily explained by the model due to Nomura et al (ref. 34). It is, of course, established that a structural transition occurs from Form 2 to Form 1 in PVF_2 on uniaxial stretching. However, present results (F.g. 10) indicate that such a conformational change may occur at a discrete yield boundary within a spherulite, or by the growth of new structure due to localised melting, for example, and a subsequent recrystallization, thus providing an orientation towards the stretch direction. Thus, it appears that on uniaxial stretching the c-axes of the polymer chains are oriented along the stretch direction and the other axes are not truly uniformly distributed in the plane perpendicular to the stretch direction. An account of the nature of the spherulitic deformation due to uniaxial stretching with respect to the present results will be published elsewhere (ref. 35). It may be noted that no distinctive changes from the observed four-leaf SALS pattern (Fig. 10a) was observed on corona poling of unstretched PVF_2 film. Furthermore, there was no noticeable change of the eight-leaf SALS patterns (Fig. 10) on corona poling of the stretched films. These observations further confirm that, in contrast to the effect of uniaxial stretching, corona poling alone, even at very high fields ($3\times10^8 Vm^{-1}$), does not produce a deformation of the spherulites.

5. CONCLUSIONS

PVF_2 films, originally containing the non-polar Form 2 type crystallites, may be made piezoelectric by corona poling. The induced piezoelectricity may be further enhanced on uniaxial stretching, followed by corona poling. The induced piezoelectricity is of dipolar origin. However, there is a difference in the sense that corona poling at fields $\frac{1}{2}3\times10^8 Vm^{-1}$ produces mainly an intermediate polar form by a cooperative rotation of the alternate polymer chains through 180^o about the c-axis

without losing its molecular conformation and the unit cell dimensions remaining unaltered, whereas the uniaxial drawing produces a direct conversion to the polar Form 1 type of structure from the non-polar Form 2 crystallites. Birefringence measurements show that the crystalline regions play the most dominant part in providing the orientational changes observed on uniaxial stretching.

ACKNOWLEDGEMENT

This work is being supported by a research grant from the U.S. Army. Two of the authors (K.D. and D.B.S.) are indebted to the Science Research Council of Great Britain for research studentships. The authors are also grateful to Dr. G. T. Davis of National Bureau of Standards, Washington D.C., U.S.A., for many valuable discussions during the progress of this work, and also for providing them with his pre-publication X-ray diffraction data.

LIST OF SYMBOLS

H_v - the mode of light scattering employing crossed polarizers, i.e. polarizer and analyser perpendicular to one another.

R_o - the radius of the spherulite.

T-G-T-G' trans-gauche-trans-gauché form.

$X_{c,v}$ - the volume fraction of crystalline polymer

d_{ij} - the piezoelectric strain coefficient (tensor); the first and the second subscripts refer to the polarization and the stress directions respectively.

Δ - the total birefringence.

Δ_a - the amorphous birefringence.

Δ_c - the crystalline birefringence.

Δ_f - the form birefringence

θ_m - the angle for which the intensity of light scattering is a maximum.

λ - the wavelength of the incident radiation.

REFERENCES

1 J.B. Lando, H.G. Olf and A. Peterlin, Nuclear magnetic resonance and X-ray determination of the structure of Poly(vinylidene fluoride), J.Polym.Sci., A-1, 4 (1966) 941.

2 R. Hasegawa, Y. Takahashi, Y. Chatani and H. Tadokoro, Crystal structure of three crystalline forms of Poly(vinylidene fluoride), Polym. J., 3, No. 5 (1972) 600.

3 K. Nakamura and Y. Wada, Piezoelectricity, Pyroelectricity and the electrostriction constant of Poly(vinylidene fluoride), J. Polym. Sci. A-2, 9 (1971) 161.

4 Y. Wada and R. Hayakawa, Piezoelectricity and Pyroelectricity of Polymers, Jap. J. Appl. Phys. 15, No. 11 (1976) 2041.

5 P.D. Southgate, Room temperature poling and morphology changes in pyroelectric polyvinylidene fluoride, Appl. Phys. Lett. 28 No. 5 (1976) 250.

6 D.K. Das-Gupta and K. Doughty, Changes in X-ray diffraction patterns of Polyvinylidene fluoride due to corona charging, Appl. Phys. Lett. 31 No. 9 (1977) 585.

7 N. Murayama, T. Oikawa, T. Katto and N. Nakamura, Persistent polarization in Poly(vinylidene fluoride), II Piezoelectricity of Poly(vinylidene fluoride) thermoelectrets, J. Polym. Sci., Polym. Phys. Ed., 13 (1975) 1033.

8 J.F. Nye, Physical properties of crystals, Oxford Univ. Press (1957) p.110.

9 H. Ohigashi, Electromechanical properties of polarized polyvinylidene fluoride films as studied by piezoelectric resonance method, J. Appl. Phys. 47 (1976) 949.

10 M. Tamura, K. Ogasawara, N. Ono and S. Hagiwara, Piezoelectricity in uniaxially stretched Poly(vinylidene fluoride), J. Appl. Phys. 45 (1974) 3768.

11 M. Oshiki and E. Fukada, Inverse piezoelectric effect and electrostrictive effect in polarized PVDF, J. Materials Sci., 10 (1975) 1.

12 P. Buchman, Pyroelectric and switching properties of polyvinylidene fluoride films, Ferroelectrics 5 (1973) 39.

13 K. Ogasawara, K. Shiratori and M. Tamura, Pyroelectricity in uniaxially stretched and polarized Poly(vinylidene fluoride), Rep. Progr. Polym. Phys. Japan, 19 (1976) 313.

14 M. Oshiki and E. Fukada, Piezoelectric effect in stretched and polarized PVDF films, Jap. J. Appl. Phys., 15 (1976) 43.

15 H.T. Jessop, On the Tardy and Sénarmond methods of measuring fractional relative retardations, Brit. J. Appl. Phys., 4 (1953) 138.

16 R.S. Stein and M.B. Rhodes, Photographic light scattering by polyethylene films, J. Appl. Phys., 31 (1960) 1873.

17 D.K. Das-Gupta and K. Doughty, Corona charging and the piezoelectric effect in Polyvinylidene fluoride, J. Appl. Phys., 49 No. 3 (1978) 4601.

18 R.S. Brockley and D.B. Shier, UCNW, Bangor (Private communication) (1978).

19 B.L. Farmer, A.J. Hopfinger and J.B. Lando, Polymorphism of Poly(vinylidene fluoride): potential energy calculations of the effects of head to head units on the chain conformation and packing of poly(vinylidene fluoride), J. Appl. Phys., 43 No. 11 (1972) 4293.

20 G.T. Davis, J.E. McKinney, M.G. Broadhurst and S.C. Roth, Electric field induced phase changes in Poly(vinylidene fluoride), J. Appl. Phys., 49 No. 10, (1978) 4998.

21 R.G. Kepler and R.A. Anderson, Ferroelectricity in polyvinylidene fluoride, J. Appl. Phys., 49 No. 3 (1978) 1232.

22 M. Tamura, S. Hagiwara, S. Matsumotu and N. Ono, Some aspects of piezoelectricity and pyroelectricity in uniaxially stretched poly(vinylidene fluoride), J. Appl. Phys. 48 No. 2 (1977) 513.

23 V. Petraccone, I.C. Sanchez and R.S. Stein, The orientation of amorphous chains in spherulites, J. Polym. Sci., Polym. Phys. Ed., 13 (1975) 1991.

24 L.E. Alexander, X-ray diffraction methods in polymer science, Wiley - Interscience, N.Y. (1964) p.269.

25 J.J. Aartsen and R.S. Stein, Scattering of light by deformed three-dimensional spherulites, J. Polym. Sci., A-2 9 (1971) 295.

26 S. Visconti and R.H. Marchessault, Small angle light scattering by elastomer-reinforced epoxy resins, Macromolecules, 7 (1974) 913.

27 C. Boisserie, R.H. Marchessault, Light scattering from epoxy-elastomer resins: A study of statistical methods in heterogeneity analysis, J. Polym. Sci., Polym. Phys. Ed., 15 (1977) 1211.

28 R.J. Shuford, A.F. Wilde, J.J. Ricca and G.R. Thomas, Characterization and piezoelectric activity of stretched and poled Poly(vinylidene fluoride) Part I: Effect of draw ratio and poling conditions, Polym. Eng. Sci., 16 No. 1 (1976) 25.

29 K. Sasaguri, S. Hosino and R.S. Stein, Relationship between morphology and deformation mechanisms of polyolefins, J. Appl. Phys., 35 No. 1 (1964) 47.

30 S. Clough, J.J. Van Aartsen and R.S. Stein, Scattering of light by two-dimensional spherulites, J. Appl. Phys., 36 No. 10 (1965) 3072.

31 S. Nomura, A. Asanuma, S. Suehiro and H. Kawai, Crystal orientation in a semi-crystalline polymer to deformation of spherulites, J. Polym. Sci., A-2 9 (1971) 1991.

32 D.Y. Yoon, C. Chang and R.S. Stein, An improved model of crystalline orientation of spherulitic polymers, J. Polym. Sci., Polym. Phys. Ed. 12 (1974) 2091.

33 S. Nomura, M. Matsuo and H. Kawai, Crystal orientation in a semi-crystalline polymer in relation to deformation of polymer spherulites. II Orientation distribution function of crystallites within crystal lamella as a function of lamellar orientation, J.Polym.Sci., Polym. Phys.Ed., 10 (1972) 2489.

34 S. Nomura, M. Matsuo and H. Kawai, Crystal orientation in a semi-crystalline polymer in relation to deformation of polymer spherulites. III Small angle light scattering, J. Polym. Sci., Polym. Phys. Ed. 12 (1974) 1371.

35. D.K. Das-Gupta and D.B. Shier, Small angle light scattering from uniaxially stretched Polyvinylidene fluoride (to be published, J. Appl. Phys. (1978).

Small-angle light scattering (SALS) from uniaxially stretched polyvinylidene fluoride

D. K. Das-Gupta and D. B. Shier

School of Electronic Engineering Sciences, University College of North Wales, Dean Street, Bangor, Gwynedd, LL57 1UT, Great Britain

(Received 7 March 1978; accepted for publication 20 June 1978)

Films (mostly of Form 2 crystal structure), 50 μm thick, of polyvinylidene fluoride (PVF_2) were uniaxially stretched at 60°C and then annealed at 120°C. Small-angle light scattering patterns (SALS) were taken of the samples in the H_v scattering mode (i.e., crossed polarizers). The results show that a four-lobe scattering pattern due to undeformed spherulites changes to an eight-lobe pattern on uniaxial stretching of PVF_2 films.

PACS numbers: 78.65.Jd

Crystalline polymers are volume filled with spherulites consisting of branched crystalline lamellae of folded chain crystals propagating from their centers.[1] Such polymers deform upon elongation, whereupon the spherulites change from spherical into ellipsoidal shape. Polyvinylidene fluoride (PVF_2) may possess at least two stable crystalline structures, i.e., Form 1 (planar zigzag polar form)[2] and Form 2 (nonpolar *T-G-T-G*[1] form).[3] Molecular conformational changes from Form 2 to Form 1 may occur in PVF_2 upon uniaxial stretching.[4-7] Small-angle light-scattering (SALS) analysis is now an established method[8-11] of characterizing morphological changes in polymeric materials. The present work reports preliminary results of changes observed in the SALS patterns upon uniaxial stretching of PVF_2 films which were provided by Kureha Chemical Industries Co. Ltd. of Japan.

PVF_2 films (mostly of Form 2 structure), 50 μm thick were uniaxially stretched at 60 °C. The stretched films were subsequently annealed at 120 °C to prevent shrinkage. A He-Ne laser beam was used to obtain the light-scattering patterns in the H_v mode. Spatial cleaning of the laser beam was achieved by locating a pinhole 6 μm in diameter at the focal plane of a biconvex lens. A collimated emerging beam 6 mm in diameter was then obtained with a second biconvex lens of suitable focal length. The experimental arrangement was similar to that of Stein and Rhodes[8] and is shown schematically in Fig. 1. The type of photographic films and the exposure time used were Ilford-HP4 and 8 sec, respectively.

Figure 2(a) shows a typical H_v scattering pattern of PVF_2 film (prior to stretching) with an approximately 7° scattering angle at maximum lobe intensity, such four-lobe patterns obtained with crossed polarizers (H_v mode) having been attributed to spherulite anisotropy.[8] It can be shown[8] that the spherulite size can be calculated from such a four-lobe scattering pattern of undeformed spherulites using

$$4\pi(R_0/\lambda)\sin(\tfrac{1}{2}\theta_m)=4.1, \tag{1}$$

where R_0 is the spherulite radius, λ is the wavelength of the incident light, and θ_m is the angle for which the intensity of scattering is maximum. The magnitudes of λ and θ_m refer to values measured within the same scattering medium. From Eq. (1) the radius of the Form 2 spherulites in PVF_2 was found to be approximately 3 μm.

It may be observed from Fig. 2 that as the draw ratio is increased the four-lobe scattering pattern changes into an eight-lobe scattering pattern. the uniaxial stretch being along the meridional direction. In order to account for the orientation of crystals in spherulites due to deformation upon stretching, it has been suggested that three separate processes of reorientation may accompany affine deforma-

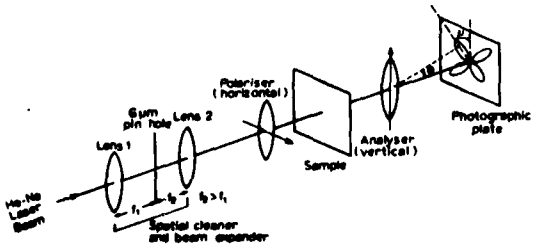

FIG. 1. The experimental arrangement to obtain light scattering patterns in the H_v mode (crossed polarizers).

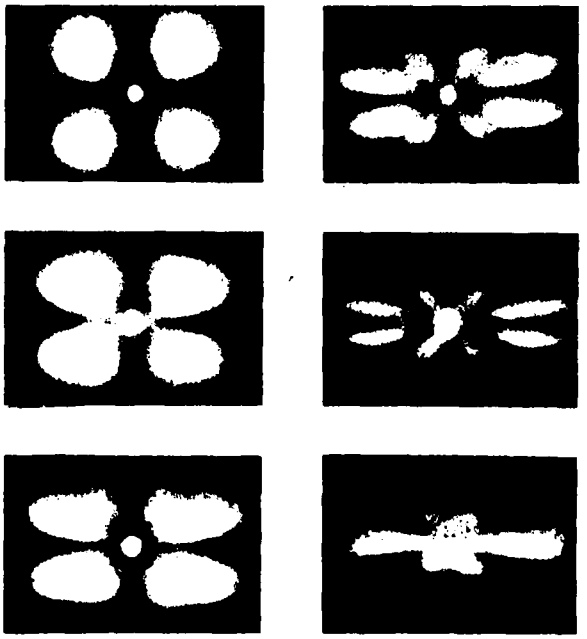

FIG. 2. SALS patterns of PVF_2 films with uniaxial stretch. a to f correspond to no stretch, 10, 30, 60, 95, and 140% stretch, respectively.

 0021-8979/78/4911-5665$01.10

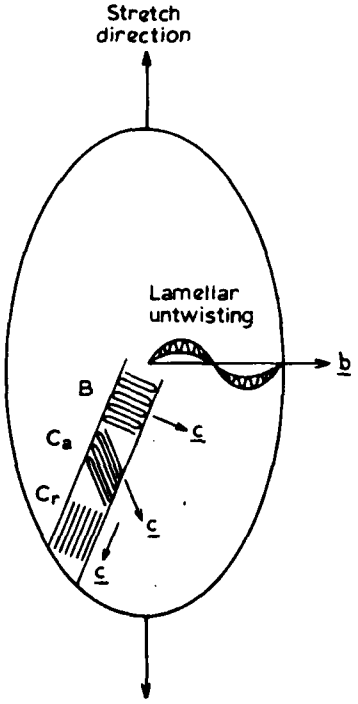

FIG. 3. Processes of spherulite deformations on uniaxial stretching (due to Nomura *et al.*[18]).

tion.[12–16] These are as follows: (i) tilting of the folded molecular chains with respect to the plane of the lamellae, (ii) twisting of the lamellae about the spherulite radius, and (iii) rotation of the *b* axis about the *c* axis of the crystal. It has, however, been pointed out[15] that the above model fails to provide a good agreement with experimental results in terms of the orientation distribution function of the reciprocal lattice vector of the (110) plane. Nomura *et al.*[15,17,18] provide an alternative theoretical model of spherulite deformation due to uniaxial stretching, which takes into account rotation of crystallites within the lamellae as well as lamellar untwisting. In this model[18] they consider the existence of two types of crystal orientations within the lamellae of the undeformed spherulite, viz., type *R* in which the crystallites (and hence the principal optical axes) are randomly oriented and type *B* in which the optical axes preferentially lie at right angles to the spherulite radius (i.e., *b*-axis radial orientation). The contribution to the light-scattering intensity in the H_v mode due to type *R* crystal orientation may be neglected. They[18] further suggest (see Fig. 3) that the type *B* crystals may be subjected to two types of *c*-axis orientation, i.e., (i) due to crystal rotation around the *a* axis associated with chain tilting (type C_a) and (ii) due to unfolding of polymer chains (type C_r). The model predicts an alignment of the *c* axis in the stretch direction. The types C_a and C_r crystals may be formed when the stretch direction is approximately parallel to the lamellar axis and lamellar untwisting will occur when the stretch direction is approximately perpendicular to the lamellar axis (see Fig. 3) which is also in agreement with Yoon *et al.*[16] The results of x-ray diffraction with uniaxially stretched low-density polyethylene were observed to be compatible with this model.[18] The computed SALS patterns[18] (theoretical) in the H_v mode show that a four-lobe pattern, which must arise due to contribution from the type *B* crystal orientation only, for undeformed spherulities may give rise to an eight-lobe pattern on uniaxial stretching when reorientations of the crystals, i.e., types C_a and C_r are considered. With increasing stretch ratio the lamellar untwisting may begin to occur and this would extend the original four-leaf-clover pattern in the meridional zone. This would also be in agreement with Van Aartsen and Stein.[9] Furthermore, the azimuthal angle μ (Fig. 3) may begin to increase from the 45° position and move progressively towards the equatorial zone with increasing stretch ratio. Subsequent to these two initial mechanisms of spherulite deformation, two other additional contributions may arise due to the formation of types C_a and C_r crystals (only at high values of stretch ratio) giving rise to eight or more lobes in the SALS pattern. Such an eight-lobe pattern has also been observed[19] on uniaxial stretching of low-density polyethylene of imperfect spherulite structure. The SALS patterns (Fig. 2) observed in the present work are in apparent agreement with Nomura *et al.*[18] in as much that, on uniaxial stretching of PVF_2 film, an eight-lobe pattern is formed. Four of the lobes move progressively towards the equatorial zone (i.e., at right angles to the stretch direction), the remaining four lobes moving initially towards the stretch direction and then increasing their azimuthal angle back to 45° at an approximately 90% stretch ratio. However, it may be observed (Fig. 2) that the scattering pattern changes into an eight-lobe type over a relatively small range of draw ratio (0–60%). This may not be satisfactorily explained by the model by Nomura *et al.*[18] which proposes a continuous change of orientation within a deforming spherulite upon elongation. Furthermore, the intensity of the scattering pattern at low draw ratio values was observed to be highest in the lobes which move to a position at right angles to the stretch direction. This is in disagreement with Nomura *et al.*[18] A possible explanation for this observed behavior of the scattering pattern at low elongation may be as follows. It is established that a structural transition from Form 2 to Form 1 in PVF_2 may occur on uniaxial stretching.[4–7] Such a conformational change may occur either at a discrete yield boundary within a spherulite or by the growth of new structures due to a localized melting, for example, and a subsequent recrystallization, thus providing an orientation towards the stretch direction. The SALS pattern may then be expected to consist of an eight-lobe-type profile superimposed with the scattering pattern of the recrystallized material which would be in evidence towards a position at right angles to the stretch direction for low elongation.

Further work is in progress to obtain (i) the intensity distribution in the SALS patterns, (ii) birefringence, and (iii) x-ray pole figures to determine the orientation distribution function.

This work is partially supported by a research grant from the U.S. Army. One of the authors (DBS) is also grateful to the Science Research Council of Great Britain for a research studentship.

[1]V. Petraccone, I.C. Sanchez, and R.S. Stein, J. Polym. Sci. Polym. Phys. Ed. **13**, 1991 (1975).
[2]J.B. Lando, H.C. Olf, and A. Peterlin, J. Polym. Sci. A-1 **4**, 941 (1966).
[3]W.W. Doll and J.B. Lando, J. Macromol. Sci. B **4**, 889 (1970).
[4]G. Cessac and J.G. Curro, J. Polym. Sci. Polym Phys. Ed. **12**, 695 (1974).
[5]M. Oshiki and E. Fukada, Jpn. J. Appl. Phys. **15**, 43 (1976).
[6]R.J. Shuford, A.F. Wilde, J.J. Ricca, and G.R. Thomas, Polym. Eng. Sci. **16**, 25 (1976).
[7]M. Latour, J. Electrostatics **2**, 241 (1977).
[8]R.S. Stein and M.B. Rhodes, J. Appl. Phys. **31**, 1873 (1968).
[9]J.J. Van Aartsen and R.S. Stein, J. Polym. Sci. A-2 **9**, 295 (1971).
[10]S. Visconti and R.H. Marchessault, Macromolecules **7**, 913 (1974).
[11]C. Boisserie and R.H. Marchessault, J. Polym. Sci. Polym. Phys. Ed. **15**, 1211 (1977).
[12]K. Sasaguri, S. Hoshino, and R.S. Stein, J. Appl. Phys. **35**, 47 (1964).
[13]K. Sasaguri, R. Yamada, and R.S. Stein, J. Appl. Phys. **35**, 3188 (1964).
[14]S.Clough, J.J. Van Aartsen, and R.S. Stein, J. Appl. Phys. **36**, 3072 (1965).
[15]S. Nomura, A. Asanuma, S. Suehiro, and H. Kawai, J. Polym. Sci. A-2 **9**, 1991 (1971).
[16]D.Y. Yoon, C. Chang, and R.S. Stein, J. Polym. Sci. Polym. Phys. Ed. **12**, 2091 (1974).
[17]S. Nomura, M. Matsuo, and H. Kawai, J. Polym. Sci. Polym. Phys. Ed. **10**, 2489 (1972).
[18]S. Nomura, M. Matsuo, and H. Kawai, J. Polym. Sci. Polym. Phys. Ed. **12**, 1371 (1974).
[19]M.Motegi, T. Oda, M. Moritani, and H. Kawai, Polym. J. **1**, 209 (1970).

J. Phys. D: Appl. Phys., 13 (1980) 95–105. Printed in Great Britain

Piezoelectricity in uniaxially stretched and corona poled polyvinylidene fluoride

D K Das-Gupta and K Doughty
School of Electronic Engineering Sciences, University College of North Wales, Dean Street, Bangor, Gwynedd LL57 1UT

Received 11 May 1979, in final form 17 August 1979

Abstract. PVF_2 films of Form 2 structure were uniaxially stretched at 60 °C up to a stretch ratio of 7:1 and subsequently corona poled at room temperature up to a surface potential of 7 kV. Structural studies of both the stretched and the stretched and poled films were made by x-ray reflection–diffraction and Laué transmission techniques. The induced piezoelectric coefficient d_{31} was also measured as a function of surface (poling) potentials of films with stretch ratios in the range 1:1 to 7:1. The results show that the induced piezoelectricity in PVF_2 may arise from two different types of conformational changes in the unit cell structure and is of dipolar origin.

1. Introduction

Piezoelectricity in polyvinylidene fluoride (PVF_2), which is a semicrystalline polymer, is significantly enhanced (Kawai 1969) on uniaxial stretching and subsequent poling at an elevated temperature with a high external electric field for an extended period of time (viz conventional poling). Fukada and Sakurai (1971) and Nakamura and Wada (1971) have studied the temperature dependence of the complex piezoelectric strain constant of uniaxially stretched and conventionally poled PVF_2 films. Oshiki and Fukada (1976) have also studied the temperature dependence of the complex piezoelectric stress constant and the electrostrictive constant of stretched and poled (conventional poling) PVF_2. They (Oshiki and Fukada 1976) suggest that the polarisation, due to external poling, may arise from the aligned dipoles within the crystalline region of PVF_2, which is in disagreement with Murayama *et al* (1975). Wada and Hayakawa (1976) review the theoretical and experimental observations on piezo- and pyroelectric properties and the nature of their origin in PVF_2. Broadhurst *et al* (1978) have developed a bulk dipolar model with compensating surface space charges and suggest that the piezo- and pyroelectricity in PVF_2 arise from bulk dimensional changes due to changes in stress and temperature, respectively.

It has been shown from x-ray diffraction studies (Shuford *et al* 1976, Das-Gupta *et al* 1979, Grandidge 1979) that, with uniaxial stretching, the crystallites in PVF_2 films may assume a preferred orientation. It has also been shown from the x-ray diffraction studies of suitably poled (both conventional and corona poling) films of PVF_2 (Kepler *et al* 1975, Shuford *et al* 1976, Das-Gupta and Doughty 1977, 1978a,b,c, Kepler and Anderson 1978, Davis *et al* 1978, Doughty 1979) that the poling may induce a structural change involving a rotation of polar unit cells of PVF_2 which aligns the dipole moments towards the direction of the poling field. The results of Raman (Latour 1976/77) and infrared (Southgate 1976,

0022-3727/80/010095+12 $01.00

Shuford *et al* 1976) spectroscopic studies of poled PVF_2 films are also in agreement with the above observations.

Present work reports the results of a systematic study of the structural changes and the corresponding enhanced piezoelectricity after corona charging of unidirectionally stretched PVF_2 films. The samples of 25 μm thick PVF_2 (Kureha), unidirectionally stretched at 60 °C (from 1 : 1 to 7 : 1 stretch ratio), were provided by The Post Office Research Centre at Martlesham Heath, Ipswich.

2. Experimental details

The method of corona charging, the step-scanning technique of obtaining x-ray diffraction profiles for a 2θ (Bragg angle) range of 17–22 ° in steps of 0·1 °, using CuKα radiations, and the method of measuring the piezoelectric strain coefficient d_{31}, were exactly the same as described elsewhere (Das-Gupta and Doughty 1978a,c). Additional x-ray diffraction data were obtained in the 2θ range 10–30 ° using an automatic recording technique (Doughty 1979). Corona charging of each sample was carried out at a constant temperature of 18 °C for 30 min. The surface potential of the polymer, which was monitored continuously with a Field Mill type electrostatic voltmeter, was observed to reach the desired values (≥ 8 kV) within 10 s after the application of the high-voltage supply to the corona point. Most of the observations were made with positively (corona) charged polymer surface; however, a limited amount of work was also carried out with negatively (corona) charged specimens. The x-ray diffraction profiles were obtained for each sample before and after corona charging. The absolute accuracy of the diffractometer (i.e. error in 2θ values), which was checked periodically using a standard silicon sample, was less than 0·01 °. However, the overall error, including that introduced in mounting the sample in the sample holder of the goniometer, was $\geq 0{\cdot}1$ °.

In addition to the x-ray diffraction profiles, Laué transmission (x-ray) patterns were also obtained in this work. It is necessary to do so as any information on orientation effects in the (001) planes, which are parallel to the direction of the incident planes, will be missing in the reflection (diffraction) mode. Laué patterns also offer an additional advantage in providing structural information on several planes simultaneously. A standard experimental arrangement was employed to obtain the Laué patterns in which a photographic film (Ilford x-ray film, type G) was placed at a distance D (8 cm) behind the sample and perpendicular to the incident beam. For a film thickness of 25 μm an exposure time of 15 h was required to record the Laué patterns. The undiffracted central beam was removed, of course, with a lead stop. The crystallographic planes in the Laué patterns were identified by using the following expression:

$$d_{hkl} = \frac{\lambda}{2} \operatorname{cosec}\left(\frac{\tan^{-1}(r/D)}{2}\right) \tag{1}$$

where d_{hkl} is the interplanar spacing, λ is the wavelength of the incident radiations (1·54 Å) and r is the radius of the observed diffraction ring (for a semi-crystalline material) in the Laué pattern.

The piezoelectric strain coefficient d_{31} was subsequently evaluated by measuring the open-circuit voltage (with a storage oscilloscope) developed across a standard mica capacitor, connected in parallel with the sample, on releasing a fixed weight (Das-Gupta and Doughty 1978a,c).

3. Results

Figure 1 shows a typical set of x-ray diffraction profiles of uniaxially stretched PVF_2 films with different stretch ratios. It may be observed that the diffraction peak intensity of the (020) plane of the Form 2 type, occurring at a 2θ value of 18·4° (Doll and Lando 1970), increases with increasing stretch ratio.

The (110) diffraction peak of the Form 2 structure, which occurs at a 2θ value of 20·15° (Doll and Lando 1970), also increases in intensity up to 3:1 stretch ratio, above

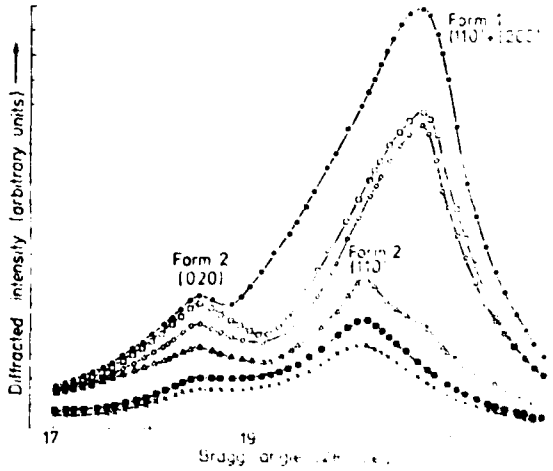

Figure 1. X-ray diffraction profiles of uniaxially stretched PVF_2 films with different stretch ratios. ●, 7:1 stretch ratio; ○, 6:1 stretch ratio; □, 5:1 stretch ratio; △, 3:1 stretch ratio; ■, 2:1 stretch ratio; ×, 1:1 stretch ratio

which it begins to disappear. The composite peak [(110)+(200)] of the polar Form 1 structure, occurring at a 2θ value of 20·8° (Lando *et al* 1966, Hasegawa *et al* 1972), is only just noticeable in the diffraction pattern of the sample with a stretch ratio of 3:1. With further increase of the uniaxial stretch ratio this composite peak becomes progressively more dominant (figure 1).

Figure 2 shows the effect of structural changes due to corona charging of the uniaxially stretched polymer (2:1 to 7:1 stretch ratio) at a surface potential of 6 kV. It may be observed that on corona charging of samples with increasing stretch ratio the Form 2 (020) peak gradually disappears. The Form 2 (110) peak also disappears on corona charging of samples with higher stretch ratios, although an enhancement of this peak occurs initially at lower stretch ratios. The composite peak [(110)+(200)], occurring at 2θ value of 20·8°, of the Form 1 structure appears on corona charging of samples with a stretch ratio of 2:1. For samples with increasing stretch ratios the magnitude of this composite peak becomes considerably enhanced on corona charging.

Laué transmission patterns of samples stretched at 2:1 and 7:1 are presented in figures 3 (plate) and 4 (plate) respectively. Figures 5 (plate) and 6 (plate) show the transmission (Laué) patterns of the same samples on subsequent corona charging at 6 kV. An identification of the diffracting planes was made by direct measurement of the radii of the rings on the negatives. Due to the large differences in the intensities of the different rings some

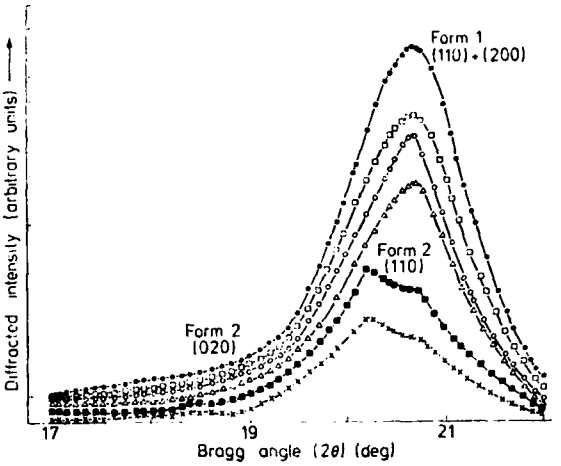

Figure 2. X-ray diffraction profiles of uniaxially stretched PVF$_2$ films (2:1 to 7:1 stretch ratio) after corona charging to a surface potential of 6 kV. Symbols: same as for figure 1.

of the photographs were split into two parts, each half receiving a different exposure time to obtain a good resolution for all the rings. Tables 1 and 2 give the radii of the Laué transmission rings for the corresponding structural diffraction planes for the 2:1 and 7:1 stretch ratios, respectively. For the sake of comparison, the corresponding d values due to Hasegawa *et al* (1972) have also been given in these tables from which it may be observed that there is good agreement with the present work.

Figure 3 shows typically a set of diffraction rings of a polycrystalline material with spherulitic morphology. As the stretch ratio is increased a preferential orientation of the

Table 1. Analysis of Laué transmission photographs (D=8 cm). 2:1 stretch ratio.

Ring radius (cm)	d value (Å)	Diffracting plane	Crystal form	d value (Å) (due to Hasegawa *et al*)
2·7	4·75	(020)	2	4·82
2·92	4·38	(110)	2	4·41
3·05	4·25	(110)+(200)	1	4·26–4·29
4·0	3·35	(012)	2	3·31
5·2	2·71	(130)	2	2·70
5·8	2·50	(200)	2	2·48
6·45	2·31	(002)	2	2·26
6·95	2·20	(220)	2	2·21

Table 2. Analysis of Laué transmission photographs (D=8 cm). 7:1 stretch ratio.

Ring radius (cm)	d value (Å)	Diffracting plane	Crystal form	d value (Å) (due to Hasegawa *et al*)
2·6–2·8	4·59–4·92	Amorphous halo	—	—
3·0–3·2	4·05–4·33	(110)+(200)	1	4·26–4·29
4·05	3·32	(021)	2	3·31
7·1	2·17	(111)+(201)	1	2·19–2·20

crystallites occurs along the stretch direction which causes the diffraction rings to break up into short arcs progressively. This is evidenced in figure 4 in which the disappearance of some of the Form 2 diffraction rings (i.e. (220), (002), (200), (130)) may also be noticed.

Figure 10 illustrates the variation of the piezoelectric coefficient d_{31} with stretch ratios for samples which were corona charged at 7 kV. The behaviour of d_{31} of the 7:1 stretched samples with corona charging potential is shown in figure 11.

Finally, figure 12 shows a comparison of the measured d_{31} values for positive and negative polarities of the corona potential at 7 kV with samples stretched in the range from 2:1 to 7:1.

4. Discussion

The diffraction profile (figure 1) of the sample with 1:1 stretch ratio indicates that only the non-polar Form 2 type of crystal structure is present in this sample. Furthermore, the Laué transmission pattern showed an absence of any preferential orientation of the crystallites in the 1:1 stretched sample. Thus, such an isotropic material with a non-polar crystal structure should not exhibit any pyro- and piezoelectricity. Now the centre of the amorphous halo for PVF_2 is centred at a 2θ value of 18·4°, which unfortunately coincides with that of the Form 2 (020) diffraction peak position (Doll and Lando 1970). However, by employing a method due to Gal'perin *et al* (1970) it may be shown from figure 1 that the contribution from the amorphous phase of the polymer to the enhancement of the (020) diffraction peak intensity remains significantly unaffected even for a stretch ratio of 7:1. This is not in disagreement with Davis and Rushworth (1976) who found the amorphous phase in drawn PVF_2 to be isotropic. The increase in the intensity of the Form 2 (020) peak with increasing stretch ratio (figure 1) may then be explained by a preferential orientation of the *b* axis of the crystallite in the thickness direction of the film. By convention, the *c* axis is commonly taken as the direction parallel to the polymer chain.

The observed increase in the intensity of the Form 2 (110) diffraction peak with increasing stretch ratio up to 3:1 (figure 1) is due to the preferential orientation of the *c* axis along the stretch direction. For higher stretch ratios, the reduction and disappearance of this diffraction peak (figure 1) may be explained by a conversion of the Form 2 (figure 7) crystallites into the Form 1 (figure 9) structure. This is evidenced by the progressive dominance of the Form 1 composite peak [(110)+(200)] at a 2θ value of 20·8° with increasing stretch ratio (figure 1). The Laué patterns (figure 4) of the stretched (7:1) polymer further support the above observations, which are also in agreement with Shuford *et al* (1976). Cessac and Curo (1974) and Latour (1976/77) also confirm from studies with polarised Raman spectroscopy that a structural change from Form 2 (figure 7) to Form 1 (figure 9) crystallite may occur in PVF_2 on uniaxial stretching at low temperature. Matsushige *et al* (1978) provide evidence (from x-ray studies) of a crystal transformation from the Form 2 structure into Form 1 type of PVF_2 at an annealing pressure of 4000 kg cm^{-2} at a temperature below the melting point (i.e. 286 °C), at this pressure, of the Form 2 crystallites. Although the temperature employed in their investigation was significantly higher than ambient, it may be pertinent to compare the electrostatic pressure generated in the corona charging process with the mechanical pressure required to convert the Form 2 crystallites into Form 1 types. Using the expression:

$$P = \tfrac{1}{2}\,\epsilon_0 \epsilon_r E^2 \tag{2}$$

where P is the pressure, ϵ_0 is the permittivity of free space, ϵ_r is the relative permittivity

of the dielectric, and E is the applied field, it would appear that the electrostatic pressure (< 100 kg cm^{-2}) is over an order of magnitude less than the pressure to bring about such a conversion by quite the same mechanism as observed by Matsushige *et al* (1978). The existence of the Form 2 (020) diffraction peak (figure 1) together with the Form 2 (021) diffraction ring (figure 3) and arc (figure 4) would indicate that a complete conversion of all the Form 2 crystallites into the Form 1 type PVF$_2$ does not occur even at the highest ratio (7:1) employed in this work. This is in agreement with the results of small-angle light scattering (SALS) patterns from uniaxially stretched PVF$_2$ films (Das-Gupta and Shier 1978, Das-Gupta *et al* 1979). Spherulitic polymers deform upon elongation whereupon the spherulites change from spherical into ellipsoidal shapes. Nomura *et al* (1974) offer a model for the alignment of the c axis (carbon–carbon axis) in the stretch direction due to (i) crystal rotation around the a axis associated with chain filtering, and (ii) unfolding of polymer chains. As a consequence the fluorine atoms of PVF$_2$ in the Form 2 structure (figure 1) may be able to overcome the steric hindrance and flip over to produce a structure resembling that of Form 1 (figure 9). Das-Gupta and Shier (1978) suggest from the observations of the SALS patterns that such a conformational change may occur either at a discrete yield boundary within a spherulite or by the growth of new structures due to a localised melting, for example, and a subsequent recrystallisation, thus providing an orientation towards the stretch direction. This model allows for the entire collection of the crystallites within a lamella to be oriented upon stretching with little disturbance to individual crystallites, so that the preferential orientation and the conversion from the Form 2 to Form 1 type of structure in PVF$_2$ may be unrelated.

On corona charging stretched PVF$_2$ (figure 2) the Form 2 (020) peak is reduced in intensity and for most samples may not be observed above the background. It is unlikely that this may be due to a complete conversion of the Form 2 crystallites to the Form 1 type crystallites because other Form 2 planes, such as (021), still give rise to significant diffraction arcs in the Laué patterns (figures 4 and 6).

It is proposed that the reduction in the Form 2 (020) peaks after corona charging may be the result of a structural change from the non-polar type of Form 2 unit cell

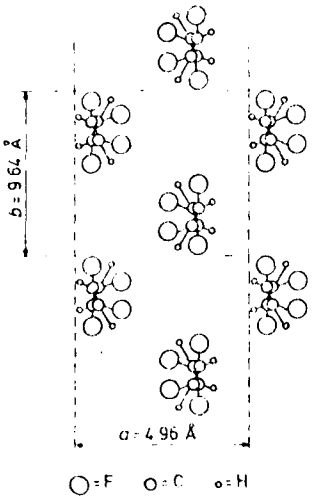

Figure 7. The unit cell of the non-polar Form 2 PVF$_2$.

(figure 7) to a polar variety of this cell without a change of lattice dimensions (Davis *et al* 1978). Such a polar variety may be produced if alternate chains in the Form 2 lattice were rotated through 180° to produce an arrangement where all the chains were parallel (Das-Gupta *et al* 1979).

The net dipole moment of 1·21 D per monomer unit (M G Broadhurst 1978, private communication) perpendicular to the Form 2 chain of PVF_2 is parallel to the *a* axis (figure 7), and the effect of a high electric field stress would be to tend to align these dipoles parallel to the field. Those chains with their *a* axis originally parallel to the surface planes will be energetically in the most favourable positions in an applied corona field and these chains may be rotated through 90° to produce a stable arrangement. Such a process would require half the chains to rotate in a clockwise direction and the other half to rotate anticlockwise so that alternate chains would appear to have rotated through 180° with respect to each other.

The result is the polar variety of the Form 2 (figure 8) as proposed by Davis *et al* (1978) and with the unit cell axes rotated through 90° as compared to the original non-

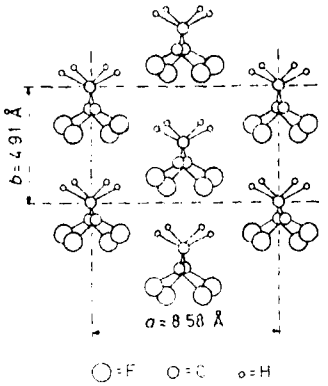

Figure 8. The unit cell of the polar Form 2 PVF_2 produced by a rotation of crystal axes through 90°, alternate molecular chains rotating in opposite directions.

polar cell (figure 7). This process leads to a preferred orientation of the *a* axis parallel to the applied field, i.e. perpendicular to the surface planes. Therefore, after poling, there will also be a preferred orientation of the *b* axis, but in this case, parallel to the film surface. As a consequence, there will be a reduction in the number of (0*K*0) planes which can be observed by the reflection-diffraction technique and this may then explain the reduction in the intensities of the Form 2 (020) diffraction peaks after corona charging (figure 2).

Thus, the changes in x-ray diffraction patterns observed on corona charging (figures 2, 4 and 6) may be adequately attributed to a change of symmetry of the Form 2 crystallites from C_{2h} to C_{2v}, together with a rotation of axes. Also, the dipoles, after corona charging, will lie preferentially along the direction of poling and will produce a polarisation which may give rise to piezoelectric behaviour.

It may, however, be noticed from figure 10 that the highest value of the piezoelectric coefficient d_{31} occurs on corona poling of samples with the highest stretch ratio of 7:1. It may be accepted from the observations of the x-ray data (figures 1 and 4) that, at this stretch ratio, the Form 2 type crystallite contents will also be the least. It should be stated

that the magnitude of d_{31} in mostly Form I (figure 9) type of crystallites (at 7:1 stretch ratio) was observed to be negligible before corona poling. Thus, although the uniaxial stretching produces an alignment of molecular chains along the stretch direction, the observed piezoelectricity necessitates that a change in the molecular axes of the Form I crystallites (figure 9) should occur to produce a net dipole moment. The increases observed in the Form I composite peak [(110)+(200)] after corona charging (figure 2) suggest that such a rotation indeed occurs which is in agreement with Latour (1977). It is established that the orthorhombic symmetry of the Form I type (figure 9) unit cell

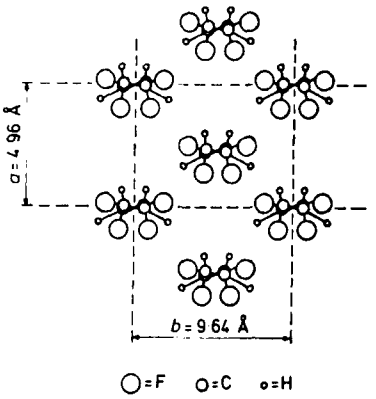

Figure 9. The unit cell of the Form I PVF_2.

results from a small (1 %) distortion of a hexagonal unit lattice (Miller and Raisoni 1976). Kepler and Anderson (1978) use this fact to suggest that a rotation of the Form I unit cell axes may thus be accomplished in 60° increments without disruption of the polymer morphology. The decrease in the width at half-height of the (110)+(200) Form I composite peak (figure 2) after corona charging may be due to (i) an increase in average crystallite size, and (ii) a reduction in the level of lattice distortions. It was observed that the crystallinity (55%) of the 1:1 stretched sample was independent of corona poling. However, Latour (1976/77) and Davis *et al* (1978) have observed a small change in crystallinity, induced by the poling field in a copolymer and the homopolymer of PVF_2, respectively. It may be noted that the recent work on the fine structure of stretched and poled PVF_2 films by Takahashi and Odajima (1979) show that stretching may introduce orientation dislocations in which a part of the long molecule tends to get oriented about its chain axis, accompanied by a $c/2$ translation due to chain twisting. Their preliminary calculations also show that the chain molecule can rotate to a metastable position in the range 130–180° oriented from the regular direction, accompanied by a slight lateral shift of the chain axis. It is feasible that a high field poling process may remove these defects by rotating the 'odd' molecules into a parallel arrangement. The removal of such defects from the Form I lattice would introduce a polarisation if it is assumed that the removal of defects applies only in the direction of the poling field. It may be difficult to calculate the contribution to the polarisation without a prior knowledge of the defect density and the distribution of orientations of the crystallite axes. Further work in this direction will be of considerable interest.

Figure 10 shows that d_{31} tends to reach a saturation level at higher stretch ratios when most of the crystal regions have been preferentially aligned as observed by Shuford *et al*

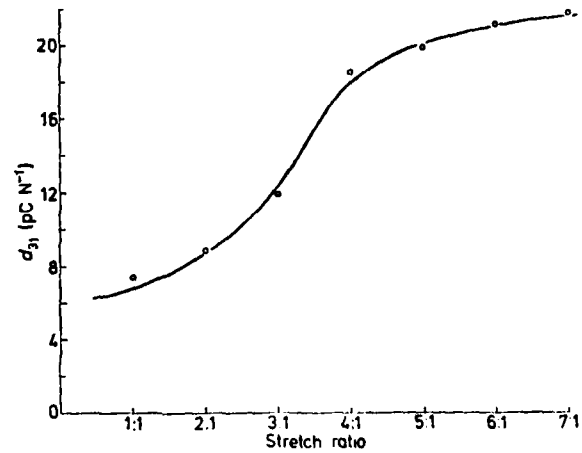

Figure 10. Variation of d_{31} with stretch ratio for samples corona charged at 7 kV.

(1976). Further stretching may only assist to align the amorphous regions which may not contribute significantly to the observed piezoelectricity in PVF_2 and this is in disagreement with Tamura *et al* (1977).

The behaviour of d_{31} with increasing charging potential at a constant stretch ratio of 7:1 (figure 11) shows that, unlike the case in figure 10, it does not reach its near-saturation value at room temperature even at a surface potential of 7 kV. This may be explained in the following manner. In the unpoled samples the crystallites may exist with all possible orientations with respect to the direction of the poling field. The crystallites will, *therefore, require* different poling fields to provide the energy necessary for an identical rotation. However, since the rotation of the Form 1 type crystallites may occur only in discrete steps of 60°, a complete alignment of all the crystallites at a specific field may not

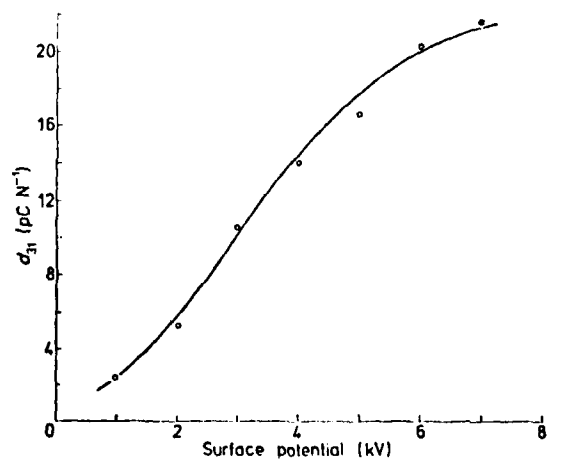

Figure 11. The behaviour of d_{31} of the 7:1 stretched samples with corona charging potential. Sample thickness = 25 μm.

be possible. The dipolar axes of the Form 1 crystallites will thus be statistically arranged at angles between $\pm 30°$ to $0°$ with respect to the direction of the poling field. A similar argument, applied to the Form 2 structure, would allow a distribution of crystallite axes between $\pm 45°$ to $0°$ to the field direction. Further work is in progress to determine the activation energies and time constants involved with these two processes from studies of structural changes and their effects on d_{31}, the variable parameters being the poling temperature, time, electric fields and stretch ratios.

Finally, figure 12 demonstrates that the observed magnitude of d_{31} is independent of the polarity of the corona charges which would be in agreement with the concept of the dipolar orientation being the dominant mechanism of the induced piezoelectricity in PVF_2.

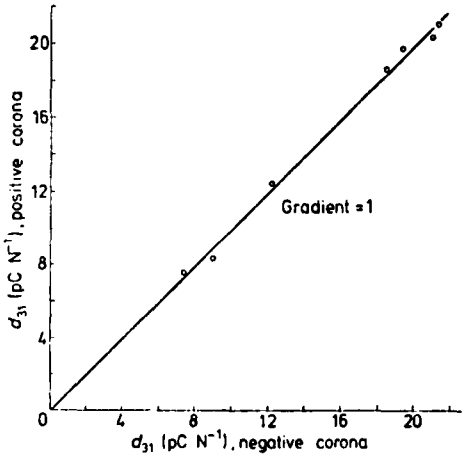

Figure 12. Comparison of measured d_{31} values for positive and negative polarities of corona at 7 kV for samples stretched 2:1 to 7:1.

5. Conclusions

Piezoelectricity, induced in polycrystalline PVF_2 films of Form 2 structure, may originate from (i) a change in symmetry from C_{2h} of non-polar Form 2 structure to C_{2v} type (polar Form 2) arising from rotations of the crystal *a* and *b* axes through 90° on corona poling, and (ii) preferential alignment and a change in the molecular axes of the Form 1 crystallites due to uniaxial stretching and subsequent corona poling.

Acknowledgments

The authors would like to thank Drs M G Broadhurst and G T Davis of the National Bureau of Standards, Washington DC, USA, Dr R J Shuford of Army Materials Research Centre, Watertown, Boston, USA, Professor A Odajima of Hokkaido University, Sapporo, Japan, and Dr P Pantelis of the Post Office Research Centre, Ipswich, UK, for many useful discussions during the progress of this work. It is also a pleasure to express

our gratitude to Dr Pantelis for providing us with the stretched PVF_2 films. Thanks are also due to Mr P Grandidge for carrying out a part of the experimental work.

This work is being financed by a research grant from the US Army.

References

Broadhurst M G, Davis G T and McKinney J E 1978 *J. Appl. Phys.* **49** 4992–7
Cessac G and Curro J G 1974 *J. Polymer Sci., Polymer Phys. Ed.* **12** 495–702
Das-Gupta D K and Doughty K 1977 *Appl. Phys. Lett.* **31** 585–7
—— 1978a *J. Appl. Phys.* **49** 4601–3
—— 1978b *IEEE Trans. IAS* **IA-14** 448–53
—— 1978c *J. Phys. D: Appl. Phys.* **11** 2415–23
Das-Gupta D K, Doughty K and Shier D B 1979 *J. Electrostatics* to be published
Das-Gupta D K and Shier D B 1978 *J. Appl. Phys.* **49** 5685–7
Davies G R and Rushworth A R 1976 *J. Mater. Sci.* **11** 782–3
Davis G T, McKinney J E, Broadhurst M G and Roth S C 1978 *J. Appl. Phys.* **49** 4998–5002
Doll W N and Lando J B 1970 *J. Macromol. Sci.–Phys.* **43** 4293–303
Doughty K 1979 *PhD Thesis* University of Wales
Fukada D and Sakurai T 1971 *Polymer J.* **2** 656–62
Gal'perin Ye L, Kosmynin B P and Smirnov V K 1970 *Polymer Sci.* **12** 2133–8
Grandidge P C 1979 *MSc Thesis* University of Wales
Hasegawa R, Takahashi Y, Chatani Y and Tadokoro H 1972 *Polymer J.* **3** 600–10
Kawai H 1969 *Jap. J. Appl. Phys.* **8** 975–6
Kepler R G and Anderson R A 1978 *J. Appl. Phys.* **49** 1232–5
Kepler R G, Graeber E J and Beeson P M 1975 *Bull. Am. Phys. Soc. Ser. 2* **20** 350
Lando J B, Olf H G and Peterlin J 1966 *J. Polymer Sci.* **4** 941–51
Latour M 1976/77 *J. Electrostatics* **2** 241–8
—— 1977 *Polymer* **8** 278–80
Matsushige K, Nagata K and Takemura T 1978 *Jap. J. Appl. Phys.* **17** 467–72
Miller R L and Raisoni J 1976 *J. Polymer Sci., Polymer Phys. Ed.* **14** 2325–6
Murayama N, Oikawa T, Katto T and Nakamura K 1975 *J. Polymer Sci., Polymer Phys. Ed.* **13** 1033–47
Nakamura K and Wada Y 1971 *J. Polymer Sci.* **9** 161–73
Nomura S, Matsuo M and Kawai H 1974 *J. Polymer Sci., Polymer Phys. Ed.* **12** 1371–81
Oshiki M and Fukada E 1976 *Jap. J. Appl. Phys.* **15** 43–52
Shuford R I, Wilde A F, Rica J J and Thomas G R 1976 *Polymer Engng Sci.* **16** 25–35
Southgate P D 1976 *Appl. Phys. Lett.* **28** 250–2
Takahashi N and Odajima A 1979 *Jap. J. Appl. Phys.* to be published
Tamura M, Hagiwara S, Matsumoto S and Ono N 1977 *J. Appl. Phys.* **48** 513–21
Wada Y and Hayakawa R 1976 *Jap. J. Appl. Phys.* **15** 2041–57

Figure 3. Laué transmission pattern of a sample stretched by 2:1

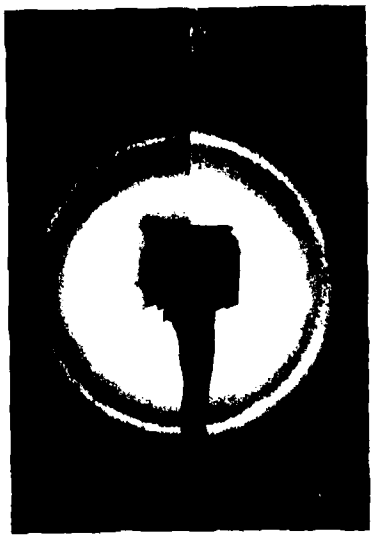

Figure 5. Laué transmission pattern of 2:1 stretch sample after corona charging to 6 kV.

Figure 4. Laué transmission pattern of a sample stretched by 7:1.

Figure 6. Laué transmission pattern of 7:1 stretch sample after corona charging to 6 kV.

Changes in x-ray diffraction patterns of polyvinylidene fluoride due to corona charging

D. K. Das Gupta and K. Doughty

School of Electronic Engineering Science, University College of North Wales, Dean Street, Bangor, Gwynedd LL57 1UT, Great Britain
(Received 9 June 1977; accepted for publication 31 August 1977)

The changes in the x-ray diffraction patterns of 16- and 25-μm-thick polyvinylidene fluoride films, caused by 6-kV corona charging at room temperature, are presented. The diffraction peaks corresponding to (100) and (020) α-crystalline forms tend to be considerably reduced while the (110) β-form peak changes in shape and position.

PACS numbers: 77.90.+k, 81.60.Jw, 61.40.Km, 73.40.Bf

Polyvinylidene fluoride (PVF_2) is a semicrystalline polymer which may exist at least in two stable crystalline forms,[1] namely, a planar zigzag polar form (β form or Form 1)[2] and a T-G-T-$\bar{G}$ nonpolar form (α form or Form 2)[3] where T, G, and $\bar{G}$ denote the trans and the two types of gauche forms, respectively. Oshiki and Fukada[4] show that a significant reduction of the α form takes place on stretching and subsequently subjecting the PVF_2 films, originally containing both α and β forms, to high dc fields over extended periods of time at elevated temperatures (i.e., poling). The infrared and Raman spectroscopic studies of Latour[5] also support such observations on poling of PVF_2 films. Tamura *et al.*[6] detected changes in the polarized infrared spectrum which indicated an orientation of β-form crystallites on poling and this is supported by the changes in the x-ray diffraction pole figure of Kepler[7] for poled and unpoled samples. Southgate[8] reports a significant reduction of the infrared absorption peaks at 762 and 975 cm^{-1}, which have been ascribed to the α form,[9] after poling using a corona charging source at voltages of up to ±6 kV at room temperature.

An attempt has been made in the present study to observe changes in molecular conformation due to corona charging of 16- and 25-μm-thick films of PVF_2 by x-ray diffraction techniques. The films were supplied by the Kureha Chemical Industry Co. Ltd., of Japan. Test samples ~3 cm^2 in area were cleaned with acetone and diffraction patterns were recorded for Bragg angles (i.e., 2θ) between 16° and 23° using the step scanning technique and Ni-filtered Cu-K radiations. The samples were then corona charged at room temperature to a surface potential ±6 kV using a similar technique to that of Southgate[8] and diffraction patterns redetermined. The results are shown in Figs. 1 and 2. Table I provides a summary of the peak positions observed (i.e., 2θ values) in the present work and the corresponding crystallographic data of PVF_2 (without corona charging) due to Hasegawa *et al.*[10] Although no internal standard

TABLE I. Summary of x-ray diffraction results of PVF_2 films (before and after corona charging).

Sample thickness ($\times 10^{-6}$ m)	Crystallographic data due to Hasegawa *et al.* Bragg angle $2\theta°$	Crystalline form	Crystallographic plane	Diffraction data (present work) Before corona charging Bragg angle $2\theta°$	Area (arbitrary units)	Integral breadth (rad)	After corona charging Bragg angle $2\theta°$	Area (arbitrary units)	Integral breadth (rad)
16	17.9	α	(100)	17.7	11.2	...	17.7	1	...
	18.4	α	(020)	18.4	3.4	...	18.4	1	...
	20.1	α	(110)	20.0	54.52	0.00614	19.4	3.3	...
	20.85	β	Composite peak (110) + (200)	20.7	45.16	0.00636	20.16	65.25	0.00883
25	20.1	α	(110)	20.15	76.5	0.00448	19.9	11.2	...
	20.85	β	Composite peak (110) + (200)	20.9	93.5	0.00537	20.6	109.6	0.00846

has been used in the present work for calibration of the spectra, the discrepancies between the observed 2θ values and those of Hasegawa *et al.*[10] do not produce differences in the magnitudes of the relevant lattice parameters in excess of 2%. It should be pointed out that there is a positional uncertainty of 2θ values in the present work, not exceeding 0.1°, associated with the mounting of the sample. As the structure factor due to the (110) peak alone in the composite β-form peak at $2\theta \simeq 20.85°$ (Table I, Hasegawa *et al.*[10]) is about 4.6 times greater than that of the other components of the peak, i.e., (200) peak,[11] this composite peak will be labelled as the (110) β-form peak henceforth.

It may be observed from Fig. 1 that after the application of corona charging the (100) and (020) α-form peaks are almost completely removed and are just visible above the background level. This was the case also for the 25-μm-thick sample. The intensity of the (110) α-form peak was observed to diminish with increasing surface potential due to corona charging. Thus for the case of a surface potential of 6 kV, which was the maximum value employed in the present work, the shoulder on the lower angle side of the (110) β-form peak (Fig. 1) may be attributed to the much reduced (110) α-form reflection rather than being a new peak. The (110) α-form and (110) β-form peaks have been resolved in Figs. 1 and 2 to show distinctly the pronounced effect of corona charging. For the sake of clarity, the diffraction pattern of the 25-μm-thick film has been shown in Fig. 2 for a restricted range of 2θ values where the (110) α-form peak, which is much reduced, may be distinctly observed as a shoulder on the (110) β-form profile after corona charging. These large reductions in the areas under the three α-form peaks (see Table I) and the observed significant increase in the area under the (110) β-form profile after corona charging indicates a change in the molecular conformation (i.e., a reduction in α-form crystallites and an increase in the β-form crystallites) in PVF_2 films which would be in

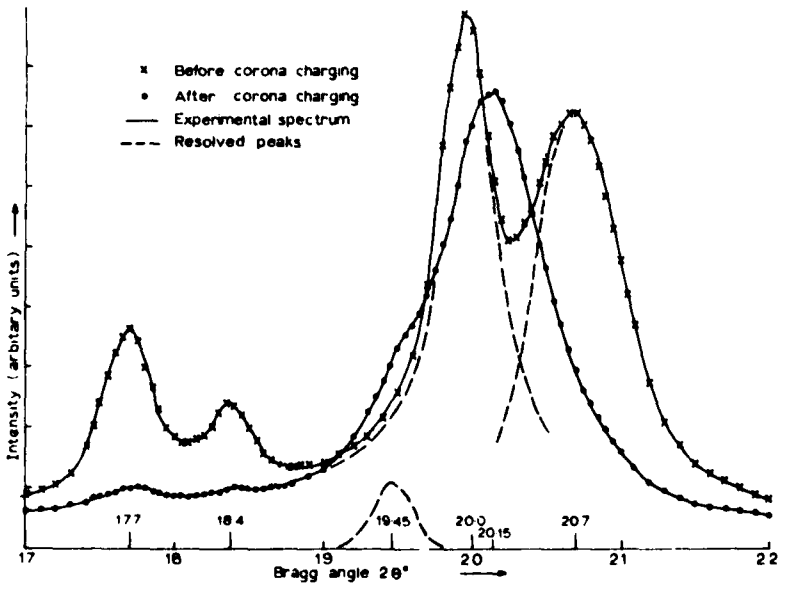

FIG. 1. X-ray diffraction spectra of 16-μm-thick sample of PVF_2 before and after corona charging.

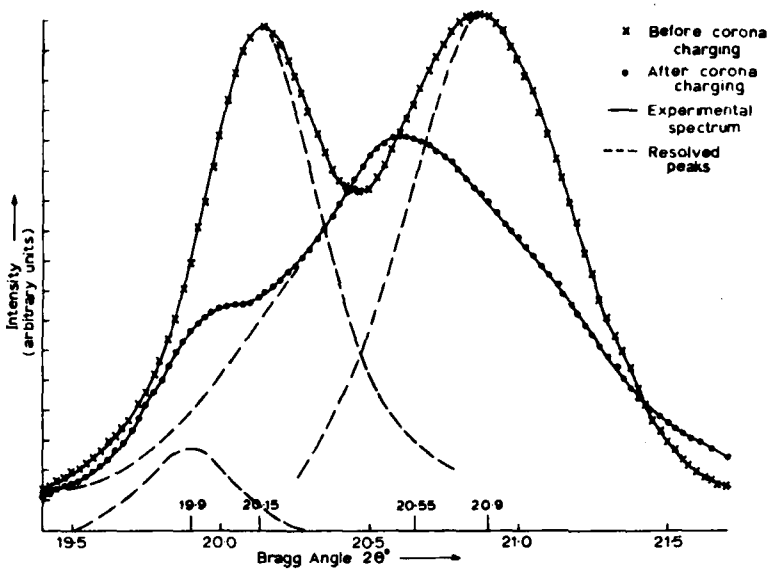

FIG. 2. X-ray diffraction spectra of 25-μm-thick sample of PVF_2 before and after corona charging.

agreement with Southgate.[8] Furthermore, the linewidths (i.e., integral breadth) of the (110) β-form diffraction profiles were also observed to increase significantly [Figs. 1 and 2 and Table 4 (Ref. 10) after corona charging] which would indicate a decrease in the β-form crystallite size and/or an increase in the lattice distortion.

Finally, it may be observed from Figs. 1 and 2 that after corona charging the peak positions (i.e., 2θ values) of the (110) diffraction profiles, in particular, the β-form peak (Fig. 1) shifted to a lower value by more than 0.5° (Table 5, Ref. 10), which is significantly greater than the positional uncertainty (i.e., $\pm 0.1°$) in the present work. This corresponds to an increase in an interplanar separation of over 3%.

A possible explanation of the results may be as follows. The high electric field stress caused by corona charging may have an effect on the PVF_2 film analogous to that of a mechanical stretching or rolling. It is established that such mechanical treatments may cause the carbon-carbon backbones to be aligned preferentially with the surface plane[11] (i.e., 110 planes). Under the action of a high electric field the electrostatic force might compress the film thickness, which in turn may relax the C-C-C bond angles thereby increasing the C-C separation. As a consequence, the fluorine atoms in the α form may be able to overcome the stearic hinderance and the C-F bonds can flip over, producing a structure resembling to that of the β form. Similar expansions may not occur in the (100) and (020) directions because of the restrictions on the separations of the individual chains. Furthermore, the high internal energy due to the coupling of the C-F dipoles in the β form would cause the crystallites to remain aligned in their own molecular field even when surface charges are removed.

Further work is in progress at present, using an internal standard, to determine quantitatively changes in lattice dimensions and distortions, crystallite size and orientation, and crystallinity in PVF_2 after corona charging.

[1]K. Okuda, T. Yoshida, M. Sugita, and M. Asahina, J. Polym. Sci. B 5, 465 (1967).
[2]J. B. Lando, H. G. Olf, and A. Peterlin, J. Polym. Sci. A-1 4, 941 (1966).
[3]W. W. Doll and J. B. Lando, J. Macromol. Sci. Phys. B 4, 889 (1970).
[4]M. Oshiki and E. Fukada, Jpn. J. Appl. Phys. 15, 43 (1976).
[5]M. Latour, J. Electrostatics 2, 241 (1977).
[6]M. Tamura, S. Hagiwara, S. Matsumoto and N. Ono, J. Appl. Phys. 48, 513 (1977).
[7]R. G. Kepler, Proc. Piezoelectric and Pyroelectric Symposium—Workshop 46, 1975 (unpublished).
[8]P. D. Southgate, Appl. Phys. Lett. 28, 250 (1976).
[9]G. Cortili and G. Zerbi, Spectrochim. Acta A 23, 285 (1967).
[10]R. Hasegawa, Y. Takahashi, Y. Chatani, and H. Tadokoro, Polym. J. 3, 600 (1972).
[11]J. H. McFee, J. G. Bergman, Jr., and G. R. Crane, Ferroelectrics 3, 305 (1972).

Corona charging and the piezoelectric effect in polyvinylidene fluoride

D. K. Das-Gupta and K. Doughty

School of Electronic Engineering Science, University College of North Wales, Dean Street, Bangor, Gwynedd, LL57 1UT, Great Britain

(Received 19 January 1978; accepted for publication 9 March 1978)

Biaxially stretched PVF_2 films were poled by corona charging over a range of surface potentials not exceeding 10 kV. Studies of x-ray diffraction patterns are presented together with the measured values of the piezoelectric constant d_{31} of such films. The results indicate that the piezoelectricity in this polymer arises from the dipolar orientation of the polar crystallites.

PACS numbers: 77.60.+v, 73.40.Bf, 68.20.+t

Polyvinylidenefluoride (PVF_2) films may possess simultaneously at least two[1] stable crystalline structures, i.e., a polar form[2] (form 1 or β form) and a nonpolar form[3] (form 2 or α form). It has been established that a single crystal of PVF_2 in the polar form which has an orthorhombic unit cell with a space group[4] $Cm2m(C_{2v}^{14})$ may possess piezo-electricity without being subjected to any external poling process. Murayama *et al*[5] suggest that in PVF_2 film, containing both form 1 and form 2 crystallites, the piezoelectricity and the pyroelectricity may increase with increasing form 1 (polar) content. Southgate[6] shows that on poling of PVF_2 films by corona charging changes in molecular conformation and an enhancement in the pyroelectric coefficient occur. Preliminary studies[7] of x-ray diffraction patterns also indicate that on poling by corona charging at 6 kV a change in molecular conformation from form 2 to form 1 takes place in PVF_2 films, orginally containing both forms. The present study is a continuation of this earlier work, and it may be divided into two parts as follows: (i) a study of x-ray diffraction patterns of (biaxially streched) PVF_2 films 25 μm thick (Kureha) with poling by corona charging at different surface potentials ($\triangleright +10$ kV) and (ii) a study of the corresponding magnitudes of the piezoelectric coefficients of such poled samples.

Poling by corona charging with a zerostat gun[7] and a technique similar to that of Southgate[6] was found to be unsuitable for uniform and repeatable surface potentials of definitive magnitudes on the polymer surface. For the present work, a micromesh control grid was introduced between the sample and the corona point which was connected to an adjustable and stabilized EHT supply. The control grid was connected to a similar but separate EHT supply which was maintained at a potential 3 kV below that of the corona point. Aluminum electrodes were vacuum deposited on one surface of circular samples of 5 cm in diameter, the metalized surface being in contact with an earthed heavy copper plate which was maintained at a constant temperature of 18 °C. Positive charges were deposited on the nonmetalized surface of the polymer, the surface potential being monitored continuously with a Field Mill type electrostatic voltmeter (Model 216, IDB, UCNW, Bangor). In all cases, the surface potential was observed to reach the desired values within 10 sec. after the application of the high-voltage supplies to the corona point and the grid. The poling time employed for each sample was 30 min at the end of which period the nonmetalized surface was earthed temporarily.

A step-scanning technique was employed to obtain the x-ray diffraction profiles of PVF_2 samples using Ni-filtered Cu-Kα radiations with a Philips x-ray diffract-

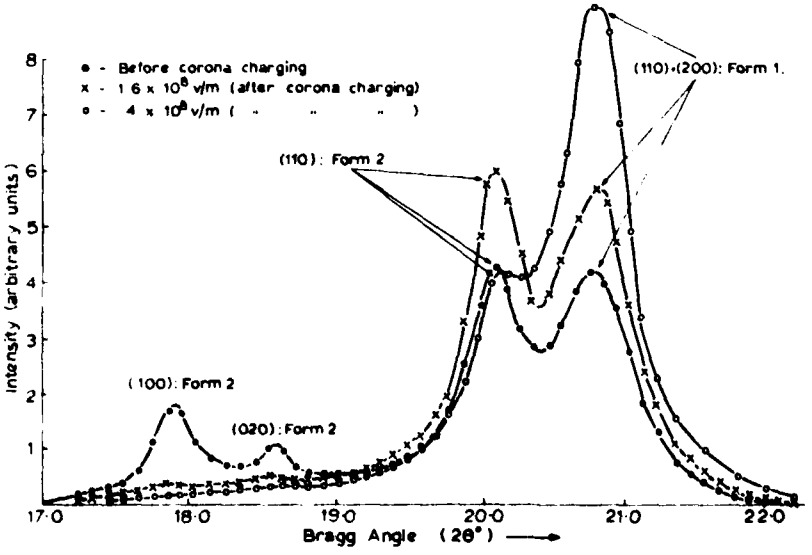

FIG. 1. X-ray diffraction pattern as a function of poling (corona charge) field.

 0021-8979/78/4908-4601$01.10

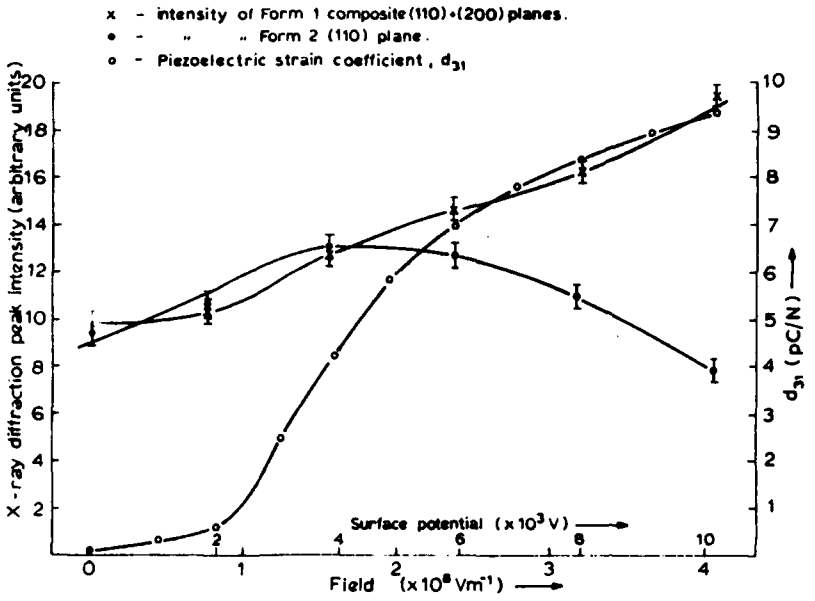

FIG. 2. Magnitude of d_{31} and peak intensities of (110) form 2 and (110)+(200) form 1 as a function of poling (corona charge) field.

ometer (Model PW1050). The evaporated aluminum electrode on one of the surface of the polymer acted as an internal standard in order to ascertain an uncertainty in the value of 2θ, where θ is the Bragg angle, not exceeding 0.1°. Figure 1 shows results of a typical and representative set of defraction profiles of PVF_2 samples which were poled by corona charging at different values of surface potentials. For the sake of comparison, a diffraction profile of an unpoled sample is also provided in Fig. 1, and it may be stated that the respective 2θ values for different structural planes in this profile are in good agreement with those due to Hasegawa *et al.*[4] It may be noted from Fig. 1 that the peak values of the diffracted intensities of the form 2 structural planes (100) and (020) decrease with increasing poling field, and finally their magnitudes become vanishingly small at fields in excess of 1.6×10^8 V m^{-1}. It may also be observed (Fig. 1) that the form 2 (110) peak intensity, on the other hand, first rises with the increasing field, not in excess of $\sim 1.6\times10^8$ V m^{-1} face potential ~4.0 KV) beyond which it decreases rapidly. The composite peak (100)+(200) of form 1, on the other hand, was observed to increase continuously as the poling field was increased. It should be stated that each individual chain molecule of forms 1 and 2 has a dipole moment normal to its chain axis, although in form 2 the chains pack in the antipolar array in a unit cell. Thus it may be expected that each chain, even in form 2, may experience a change in orientation due to the interaction with the poling field. Therefore, it is suggested that the increases in the height of the form 1 composite peak (110)+(200) are due to a change in the orientatation and aligment in the lower-field region which is in agreement with Kepler.[8] The behavior of the form 2 peaks, i.e. (100), (020), and (110), may be explained by a modification of form 2 due to an orientation of the resultant dipole moments of individual chains in the low-field region. Furthermore, with fields in excess of $\sim 1.6\times10^8$ V m^{-1}, a change into a form 1 type of crystallite may be progressively completed. This observation is in agreement with a previous report by the present worker.[7] However, in contrast to the previous work,[7] no peak shifts in 2θ values were observed with the present method of corona charging even for the highest surface potential employed (i.e., 10 kV or a field of 4×10^8 V m^{-1}). Although, unlike in the present work, an internal standard was not used in the previous work,[7] the observed peak shifts for both form 1 (110)+(200) and form 2 (100) profiles with corona charging by a zerostat gun were well outside the limits of measurements and setting errors. The reason for this discrepancy is not understood but may be due partly to a higher localized poling by the zerostat gun.

Following the x-ray analysis, a second aluminum electrode was evaporated on the other surface of the poled samples which was then left for 24 h with the electrodes short circuited. The piezoelectric coefficient d_{31} was then measured for samples poled at different surface potentials using a conventional static method of the release of a fixed weight at a constant temperature using an electropneumatic solenoid valve. A Tektronix Storage Oscilloscope (Mode 549 with a 1 A7 amplifier) was used to monitor the piezoelectric charge. Figure 2 shows the variation of d_{31} with poling fields together with the changes in the peak values of form 2 (110) and form 1 (110)+(200) diffraction profiles. The behavior of the piezoelectric coefficient d_{31} (Fig. 2) as a function of the poling field (or surface potential after corona charging) may be observed to be similar to that of the pyroelectric coefficient with the permanent polarization in PVF_2 after corona charging (Ref. 6).

It is suggested that up to a poling field of $\sim 1.6\times10^8$ V m^{-1}, the piezoelectricity in PVF_2 may arise from dipolar orientations of both form 1 crystallites and the new intermediate modifications of form 2 crystallites. Above this field, the piezoelectricity in this polymer

may be entirely due to the dipolar orientation of the form 1 type of molecules.

Finally, it may be stated that corona charging of polymer films at ordinary temperatures may be more satisfactory method of poling than the conventional method employed at elevated temperatures for comparable values of the piezoelectric coefficients.

This work is financially supported by a reserach grant from the U.S Army.

[1]K. Okuda, T. Yoshida, M. Sugita, and M. Asahina, J. Polym. Sci. B 5, 465 (1967).
[2]J. B. Lando, H. G. Olf and A. J. Peterlin, J. Polym. Sc A 4, 941 (1966).
[3]W. W. Doll and J. B. Lando, J. Macromol Sci. Phys. E 309 (1970).
[4]R. Hasegawa, Y. Takahashi, Y. Chatani, and H. Tadol Polym. J. 3, 600 (1972).
[5]N. Murayama and H. Hashizumi, J. Polym. Sci. Polyı Phys. Ed. 14, 989 (1976).
[6]P. D. Southgate, Appl. Phys. Lett. 28, 250 (1976).
[7]D. K. Das-Gupta and K. Doughty, Appl. Phys. Lett. 31 (1977).
[8]R. G. Kepler and R. A. Anderson, J. Appl. Phys. 49, 1 (1978).

J. Phys. D: Appl. Phys., Vol. 11, 1978. Printed in Great Britain

Piezo- and pyroelectric behaviour of corona-charged polyvinylidene fluoride

D K Das-Gupta and K Doughty
School of Electronic Engineering Science, University College of North Wales, Dean Street, Bangor, Gwynedd LL57 1UT

Received 28 June 1978

Abstract. Biaxially stretched polyvinylidene fluoride (PVF_2) films of 25 μm thickness were poled by corona charges at surface potentials of 10 and 5 kV. X-ray diffraction studies suggest that structural changes from the non-polar Form 2 type to the polar Form 1 type occur, via an intermediate polar Form 2 type, in PVF_2 on corona charging. The similarity in behaviour of the reversible pyroelectric coefficient p, and the piezoelectric strain coefficient d_{31} with temperature suggest that these two phenomena in PVF_2 may have a common origin.

1. Introduction

Polyvinylidene fluoride (PVF_2) is a semi-crystalline polymer which may exist in at least two stable forms simultaneously, i.e., a planar zig-zag (all-trans conformation) polar form (Form 1 or β-form) with two monomer units (—CH_2—CF_2) per unit cell belonging to the space group $C_mC2_m(C_{2v}^{14})$ (Lando *et al* 1966, Hasigawa *et al* 1972) and the T–G–T–G′ form (Form 2 or α-form) with the space group $P2_1/C(C_{2h}^5)$ (Doll and Lando 1970). In the Form 1 unit cell structure the dipole moments of each monomer unit (2·1 *D*) are parallel to each other and oriented in a direction perpendicular to the polymer chain axis (Nakamura and Wada 1971). As a result, there is a net dipole moment within the Form 1 type unit cell. In the T–G–T–G′ conformation there is also a dipole moment normal to the chain axis, but in the Form 2 unit cell the adjacent chains pack with their dipoles in an antiparallel array. Thus the Form 2 unit cell has no net dipole moment. Thus a single crystal of PVF_2 Form 2 structure may not be expected to be piezo- or pyroelectric whereas the Form 1 type structure will exhibit these effects without any external poling. A poling may be achieved by applying a high electrical stress to the polymer at an elevated temperature for an extended period of time and subsequently cooling the specimen to the ambient temperature in the presence of the external electric field (i.e. conventional poling). The relationship between the dielectric displacement D, the electric field F, the relative permittivity ϵ_r and the frozen-in non-equilibrium polarisation P is given by

$$D = \epsilon_0 \epsilon_r F + P \tag{1}$$

where ϵ_0 is the permittivity of free space. For $F=0$, i.e. with a short-circuited poled sample, we have from equation (1)

$$\left|\frac{\partial D}{\partial S}\right|_{F=0,T} = \left|\frac{\partial P}{\partial S}\right|_{F=0,T} = \left|\frac{\partial Q/A}{\partial S}\right|_{F=0,T} \simeq \frac{1}{A}\left(\frac{\partial Q}{\partial S}\right)_{F=0,T} \tag{2}$$

where S is the stress, Q the charge liberated, A the electrode area and T the temperature.

0022-3727/78/0017-2415 $02.00

The piezoelectric strain coefficient is defined thus:

$$d_{ij}=\frac{1}{A}\left(\frac{\partial Q}{\partial S}\right)_{F=0,\,T} \tag{3}$$

where $i=1$, 2 and 3 and $j=1$, 2, 3, 4, 5 and 6. Similarly, the pyroelectric coefficient may be expressed thus:

$$p=\frac{1}{A}\left(\frac{\partial Q}{\partial T}\right)_{F=0,\,S}=\frac{1}{A}\frac{\partial Q}{\partial t}\cdot\frac{\partial t}{\partial T}=\frac{1}{A}I\frac{\mathrm{d}t}{\mathrm{d}T} \tag{4}$$

where I is the short-circuited current through the sample and $\mathrm{d}T/\mathrm{d}t$ is its rate of rise of temperature.

The piezoelectric matrix components for PVF_2 with Form 1 structure with the space group C_{2v} are as follows (Nye 1957):

$$d_{ij}=\begin{pmatrix}0 & 0 & 0 & 0 & d_{15} & 0\\ 0 & 0 & 0 & d_{24} & 0 & 0\\ d_{31} & d_{32} & -d_{33} & 0 & 0 & 0\end{pmatrix} \tag{5}$$

and the corresponding pyroelectric components are

$$p=\begin{pmatrix}0\\ 0\\ -p_3\end{pmatrix}. \tag{6}$$

Ogasawara *et al* (1976) and also Murayama and Hashizumi (1976) have shown that for identical poling conditions the piezo- and pyroelectricity in PVF_2 are linearly related with each other. It is also established that the piezoelectricity in PVF_2 increases with increasing Form 1 contents (Murayama *et al* 1975). Wada and Hayakawa (1976) review the piezo- and pyroelectric properties and the nature of their origin in PVF_2.

It has been shown that a significant structural change from Form 2 to Form 1 may occur on corona poling of PVF_2, originally containing both the forms (Southgate 1976, Das-Gupta and Doughty 1977, McKinney and Davis 1978).

The present work reports the results of a study of the structural behaviour and its relevance on d_{31} and p after repeated thermal cycling of corona-charged PVF_2 films.

2. Experimental details

25 μm thick biaxially stressed PVF_2 films containing both Form 1 and Form 2 type of crystallites were employed in this work and the films were kindly provided by the Kureha Chemical Industries Company Limited of Japan. Aluminium electrodes of 5 cm in diameter were vacuum-deposited on one surface of each sample which was then held under pressure between two short-circuited aluminium plates and conditioned in an oven at a constant temperature of 120 °C for 15 h. X-ray diffraction profiles of each sample were subsequently obtained for a 2θ range of 17–22°, where θ is the Bragg angle, using CuKα radiations and a step-scanning technique as described in a previous work (Das-Gupta and Doughty 1978). The evaporated aluminium electrode on one face of each sample acted as an internal standard and the uncertainty in the observed value of 2θ at the peak of a diffraction profile did not exceed 0·1°. Pairs of samples were then corona-

charged at a time by a method described elsewhere (Das-Gupta and Doughty 1978) for 100 s to the desired values (i.e. +5 kV and +10 kV) of the surface potential. X-ray diffraction patterns for each of the corona charged pair of samples were recorded for the same range of 2θ values, described above. Each sample was then shorted between two sheets of aluminium for 24 h at 20 °C. Following this procedure, conducting silver paste was painted on the non-metallised surface of each sample which was then mounted on a circular aluminium block of 5 cm in diameter, located on a copper heating block. A programmed power supply was employed to raise the temperature of the sample from 20 to 90 °C at a heating rate of 2 °C min^{-1}, the temperature being recorded continuously by a Keithley electrometer, Type 602. The cooling of the sample from a high temperature to ambient condition was achieved with liquid air in an evacuated double-walled liquid dewar which was attached to the copper heating plate. After the first thermal cycle (i.e. 20°–90°–20 °C) the magnitude of short-circuited current through the specimen was observed to be repeatable on successive runs. The electrode of silver paste was then removed with acetone and the x-ray diffraction pattern of the corona-poled sample was obtained again.

A second aluminium electrode was then vacuum-deposited on the non-metallised surface of the other sample of the corona-charged pair which was then left for 24 h with the electrodes short-circuited. The piezoelectric strain coefficient d_{31} of this specimen was subsequently measured in a temperature controlled oven using a conventional static method of releasing weight by means of an electropneumatic solenoid valve. A standard mica capacitor was connected in parallel with the sample and the voltage developed across it due to the release of charges was monitored with a Type 549 Tektronix storage oscilloscope and a Type 1A7 amplifier. These measurements were carried out with each sample at steps of 5 °C in the temperature range of 20–90 °C with a rate of rise of temperature of 4 °C min^{-1} and d_{31} values were computed. The sample was then allowed to cool to 20 °C before further measurements of d_{31} were made for the second and further subsequent thermal runs. Finally, the behaviour of d_{31} with annealing at temperatures up to 150 °C was investigated in which the sample was subjected to each annealing temperature for 15 h under short-circuited conditions.

3. Results

Figure 1 shows the effects of corona charging on the structure of PVF_2, originally containing both Form 1 and Form 2 crystallites. The observed 2θ values, i.e. angular positions of diffracted peak intensities, for respective structural planes for the unpoled specimen are in good agreement with Hasegawa *et al* (1972). It may be noticed that whilst the peak intensities of Form 1 composite profile of (110)/(200) planes and Form 2 (110) plane increase those of Form 2 (100) and (020) planes become vanishingly small (see figure 1) on corona poling at a potential of 5 kV. However, on increasing the charging potential to 10 kV, the Form 2 (110) peak intensity was observed to reduce significantly whilst that of the Form 1 composite peak (110)/(200) enhanced considerably. These observations are in agreement with those previously reported by the present workers (Das-Gupta and Doughty 1978).

A typical behaviour of thermally stimulated (short-circuit) currents (TSC) for the first heating cycle with PVF_2 films, poled at two different surface potentials of 5 and 10 kV, are shown in figure 2. Both curves display a broad peak at ~49 °C and have similar profiles to those reported by other workers (Cresswell *et al* 1972, Pfister and

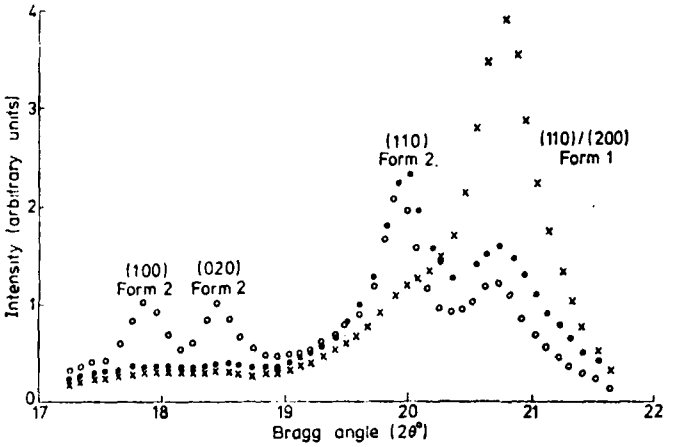

Figure 1. X-ray diffraction patterns of 25 μm thick PVF_2 film before (○) and after corona poling to (●) 5 kV, (×) 10 kV.

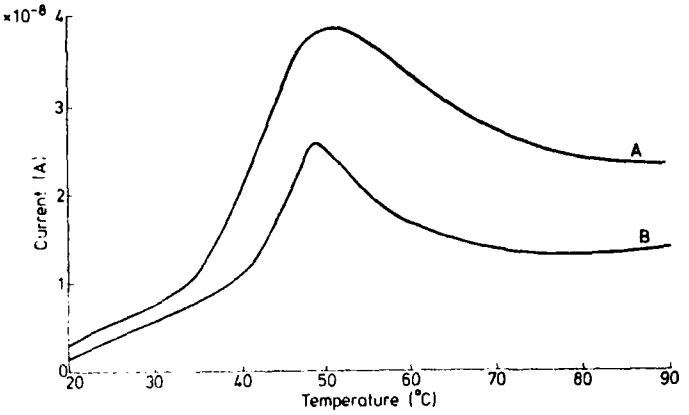

Figure 2. Thermally stimulated current (TSC) during the first heating cycle (irreversible) in corona charged PVF_2 film of 25 μm thickness: A, Corona potential 10 kV, charging time 100 s and charging temperature 20 °C; B, Corona potential 5 kV, otherwise as in A.

Abkowitz 1976, Sharp and Garn 1976). In figure 3 are presented the typical behaviour of the true (i.e. reversible) pyroelectric currents for the second and successive cycles with temperature, which are about an order of magnitude lower than those for the TSC currents (irreversible), observed during the first cycle (figure 2). The pyroelectric coefficient p was calculated from these plots (figure 3) using equation (4) and the magnitude of p in curve A (figure 3, 10 kV case) appears to be $\sim 3 \times 10^{-5}$ C m^{-2} K^{-1} at 20 °C, rising to a value of 8×10^{-5} C m^{-2} K^{-1} at 90 °C. The corresponding values of p for curve B (figure 2, 5 kV case) are $\sim 2 \times 10^{-5}$ C m^{-2} K^{-1} and 6×10^{-5} C m^{-2} K^{-1} respectively. The largest yet reported magnitude of p at room temperature for conventionally poled PVF_2 (Peterson *et al* 1974) is $4{\cdot}1 \times 10^{-5}$ C m^{-2} K^{-1} which is in good agreement with the present work in which corona poling has been employed. The magnitude p (figure 3) seems to increase linearly with temperature up to ~ 60 °C beyond which there is evidence of super-linear rate of increase which is also in agreement with other workers (Burkard and

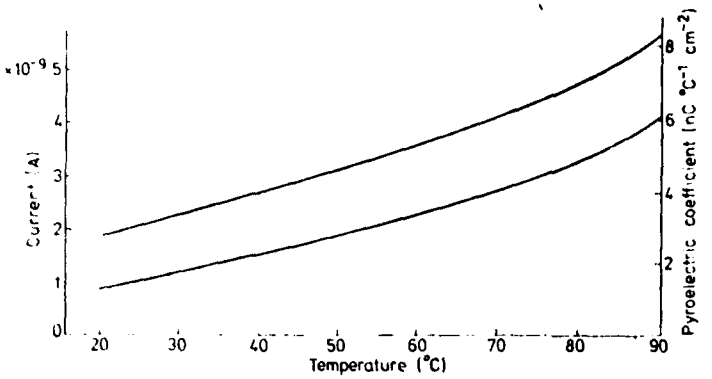

Figure 3. Thermally stimulated current (reversible) during the second heating cycle and the pyroelectric coefficient with corona charged PVF_2 film of 25 μm thickness. Poling conditions for curves A and B are the same as in figure 1.

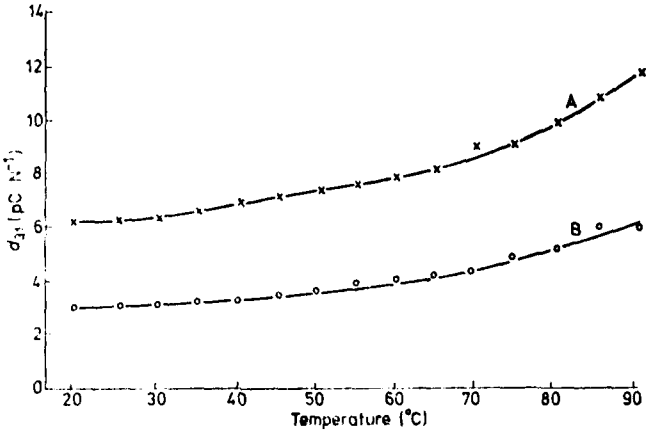

Figure 4. The behaviour of the (reversible) piezoelectric strain coefficient d_{31} of corona charged PVF_2 film of 25 μm thickness. Poling conditions for curves A and B are the same as in figure 1.

Pfister 1974, Sharp and Garn 1976). The temperature dependence of the (reversible) piezoelectric strain coefficient d_{31} for the two different poling conditions is shown in figure 4. The magnitude of d_{31}, observed in the present work, with the corona-poled samples, is in agreement with that observed by other workers (Murayama *et al* 1975, Kepler and Anderson 1978a,b) using conventional poling technique at comparable electrical stresses. Figure 5 shows that repeated cycling from 20–90 °C has little effect on the structure of corona-poled PVF_2 films. Finally, figure 6 is a plot of normalised values of d_{31} as a function of the annealing temperature and it shows that approximately half the activity still remains even after annealing at 140 °C. It may be mentioned that with conventionally poled samples Pfister *et al* (1973) observed the polarisation to decay markedly in PVF_2 at a temperature ~ 100 °C.

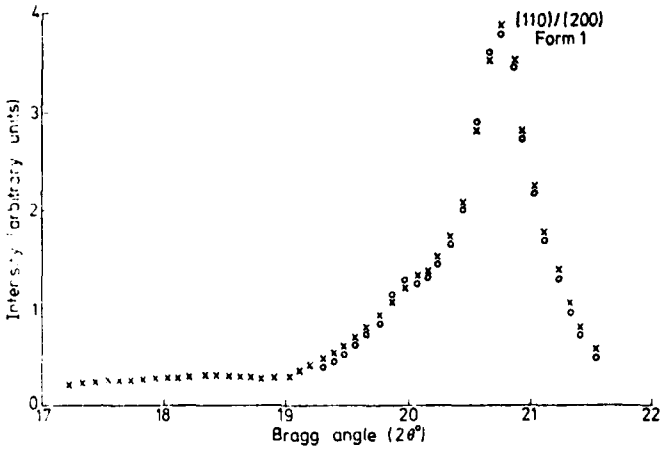

Figure 5. Effect of thermal aging on the x-ray diffraction profiles of corona-charged (10 kV case) PVF_2 film of 25 μm thickness: × before thermal cycling, ○ after several thermal cycles between 20-90 °C.

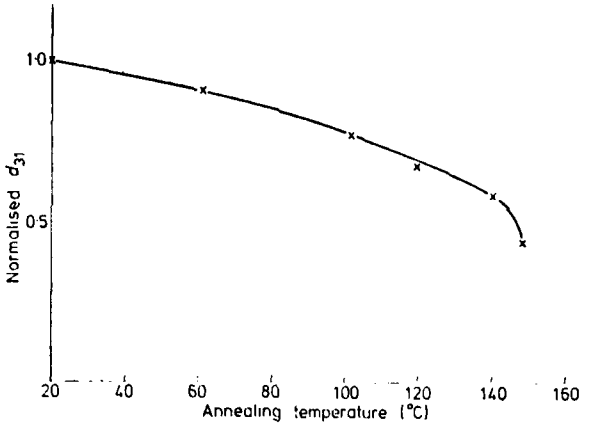

Figure 6. Decay of d_{31} (normalised) as a function of annealing temperature.

4. Discussion

It is obvious from figure 1 that the (corona) poling has a significant influence on the structure of both Form 1 and Form 2 crystallites in PVF_2. It is established that the piezoelectric response may be considerably enhanced on poling of this polymer, containing mostly Form 2 type crystallites, at a DC field of $7{\cdot}8 \times 10^7$ V m^{-1} and subsequently annealed.

In view of the above observations and assuming that a model of dipolar orientation on poling to be responsible for the induced piezo- and pyroelectricity in both Form 1 and Form 2 PVF_2 (Mopsik and Broadhurst 1975), the observed enhancement of the diffraction peak intensity of the Form 2 (110) plane in the present work (figure 1) may be explained in the following manner (Das-Gupta and Doughty 1978, Davis *et al* 1978).

On corona poling (5 kV case) of PVF_2 films containing both Form 1 and Form 2 crystallites, a conversion of Form 2 unit cell to a polar intermediate form, but still maintaining the T–G–T–G′ structure of the polymer chains, may occur due to only a rotation of alternate chains about the chain axis through 180° without any alteration in the (Form 2) unit cell dimensions. The stability of such an intermediate polar form with the unit cell dimensions of the Form 2 structure, may not violate the conditions for the minimum potential energy requirement (Farmer *et al* 1972). Such a model will also explain the observed reduction of the peak heights in the reflection–diffraction profiles of Form 2 (100) and (020) planes. The increase in the height of the Form 1 composite peak (110)/(200) (figure 1) is due to an orientation and alignment of the dipoles due to corona-poling which is in agreement with Kepler *et al* (1978a, b). On further increase of the corona poling voltage (10 kV) a conformational change occurs in which the intermediate polar form is finally converted to a polar zig-zag Form 1 type of structure. This is also in agreement with Das-Gupta and Doughty (1978) and Davis *et al* (1978).

There is as yet no definitive knowledge on the origin of piezo- and pyroelectricity in PVF_2 which may arise from two causes: (i) oriented dipoles and (ii) trapped charges in the bulk. Wada and Hayakawa (1976) observe that the unit cell structure of Form 1 crystal has a large spontaneous polarisation, P_f of 0·13 C m^{-2} which increases with increasing poling field. An integration of the liberated (irreversible) charges for the first TSC runs for the curves A and B in figure 2 yields polarisation values of ~0·02 and 0·01 C m^{-2} respectively. Pfister *et al* (1973) show that such irreversible polarisation is approximately proportional to the (conventional) poling field which is in agreement with the present work where corona poling was employed. The activation energies, calculated from the initial slope to the peak positions of the curves A and B in figure 2 (Garlick and Gibson 1948) were found to be 1·4 and 1·2 eV. For these calculations (i.e. polarisation and activation energies) the reversible pyroelectric currents were subtracted out from the irreversible TSC currents of the first cycles. The values obtained for the activation energies in this work are lower than those due to Sharp and Garn (1976) who, however, point out that the position and the magnitude of TSC peaks are dependent on the time interval between the poling and the measurement, i.e., 'rest-time'. The activation energy values would indicate the energy levels of the traps in the bulk of the polymer from which space charges are irreversibly liberated during the first cycle of the TSC run.

An integration of the pyroelectric currents in curves A and B from 20 to 90 °C (figure 3) produces values of ~0·004 and 0·002 C m^{-2} respectively for the residual polarisation P_r, in the bulk of the polymer, which are about 20% of the magnitudes of the irreversible space charge polarisation (curves A and B, figure 2). These values of P_r are similar to those obtained by Oshiki and Fukada (1976).

Using a rigid dipole model, Lines and Glass (1977) estimate for the pyroelectric coefficient

$$p=\frac{dP}{dT}=0{\cdot}07E\times 10^{-5}\ \text{C cm}^2\ \text{K}^{-1} \tag{8}$$

where E is in 10^8 V m^{-1}. The experimentally observed values of p in the present work (curves A and B in figure 3) are considerably higher than those predicted by the equation (8). Thus the assumption of rigid dipoles may not be valid which is in agreement with Lines and Glass (1977) who further add that a rotation of C—F and C—H bonds with temperature may be the dominant mechanism for pyroelectricity in PVF_2. In this respect a small change in the x-ray pole figure has indeed been noticed by Kepler *et al* (1975) after poling Form 1 type PVF_2 films. It may also be noted that the crystallinity

of polyethylene was observed to decrease from 67% to 57% on increasing the temperature from 25 to 110 °C (Kavesh and Shultz 1970). Following this argument, Kepler and Anderson (1978) observe that if similar changes in crystallinity were to occur in PVF_2, the magnitude of the pyroelectric coefficient would be $5{\cdot}9 \times 10^{-5}$ C m^{-2} K^{-1}. However, such a change in crystallinity in PVF_2 with temperature has yet to be reported. Tamura *et al* (1977), on the other hand, suggest that the origin of piezo- and pyroelectricity in PVF_2 is dipolar orientation of the Form 1 type of crystals, embedded in the amorphous phase, along the direction of the poling field. They, however, add that the occurrence of such an orientation may be subject to the degree of crystallinity and the crystallite size.

In view of the similarity in behaviour of the pyroelectric coefficient p (figure 3) and the piezoelectric strain coefficient d_{31} (figure 4) in PVF_2, it may be suggested that the two phenomena have a common origin. Furthermore, the polarity of p was observed to be opposite that of d_{31} in the present work. Following Nakamur and Wada (1971) it may thus be argued that the origin of the two phenomena in this polymer is dipolar orientation and not embedded true charges, distributed asymmetrically in the bulk. There is, however, a possibility that a part of the pyroelectricity observed in this polymer may, in fact, be of secondary nature, arising due to the piezoelectricity when the specimen undergoes thermal expansion against its constraints. Such a possibility has, of course been discussed by Kepler and Anderson (1978). It may be observed from figures 3 and 4 that p and d_{31} are linearly related with each other for identical poling conditions. This is in agreement with Murayama and Hashizumi (1975) and Ogasawara (1976) also employed the conventional poling technique.

Finally, it is suggested that the corona charging may be a useful method as the dielectric may be poled at room temperature in a very short period of time without any sacrifice of the magnitudes of the pyro- and piezoelectric responses. The present results also indicate that the origin of the pyro- and piezoelectricity in PVF_2 with corona poling may not be different from that with the conventional poling. Furthermore, it appears that a PVF_2 film, poled by corona charging at room temperature, is structurally stable (figure 5) and retains a significant percentage of the piezoelectric strain coefficient (figure 6) d_{31}, even at 140 °C which is well above its poling temperature.

Acknowledgments

This work is being financed by a research grant from the U.S. Army. One of the authors (KD) is also grateful to the Science Research Council of Great Britain for a research studentship. It is a pleasure to express our gratitude to Dr G T Davis of the National Bureau of Standards, Washington, DC, and Dr R Shuford of the Army Materials and Mechanics Research Centre, Watertown, Ma, USA, for many useful discussions and a supply of PVF_2 films during the progress of this work. The authors would also like to thank Kureha Chemical Industries Company Limited of Japan for the generous supply of PVF_2 films.

References

Burkard H and Pfister G 1974 *J. Appl. Phys.* **45** 3360–4

Creswell R A, Perlman M M and Kabayama M A 1972 *Dielectric Properties of Polymers* ed. F E Karasz (New York: Plenum) pp 295–312

Das-Gupta D K and Doughty K 1977 *Appl. Phys. Lett.* **31** 585–7
—— 1978 *J. Appl. Phys.* **49** 4601–3
Davis G T, McKinney J E, Broadhurst M G and Roth S C 1978 *J. Appl. Phys.* to be published
Doll W N and Lando J B 1970 *J. Macromol. Sci.—Phys.* **B4** (4) 309–29
Farmer B L, Hopfinger A J and Lando J B 1972 *J. Appl. Phys.* **43** 4293–303
Garlick G F J and Gibson A F 1948 *Proc. Phys. Soc.* A **60** 574–91
Hasegawa R, Takahashi Y, Chatani Y and Tadokoro H 1972 *Polymer J.* **3** 600–10
Kavesh S and Shultz J M 1970 *J. Polym. Sci.* A-2 **8** 243–76
Kepler R G and Anderson R A 1978a *J. Appl. Phys.* **49** 1232–5
—— 1978b *J. Appl. Phys.* to be published
Kepler R G, Graeber E J and Beeson P M 1975 *Bull. Am. Phys. Soc.* Ser 2 **20** 350
Lando J B, Olf H G and Peterlin 1966 *J. Polym. Sci.* A-1 **4** 941–51
Lines M E and Glass A M 1977 *Principles and Applications of Ferroelectrics and Related Materials* (Oxford: Clarendon Press) p 558
McKinney J E and Davis G T 1978 *Organic Coatings and Plastics Chemistry* **38** 271–7
Mopsik F I and Broadhurst M G 1975 *J. Appl. Phys.* **46** 4204–7
Murayama N and Hashizumi H 1976 *J. Polym. Sci., Polym. Phys. Ed.* **14** 989–1003
Murayama N, Oikawa T, Katto T and Nakamura N 1975 *J. Polym. Sc., Polym. Phys. Ed.* **13** 1033–47
Nakamura K and Wada Y 1971 *J. Polym. Sci.* A-2 **9** 161–73
Nye J F 1957 *Physical Principles of Crystals* (Oxford: Clarendon Press) p 110
Ogasawara K, Shiratori K and Tamura M 1976 *Rep. Prog. Polym. Phys., Japan* **19** 313–6
Ohigashi H 1976 *J. Appl. Phys.* **47** (3) 949–55
Oshiki M and Fukada E 1976 *Japan. J. Appl. Phys.* **15** 43–52
Peterson R L, Day G R, Gruzensky P M and Phelan R J (Jr) 1974 *J. Appl. Phys.* **45** (8) 3296–303
Pfister G and Abkowitz M A 1974 *J. Appl. Phys.* **45** (3) 1001–8
Pfister G, Abkowitz M and Crystal R G 1973 *J. Appl. Phys.* **44** (5) 2064–71
Sharp E J and Garn L E 1976 *Appl. Phys. Lett.* **29** 480–2
Southgate P D 1976 *Appl. Phys. Lett.* **28** 250–2
Tamura M, Hagiwara S, Matsumoto S and Ono N 1977 *J. Appl. Phys.* **48** 513–21
Wada Y and Hayakawa R 1976 *Japan. J. Appl. Phys.* **15** 2041–57

PUBLICATION G.

THE AGEING OF CORONA CHARGED POLYVINYLIDENE-FLUORIDE (PVF_2)

D. K. Das-Gupta & K. Doughty
School of Electronic Engineering Science
University College of North Wales
Dean Street, Bangor, Gwynedd, LL57 1UT, G.B.

Abstract

The effect of ageing due to annealing of corona charged PVF_2 films has been studied by observations of (i) changes in the X-ray diffraction patterns and (ii) decay of the piezoelectric strain coefficient d_{31}. Annealing at progressively higher temperatures was observed to produce a gradual depolarization although considerable piezoelectricity was still remanent even at 150°C. The structural morphology of the corona charged PVF_2 was not significantly altered by annealing at temperatures up to 150°C.

1. Introduction

There is a great need of new materials associated with significant piezoelectric and pyroelectric responses which may be used in a wide range of measurement technology including non-linear optics, acoustic detection and thermal imaging. Polymeric materials, because of their simplicity of fabrication, economy, flexibility, toughness and sensitivity to changes in pressure and temperature are obviously attractive for useful applications mentioned above, although their piezoelectric and pyroelectric responses are considerably less than those of ceramics and other ferroelectric compounds, such as tryglycine sulphate (TGS). Polyvinylidenefluoride (PVF_2) has attracted much attention recently because it has the highest piezo- and pyroelectric coefficients among polymeric materials. Furthermore, it is a semi-crystalline polymer and the glass transition temperature of its non-crystalline phase is well below ordinary temperatures ($T_c \sim -51$°C). PVF_2 may possess at least two stable crystalline structures, i.e. the planar zig-zag polar form (Form 1 or β-form)[2] with a dipole moment of 2.1 D[3] which is oriented along the b-axis (perpendicular to chain axis) and the non-polar T-G-T-G Form 2 (i.e. α-form)[4]. Murayama et al[5] show that the piezoelectric response in PVF_2 increases with increasing Form 1 contents with the same poling (conventional technique) conditions. The conventional technique of poling is to subject the polymer to a high electrical stress at a suitable elevated temperature and then cool it down to ambient temperature in the presence of externally impressed electric field. It has also been suggested that the piezo- and pyroelectric coefficients in PVF_2 are linearly related[6,7] with each other for identical poling (conventional technique) conditions. It is established that the piezo- and pyroelectricity in PVF_2 are enhanced by poling with high electric field as described above. Oshiki & Fukada[8] suggest that a conformational change from Form 2 to Form 1 (i.e. polar) may occur on stretching and such poling of PVF_2 films, originally containing both the forms. This is in agreement with the infrared[6,10,11], Raman[9] and X-ray diffraction studies[12] of other workers. These facts are in agreement with the observations that the piezo- and pyroelectricity in PVF_2 are due to one of the two following mechanisms: (i) strain and temperature dependence of spontaneous polarization[13] (i.e. dipolar model) and (ii) heterogeneity and embedded charges in the film[14].

Recently Southgate[15] has shown that instantaneous poling of PVF_2 may be accomplished at ambient temperature by corona charging. In this work he observed a significant change in molecular conformation from Form 2 to Form 1 in PVF_2, originally containing both the forms, after corona charging. These results have also been confirmed by X-ray diffraction studies[16] of corona charged PVF_2. These facts tend to suggest that a dipolar orientation in crystalline and(or) amorphous phase may occur in PVF_2 with both conventional poling and by corona charging. However, there is some evidence[5,7] which suggests that the origin of piezo- and pyroelectricity in PVF_2 may be due to charge injection (homocharge)and/or charge separation at defect regions(heterocharge) of Form 1 crystallites in addition to dipolar orientation. It is also of interest to note that Ohigashi[2] has been successful in obtaining considerable piezoelectric response from poled films of biaxially oriented PVF, in which the crystallites are mostly in the non-polar Form 2 structure. Thus, it appears that there is as yet no definitive knowledge of the origin of piezo- and pyroelectricity in PVF_2, although there is agreement on one specific observation that a polar crystalline form is perhaps necessary for a maximum response.

The relevance of the changes in the crystallite structure (i.e. from Form 2 to Form 1) on poling is not yet understood. Present work reports the results of the following studies of ageing in corona charged PVF_2: (i) the nature of decay of the piezoelectric strain coefficient, d_{31} and (ii) X-ray diffraction profiles.

2. Poling of Samples

Films of PVF_2 of thickness 25 and 50μm, both biaxially oriented were kindly provided by the Kureha Chemical Co. Ltd. of Japan. Preliminary structural studies of the films by X-ray diffractometry indicated the presence of both Form 1 and Form 2 in the 25μm thick film whereas the 50μm thick was observed to be only of Form 2 composition. Aluminium electrodes were vacuum deposited on one surface of circular samples of 5cm. diameters, the metallized surface being in contact with an earthed heavy copper plate at a constant temperature environment. Positive charges were deposited on the non-metallized surface of the polymer, the surface potential being continuously monitored by a Field-Mill type electrostatic voltmeter (Model 216, IDB, UCNW, Bangor). A micromesh control grid was introduced between the sample and the corona tip which was connected to a stabilized and an adjustable high voltage supply. The micromesh control grid was connected to a separate but similar high voltage supply which was always maintained at a potential of 3kv lower than that of the corona point. The surface potential of the polymer film was observed to reach the desired values, in all cases, within 10 seconds after the application of the high voltage supply to the micromesh grid and the corona point. The maximum voltage employed at the corona tip (limited by the electrical breakdown of samples) were +10Kv and +14Kv for the 25 and 50 μm thick films respectively. Corona charging was carried out at different values of surface potential for a poling time of 5 minutes in each case. The poling temperature was 18°C for the majority of the samples. however, a limited number of samples were poled at −80°C and at +100°C.

CH1287-2/78/0000-0023$00.75

3. X-ray Diffraction Profiles

X-ray diffraction profiles of PVF_2 samples were obtained with a Philips Diffractometer (Type PW1050) using Ni-filtered Cu-kα radiations and a step scanning technique in the range of 2θ-values of 17° to 22°. The metallized aluminium surface of the polymer was used as an internal standard in order to ascertain an uncertainty in the value of 2θ of less than 0.1°.

4. Measurement of Piezoelectric strain coefficient d_{31}

Following corona charging a second aluminium electrode was evaporated on the unmetallized surface of the polymer. The electrodes of the poled sample was then short circuited for 15 hours to remove extraneous charges. The magnitude of d_{31} was then determined by a conventional static method of the release of a fixed weight at ambient temperature using an electro-pneumatic solenoid valve. A Tektronix storage oscilloscope (Mode 549 with 1A7 amplifier) was used to monitor the voltage developed across a standard mica capacitor by piezoelectricity. The samples were then annealed (with electrodes short circuited) in a thermostatically controlled (within ±2° of desired values) oven for a further period of 15 hours. At the end of this period the samples were allowed to cool down to the ambient temperature for one hour before d_{31} was remeasured.

5. Results and Discussion

Figure 1 shows the X-ray diffraction profiles of 25μm thick PVF_2 films after corona charging at different surface potentials together with that of the unpoled polymer. The 2θ-values of the respective peaks for the unpoled sample are in good agreement with those due to Hasegawa et al[22]. The observed

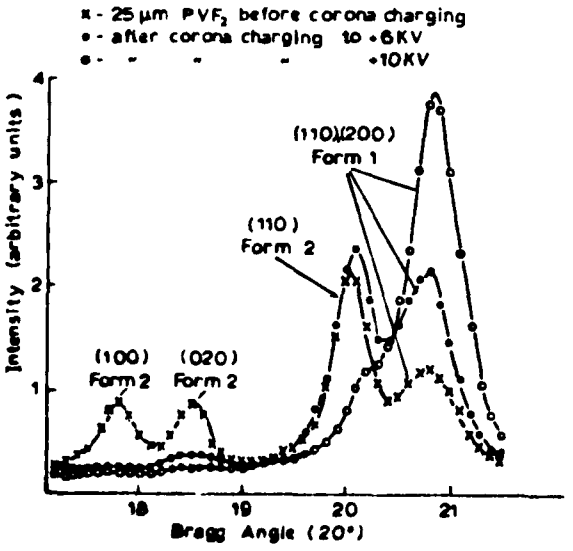

Figure 1: X-ray diffraction pattern before and after corona charging.

increase in the intensity of the (110) Form 2 peak for a surface potential of 5 Kv compared to annihilation of the other two Form 2 peaks, (i.e. (100) and (020)) and at the same time an enhancement in the intensity of the composite Form 1 peak (i.e. (110)+(200)) suggest that an intermediate structural conformation may have occurred. With poling at a higher corona tip potential (+10kv) a significant increase in the intensity of the Form 1 composite peak (110/200) and a very considerable reduction in that of Form 2 (110) peak would indicate that a change into Form 1 type of crystallites may have progressively completed. It was observed that subsequent heat treatment (i.e. annealing) has little effect on the X-ray diffraction profiles (Figure 2), and the Form 2 (100) and (020) peak do not appear. However, slight differences in the intensities of Form 1 composite peak (110/200) (which is in agreement with Kepler et al[12]), and Form 2 (110) peaks were observed after annealing at 140° in relation to their respective pre-annealed magnitudes.

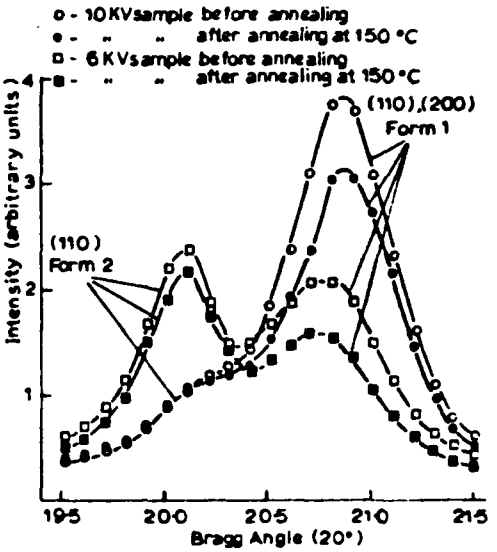

Figure 2: X-ray diffraction pattern of PVF_2 (25μm) before and after annealing.

This may be due to an onset of molecular motion in the crystalline region of the polymer at this temperature. A total of 16 samples for each of the two thicknesses (i.e. 25 and 50μm) were employed in the present work on ageing.

The magnitude of d_{31} was measured for each of these 32 samples (after short circuited condition for 15 hours) and its range was observed to be from 0.09pC/N to 7.8pC/N for different poling (corona charge) fields. Figure 3 shows typical behaviour of d_{31} as a function of the poling field for 25 and 50μm thick samples. It may be noticed (Figure 3) that the non-polar (Form 2) 50μm thick samples show comparable piezoelectric response at higher fields (>1.3×10^6 Vm^{-1}) to that of the polar (Form 1) 25μm thick samples. It may also be observed that the non-polar material has very little piezoelectric response at fields less than 1×10^6 Vm^{-1}. The non-polar material was observed to have a lower electrical breakdown strength than that of the polar and the reason for this is not yet apparent.

After annealing at 60°C the piezoelectric response was observed to decay slightly for all samples and this may be due to the onset of a molecular motion in the crystalline region of the Form 2 contents which occurs at ~70°C.

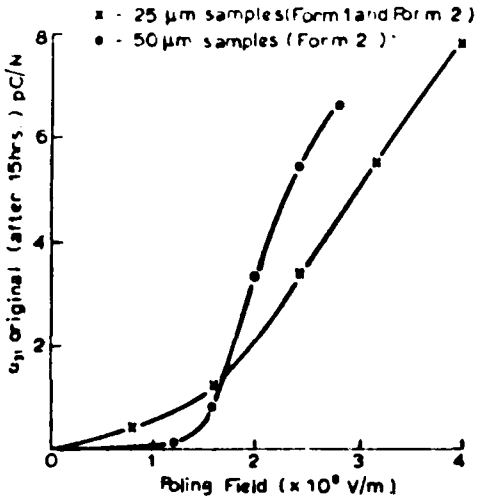

Figure 3: Behaviour of d_{31} with poling field.

Increasing the annealing temperature further reduced the magnitude of d_{31}, as shown in Figure 4. Each vertical line (downwards) represents the decay of d_{31} in a sample, (poled at a particular field and after annealing at increasing temperatures), in relation to the original pre-annealed value. It may be observed (Figure 4) that for a given annealing temperature all points lie in a straight line which suggests that the piezoelectricity in all the samples decay in the same way irrespective of the poling temperature and the molecular conformation. Linear regression has been applied to each set of measured data and the gradients give an indication of the decay of piezoelectricity (or persistent polarization) after annealing of the samples.

Figure 5 is a plot of the normalized value of d_{31} as a function of annealing temperature and it shows that approximately half the activity remains even after annealing at 150°C. It may be mentioned that with conventionally poled samples Abkowitz et al[18] observed the polarization to decay markedly at temperature ~100°C.

The present results show that with corona charging, the poling temperature may not have noticeable influence on the rate of ageing. This has the advantage that a satisfactory poling may be completed in PVF_2 by corona charging at ambient temperature in a very short time. As the behaviour

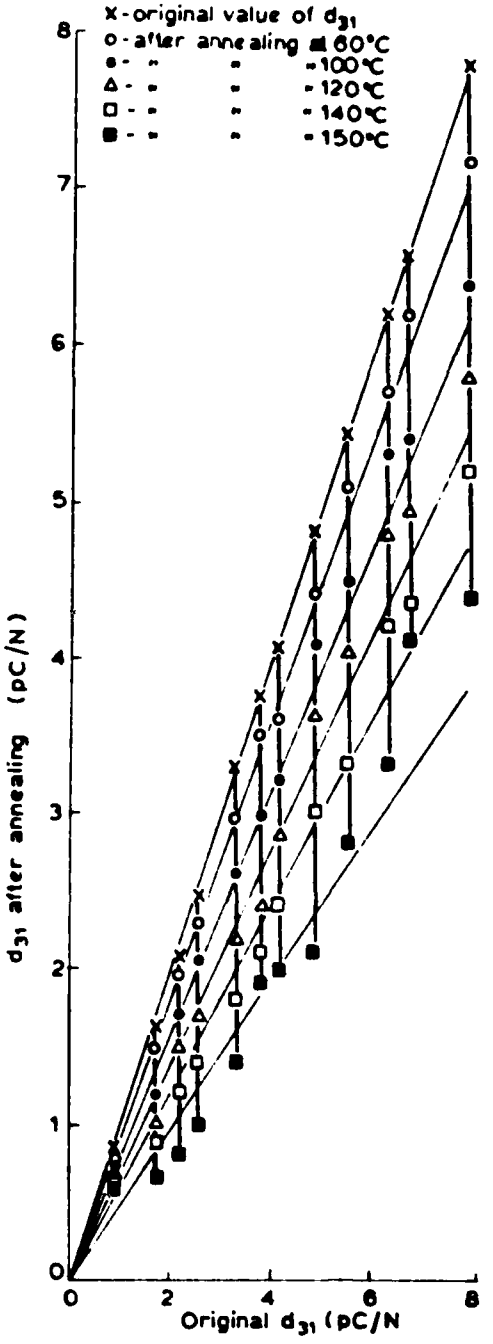

Figure 4: Ageing of d_{31}, after annealing.

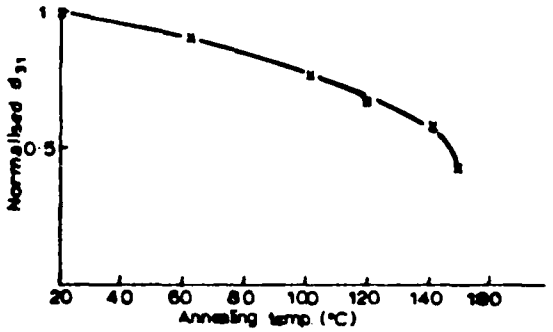

Figure 5: Decay of d_{31} (normalized) as a function of annealing temperature.

of the decay of d_{31} in both 25 (Form 1 and Form 2 crystallites) and 50μm (Form 2 crystallites) is similar it suggests that the mechanism of polarization in these two materials with different molecular conformation may also be identical, although no Form 1 (110/200) structural peak was observed with the poled 50μm thick samples. However, a recent report[23] shows the evidence of the presence of Form 1 crystallites after corona poling of PVF_2 containing Form 2 structure. Now it should be stated that each individual chain molecule of Form 2 has a dipole moment normal to its chain axis, although the chains pack in the anti polar array in a unit cell. Thus it may be expected that each chain may experience a change in orientation due to the poling field, giving rise to piezoelectricity in PVF_2 even in the absence of any Form 1 crystallites.

Acknowledgement

This work is being financed by a research contract with the U.S. Army. The authors are grateful to Mr. R. S. Brockley for invaluable assistance in the measurement of the piezoelectric strain constant. One of the authors is also grateful to the Science Research Council of Great Britain for a research studentship grant.

References

1. K. Okuda, T. Yoshida, M. Sugita & M. Asahina, J. Polym. Sci., B5, 465 (1967).
2. J.B. Lando, H.G. Olf & A. Peterlin, J. Polym. Sci., A-1, 4, 941 (1966).
3. K. Nakamura & Y. Wada, J. Polym. Sci., A-2, 9, 161 (1971).
4. W.W. Doll & J.B. Lando, J. Macromol. Sci., Phys., B4(4), 889 (1970).
5. N. Murayama, T. Oikawa, T. Katto & N. Nakamura, J. Polym. Sci., Polym. Phys. Ed., 13, 1033(1975).
6. K. Ogasawara, K. Shiratori & M. Tamura, Rep. Progr. Polym. Phys. Japan, 19, 313 (1976).
7. N. Murayama & H. Hashizumi, J. Polym. Sci., Polym. Phys. Ed., 14, 989 (1976).
8. M. Oshiki & E. Fukada, Jap. J. Appl. Phys., 15(1), 43 (1976).
9. M. Latour, J. Electrostatics, 2, 241 (1977).
10. M. Tamura, S. Hagiwara, S. Matsumoto & N. Ono, J. Appl. Phys., 48, 513 (1977)
11. R.J. Shuford, A.F. Wild, J.J. Ricca & G.R. Thomas, Polym. Eng. Sci., 16(1) 1976.
12. R.G. Kepler & R. A. Anderson, J. Appl. Phys., 49(1), 1978.
13. K. hayakawa & Y. Wada, Rep. Progr. Polym. Phys. Japan, 15, 377 (1972).
14. K. Hayakawa & Y. Wada, Advances in Polym. Sci., 11, 1 (1973).
15. P.D. Southgate, Appl. Phys. Lett., 28(5), 250 (1976).
16. D.K. Das-Gupta & K.Doughty, Appl. Phys. Lett. 31(9), 585 (1977).
17. N. Murayama, J. Polym. Sci., Polym. Phys. Ed., 13, 929 (1975).
18. G. Pfister, M. Abkowitz, & R.G. Crystal, J. Appl. Phys., 44, 2064 (1973).
19. G.W. Day, C.A. Hamilton, R.L. Peterson, R.J. Phelan, Jr., & L.D. Mullen, Appl. Phys. Lett., 24, 456 (1974).
20. R.J. Phelan, Jr., R.L. Peterson, C.A. Hamilton & G.W. Day, Ferroelectrics 7, 375 (1974).
21. H. Ohigashi, J. Appl. Phys., 47(3), 949 (1976).
22. R. Hasegawa, Y. Takahashi, Y. Chatani & H. Tadokoro, Polym. J., 3(5), 600 (1972).
23. J.E. McKinney & G.T. Davis, NBS Technical Report (N00014-78-0015), to be published in ACS Polymer Preprints, December 1, 1977.

448 IEEE TRANSACTIONS ON INDUSTRY APPLICATIONS, VOL. IA-14, NO. 5, SEPTEMBER/OCTOBER

On the Nature of Poling by Corona Charging and the Pyroelectric Effect in PVF_2

DILIP K. DAS-GUPTA AND KEVIN DOUGHTY

Abstract—**The effect of corona charging (at 12.5 kV) of polyvinylidine fluoride (PVF_2) is studied by infrared spectroscopy and X-ray diffraction techniques. The results show that changes in molecular conformation occur with such a poling process that is in agreement with Southgate. The pyroelectric coefficient was observed to increase significantly after such a poling, reaching a maximum value of ~3 nC/cm^{2}K at ~343 K. It is suggested that the pyroelectricity in PVF_2 at this temperature is due to dipolar orientation.**

I. INTRODUCTION

POLYVINYLIDENE fluoride (PVF_2) is a semicrystalline polymer of monomer unit $CH_2 = CF_2$. It may exist in at least two stable forms [1], i.e., planar zigzag polar (β-form or Form 1) form [2] with an electric dipole moment of 2.1D[3] that is oriented along the b-axis (perpendicular to the chain axis) and the trans-gauche trans-gauche nonpolar (α-form or Form 2) form [4]. The β-form has an orthorhombic unit cell with a space group $Cm2m(C_{2v}{}^{14})$ [5] and a single crystal of this form will exhibit piezoelectric effect without any external poling. Murayama *et al.* [6] shows that in PVF_2 film containing both α- and β-forms, the piezoelectric response increases with increasing β-form content. Murayama and Hashizumi [7] further observes that its pyroelectric response is also related to the β-form. It is established that the piezoelectric and pyroelectric responses in PVF_2 may be enhanced by poling of oriented films with high electric field. Oshiki and Fukada [8] shows that a significant molecular conformation, i.e., a conversion from α-form to β-form may take place on stretching and poling of PVF_2 films originally containing both α- and β-forms. Latour [9] also supports this observation from the infrared and Raman spectroscopic studies of poled PVF_2 films. An orientation of the β-form crystallites on poling was observed by Tamara *et al.* [10] from their polarized infrared spectral studies, and this is also supported by the changes in the X-ray pole figures due to Kepler [11] for unpoled and poled samples. Shuford *et al.* [12] also observed that increases in the draw ratio produces increasing conformal changes in PVF_2 from α-form to β-form, thereby increasing its piezoelectric property. Southgate [13] reports a significant reduction of the infrared absorption peaks at 762 and 975 cm^{-1} (attributed to α-form) after corona charging of PVF_2 films.

Paper IUSD 78-9, approved by the Electrostatic Processes Committee of the IEEE Industry Applications Society for presentation at the 1977 Industry Applications Annual Society Meeting, Los Angeles, CA, October 2-6. This work is being supported by a research grant from the U.S. Army. Manuscript released for publication April 12, 1978.

The authors are with the School of Electronic Energy Science, University College of North Wales, Bangor, Gwynedd, LL57 1UT, United Kingdom.

The different mechanisms that have been proposed for origin of piezo- and pyroelectricity may be summarized follows.

i) Dipolar Orientation: Only the crystalline regions of polymer align permanently with the poling field, and only component of the chain axis that lies on the plane of the contributes to polarization. This view is supported to cer extent by the X-ray data of Kepler *et al.* [14]. Hayakawa e [15] suggest that the changes in polarization of the (dipoles about the C-C backbone due to the poling field in direction of the chain axis may be responsible for the pi electric effect in PVF_2

ii) Charge Trapping: Murayama *et al.* [6] and Pfister e. [16] suggest that the piezoelectricity and pyroelectricity PVF_2 may originate from trapped charge (thermoelec behavior), the β-form providing the trap centers. They furt suggest that the persistent polarization of PVF_2 electrets c sists of a) trapped homocharge (i.e., injected holes) and b) heterocharge that appears after the decay of the homocha Finally, Murayama and Hashizume suggest that the pie electricity and pyroelectricity may arise from the same sistent polarization.

iii) Electrostriction: Oshiki and Fukada [17] suggest t electrostriction in the presence of a residual electric field i poled sample is responsible for the piezoelectricity in PV films.

It has also been reported by Osaki *et al.* [18] that whe static electric field is applied to PVF_2 at high temperatu the magnitude of ϵ'' (the imaginary part of complex perm tivity ϵ^*) decreases quite significantly. They attribute this the ionic impurities and to their electrolysis on application a dc field.

It may be observed from the above discussion that there i considerable need to make a systematic study of the nat and mechanism of poling (both macroscopic and microsco aspects) and their relevance to the piezoelectricity and py electricity in PVF_2.

These considerations provide a basis of the present progr of work with corona charged PVF_2 that may be divided in three parts that are i) studies of infrared resonance absorpti spectra, ii) studies of X-ray diffraction patterns, and iii) py electric current studies.

Measurements were made with biaxially oriented 16 and μm thick PVF_2 films (Kureha Chemical Industry Compar Ltd., Japan). The pyroelectric studies were made at a chamb pressure of 10^{-6} torr. The corona charging of the PVF_2 12.5 kV was carried out by employing a similar technique that of Southgate [13] using a high-energy piezoelect

0093-9994/78/0900-0448$00.75

AD-A084 448 UNIVERSITY COLL OF NORTH WALES BANGOR F/G 11/9
A STUDY OF THE NATURE AND ORIGINS OF PYROELECTRICITY AND PIEZOE--ETC(U)
JAN 80 D K DAS-GUPTA DA-ERO-77-G-088
UNCLASSIFIED NL

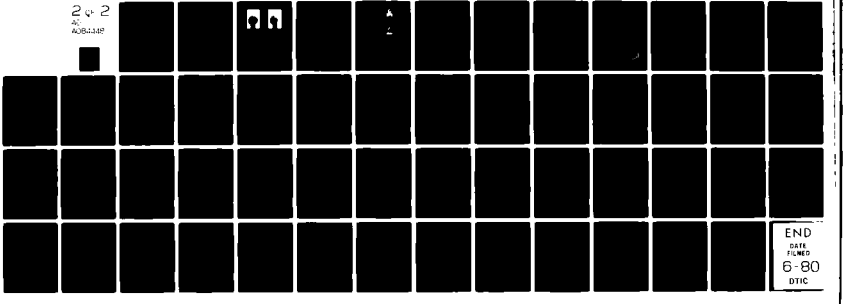

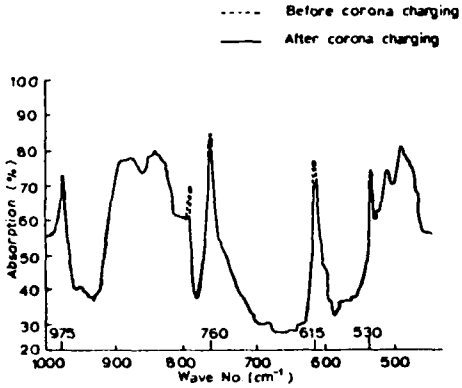

Fig. 1. Infrared spectra of 25 μm thick PVF_2 before and after corona charging.

corona discharge gun (zerostat) at 293 K. The magnitude of the charge on each sample and that of the corresponding polarization produced by the applied field, were determined with a Field Mill type electrostatic voltmeter and a Keithley electrometer (type 602) connected across a series 0.1 μF mica capacitor.

II. STUDIES OF INFRARED RESONANCE ABSORPTION SPECTRA OF PVF_2 BEFORE AND AFTER CORONA CHARGING

A Grubb-Parsons "spectromajor" infrared spectrometer with a polarizer was used in the "double-beam" mode in the region 1600-450cm^{-1}. The preferred orientation of the samples in relation to the polarizer of the spectrometor was determined initially by repeated trials and inspection of the spectra in steps of 10° rotation of the polarizer. Fig. 1 shows the infrared spectra of 25 μm thick PVF_2 film with and without corona charging from which it may be noticed that the absorption peak amplitudes at 530, 615, 760, 800, and 975 cm^{-1} have all been reduced after corona charging at room temperature (~20°C). These vibrations are attributed to the α-form of the polymers and have been ascribed to $CF_2(\delta)_o$, CF_2(wag), $CF_2(\delta)_i$, skeletal, [or CH_2 (rock)$_i$] and skeletal modes, respectively. Here the standard symbol δ represents "bending in plant," and the subscripts i and o identify in-phrase and out-of-phase, respectively. These results are in agreement with Southgate [13], except that unlike his spectra, no new vibrational peak at 1155 cm^{-1} was observed after corona charging in the present work. It should be noted that Southgate [13] also observed an increase in the amplitude of the vibrational peak at 510 cm^{-1}, which is attributed to the β-form, after annealing the corona charged sample. The most noticeable reduction in the amplitude of a vibrational peak after corona charging occurs at ~800 cm^{-1} in the present work (Fig. 1).

A possible explanation of the reductions of amplitudes of some of the vibrational peaks of the α-form (Fig. 1) after corona charging may be as follows. If the C-C bond of the α-form is allowed to relax due to the presence of a high electrostatic force arising from the surface charges, the F-F repeat distance will increase, which in turn may reduce the stearic hindrance of the fluorine atoms. This will allow the fluorine atoms to reorientate to a structure somewhat resembling the β-form. In such a model, there will be an increase in the skeletal repeat distance resulting in a diminshed stearic hindrance of the C-F unit in each chain. This may cause some preferential alignment of the C-F dipole in the electrostatic field resulting in a structure somewhat akin to the β-form. On subsequent annealing of the sample, further transition towards β-form structure may be enhanced, which would be in agreement with the observation of Southgate (i.e., an increase in the amplitude of the β-form vibrational peak at 510 cm^{-1} subsequent to corona charging and annealing). This would also result in an increase in density of the polymer because of the easier packing of the β-form chains. However, above suggestions should be treated with caution, and further work is necessary to determine whether changes in the skeletal repeat distance is due to changes in the C-C bond length or due to changes in the C-C-C interangle.

III. STUDIES OF X-RAY DIFFRACTION PATTERNS OF PVF_2 BEFORE AND AFTER CORONA CHARGING

A study of changes in molecular conformation of 16 μm and 25 μm thick PVF_2 films due to corona charging using a Philips X-ray diffractometer type PU 1025 is reported. Diffraction patterns were obtained with test samples of area ~3 cm^2 for Bragg angles (i.e., 2θ-values) between 16° and 23° using the step scanning technique and Ni-filtered Cu-Kα radiation. The sample was then corona charged at room temperature at ±12.5 kV, and the diffraction pattern was obtained again for the same range of Bragg angle as stated above. Figs. 2 and 3 show the diffraction patterns for the 16 and 25 μm thick samples, respectively, and Table I summarizes the results of the present work, and in addition, it provides the relevant crystallographic data of PVF_2 due to Hasegawa *et al.* [5] for the purpose of comparison. It may be observed from Table I that the discrepancies between the θ-values in this paper and those of Hasegawa *et al.* [5] do not produce differences in the lattice parameter in excess of 2 percent, although no internal standard has been used in this work. The positional uncertainty of 2θ-values associated with the mounting of the samples in the present work does not exceed ±0.1°. According to Kepler, the structure factor due to (110) peak alone in the composite β-form peak at $2\theta \cong 20.85°$ is ~4.6 times greater than that of its other component (200) peak. This peak will henceforth be called (110) β-form peak in this paper.

Fig. 2 shows that for 16 μm thick sample after corona charging the (100) and (020) α-form peaks are very significantly reduced or are almost completely removed. This was also observed for the 25 μm thick sample of PVF_2. Furthermore, the (110) α-form peak was considerable reduced after corona charging when it seemed to appear as a shoulder on the lower angle side of the (110) β-form peak (Fig. 2). This may be more clearly observed in Fig. 3 where the diffraction patterns have been shown for a restricted range of 2θ-values for the both Figs. 2 and 3. It may be argued that corona poling has substantially reduced the amounts of both of the original α and β phase material and replaced it by a different crystallite

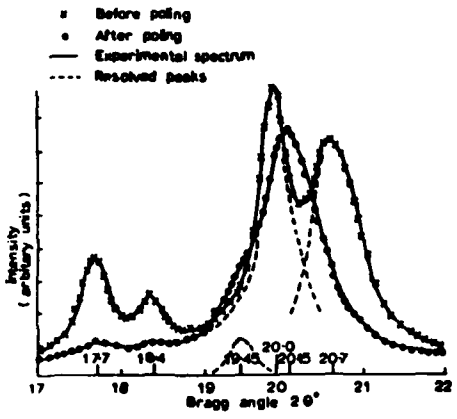

Fig. 2. X-ray diffraction spectra of 16 μm sample of PVF_2 before and after corona charging.

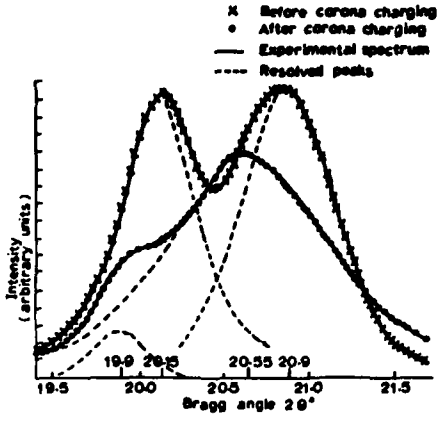

Fig. 3. X-ray diffraction spectra of 25 μm sample of PVF_2 before and after corona charging.

TABLE I
SUMMARY OF X-RAY DIFFRACTION RESULTS OF PVF_2 FILMS BEFORE AND AFTER CORONA CHARGING

Sample thickness	Crystallographic data due to Hasegawa et al[5]			Diffraction data (present work)					
				Before corona charging			After corona charging		
x 10^{-6}m)	Bragg angle 2θ°	Crystalline form	Crystallographic plane	Bragg angle 2θ°	Area (arbitrary units)	Integral breadth (radians)	Bragg angle 2θ°	Area (arbitrary units)	Integral breadth (radians)
16	17.9	α	(100)	17.7	11.2	-	17.7	1	-
	18.4	α	(020)	18.4	3.4	-	18.4	1	-
	20.1	α	(110)	20.0	54.52	0.00614	19.4	3.3	-
	20.85	β	Composite peak (110)+(200)	20.7	45.16	0.00636	20.16	65.25	0.00883
25	20.1		(110)	20.15	76.5	0.00448	19.9	11.2	-
	20.85		Composite peak (110)+(200)	20.9	93.5	0.00537	20.6	109.6	0.00846

population. Then, since the IR spectra of the resulting sample indicates that the chains are primarily in a planar zigzag confirmation, one can make the assumption that the new diffraction peaks arise from a distribution of small distorted β (or γ) phase-like crystallite. It may also be observed from Figs 2 and 3 and Table I that the line width (i.e., integral breadth) of the (110) β-form diffraction profile increases significantly after corona charging that would suggest a reduction of the β-form crystallite size and/or an increase in the lattice distortion.

Finally, the peak positions (i.e., 2θ-values) and the (110) diffraction profile, in particular, β-form peak was observed to shift after corona charging to a lower value by more than 0.5° (Fig. 2) which is well outside the limit of the positional uncertainty in the present work. Such a shift would correspond to an increase in the interplanar separation of over 3 percent that would be compatible with the observations in the infrared spectra in Section II.

Laue Photographs: Confirmation of molecular structural changes due to corona charging were also obtained from flat film X-ray photographs of 25 μm thick PVF_2 samples using a Laue-type X-ray transmission camera (Figs. 4 and 5). Due to the large difference in intensity, each photograph is split into two parts, each half receiving a different exposure time to obtain a good resolution. From a knowledge of the sample to film distance D, the crystallographic planes were identified by measuring the radii of the rings r in Figs. 4 and 5 and using the following relationships:

$$X = 2d_{hkl} \sin \theta \tag{1}$$

and

$$2\theta = \arctan r/D \tag{2}$$

where λ is the wavelength of the X-ray (= 1.54 Å) and other symbols have their usual meanings.

Table II summarizes the results of these observations for both Figs. 4 (before corona charging) and 5 (after corona charging). The most noticeable features of the Laue photograph after corona charging (Fig. 5, Table I) are as follows:

Fig. 4. Laue transmission (X-ray) pattern for PVF_2 before corona charging.

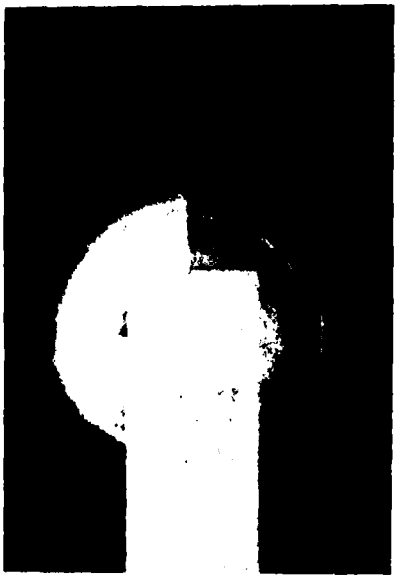

Fig. 5. Laue transmission pattern (X-ray) pattern for PVF_2 after corona charging.

TABLE II
SUMMARY OF OBSERVED LAUE DIFFRACTION PATTERNS OF PVF_2 FILMS BEFORE AND AFTER CORONA CHARGING

Radius of rings cms	$2\theta^\circ$	d_{hkl} spacing Å	Crystalline form	Crystallographic planes	Intensity (before corona charging Figure 4)	Intensity (after corona charging, Figure 5)
3.275	18.5	4.79	α	020	Very strong	Strong
3.65	20.4	4.35	α	110	Strong	Absent
3.75	20.9	4.24	β	(110)+(200)	Strong	Very strong
4.9	26.6	3.35	α	021	Strong	Fairly strong
5.15	27.7	3.22	α	111	Very weak	Absent
6.15	32.1	2.79	α	121	Weak	Absent
6.45	33.3	2.69	α	130	Weak	Weak
7.25	36.5	2.46	β	(310)+(020)	Absent	Weak
7.9	38.9	2.31	α	131	Weak	Weak
8.70	41.6	2.17	α	140	Weak	Weak

i) the disappearance of the α(110) α-form ring that is in agreement with X-ray diffraction patterns in Figs. 2 and 3,
ii) fall in intensity of other α-form rings,
iii) appearance of an extra ring that may be ascribed to a composite β-form ring due to (310) and (020) planes.

These results further verify the previous observations that significant changes in the molecular conformation of PVF_2 films occur on corona charging.

Further work is in progress at present to determine quantitatively, using an internal standard, the crystallite size and orientations, and lattice distortions after corona charging and their effects on the pyroelectricity and piezoelectricity in PVF_2 films.

IV. MEASUREMENT OF PYROELECTRIC COEFFICIENT OF PVF_2 AFTER POLING

The pyroelectric coefficient p is the change in internal polarization of a dielectric material with temperature T and may be expressed as

$$p = \frac{1}{A} \cdot \frac{dQ}{dT} \tag{3}$$

where A and Q represent electrode area and charge, respectively. The direct and probably the most accurate method of determining the pyroelectric coefficient is to measure the short circuited current through a pyroelectric material at a

constant rate of change in temperature. The pyroelectric current density J_{pyro} is given by

$$J_{pyro} = p\frac{dT}{dt}. \tag{4}$$

Thus a plot of J_{pyro} versus T gives directly the pyroelectric coefficient. Equation (2) also shows that

$$J_{pyro} = 0, \qquad \frac{dT}{dt} = 0.$$

Hence any current measured at a constant temperature would contribute erroneously to the evaulation of the pyroelectric coefficient p, and this must be eliminated. In the direct method determination of the pyroelectric coefficient, p is made by measuring the short circuited current that flows from one electrode to the other for a constant rate of change in temperature. This method has been employed with PVF_2 films that were poled by two separate methods, i.e., i) by subjecting the sample to a strong dc field at elevated temperature and then slowly cooling with the applied field to 298 K and ii) by corona charging at 12.5 kV at room temperature. All pyroelectric current measurements were made at a chamber pressure of $<10^{-5}$ torr.

Method 1, Poling by a dc Field: Two measuring electrodes of gold were evaporated across each sample of 25 μm thickness. The electrode thickness and area were ~250 Å and 2 cm^2. Each sample was also provided with an evaporated gold guard ring electrode to minimize the surface currents. The sample was conditioned in the measuring vacuum chamber by heating it in the short circuited condition to 383 K. The temperature was then lowered to the desired poling temperature. At each appropriate poling temperature, the short circuit was removed, and the poling electric field of $10^7 Vm^{-1}$ was applied to the sample that was then slowly cooled to 298 K. The sample was then short circuited again, and the discharge current was monitored for 10^3 s at this constant temperature (i.e., 298 K). Such a procedure obviously has the advantage of reducing the nonpyroelectric irreversible component from the intended measurement of the reversible pyroelectric current. The temperature was then raised at a rate of 5°/10 min until the poling temperature was reached. The short circuited sample was then cooled again to 298 K and reheated to the poling temperature at the same rate mentioned above (second cycle). The pyroelectric coefficient was obtained from the data provided by the third cyclic operation for each poling temperature. In Fig. 6, curve B shows the magnitudes of the pyroelectric coefficients measured at respective poling temperatures from which it may be observed that the pyroelectric coefficient rises sharply at poling temperatures >323 K, reaching a maximum value of 1.9 nC/cm^2K at ~343. At poling temperatures in excess of 353 K, the pyroelectric coefficient was observed to decrease slightly. Similar behavior of the pyrelectric coefficient was also observed by Burkard and Pfister [20]. It may be of interest to note that Shuford *et al.* [12] and Tamura *et al.* [21] also observed a similar temperature

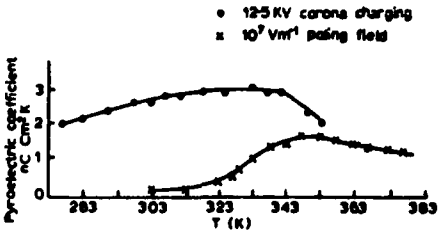

Fig. 6. Pyroelectric coefficient of 25 μm thick PVF_2.

dependence of the piezoelectric constant in oriented and poled (by dc field) PVF_2. It should be noted that PVF_2 has a structural relaxation peak at ~343 K due to a molecular motion in the crystalline region [22]. Thus the observed increase in the magnitude of the pyroelectric coefficient in PVF_2 with poling temperature in the range 303-383 K may probably be related to the molecular motions in the crystalline phase enabling the orientation of the CF_2 dipoles with the poling field at 350 K. As the temperature is lowered,

Method 2, Poling by Corona Charging: The sample was charged at ±12.5 kV at room temperature with an earthed silver electrode and following a procedure similar to that of Southgate [13]. A second silver electrode was then painted on the other face of the sample before locating it in the vacuum chamber. The cyclic method extending over three cycles, as described in the previous method, was again employed for the measurement of the pyroelectric current, except in the present case the highest temperature was restricted to 353 K.

Fig. 6, curve A shows the behavior of the pyroelectric coefficient with temperature in the range 278-353 K after corona charging at room temperature. It may be noticed that the pyroelectric coefficient has been much enhanced by poling the sample with corona charging, reaching a maximum value of ~3 nC/cm^2K at ~343 K. However, in this case, the pyroelectric coefficient has an appreciable magnitude (~1.8 nC/cm^2K) even at temperatures lower than 283 K. It may be mentioned that the polarization achieved by corona charging in the present case reached a magnitude of ~2 × $10^{-5}C\ cm^{-2}$, which, according to Southgate [13], is sufficient to align all the dipoles of the β-phase. The considerable electrostatic pressure (~30 atmosphere in the present case) has a similar effect as making the sample oriented, which in turn enhances the reversible pyroelectricity in PVF_2.

Further work is in progress to study the pyroelectric and piezoelectric behavior of PVF_2 after corona charging at different temperatures.

IV. CONCLUSIONS

Measurements of i) infrared absorption and ii) X-diffraction patterns by PVF_2 films show that changes in molecular conformation (i.e., α-form to β-form) occur on poling by corona charging. The magnitude of the reversible pyroelectric coefficient is enhanced by this process. It is suggested that the observed pyroelectricity, at temperatures at least up to 385 K, is due to dipolar orientations.

REFERENCES

[1] K. Okuda, *et al., J. Polym. Sci.*, vol. B5, 1967.
[2] J. B. Lando, H. G. Old, and A. Peterlin, *J. Polym. Sci.*, A-1, vol. 4, 1966.
[3] K. Nakamura and Y. Wada, *J. Polym. Sci.* A-2, vol. 9, 161 (1971).
[4] W. W. Doll and J. B. Lando, *J. Macromol. Sci. Phys.*, vol. B4(4), 1970.
[5] R. Hasegawa, *et al., Polym. J.*, vol. 3(5), 1972.
[6] N. Murayama, *et al., J. Polym. Sci., Polym. Phys. Ed.*, vol. 13, 1033 (1975).
[7] N. Murayama and H. Hashizume, *J. Polym. Sci., Polym. Phys. Ed.*, vol. 14, 1976.
[8] M. Oshiki and E. Fukada, *Jap. J. Appl. Phys.*, vol. 15(1), 1976.
[9] M. Latour, *J. Electrostatics*, vol. 2, 1977.
[10] M. Tamura, *et al., J. Appl. Phys.*, vol. 48, 1977.
[11] R. G. Kepler, *Proc. Piezoelectric and Pyroelectric Sym.*—Workshop, vol. 46, Sept. 1975.
[12] R. J. Shuford, *et al., Polym. Eng. Sci.*, vol 16 (1), 1976.
[13] P. D. Southgate, *Appl. Phys. Lett.*, vol. 28 (5), 1976.
[14] R. G. Kepler, E. G. Graber and P. M. Beegon, *Bull. Am. Phys. Soc.*, A-1, vol. 4, 1966.
[15] R. Hayakawa, *et al.: Reports and Prog. Polym. Phys.*, Japan, vol. 16 1973.
[16] G. Pfister, M. D. Abkowitz, and R. G. Crystal, *J. Appl. Phys.*, vol. 44 1973.
[17] M. Oshiki and E. Fukada, *J. Mat. Sci.*, 10, vol. 1, (1975).
[18] S. Osaki, S. Uemura and Y. Ishida, *J. Polym. Sci.*, A-2, vol. 9, 585 (1971).
[19] R. L. Byer and C. B. Roundy, *IEEE Trans. Sonics, Ultrason.*, vol. 19, 1972.
[20] H. Burkard and G. Pfister, *J. Appl. Phys.*, vol. 45 (8), 1974.
[21] M. Tamura, *et al., J. Appl. Phys.*, vol. 48 (2), 1977.
[22] H. Kakutani, *J. Polym. Sci.*, A-2, vol. 8, 1970.

Dilip K. Das-Gupta obtained the Ph.D. degree in physics from the University of London, London, England, in 1961.

Before 1961, he worked as an Instrument Engineer with The Elliott Bros. Ltd. and The Distillers Company Ltd. of Great Britain. In 1961, he joined the Department of Physics of Birkbeck College (London University) as a Research Assistant. He was appointed a Lecturer at the University College of North Wales. Bangor, where he now teaches electrical material science. His research interest is electronic properties of polymeric insulators.

Kevin Doughty was born in Caernarvon, Great Britain. He received the B.Sc. degree with Honors in physics from the University of Wales in 1975. He is at present reading for the Ph.D. degree in electronic engineering at the School of Electronic Engineering Science, University College of North Wales, Bangor, Gwynedd. The subject of his research is X-ray diffraction studies of polyvinylidene fluoride under electrical stress.

Pyroelectricity in polyvinylidene fluoride

D. K. Das-Gupta and J. S. Duffy

School of Electronic Engineering Science, University College of North Wales, Dean Street, Bangor, Gwynedd, LL57 1UT, Great Britain

(Received 9 June 1978; accepted for publication 8 August 1978)

The magnitude of the pyroelectric coefficient in polyvinylidene fluoride was observed to increase significantly on maintaining the poling field while cooling the samples from elevated poling temperatures to ambient temperature. The results of the measurement of the depolarization currents with repeated thermal cycling of poled specimens from temperatures well above that of poling conditions to 30°C suggest that dipolar reorientations may be responsible for the pyroelectricity in PVF_2. These observations hold for both the conventional poling and the corona charging of PVF_2 films, originally containing form 1 and form 2 crystallites.

PACS numbers: 77.70.+a

Piezoelectricity and pyroelectricity may be significantly enhanced in several polymers[1-3] following an application of high electrical stress at an elevated temperature for an extended period of time and finally cooling the polymer to room temperature without removing the field (i.e., conventional poling technique). Of the pyroelectric polymers available, polyvinylidene fluoride (PVF_2) is of particular interest because of the comparatively large pyroelectric response which may be obtained from it after suitable poling. A PVF_2 electret may be used as an optical detector for infrared radiations.[4-6] PVF_2 is a semicrystalline polymer which may exist in at least two stable forms,[7] viz., a planar zigzag polar form (form 1 or β form) and the nonpolar form (form 2 of α form) with *T-G-T-G'* conformation. It has been shown[8] that the piezoelectric response of PVF_2 increases with increasing form 1 contents with the same poling conditions. It has also been suggested that the piezoelectric and pyroelectric coefficients in PVF_2 are linearly related with each other[9,10] for identical poling conditions. The piezoelectric properties of PVF_2 and the nature of their origin have been reviewed by Wada and Hayakawa.[11] It has been shown that a significant change in molecular structure from form 2 to form 1 may occur in PVF_2,[12-14] originally containing both the forms, after corona charging. The present work reports the results of a study of the pyroelectric behavior of 25-μm-thick PVF_2 films after (i) conventional poling and (ii) corona charging. The polymer films were kindly porovided by the Kureha Chemical Co. Ltd. of Japan.

For conventional poling, gold electrodes 2.5 cm in diameter and 250 Å thick were vacuum deposited on the two surfaces of each sample. Prior to poling, the sample was conditioned at a constant temperature of 110 °C for 12 h with its electrodes short circuited, at a chamber pressure of $< 10^{-5}$ Torr. The poling was also carried out at this chamber pressure, the variable parameters being electric field, time, and temperature.

For corona poling an aluminum electrode was vacuum deposited on one surface of each sample, the metallized surface being in contact with an earthed copper plate which was maintained at a constant temperature of 18 °C. A micromesh control grid was introduced between the nonmetallized surface of the polymer and the corona tip which was connected to an adjustable and stabilized E.H.T. supply. The control grid was connected to a similar but separate E.H.T. supply which was maintained at a potential of 3 kV below that of the corona point. Positive charges were deposited on the nonmetallized surface of the polymer, the surface potential being monitored continuoully with a Field-Mill-type electrostatic voltmeter. A second aluminum electrode was then vacuum deposited on the nonmetallized surface of the corona-poled sample. All pyroelectric measurements were made at a chamber pressure of $< 10^{-5}$ Torr. Each poled sample (conventional and corona poling) was short-circuited in the evacuated measurement chamber and heated to 90 °C for >2 h, after which the sample was cooled to room temperature. This first thermal run may be called a depolarization or irreversible cycle and is a measure of the absorbed charge during the poling process. All subsequent thermal cycles, i.e., heating the short-circuited samples at a constant rate to a desired temperature and subsequent cooling to room temperature, were observed to produce "reversible" or "true pyroelectric current".[10,15,16] Such pyroelectric currents have been observed with form 1[17] type PVF_2 and also in specimens containing form 1 and form 2 crystallites.[18] The pyroelectric coefficient p was calculated from the observed short-circuited current I, using

$$p=\frac{1}{A}\frac{dQ}{dT}=\frac{1}{A}\frac{dQ}{dt}\frac{dt}{dT}=\frac{1}{A}I\frac{dt}{dT}, \tag{1}$$

where A is the area of the electrode and dT/dt if the rate of rise in temperature, which was 2 °C/min in the present work.

Figure 1 shows the typical behavior of the reversible pyroelectric coefficient of PVF_2 with temperature after conventional poling at 80 °C with a poling field of 9×10^7 V m^{-1} for a poling time of 10^4 s. The pyroelectric coefficient was observed to be repeatable up to ~90 °C. It may be noted from Fig. 1 that on maintaining the poling field during the cooling of the sample (~20 min) to room temperature, the magnitude of the pyroelectric coefficient was enhanced significantly by ~65%. This is in disagreement with Blevin[19]; however, it may be stated that the relative difference in the magnitudes of the pyroelectric currents in the two cases (Fig.

 0021-8979/79/010561-03$01.10

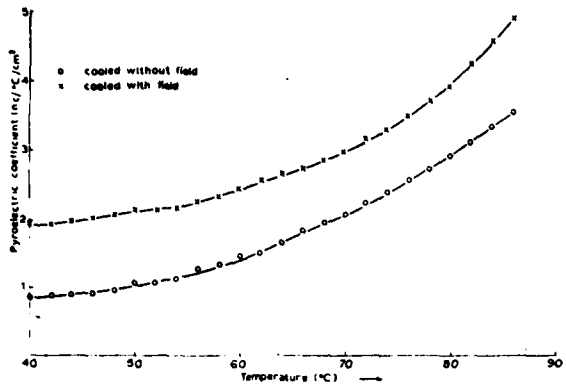

FIG. 1. Pyroelectric coefficient/temperature characteristic for 25 μm-thick PVF_2 with conventional poling. The poling parameters are $E_p = 9 \times 10^7$ V m^{-1}, $T_p = 80$ °C, and $t_p = 10^4$ s.

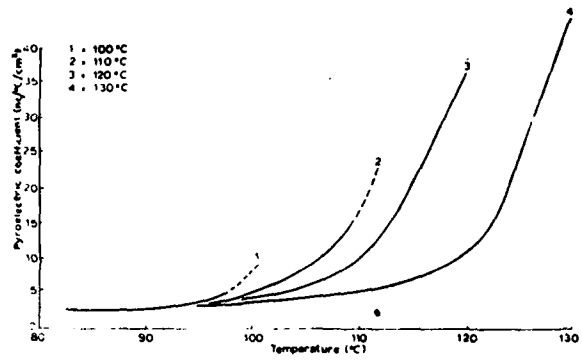

FIG. 2. Pyroelectric coefficient/temperature behavioir for 25 μm-thick PVF_2 with thermal cycling above the poling temperature (conventional poling case). The poling parameters are as stated in Fig. 1.

1) was observed to be progressively less pronounced with the increase in the poling temperature from 60 to 80 °C. The polarity of the short-circuited pyroelectric current was found to be opposite to that of the charging current during the poling process. Furthermore, the pyroelectric coefficient was observed to be of opposite polarity to that of the piezoelectric strain coefficient[20] d_{31}. In this respect,[3] the origin of the pyroelectricity in PVF_2 may be attributed to a mechanism of dipolar orientation rather than that of an asymmetrical distribution of true charges. The spontaneous polarization P_s of the form 1 crystal of PVF_2 is stated[11] to be 13 μC/cm^2. An integration of the liberated charges during a pyroelectric measurement after the first thermal cycling yields a value of $\sim 0.6\,\mu$C/cm^2 for the residual polarization P_r in the present work. This value is $\sim 5\%$ of the magnitude of P_s for the form 1 crystal. A similar value of P_r was also observed by Oshiki and Fukada[21] who found it to be reproducible after the first thermal cycle. The polarization P, induced in a material with a dilute assembly of rotating dipoles due to a poling field E_p at a poling temperature T_p, may be given by

$$P = N\mu^2 E_p / 3kT_p, \tag{2}$$

where N is the density of dipoles, μ is the dipole moment, and k is Boltzmann's constant. This model assumes perfect crystallinity and a complete alignment of all the dipoles along the poling field. Assuming $N = 1.8 \times 10^{22}$/cm^3, $\mu = 2.1$ D, $E_p = 9 \times 10^5$ V cm^{-1}, and $T_p = 80$ °C for the present case, P appears to be $\sim 0.5\,\mu$C/cm^2, which is in agreement with the magnitude of P_r and with Lines and Glass.[22] However, this agreement may be essentially fortuitous as Eq. (2) is strictly not applicable to the present case, i.e., a condensed phase with an inherent strong coupling between the dipoles along the chain, together with the associated electrical and mechanical interactions with adjacent chains. Partial orientation of the CF_2 group in a form 1 crystallite[23] and minor changes in the x-ray pole figure[24] along the direction of the external electrical stress have been reported. Conformational changes from form 2 to form 1, induced by corona charging, have also been reported[12,13,20,25] for PVF_2, originally containing both the forms. It may, however, be stated that a contribution to the polarization in PVF_2 may also arise due to charges injected by the electrodes during the poling.[18]

In order to investigate the behavior of pyroelectricity on heating of the sample to temperatures higher than that at which the specimens were poled, a method of thermal cleaning[26] was employed. The short-circuited poled sample was heated from 30 °C to temperatures above 80 °C in steps of 10 °C for successive thermal cycles. Figure 2 shows the behavior of the pyroelectric coefficient with repeated thermal cycling to higher temperatures after the initial cycle (not shown in Fig. 2). Unlike the results of Murayama and Hashizumi,[10] no peak was observed in the magnitude of the pyroelectric current during the thermal cycling. However, it should be pointed out that the samples used in the present work contained both forms in contrast to only form 1 content employed by Murayama and Hashizumi.[10] It may be observed(Fog. 2) that the pyroelectricity in PVF_2 shows good stability with no decay below 90 °C whereupon it starts to decay. Repeated thermal cycling between 25 and 100 °C in the TSC measurements due to Abkowitz and Pfister[27] also shows a reduction of space charge in PVF_2. Furthermore, Van Turnhout[28,29] indicates that space charges may be released at temperatures greater than the dipolar relaxation maxima. In this respect it is of interest to note that the structural relaxation temperatures due to molecular motions in

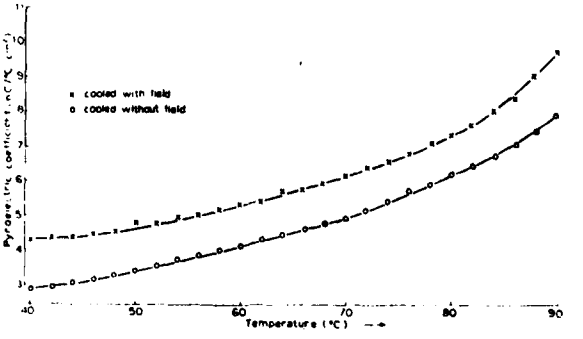

FIG. 3. Pyroelectric coefficient/temperature characteristic for 25 μm-thick PVF_2 with corona poling. The poling parameters are $E_p = 2.8 \times 10^8$ V m^{-1}, $T_p = 100$ °C, and $t_p = 300$ s.

the crystalline regions (i.e., α_c) are ~ 70 °C (form 2 crystal) and 110–130 °C (form 1 crystallites).[30] These observations may suggest that at least two mechanisms may be responsible for the pyroelectricity in PVF_2, both of which contribute to the stable and reversible pyroelectric coefficient up to a temperature of ~ 90 °C, above which one of the mechanisms (i.e., space charge) may decay. For the stable component of the pyroelectric current a dipolar reorientation in the molecular chains producing a change in the structural conformation in PVF_2 may be the dominant mechanism.

Figure 3 shows the behavior of the pyroelectric coefficient with temperature in corona-charged PVF_2 films. An increase of $\sim 33\%$ in the magnitude of p was observed in this case when the specimen was cooled in the presence of the corona poling field. We suggest that the greatest advantage of corona poling seems to be the ability to exert larger fields at high temperatures in comparison with conventional poling, thus enhancing the magnitude of the internal polarization and hence that of the pyroelectric coefficient (see Figs. 1 and 3). It was also observed that the poling time may be significantly reduced with corona poling. The exact reasons for these virtues with corona poling are yet to be understood. However, because of the similarity in the nature of variation of the pyroelectric coefficient in the two cases (Figs. 1 and 3), it is suggested that corona poling does not induce any additional or different mechanisms in PVF_2 to those suggested for the conventional poling. It should also be mentioned that the results with the repeated thermal cycling of PVF_2 films which were corona charged at 20 °C showed no decay of the pyroelectric coefficient up to a temperature of ~ 90 °C.

Further work is in progress with the measurement of the pyroelectric coefficient using a dynamic method with a modulated laser beam in which a fast heating rate is being employed.

This work is being supported by a research grant for the U.S. Army. The authors would like to thank K. Doughty for useful discussions and also for poling the specimens by corona charging during the progress of this work.

[1]H. Kawai, Jpn. J. Appl. Phys. **8**, 975 (1969).
[2]J. G. Bergman, Jr., J. H. McFee, and G. R. Crane, Appl. Phys. Lett. **18**, 203 (1971).
[3]K. Nakamura and Y. Wada, J. Polym. Sci. **9**, 161 (1971).
[4]A. M. Glass, J. H. McFee, and J. G. Bergman, Jr., J. Appl. Phys. **42**, 5291 (1971).
[5]G. W. Day, C. A. Hamilton, R. L. Peterson, R. J. Phelan, Jr., and L. D. Mullen, Appl. Phys. Lett. **24**, 456 (1974).
[6]R. J. Phelan, Jr., R. J. Mahler, and A. R. Cook, Appl. Phys. Lett. **19**, 337 (1971).
[7]J. B. Lando, H. G. Olf, and A. Peterlin, J. Polym. Sci. A-1, **4**, 941 (1966).
[8]N. Murayama, T. Oikawa, T. Katto, and N. Nakamura, J. Polym. Sci. Polym. Phys. Ed. **13**, 1033 (1975).
[9]K. Ogasawara, K. Shiratori, and M. Tamura, Rep. Prog. Polym. Phys. Jpn **19**, 313 (1976).
[10]N. Murayama and H. Hashizumi, J. Polym. Sci. Polym. Phys. Ed., **14**, 989 (1976).
[11]Y. Wada and R. Hayakawa, Jpn. J. Appl. Phys. **15**, 2041 (1976).
[12]P. D. Southgate, Appl. Phys. Lett. **28**, 250 (1976).
[13]D. K. Das-Gupta and K. Doughty, Appl. Phys. Lett. **31**, 585 (1977).
[14]J. E. McKinney and G. T. Davis, NBS Technical Report No. 0014-78-0015, 1978 (unpublished).
[15]H. Burkard and G. Pfister, J. Appl. Phys. **45**, 3360 (1974).
[16]L. E. Garn, IEEE Trans. **PHP-10**, 208 (1974).
[17]N. Murayama, *Microsymposium on Electrical Properties of Polymers*, (The Society of Polymer Science, Tokyo, 1972).
[18]G. Pfister, M. Abkowitz, and R. G. Crystal, J. Appl. Phys. **44**, 2064 (1973).
[19]W. R. Belvin, Appl. Phys. Lett. **31**, 6 (1977).
[20]D. K. Das-Gupta and K. Doughty, J. Appl. Phys. **49**, 4602 (1978).
[21]M. Oshiki and E. Fukada, Jpn. J. Appl. Phys. **15**, 43 (1976).
[22]M. A. Lines and A. M. Glass, *Principles and Applications of Ferroelectrics and Related Materials* (Clarendon Press, Oxford, (1977), p.557.
[23]S. Hagiwara, S. Matsumoto, and M. Tamura, 36th Annual Meeting of the Japan Society of Applied Physics, 1975 (unpublished).
[24]R. G. Kepler, E. J. Graeber, and P. M. Beeson, Bull. Am. Phys. Soc. **20**, 350 (1975).
[25]G. T. Davis, J. E. McKinney, M. G. Broadhurst, and S.C. Roth J. Appl. Phys. **49**, 4998 (1978).
[26]M. M. Perlman, J. Appl. Phys. **42**, 2645 (1971).
[27]M. Abkowitz and G. Pfister, J. Appl. Phys. **46**, 2559 (1975).
[28]J. Van Turnhout, Polym. J. **2**, 173 (1971).
[29]J. Van Turnhout, Ph. D. thesis (Leiden, 1972); TNO Central Laboratorium Communication No. 471 (unpublished).
[30]H. Kakatuni, J. Polym. Sci. A-2 **8**, 1177 (1970).

*PG JAPIA,800200R9M068

Pyrolelectric transient response of polyvinylidene fluoride

D. K. Das•Gupta and K.•Doughty
School of Electronic Engineering Science, University College of North Wales, Dean Street, Bangor, Gwynedd LL57 1UT, Great Britian

(Received 30 May 1979; accepted for publication 24 August 1979)

The pyroelectric responses of conventionally poled films of polyvinylidene fluoride to a step input of radiation have been analyzed and shown to be well described by the superposition of two decaying exponentials governed by the thermal and the electrical time constants of the system respectively. The peak response of the pyroelectric current transient was observed to be proportional to both the pyroelectric coefficient d_{31} for PVF_2 films of 25 μm thickness so that the peak current response curve may be used to evaluate $p(T)$ and d_{31}.

PACS numbers: E/T;8077.70. + a, 77.60. + v
*JN #56 GB #80 10 #81 Organic Compounds :T1; Pyroelectric Effect :Q1; Fluorides; Transients; Polyvinyls; Films; Mathematical Models; Radiations; Electric Current; Thickness;

INTRODUCTION

Pyroelectricity may be manifested in principle, in any material with any one of the following ten structural space groups,[1,2] C_1, C_s, C_{1v}, C_6, C_{6v}, C_2, C_{2v}, C_3, and C_{3v}. Polyvinylidene fluoride (PVF_2) may possess simultaneously two stable structural forms, viz., polar zig-zag Form 1 (β-form)[3,4] and nonpolar Form 2 (α-form)[5] with C_{2v} and C_{2h} space groups respectively. It is now well established that piezo- and pyroelectricity in may be induced in both Form 1 and Form 2 of this polymer by subjecting it to a suitable external field at an elevated temperature for an extended period of time (i.e., conventional poling) or by corona potential at high values of surface potentials at ordinary or even low temperatures. Besides dipolar orientations there are three other possible origins of polarization in a polymer electret. These are (i) charge injected from the poling electrodes; (ii) charge separation in the material over microscopic distances; and (iii) charge separation on a molecular scale.

The first of these charges is known as homocharge because the polarity of the injected charge is the same as that of the injecting electrode. The other two mechanisms, together with the dipolar orientations, give rise to heterocharge. It may be shown[7] that the pyro- and piezoelectric responses of polymers may exhibit the same polarity if they arise from an asymmetric distribution of space charge in the bulk. Conversely, should the origin of these two phenomena be of dipolar nature, the polarities of the respective signals will be dissimilar. Pfister *et al.*[7] suggested that the dominant mechanism of pyroelectricity in PVF_2, after short poling time, is charge injection whereas with long poling time, the dipoles orientation also makes an additional contribution. Recent work shows that the piezo- and pyroelectricity, induced on poling of PVF_2 films of Form 2 structure, may originate from a change in symmetry from C_{2h} to a polar form of C_{2v} type arising of rotations of the crystal a and b axes through 90° around the c axis (carbon-carbon axis). In Form 1 type structure, on the other hand, these two phenomena may originate from a preferential alignment and a change in the molecular axes of the crystallites on suitable poling.

The pyroelectric response of a material may be determined by three methods, viz., (i) the direct method,[12] which is perhaps the most accurate technique; (ii) the dynamic method[13-19] of using interrupted thermal radiations, and (iii) the charge integration method[20] which is perhaps the least attractive technique in which the measured current may also include additional components, i.e., thermoelectric current. It has been shown that[15] the measured data of the dynamic method may be calibrated against those of the direct method to provide a satisfactory technique for determining the suitability of various target materials for use in pyroelectric detectors.

In a recent paper the results of a study of the pyroelectric behavior of PVF_2, using the direct method,[12] have been reported. The present work is a continuation of this study in which both the direct and the dynamic methods have been employed to study the pyroelectric response of PVF_2. Furthermore, the piezoelectric response of this polymer has also been measured in this work for poling conditions which were identical for the pyroelectric study.

EXPERIMENTAL TECHNIQUE AND RESULTS

Biaxially stretched PVF_2 films of 25 μm thickness, containing both Form 1 and Form 2 crystallites were used in this

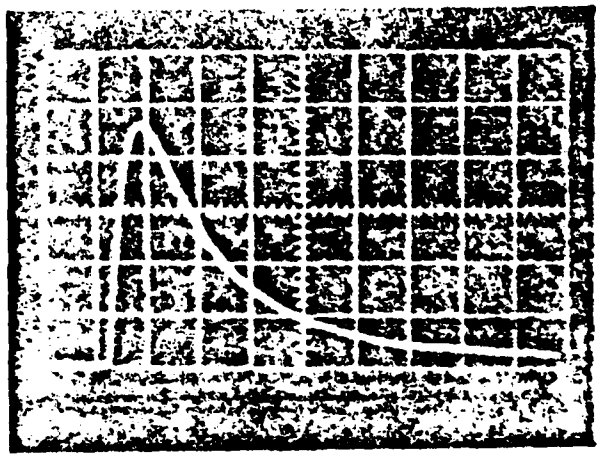

FIG. 1. Pyroelectric transient response of PVF_2

work. The films were provided by the Kureha Chemical Industries Co. Ltd. of Japan. Evaporated aluminium electrodes of 500 Å thickness and 1.6 cm^2 in area, were employed for the conventional poling of the polymer at room temperature, the range of the poling field being 8×10^7–2×10^8 V cm^{-1}. A Brandenburg-type 470 high stability photomultiplier EHT supply was used for poling the samples. For the dynamic measurement of the pyroelectric current a Spectra-Physics He-Ne laser (Model 133) with a wavelength of 632.8 nm was employed. The output power from the laser was measured with a Hilger and Watts thermopile (Model FT 16.1/696) and was observed to be 0.94 mW. The divergence angle of the laser beam was 0.063° which indicates a good collimation of the beam. The poled specimen (electret) was mounted on a heat-sinked sample holder with x-y vernier adjustments so that the laser beam impinged as near as possible to the center of the electrode. The back electrode was earthed to the heat sink. The response due to a step pulse was fed to a storage oscilloscope via a Keithley electrometer. The responses obtained were found to be repeatable to an accuracy better than 3%. The diameter of the laser beam on the sample was ~2.5 mm.

Figure 1 shows a typical pyroelectric response to a step input of the incident radiations. Such responses were obtained after eliminating the irreversible pyroelectric components (i.e., to applied space charges) by thermal cycling (up to 80 °C) of the poled samples.

The pyroelectric coefficient p was measured using the direct method and the experimental details were identical to those described before.[21] Figure 2 shows a typical set of results indicating the behavior of the reversible pyroelectric response in the temperature range of 18–38 °C. The piezoelectric coefficient d_{31} was measured as a function of poling field using a conventional technique of the release of a fixed weight at a constant temperature and the experimental details were identical to those described in an earlier work.[9] In Fig. 3 the results of the dynamic pyroelectric response have been plotted against the pyroelectric coefficient (obtained by the direct method) together with the piezoelectric coefficient d_{31} for each of the four samples described in Table I. It should be noted that all samples were preconditioned before poling by heating them in short circuited conditions for ~15 h at 120 °C.

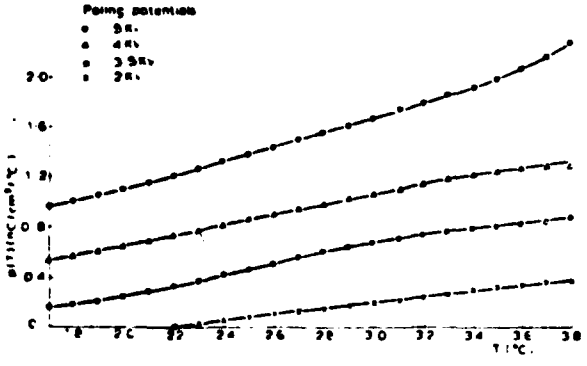

FIG 2 Pyroelectric coefficient against temperature

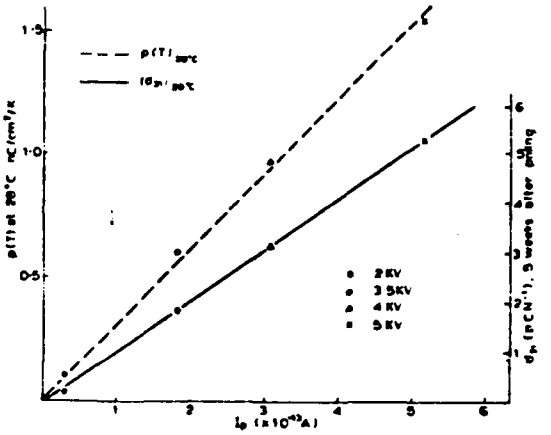

FIG. 3. Calibration of peak response I_p against pyroelectric coefficient $p(T)$ at 28 °C and piezoelectric coefficien: d_{31} at 20 °C.

DISCUSSION

An analysis of the pyroelectric current transients arising from a step input of radiation may provide useful information for pyroelectric detectors. It may be shown that[22]

$$I(t) = \frac{F_0 A p(T)}{P C_p a}\left(\frac{1}{1-\theta}\right) \times\left[\left(\exp-\frac{t}{\tau_T}\right)-\left(\exp-\frac{t}{\tau_E}\right)\right], \qquad (1)$$

where $I(t)$ is the pyroelectric current; F_0 is the radiation power absorbed per unit area of the electroded material; A is the area of the electroded sample; $p(T)$ is the pyroelectric coefficient of the material; P is the density of the material (gm/cm^3); C_p is the specific heat (J g °C); a is the sample thickness (cm); θ is the τ_E/τ_T; τ_E is the electrical time constant of the system ($= RC$); C and R represent the effective capacitance of the system comprising the material, load and the input capacitances and resistances; τ_T is the thermal time constant of the system ($= CT/G_T$); C_T is the thermal capacity $= PC_p aA$; G_T is the thermal conductance of the coupling between the sample and the ambient (radiative, convective and conductive). Here it has been assumed that $\tau_E \neq \tau_T$. Equation (1) represents the difference between two exponentials with the same initial value, but decaying with two time constant τ_E and τ_T. The peak value of the current I_p and the time t_p for the pyroelectric current to reach this value are given by[22]

TABLE I Calibration table for 25-μm thick PVF_2 film.

Poling potentials	$p(T)$ from Fig. 2 (direct method) nC/cm^2 °C	$I_p(\times10^{-13}A)$ at 20 °C step response (dynamic method)	$(\times10^{-4}$ cm^2 °C/sec) $I_{p/pT}$
5KV	1.55 at 28 °C	5.2	3.35
4KV	0.98 at 28 °C	3.05	3.11
3.5KV	0.6 at 28 °C	1.85	3.08
2KV	0.18 at 28 °C	0.58	3.22

$$I_p = \frac{F_0 p(T) A}{P C_p a} \theta \frac{\theta}{1-\theta} \tag{2}$$

and

$$t_p = \tau_E \ln \frac{\theta}{1-\theta}. \tag{3}$$

The initial slope K, of the pyroelectric response to a step input radiation may be given by[22]

$$K = \left.\frac{dI(t)}{dt}\right|_{t=0} = \left(\frac{F_0 P(T) A}{P C_p a}\right)\left(\frac{1}{\tau_E}\right). \tag{4}$$

These equations were used to analyze the shapes of the pyroelectric current transients in this work.

Now Eq. (2) may be rewritten thus:

$$I_p = \beta p(T), \tag{5}$$

where

$$\beta = \frac{F_0 A}{P C_p a} \theta \frac{\theta}{1-\theta} \tag{6}$$

The magnitude of β should thus be a constant for a given sample and electrode geometry provided the incident radiative power and the electrical and thermal time constants remain invariant. This is demonstrated in Table I which gives the magnitude of β for a typical set of samples of indentical thickness and electrode areas, but poled with different electric fields. The values of the pyroelectric coefficient $p(T)$ and the pyroelectric current I_p were obtained directly from Fig. 2 (i.e., the results of the direct method) and the step responses of the dynamic method, respectively. It may be observed that the magnitude of β values in Table I are in reasonable agreement with each other. Although the magnitude of $p(T)$ was chosen to be at 28° for this comparison (Table I), the above argument should still hold for other temperatures as the characteristics of $p(T)/T$ (Fig. 2) are similar in shape for different poling field. It is worth noting that there may exist a threshold field of 1.18×10^8 V cm^{-1} at ordinary temperature below which no significant pyroelectric response was observed in PVF_2 in this work. In agreement with the previous work[11,21] the observed magnitudes of $p(T)$ are much higher than those which may be expected from the expression[2]

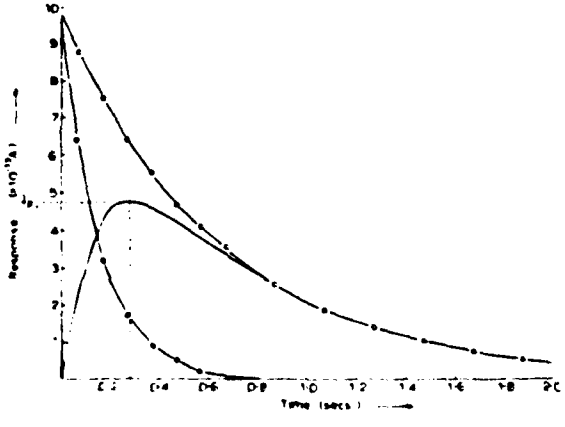

FIG 4 Pyroelectric transient response separated into thermal and electrical components

TABLE II Comparison of calculated and observed parameters.

Parameters	Calculated	Observed
$\beta = \frac{F_0 A}{P C_p a} \theta \frac{\theta}{1-\theta}$	3.02×10^{-4} (cm^2 °C/sec)	3.19×10^{-4} (cm^2 °C/sec)
$I_p = \beta p(T)$	4.72×10^{-13} (amp)	4.75×10^{-13} (amp)
$t_p = \tau_E \ln \frac{\theta}{\theta-1}$ (time at which maximum I_p occurs)	0.30 sec	0.28 sec
$K = \frac{F_0 p(T) A}{P C_p a} \frac{1}{\tau_E}$	4.72×10^{-12} (amp/sec)	5×10^{-12} (amp/sec)

$$p(T)_{20\,^\circ C} = \frac{dP_s}{dt} = 0.07E \times 10^{-5} \ (\text{cm}^2\ \text{K}^{-1}), \tag{7}$$

where E is the electric field in 10^8 V m^{-1}.

This would suggest that the rigid dipolar model may not be valid, in which case a rotation of C-F and C-H bonds may be the dominant factor, or pyroelectricity in PVF_2 may arise from other causes. A similar conclusion was also reached by Kepler and Anderson[23] when they attempted to separate the components of pyroelectricity into primary pyroelectricity and secondary pyroelectricity. Their results show that the secondary pyroelectricity, in which the sample shape and size are not held constant during the temperature change, may only account for about half the total pyroelectricity observed in this material. They[23] further suggest that a reversible temperature-dependent crystallinity may be responsible for the rest of the observed, pyroelectric response. It is not difficult to envisage the number of dipoles changing by virtue of such a reversible temperature-dependent crystallization so that as the temperature decreases there may be a slight increase in the number of repeat units associated with the crystal. Indeed a significant increase may occur if only one in every 10 000 crystallizes or melts per degree change in temperature have been observed,[24] it is possible that the x-ray diffraction technique of measuring the crystallinity may lead to anomalous results due to the thermal scattering parameters of the atoms changing with temperature

Pyroelectric transients for step input radiations were analyzed for at least 13 samples[24] for each poling field. The observed nature of the pyroelectric transient response (Fig 1) is in agreement with those obtained for other pyroelectric

materials, (for example, Triglycine sulphate and Barium titanate,[13] Triglycine Sulphate and Strontium-Barium Niobate,[22] etc) and PVF_2.[26,27] Using the method due to Simhony and Shaulov[22] these transients were then analyzed. Figure 4 shows an enlarged representation of such a transient as shown in Fig. 1. The decay of this transient would be largely dependent on the thermal time constant τ_T, provided it is much larger than the electrical time constant τ_E. When an exponential was drawn to fit the tail of the transient response it was found to correspond exactly (Fig. 4) and the thermal time constant (τ_T) of 0.654 s was thus evaluated. As the pyroelectric response is made of two time constant τ_T and τ_E the exponential for the electrical time constant (τ_E) was constructed (Fig. 4) using the superposition principle and the magnitude of τ_E was observed to be 0.16 s. Now in the dynamic method the electrometer (Keithley 602) was used entirely on the 10^{-11}A range where the effective input resistance is 10^8 ohms. The input capacitance of the electrometer is ~20 pF and the capacitance of the sample with the sample holder, measured with a general radio bridge, type 1621, at 1 kHz was found to be 1.0195 nF. Thus the effective capacity and the time constant (τ_E) of the equivalent electrical measuring system (including the sample) are ~1.04 nF and 0.10 s respectively, the latter value being not too dissimilar from that evaluated from the transient response (Fig. 4). Table II gives the summary of the analysis of the transient responses shown in Fig. 4. To evaluate β (Table II) from Eq. (6), the magnitude of ρC_p[15,26] was taken to be 2.4 J/°C cm^3. It may be observed from Table II that there is good agreement between the expected shape[22] of the pyroelectric step response of an electret and the observed current decay in PVF_2 with a step input of radiations. Thus it should be possible to determine the pyroelectric coefficient from such a step response provided the calibration curve for $p(T)/T$ is available using the analysis due to Simhony and Shaulov[18] for a particular material with a particular thickness. β values will, of course, be dependent on sample thickness as their analysis assumes that the absorption of the incident radiations mostly occur uniformly in the bulk of the material and its thickness is within the absorption depth for the black body radiations at 500 K, which for poled PVF_2 samples appear to be ~30 μm.[28]

The observed behavior of the piezoelectric coefficient d_{31}, with the poling field (conventional) is in agreement with other workers[24,29,30] although there is no strong evidence of the existence of a threshold field which has been observed with 50-μm-thick films.[24,29] This may be due to the fact that unlike 25-μm-thick samples, consisting of both the polar Form 1 and the nonpolar Form 2 crystallites, the 50-μm-thick samples, for which a threshold polarizing field has been observed[29] ($> 8\times10^7$ Vm^{-1}) (Refs. 24, 31) is of Form 2 structure only. In agreement with other workers[20,25,27] the induced piezoelectricity was also observed to be quite stable at room temperature.

It may be observed from Fig. 3 that the peak of the pyroelectric transient I_p is linearly related to both the piezoelectric coefficient d_{31}, and the pyroelectric coefficient, measured by the direct method. Thus for the 25-μm-thick Kureha sample these three parameters may be explained in the following manner:

$$p_{24^\circ C}/I_{p(20^\circ C)} = 3.13\times10^3 \text{ s C m}^{-2}\,^\circ\text{C}^{-1} \quad (8)$$

and

$$d_{31(\text{after 5 weeks})}/I_{p(20^\circ C)} = 10\text{s}N^{-1}. \quad (9)$$

The linear relationship between $p(T)$ and I_p may be due to the fairly long time constants (> 0.1 s) involved in the transient measurement technique compared to the pulse techniques of other workers.[16,18,19] This effectively approaches the time scale of the direct method[12] so that differences which may occur in pyroelectric measurements due to the creation of an expanded space charge region[32,33] may be minimized.

The contribution of piezoelectricity to the pyroelectric response has been discussed in detail[16,17] but has been found not to be the dominant factor PVF_2.[23] However, the similar behavior of d_{31} and $p(T)$ with temperature[11] suggests that piezoelectricity and pyroelectricity may have a common origin and it may not be surprising that I_p is proportional to d_{31}.

Further work is in progress to study the effects of the following parameters on the dynamic pyroelectric response of PVF_2: (i) sample thickness, (ii) frequency of chopped radiations, (iii) front electrode material and its thickness, and (iv) heat transfer arrangement.

ACKNOWLEDGMENTS

The authors are grateful to G.C. McCawley for performing much of the experimental work. This work is being financed by a research grant from the U.S. Army.

[1] W.G. Cady, *Piezoelectricity*, 1st ed. (McGraw-Hill, New York, 1946), p. 699.
[2] M.E. Lines and A.M. Glass, *Principles and applications of ferroelectrics and related materials* (Clarendon, Oxford, 1977), p. 608.
[3] J.B. Lando, H.G. Olf, and A. Peterlin, J. Polym. Sci. A-1 4, 941 (1966).
[4] R. Hasegawa, Y. Takahashi, Y. Chatani, and H. Tadokoro, Polym. J. 3, 600 (1972).
[5] W.N. Doll and J.B. Lando, J. Macromol. Sci.—Phys. B4(4), 309 (1970).
[6] K. Nakamura and Y. Wada, J. Polym. Sci. A-2 9, 161 (1971).
[7] G. Pfister, M. Abkowitz, and R.G. Crystal, J. Appl. Phys. 44, 2064 (1973).
[8] R.G. Kepler and R.A. Anderson, J. Appl. Phys. 49, 1232 (1978).
[9] D.K. Das-Gupta and K. Doughty, J. Appl. Phys. 49, 4601 (1978).
[10] G.T. Davis, J.E. McKinney, M.G. Broadhurst, and R.C. Roth, J. Appl. Phys. 49, 4998 (1978).
[11] D.K. Das-Gupta and K. Doughty, J. Phys. D., 11, 2415 (1978).
[12] R.L. Byer and C.B. Roundy, IEEE Trans. Sonis and Ultrason., SU-19, 333 (1972).
[13] A.G. Chenoweth, J. Appl. Phys. 27, 78 (1956).
[14] E.H. Putley, "The Pyroelectric Detector", in *Semiconductors and Semimetals 5 Infrared Detectors*, edited by R.K. Willardson and A.C. Beer, (Academic, New York, 1970), p. 259.
[15] L.E. Garn and E.J. Sharp, IEEE Trans. Hybrid & Packaging PHP10(4), 208 (1974).
[16] R.E. Collins, Proc. IEEE 34, 381 (1973).
[17] R.E. Collins, Rev. Sci. Instrum. 48, 883 (1977).
[18] P. Lautenschlean, G. Drefus, and J. Lewiner, Phys. Rev. Lett. 38, 46 (1977).
[19] A.S. DeReggie, C.M. Cuttman, F.J. Mopsic, G.T. Davis, and N.G. Broadhurst, Phys. Rev. Lett. 40, 413 (1978).
[20] A.M. Glass, J. Appl. Phys. 40, 413 (1978).
[21] D.K. Das-Gupta and J.S. Duffy, J. Appl. Phys. 50, 561 (1979).
[22] M. Simhony and A. Shaulov, J. Appl. Phys. 42, 3741 (1971).
[23] R.G. Kepler and R.A. Anderson, J. Appl. Phys. 49, 4490 (1978).

[24]K. Doughty, Ph.D. thesis, University of Wales, 1979.
[25]G.C. McCawley, M.Sc. thesis, University of Wales, 1979.
[26]A.M. Glass, J.H. McFee and J.F. Bergman, Jnr., J. Appl. Phys. 42, 5219 (1971).
[27]J.H. McFee, J.G. Berman, J., and G.R. Crane, Ferroelectrics 3, 305 (1972); IEEE Trans. Sonis & Ultrason., SU-19, 305 (1972).
[28]D.K. Das-Gupta and K. Doughty, Ferroelectrics (to be published).
[29]N. Murayama, J. Polym. Sci., Polym. Phys. Ed. 13, 929 (1975).
[30]R.S. Brockley, Ph.D. thesis, University of Wales, 1979.
[31]H. Kawai, Jpn. J. Appl. Phys. 8, 1975 (1969).
[32]P. Bloomfield, I. Lefkowitz, and A.D. Aranoff, Phys. Rev. B 4, 974 (1971).
[33]P. Bloomfield, A. DeReggie, S. Roth, S. Edelman, I. Lefkowitz, and R. Lontz, Bull. Am. Phys. Soc. 22, 282 (1977).

A STUDY OF THE PYROELECTRIC BEHAVIOR OF POLYVINYLIDENE FLUORIDE

D. K. Das-Gupta and K. Doughty
School of Electronic Engineering Science
University College of North Wales
Dean Street, Bangor, Gwynedd, G.B.

INTRODUCTION

The pyroelectric coefficient of a material may be determined by three methods:

1. the direct method,[1] which is the most accurate technique;
2. the dynamic method,[2,3] using interrupted thermal radiations;
3. the charge integration method[4] in which the measured coefficient may include unwanted components such as those due to thermoelectric currents.

It has been shown[5] that the measured data of the dynamic method may be calibrated against those of the direct method, providing a satisfactory technique for quickly determining the suitability of various target materials for use in pyroelectric detectors.

Polyvinylidene fluoride (PVF_2) is a semi-crystalline polymer which may exist in at least two stable crystalline forms; viz. a polar Form 1 and a non-polar Form 2.[6] It may be made to exhibit pyroelectric behavior after polarization in a high d.c. field to align the polar crystallites of the Form 1 type structure.[7] Also, high-field treatment may produce a polar variety of the Form 2 type crystallites which subsequently may be converted to the Form 1 structure.[8-11].

Some workers have reported considerable non-uniformity of poling in films of poled PVF_2 with pyroelectric[12] and piezoelectric[13] activity decreasing from a maximum at the positive electrode to a minimum at the negative electrode--

constants; viz., the thermal time constant τ_T and the electrical time constant τ_E. These two components have been separated in figure 3 from which it may be observed that $\tau_T = 0.65$ seconds and $\tau_E = 0.16$ seconds. The peak values of the current transients, I_p, were measured for each face nearer to the laser.

Uncharged samples were studied by the I.R. transmission technique[10] and the magnitude of the 795cm^{-1} absorption peak due to the CH_2 rock[16] was measured. The same absorption peak was studied by the A.T.R. technique for both surfaces of the film.[10]

Samples were prepared for corona charging in pairs--one for I.R. analysis and one for pyroelectric measurements. An electrode was evaporated onto only one side of each sample in the same configuration as for the conventionally poled samples and positive corona charges were deposited up to surface potentials of 5, 7.5 and 10KV, respectively, by the technique described in the literature.[8,10] Following the charging process, a record aluminium electrode was evaporated onto the corona side of the samples for pyroelectric measurements, and I_p and p(T) were measured as before. The aluminium electrode was then removed from the other set of samples using NaOH solution and infra-red absorption spectra measurements were obtained.

RESULTS AND DISCUSSION

An analysis of pyroelectric current transients arising from a step input of radiation yields[15]

$$I(t) = \frac{F_o A\, p(T)}{P\, C_p\, a}\left(\frac{1}{1-\Theta}\right)\left[\left(\exp -,^{t/\tau_T}\right) - \left(\exp - {}^{t/\tau_E}\right)\right] \quad (1)$$

where I(t) = Pyroelectric current
F_o = Radiation power absorbed per unit of electrode meter
A = Area of electroded sample
p(T) = Pyroelectric coefficient
P = Sample density

C_p = Specific heat of material
a = Sample thickness
τ_E = Electrical time constant of system
τ_T = Thermal time constant of sample configuration
Θ τ_E/τ_T

Differentiating equation (1) to find the maximum of I(t) we have

$$I_p = \frac{F_o P(T)\, A}{P\, C_p\, a}\ \Theta^{\Theta/1-\Theta} \qquad (2)$$

$$\text{at} \quad t_p = \frac{\tau_E \ln\Theta}{\Theta - 1} \qquad (3)$$

Substituting the value of Θ obtained from figure 3 into equation (3) we have t_p = 0.3 secs. which is in good agreement with the 0.28 secs. observed.

Equation (2) shows that I_p is directly proportional to the pyroelectric coefficient, p(T), for a constant value of Θ. Values of p(T) and I_p for each sample are given in table 1. The measured values of I_p have been plotted against their respective values of p(T) for the conventionally- and corona-poled samples in figures 4 and 5, respectively.

From figure 4 it may be observed that p(T) measured at 28°C is proportional to I_p, measured at the positive face, but not proportional to I_p at the negative face. The I_p^+ (i.e., front face with positive polarity) response is in each case greater than I_p^- (i.e., front face with negative polarity) which is consistent with the results of other workers.[12] Since the differences become progressively less as the poling field is increased, it demonstrates that the non-uniformity of poling decreases as the poling level increases.

In the case of corona-charged samples (figure 5) p(T) is related linearly to I_p^- but is not proportional to I_p^+ in the same way. Furthermore, I_p^+ is less than I_p^- in each case and the gradients of the p(T) versus I_p plot in figure 5 are smaller than those in figure 4.

which may suggest that the metal-polymer-metal interfaces may play an important role in the poling process.

In this work the pyroelectric responses from each face of both conventionally- and corona-charged samples of PVF_2 have been studied by a transient technique and compared to the results of the direct method. Also, the infra-red absorption at $795cm^{-1}$, due to the Form 2 type molecular chains, has been studied for the corona-charged samples by conventional infra-red spectroscopy (to examine the bulk), and Attenuated Total Reflection Spectroscopy (to probe the surface structure). This may allow a comparison of structural differences in the bulk and at the surfaces to be made before and after poling.

EXPERIMENTAL TECHNIQUES

Twenty-five μm thick samples of biaxially stretched films containing crystallites of both Form 1 and Form 2 were supplied by the Kureha Chemical Co., Ltd. of Japan. For conventional poling, aluminium electrodes of $1.6cm^2$ area and 500Å thickness were evaporated onto each surface. These samples were then poled at room temperature at fields from $8x10^7 Vm^{-1}$ to $2x10^8 Vm^{-1}$.

The pyroelectric coefficients p(T) of these samples were measured by a direct method described in a previous paper[14] and a set of typical results showing reversible pyroelectric behavior is shown in figure 1 in the temperature range of 18-38°C.

The samples were then mounted in a sample holder with the back electrode earthed to a heat sink. The front electrode was fed to a Keithley electrometer (Model 602) operated in the fast mode whose output was monitored on a storage oscilloscope. A laser with a 0.94mw. output was directed at the center of the sample producing an illuminated area of ∿2.5mm diameter. This beam was interrupted using a cable-released shutter timed at one-thousandth of a second, and the response of the sample to a step pulse was measured. A typical response curve is shown in figure 2.

The observed response of a pyroelectric detector may be analyzed as the difference between two exponentials decaying from the original value with different time

Since the value of p(T) obtained after corona charging at 5KV is similar to that obtained by conventional poling with the same field (table 1), then it is likely that a surface effect is responsible for the measured low values of I_p+ after corona charging.

Figure 6 shows the Optical Density Ratios of the $795cm^{-1}$ I.R. absorption peak at different poling potentials for the bulk and for the two surfaces. It may be observed that the reduction in the peak intensity at the corona-charged surface is much less than in the bulk and at the negative (earthed) electrode. The reduction of the level of the absorption peak is an indication of the degree of poling[10] and, therefore, this result confirms that nonuniform poling exists at the positive electrode of corona-charged samples. This is in agreement with a report[17] of a slight nonuniform charge distribution at each surface of a plasma-poled sample of PVF_2.

CONCLUSIONS

It has been shown that a nonuniformity of poling exists in all samples of PVF_2, poled at room temperature. However, while the nonuniform poling of conventionally-poled samples is familiar, it is very different from that of corona-charged samples. Further work will be required to probe the nonuniform charging and this will involve the use of chopped radiation at various frequencies in order to alter the depth of penetration of the heat pulses into the samples.

ACKNOWLEDGMENTS

The authors are grateful to Mr. G. C. McCawley for performing some of the pyroelectric measurements, and to Dr. P. Pantelis of the Post Office Research Centre, Martlesham, for measuring the A.T.R. spectra. This work is being financed by a research grant from the U.S. Army (European Office).

REFERENCES

1. R. L. Byer and C. B. Roundy, IEEE Trans. Sonic &

Ultrasonics SU-19, 333 (1972).
2. A. G. Chenoweth, J. Appl. Phys. 27, 78 (1956).
3. E. H. Putley, The Pyroelectric Detector, in Semiconductors and Semimetals, Volume 5, R. K. Willardson and A. C. Beer, eds., Academic Press, New York, 1970, p. 259.
4. A. M. Glass, J. Appl. Phys. 40, 4699 (1969).
5. L. E. Garn and E. J. Sharp, IEEE Trans. Hybrid and Packaging, PHP-10, 208 (1974).
6. R. Hasegawa, Y. Takahashi, Y. Chatani and H. Tadokoro, Polym. J. 3, 600 (1972).
7. R. G. Kepler and R. A. Anderson, J. Appl. Phys. 49, 1232 (1978).
8. D. K. Das-Gupta and K. Doughty, J. Appl. Phys. 49, 4601 (1978).
9. G. T. Davis, T. E. McKinney, M. G. Broadhurst and R. C. Roth, J. Appl. Phys. 49, 4998 (1978).
10. K. Doughty, Ph.D. Thesis, University of Wales, G.B., 1979.
11. D. K. Das-Gupta and K. Doughty, J. Phys. D. 11, 2415 (1978).
12. R. L. Peterson, G. W. Day, P. M. Gruzensky and R. J. Phelan, Jr., J. Appl. Phys. 45, 3296 (1974).
13. S. Hunklinger, H. Sussner and K. Dransfeld, Festkörperprobleme XVI, 276 (1976).
14. D. K. Das-Gupta and J. S. Duffy, J. Appl. Phys. 50, 561 (1979).
15. M. Simhony and A. Shaulov, J. Appl. Phys. 42, 3741 (1971).
16. M. Kobayashi, K. Tashiro and H. Tadokoro, Macromolecules 8, 2 (1975).
17. A. S. De Reggi, Unpublished results presented to Working Group on Piezo- and Pyroelectric Polymers, N. B. S., Washington, D.C., November 3, 1977.

TABLE 1 Summary of Measured Pyroelectric Data

Field (Vm^{-1})	Poling Method	p(T) at 28°C (nC/cm^2 °C)	I_p^+ ($\times 10^{-13}$ A)	I_p^- ($\times 10^{-13}$ A)
8×10^7	Conventional	0.18	0.58	0.31
1.4×10^8	"	0.6	1.85	1.48
1.6×10^8	"	0.98	3.05	2.8
2×10^8	"	1.55	5.2	5.05
2×10^8	Corona	1.6	4.9	5.1
3×10^8	"	2.55	6.6	7.6
4×10^8	"	3.1	7.5	9.1

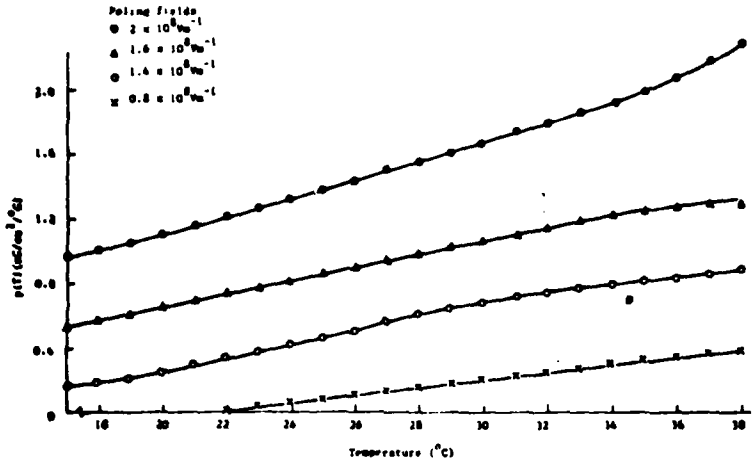

FIGURE 1 Reversible pyroelectric behavior of samples poled conventionally at room temperature.

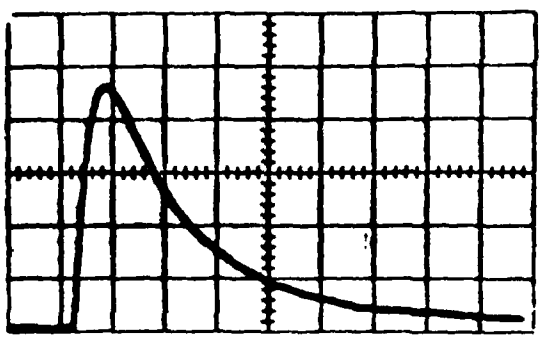

FIGURE 2 Typical pyroelectric response to a step of radiation.

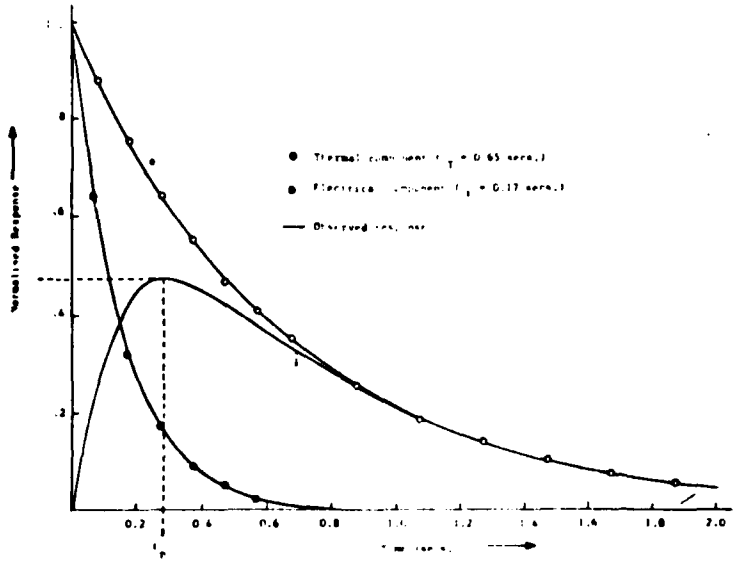

FIGURE 3 Separation of pyroelectric step response into thermal and electrical components.

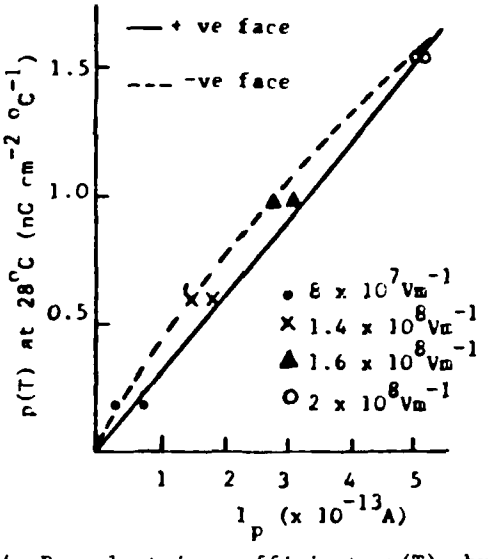

FIGURE 4 Pyroelectric coefficient, p(T), by the direct method versus the peak transient response current, I_p, for conventionally-poled samples.

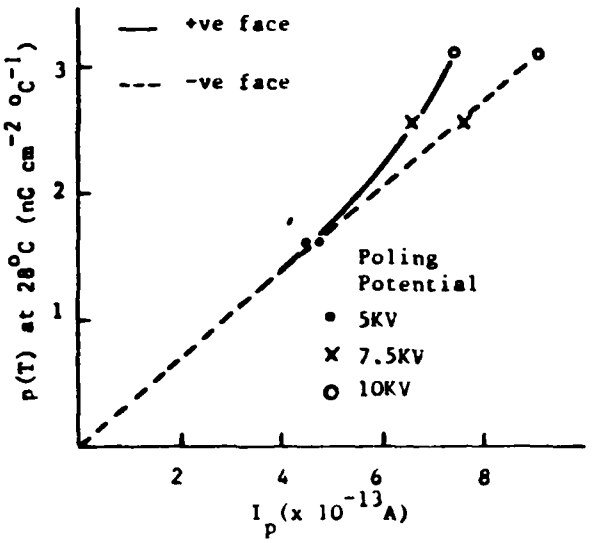

FIGURE 5 Pyroelectric coefficient, p(T), by the direct method versus the peak transient response current, I_p, for corona-charged samples.

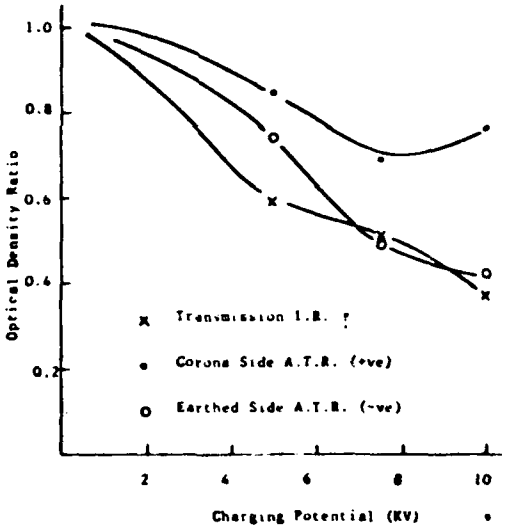

FIGURE 6 Optical density ratios of 795cm^{-1} I-R absorption peak with corona poling potential, by transmission (x) and ATR technique (o, •).

THERMAL AGING EFFECTS IN CORONA CHARGED POLYVINYLIDENE FLUORIDE

D. K. Das Gupta and K. Doughty
School of Electronic Engineering Science
University College of North Wales
Bangor, Gwynedd, Great Britain

INTRODUCTION

Polyvinylidene fluoride (PVF_2) is a semicrystalline polymer which may exist in at least two stable forms[1] simultaneously, ie.., a planar zig-zag polar form (Form 1 or β-form) with two monomer units $-CF_2-CH_2-$ per unit cell belonging to the space group $Cm2m(C_{2v}^{14})$ and the non-polar T-G-T-G' form (Form 2 or α-form) with the space group $P2_1/C(C_{2h}^5)$. In the Form 1 structure each monomer unit of PVF_2 has a dipole moment of 2.1D ($\equiv 7.01 \times 10^{-30}$ Coulomb-metre) which is oriented perpendicular to the polymer chain axis. It has been suggested[2] that in PVF_2 films, containing both Form 1 and Form 2 crystallites, the piezo- and pyro-electric responses may increase with increasing Form 1 content. It is also established that the piezo- and pyroelectric responses in oriented PVF_2 films are enhanced on poling (i.e. subjecting the polymer to a high electrical stress at an elevated temperature for an extended period of time). Oshiki and Fukada[3] observe a conversion from Form 2 to Form 1 on stretching and subsequent poling of PVF_2 films. It has also been shown[4] that a change in molecular structure may occur in bi-axially oriented PVF_2 films subsequent to poling by corona charging. These facts tend to suggest that a dipolar orientation in the crystalline and (or) amorphous phase may occur in PVF_2 on poling. The relevance of the changes in the crystalline structure on poling and the nature of the stability of the PVF_2 thermoelectrets on subsequent thermal cycling are not yet understood.

The present work reports the results of the following studies of age-ing of corona charged PVF_2 with repeated thermal cycling in the temperature range 20°-170°C; (i) the nature of the thermally stimulated currents, (ii) the

behaviour of the piezoelectric strain coefficient d_{31}, and (iii) X-ray diffraction profiles.

EXPERIMENTAL

25 μm thick PVF_2 films containing both Form 1 and Form 2 were employed in this work and the films were kindly provided by the Kureha Chemical Industries Company Limited of Japan. Aluminium electrodes of 5 cm diameter were vacuum deposited on one surface of each sample, the metallized surface being in contact with an earthed heavy copper plate at a constant temperature of 20°C. Each sample was then held between two short circuited aluminium plates and conditioned in an oven at 120°C for ~15 hours. Pairs of samples were then corona charged for 100 seconds to the desired surface potential (5 kV and 10 kV in the present study) following a technique described in a previous work.[5] X-ray diffraction profiles of the corona charged PVF_2 films were then recorded for Bragg angles θ, in the range of 17°-22° with $C_uK\alpha$ radiations using a step scanning technique. The evaporated aluminium electrode on one of the surfaces of the polymer acted as an internal standard and the uncertainty in the value of 2θ was observed not to exceed 0.1°. Samples were then shorted between two sheets of aluminium for 24 hours at 20°C. Following this procedure, conducting silver paste was painted on the non-metallized surface of each sample which was then mounted on a circular aluminium block of 5 cm in diameter, located on a copper heating plate. A programmed power supply was employed to raise the temperatures of the sample at a constant rate of 2°C/minute from 20° to 90°C, the temperature being recorded continuously. The cooling of the sample to 20°C was achieved by employing liquid air in a double walled and evacuated metallic dewer attached to the copper heating plate. After the first thermal cycle (i.e. 20°-90°-20°C) the magnitude of the short circuited current was observed to be repeatable on successive runs. The electrode of silver paste was then removed with acetone and the X-ray pattern was obtained again.

A second aluminium electrode was then vacuum deposited on the non-metallized surface of the other sample of the corona charged pair. The piezoelectric strain coefficient d_{31} of this specimen was then measured using a conventional static method of releasing a fixed weight in a temperature controlled oven. The d_{31} values were measured in the temperature range of 20°-90°C at steps of 5°C. The sample

was allowed to cool to 20°C again before further measurements of d_{31} were made for the second and each subsequent thermal run.

RESULTS

Figure 1 shows the thermally stimulated currents for the first heating cycle with PVF_2 films, poled at two surface potentials of 5 kV and 10 kV. Both curves show a peak at ~49°C and have similar profiles to those reported by other workers. The activation energies, calculated by the slope of the initial rise method, are 1.4 eV and 1.2 eV for the 10 kV and 5 kV poling voltages respectively.

In Figure 2 are presented the behaviour of the true (i.e., reversible) pyroelectric currents with temperature which are about an order of magnitude lower than those for the first cycle (irreversible), shown in Figure 1. The pyroelectric coefficient p may be calculated from these plots using the following expression:

$$p = \frac{dp}{dT} = \frac{1}{A}\frac{dQ}{dT} = \frac{1}{A}\frac{dQ}{dt} \cdot \frac{dt}{dT} = \frac{1}{A} \cdot I \frac{dt}{dT} \quad \ldots\ldots \qquad (1)$$

where p is the polarization, T the temperature, Q the charge and dT/dt the rate of heating. The magnitude of p in curve A (Figure 2) appears to be ~4 nC/°C/cm^2 at 20°C, rising to a value of ~8 nC/°C/cm^2 at 90°C. The corresponding values of p for curve B are ~2 nC/°C/cm^2 and 6 nC/°C/cm^2 respectively. In both cases the behaviour p seems to increase linearly with temperatures up to 60°C beyond which there is evidence of nonlinear and faster rate of increase in magnitude. The behaviour of the piezoelectric strain coefficient d_{31} shows a similarity with those for the pyroelectric coefficient (see Figure 3). However, it should be noted that the difference in the magnitude of d_{31} between the first and the second heating cycle is considerably less (~20%) than that for the pyroelectric case, discussed above.

Figure 4 shows the effect of corona charging on the structure of PVF_2. The observed changes are in good agreement with those previously reported by the present workers[5] and show that with increasing poling fields a conversion of Form 2 to perhaps a polar form without losing its T-G-T-G' structure and then finally to Form 1 structure. Figures 5 and 6 show that repeated thermal cycling has little effect on the structure of poled PVF_2 films.

DISCUSSION

It has been suggested[5] that an intermediate polar Form 2 type of structure with T-G-T-G' chain conformation may arise on poling of non-polar Form 2 type of crystallites at fields not exceeding 2×10^8 Vm^{-1}. Furthermore, such a conversion which may account for the observed piezo- and pyroelectricity in PVF_2, could be produced by a rotation of chains, resulting in a symmetry similar to that of Form 1 and this would also be in agreement with Davis et al.[6] However, a conversion of non-polar Form 2 into a polar Form 2 structure would involve rotations which would be similar in nature to those occurring during the so-called α_c dielectric relaxation of Form 2 structure at ~70°C.[7] Then it may be expected that the structure together with the piezo- and pyroelectricity may be unstable above this temperature. The present results indicate, however, that this is not the case for temperatures at least up to ~90°C. The lack of changes observed in the X-ray diffraction pattern of poled specimens before and after thermal cycling clearly indicates that the new structures, produced by 5 kV and 10 kV poling voltages, are quite stable.

Furthermore, no relaxation behaviour, for example, a significant change in the magnitude of p or d_{31}, was observed at temperatures around 70°C. Although the first cycle of thermally stimulated current trace (Figure 1) may indicate a presence of such a behavior, the dissimilar nature of d_{31} (Figure 3) with temperature would eliminate the role of such irreversible polarization for the origin of piezo- and pyroelectricity unless a different mechanism was responsible for the two phenomena. In view of the similarity in behaviour of the pyroelectric current (Figure 2) and d_{31} (Figure 3) with temperature this would appear to be unlikely and it may be suggested that the two phenomena have a common origin. In this sense, there is a possibility that a part of the pyroelectricity, observed in this polymer, may, in fact, be of secondary nature, arising due to piezoelectricity when the specimen undergoes thermal expansion against its constraints. Such a possibility has, of course, been discussed by Kepler and Anderson.[8]

ACKNOWLEDGEMENT

This work is financed by a research grant from the U.S. Army.

REFERENCES

1. J. B. Lando, H. G. Olf and A. Peterlin, J. Polym. Sci., A-1 4, 941 (1966).
2. N. Murayama and H. Hashizumi, J. Polym. Sci., Polym. Phys. Ed. 14, 989 (1976).
3. M. Oshiki and E. Fukada, Jap. J. Suppl. Phys. 15(1), 43 (1976).
4. D. K. Das Gupta and K. Doughty, Appl. Phys. Lett. 39(9), 585 (1977).
5. D. K. Das Gupta and K. Doughty, to be published, J. Appl. Phys., July (1978).
6. G. T. Davis, J. E. McKinney, M. G. Broadhurst and S. C. Roth, submitted to J. Appl. Phys.
7. H. Sasabe, S. Saito, M. Asahina and H. Kakutani, J. Polym. Sci., A-2 7, 1405 (1969).
8. R. G. Kepler and R. A. Anderson, to be published in J. Appl. Phys.

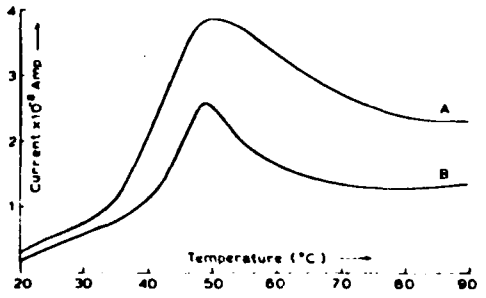

FIGURE 1 Thermally stimulated current during the first heating cycle (irreversible) from 25 μm thick and corona charged PVF_2: Curve A: Corona potential 10 kV, charging time 100 seconds and charging temperature 20°C. Curve B: As in Curve A but corona potential 5 kV. Heating rate: 2°C per minute.

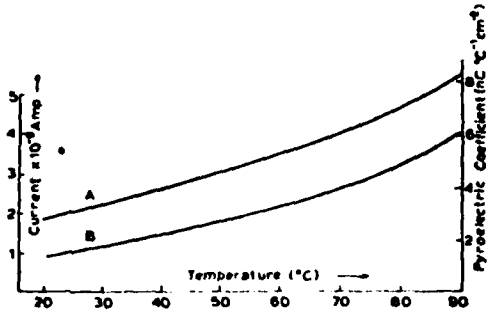

FIGURE 2 Thermally stimulated current and pyroelectric coefficient with 25 μm thick and corona charged PVF_2 during the second cycle (reversible pyroelectric current). Poling conditions for Curves A and B and the heating rate are the same as in Figure 1.

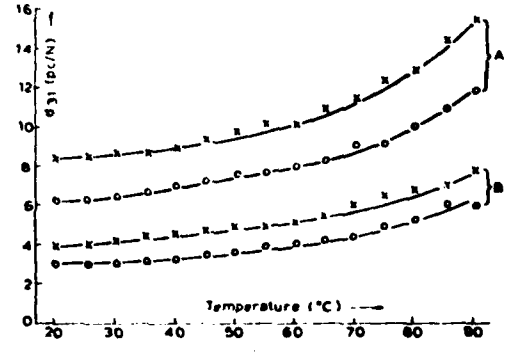

FIGURE 3 The behavior of the piezoelectric strain coefficient d_{31} of corona charged PVF_2 with temperature. Poling conditions are as in Figure 1; X first cycle and 0 second cycle.

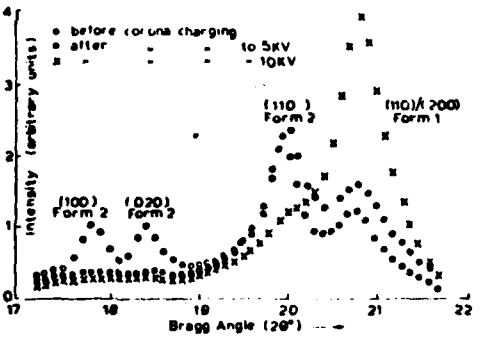

FIGURE 4 X-ray diffraction pattern of 25 μm thick PVF_2 before and after corona poling. Poling time and temperature are the same as in Figure 1.

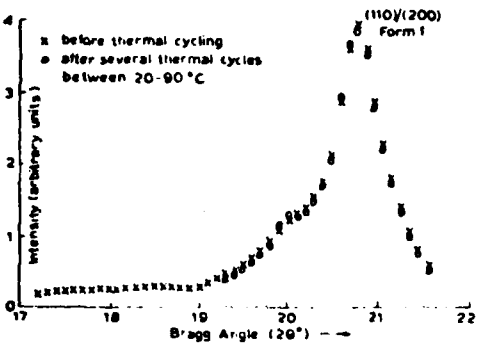

FIGURE 5 Effect of thermal aging on the X-ray diffraction profiles of corona charged (10 kV) PVF_2 of 25 μm thickness.

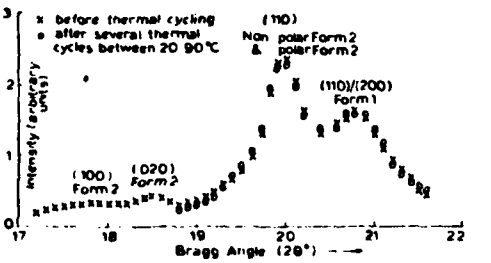

FIGURE 6 As in Figure 5 except corona poling at 5 kV.

A STUDY OF THE NATURE AND ORIGIN OF HIGH FIELD POLARIZATION IN POLYVINYLIDENE FLUORIDE

D. K. Das Gupta and R. S. Brockley
University College of North Wales
Bangor, Wales

INTRODUCTION

It is established that significant electrostatic, piezoelectric and pyroelectric responses may be obtained from electrically polarised polyvinylidene fluoride (PVF_2) films.[1-11] Although in recent years the pyro- and piezoelectric properties of PVF_2 have received considerable attention, as yet we have no clear understanding of the nature and origin of the high field polarization in this material and it appears that its electrical properties are extremely complex.

It is generally accepted that the origin of polarisation induced in a dielectric material with an external field is due to one of the following phenomena: (i) electrode polarisation, (ii) dipole orientation, (iii) charge injection, (iv) tunnelling of charge carriers from the electrodes to empty traps, and (v) hopping of charge carriers through localised states. With the exception of the hopping mechanism, the above processes have been reviewed by Wintle.[12] A study of depolarisation currents with respect to suitable variables, i.e. time, electric field, temperature, electrode materials and sample thickness, can help to identify the exact mechanism of polarisation in a dielectric material. The present work reports on an investigation of the absorption and depolarisation currents in PVF_2 with respect to the variables above.

EXPERIMENTAL

PVF_2 films of 50, 25 and 16 μm thickness were provided by the Kureha Chemical Co. Ltd., Japan. The bulk of the measurements were made with 25μm thick, uniaxially

oriented samples; however, a few were also made with 50μm thick, biaxially oriented and 16μm thick, uniaxially oriented samples. The experimental techniques (method of sample preparation, vacuum deposition of electrodes, effective electrode area and geometry, preconditioning of samples at 393K, and the measurement procedure for absorption and depolarisation currents after the application and removal of step voltages) used in this work have been described by Das Gupta and Joyner.[13,14] All measurements were made at a chamber pressure of $\simeq 10^{-6}$ Torr.

RESULTS

Time Dependence

Figure 1 shows typical examples of the time dependence of the charging and discharging currents which were obtained in the temperature range of 118-383K with electric fields in the range 10^4 - 5 × 10^7 Vm^{-1}. The charge and discharge transients are seen to be coincident at low temperatures (118-263K). However, at higher temperatures and longer times, departure from coincidence occurs, probably because of the onset of a quasi-steady state conduction which became predominant in the charging transients at temperatures in excess of 268K. Furthermore, with increasing temperature, the effect is observed at shorter times. In general, the discharge current was observed to decay as

$$I(t) = A(t)\, t^{-n} \qquad (1)$$

where I is the current, t is the time after application or removal of step voltage, A(T) is a temperature-dependent factor, and $n \simeq 1$.

Temperature Dependence

Typical examples of discharge currents at prescribed times (isochronals) in the temperature range of 118-383K are shown in Fig. 2. Similar isochronals were observed for electric fields over the range 10^4 Vm^{-1} - 5 × 10^7 Vm^{-1}. Two peaks are noted at approximately 233K and 373K. The positions of both peaks were observed to shift to lower temperatures with increasing times, which indicates thermal activation in both cases.

Field Dependence

Figures 3 and 4 show typical examples of the field dependence and the isochronals of the current transients at 313K. Again, the charging currents are observed to deviate from coincidence with the discharge currents at shorter times with increasing electric fields. This indicates that at higher fields (and temperatures) the quasi steady-state conduction current components of the charging transients become more prominent. Over the range of electric field covered in this work, the field dependence of the current transients can be expressed by the following relationship:

$$I(t) = k(t)F^p \qquad (2)$$

where k is independent of the field, and F and $p \simeq 1$, except in the case of the charging current where p was observed to increase to a value of 1.7 at the highest field (5×10^7 Vm^{-1}).

Effect of Electrode Materials

Most of the measurements were made with gold electrodes; however, a limited number of measurements were made with indium and aluminium electrodes. Figure 5 shows a typical example of the field dependence of the charging and discharging isochronals at 10^2s with these electrode materials. The results suggest that the absorption current is PVF_2 is not dependent on these electrode materials within the range of field employed.

Thickness Dependence

As stated earlier, most of the measurements were made with 25μm thick, uniaxially oriented films; however, a limited number of absorption current studies were also made with 50μm thick, biaxially oriented and 16μm thick, uniaxially oriented films. Figure 6 shows the field dependence of the charging and discharge current isochronals (10^2S) with films of these thicknesses. Within this limited range of observations, it is evident that the absorption current in PVF_2 is independent of the sample thickness.

DISCUSSION

The isochronal characteristics (Fig. 2) show that at least two relaxations (at ~233K and 373K) occur in PVF_2.

Low Temperature Region (118-263K)

The mirror image nature of the charging and discharge currents argues against a model due to trapped space charge arising from charge injection.[12,15] The observed temperature dependence and the lack of significant electrode and sample thickness effects eliminates a tunnelling model[16] as the source of the absorption current. Furthermore, the absence of any significant effect of electrode materials and the magnitude of the observed initial slope of the absorption and depolarisation currents (n-value > 0.5) appears to exclude an electrode polarisation model.[17,18] A hopping mechanism due to Lewis[19] in which the charge carriers do not reach the conduction band (i.e. no dc conduction), requires the presence of localised trap sites distributed in energy. The observed discharge current transients, with n-value ≈1 over a long period of time, may not be incompatible with such a model, assuming that band tailing occurs in a partly amorphous material[20] which may produce localised states. The broad isochronal peak observed at ~233K in the present work may be explained also by the overlapping of a number of relaxations of different dipolar assemblies. Molecular motions in PVF_2 have been studied extensively by dielectric techniques (small signal ac measurements) in recent years.[21-24] The isochronal peak observed in the present work correlates with those obtained by dielectric measurements and also with the thermally stimulated current peak observed by Pfister and Abkowitz.[25] The dielectric measurements[21-24] reveal that there are at least three distinct relaxation regions in PVF_2: (i) an α relaxation at 373-423K, (ii) a β relaxation at 223-273K, and (iii) a γ relaxation at ~203K. Respectively, these three relaxations have been attributed[23] to: (i) molecular motions in the Form I and Form II crystalline material, specifically an α_1 absorption at 343K in the Form II-nonpolar material and an α_2-absorption at 383K in the Form I-polar material, (ii) micro-Brownian motion of the main chains in the amorphous phase and (iii) local mode oscillations of the frozen main chains. These observations are also in agreement with NMR measurements.[21] Furthermore, PVF_2 has two distinct dipole

groups in the main chain: C-F (calculated[22] dipole moment = 1.53D) and C-H (calculated[22] dipole moment = 0.4D).

We suggest that the low temperature peak observed at ~233K in the present study is due to a structural motion in the main chain of PVF_2 with associated overlapping dipolar relaxations of different dipole groups.

High Temperature Region ($273 < T < 383K$)

Using similar arguments to those above, the results in the high temperature region suggest that mechanisms such as tunnelling, electrode polarisation, and space charge are not responsible for the absorption current in PVF_2. The high temperature isochronal peak (Fig. 2) at ~373K is in good agreement with the dielectric data[21-24] and may be adequately explained by structural motions involving overlapping dipolar relaxations in the crystalline phase of the polymer.

Further work is in progress to extend the studies of the absorption and depolarisation currents in PVF_2 to the upper limit of the high temperature region (~445K).

REFERENCES

1. H. Kawai, Jap. J. Appl. Phys. 8, 975 (1969).
2. E. Fukada and S. Takashita, Jap. J. Appl. Phys. 8, 960 (1969).
3. K. Nakamura and Y. Wada, J. Polym. Sci. 9, 161 (1971).
4. R. Hayakawa and Y. Wada, Adv. Polym. Sci. 11, 1 (1973).
5. Y. Wada and R. Hayakawa, Jap. J. Appl. Phys. 15, 2041 (1976).
6. N. Murayama, J. Polym. Sci. 13, 929 (1975).
7. N. Murayama, T. Oikawa, T. Katto and K. Nakamura, J. Polym. Sci. 13, 1033 (1975).
8. N. Murayama and H. Hashizumi, J. Polym. Sci. 14, 989 (1976).
9. G. T. Davis and M. G. Broadhurst, Proc. Conf. on Electrets, Sao Carlos, (1975); to be published by the Brazilian Academy of Sciences.
10. M. Oshiki and E. Fukada, Jap. J. Appl. Phys. 15, 43 (1976).
11. R. J. Shuford, A. F. Wilde, J. J. Ricca and G. R. Thomas, Polym. Eng. Sci. 16, 1 (1976).
12. H. J. Wintle, J. Non-Cryst. Solids 15, 471 (1974).
13. D. K. Das Gupta and K. Joyner, J. Phys. D. 9, 829 (1976).

14. D. K. Das Gupta and K. Joyner, J. Phys. D. 9, 2041 (1976).
15. R. H. Walden, J. Appl. Phys. 43, 1178 (1972).
16. H. J. Wintle, J. Appl. Phys. 44, 2514 (1973).
17. P. M. Sutton, J. Amer. Ceram. Sco. 47, 219 (1966).
18. J. R. Maçdonald, J. Chem. Phys. 54, 2026 (1971).
19. T. J. Lewis, Conf. on Electrical Properties of Organic Solids, Wroclaw, Poland, Inst. Phys. Chem. Ser. No. 7, Conf. No. 1, 146 (1974).
20. N. F. Mott, Adv. Phys. 16, 49 (1967).
21. H. Sasabe, S. Saito, M. Asahina and H. Kakutani, J. Polym. Sci., A-2 7, 1405 (1969).
22. S. Yano, J. Polym. Sci., A-2 8, 1057 (1970).
23. H. Kakutani, J. Polym. Sci, A-2 8, 1177 (1970).
24. K. Nakagawa and Y. Ishida, J. Polym. Sci., Polym. Phys. Ed. 11, 1503 (1973).
25. G. Pfister and M. A. Abkowitz, J. Appl. Phys. 45 (3), 1001 (1974).

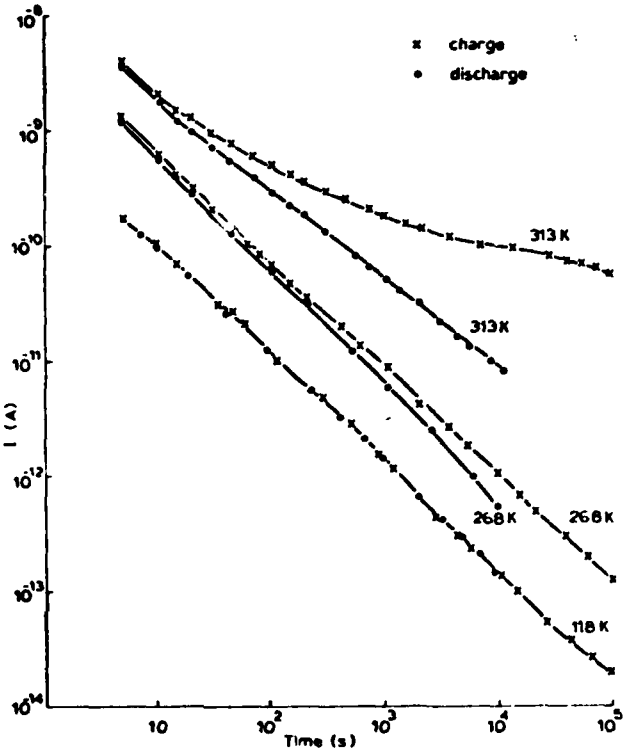

FIGURE 1 Time dependence of the charging and discharging currents at a field of 2×10^7 Vm^{-1} over the temperature range 118 - 313 K. (Sample thickness: 25 μm; evaporated gold electrodes.)

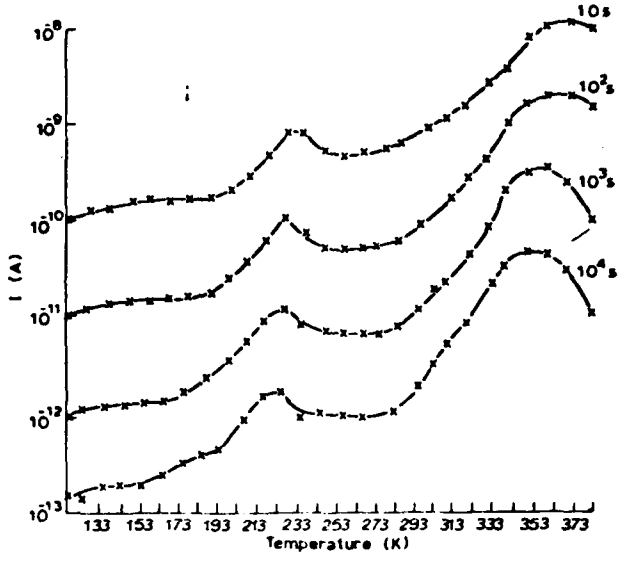

FIGURE 2 Temperature dependence of isochronal discharge currents at a field of 2×10^7 Vm^{-1}; (25-μm-thick samples with gold electrodes).

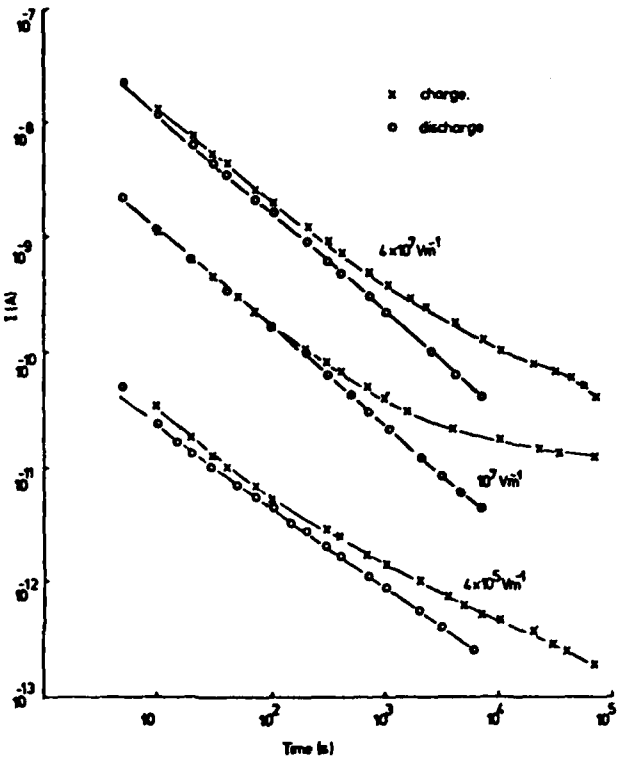

FIGURE 3 Time dependence of charging and discharging currents at different electric fields at 313 K (25-μm-thick samples with gold electrodes).

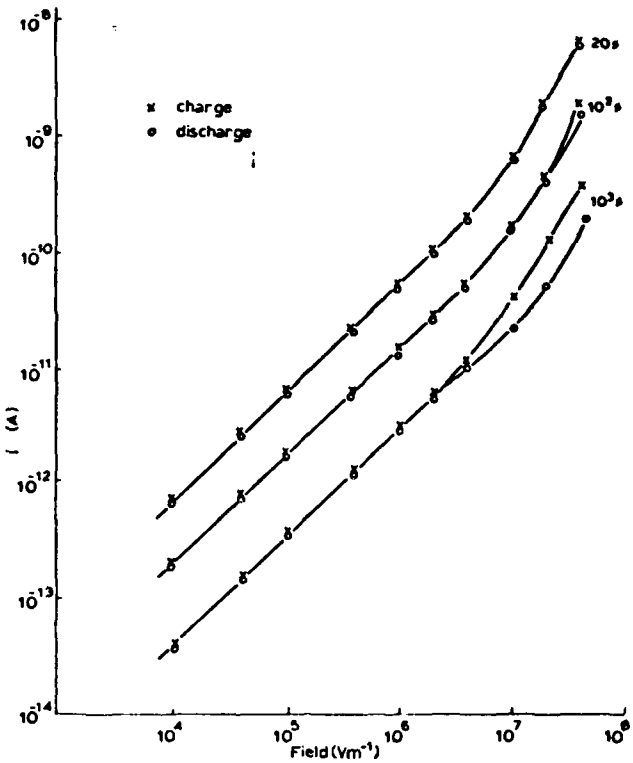

FIGURE 4 Field dependence of isochronal charging and discharging currents at 313 K (25-μm-thick samples with gold electrodes).

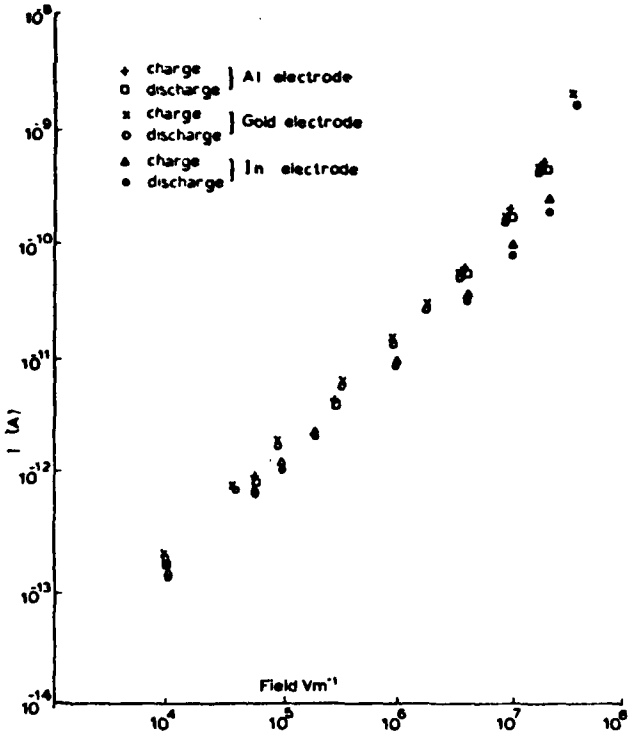

FIGURE 5 Electrode dependence of the isochronal charging and discharging currents at 313 K (10^2 s isochrones; 25-μm-thick samples).

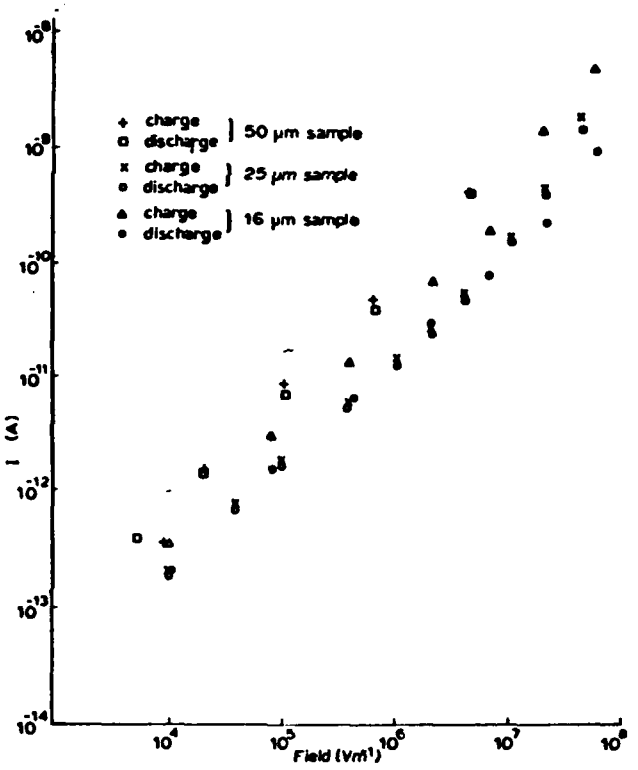

FIGURE 6 Thickness dependence of the isochronal charging and discharging currents at 313 K (10^2 s isochrones with gold electrodes).

"ON THE NATURE OF PIEZOELECTRICITY IN POLYVINYLIDENE FLUORIDE"

D. K. Das-Gupta and K. Doughty

School of Electronic Engineering and Science, University College of North Wales, Dean Street, Bangor, Gwynedd, LL57 1UT, G.B.

Abstract

The effect of poling of polyvinylidene fluoride with corona charging (∮ 12KV) has been studied by X-ray diffraction technique. The results indicate that changes in molecular conformation occur with such a poling process which is in agreement with Southgate[1] and a previous study by the present authors[2]. The piezoelectric strain coefficient d_{31} was observed to increase significantly with such a poling process, reaching a maximum value of ~10pC/N. It is suggested that the piezoelectricity in polyvinylidene fluoride is due to a dipolar orientation.

1. Introduction

Polyvinylidene fluoride (PVF_2) is a semicrystalline polymer of the monomer unit ($CH_2 = CF_2$). It has been shown that it may exist in at least two stable forms[3] simultaneously, i.e. (i) planar zig-zag polar form[4] (Form 1 or β-form) with an electric dipole moment of 2.1D[5] along the b-axis (perpendicular to the chain axis) and (ii) the non-polar form (Form 2 or α-form)[6]. It is also established that a single crystal of PVF_2 in the polar form which has an orthorhombic unit cell with a space group[7] Cm2m(C_{2v}^{14}) may possess piezoelectricity without any external poling. It has been suggested[8] that in PVF_2 films, containing both 'Form 1 (polar) and Form 2 (non-polar)', the piezo- and pyroelectricity may increase with increasing 'Form 1' content. It is also established that the piezo- and the pyroelectric responses in

oriented PVF_2 films are enhanced on poling (i.e. subjecting the polymer at a high temperature to a high electric field for a length of time). Oshiki and Fukada[9] observe a conversion from 'Form 2' to 'Form 1' on stretching and subsequent poling of PVF_2 films, originally containing both 'Form 1' and 'Form 2' and this has also been supported by Latour[10] and Shuford et al[11].

The present workers have previously shown[2] that a change in molecular conformation may take place in biaxially oriented PVF_2 films subsequent to poling by corona charging. The current study is a continuation of this earlier work and it may be divided into two parts which are as follows: (i) studies of X-ray diffraction patterns of PVF_2 films after poling with corona charging at different surface potentials not exceeding 12.2KV (i.e. a field of $\sim 4.8 \times 10^8$ Vm^{-1}) and (ii) studies of the corresponding magnitudes of the piezoelectric coefficients of the poled samples.

2. Poling by corona charging

Poling by corona charging using a Zerostat gun[2] and a technique similar to that of Southgate[1] was found to be unsuitable for controlling a uniform and repeatable surface potential on the polymer surface. For the present work a micromesh control grid was introduced between the sample and the corona point which was connected to an adjustable high voltage supply. The control grid was connected to a separate high voltage supply and maintained at 3KV below that of the corona point. Aluminium electrodes were vacuum deposited on one surface of circular samples of 5cm diameter and of 25μm thickness. Positive charges were deposited on the non-metalised surface of the polymer, the metalised surface being in contact with an earthed heavy copper plate which was

maintained at a constant temperature of 18°C. The surface potential was monitored continuously with a Field Mill type electrostatic voltmeter (Model 216, IDD, UCNW). The surface potential was observed to reach the desired values in all cases within 10 seconds after the application of E.H.T. to the corona point and the grid. The poling time employed for each sample was 30 minutes at the end of which period the non-metalised surface was earthed temporarily.

3. X-ray diffraction patterns

A step scanning technique was employed to obtain the X-ray diffraction profiles of PVF_2 samples using N_i-filtered Cu-Kα radiations with a Philips X-ray diffractometer (Model PW1050). In fact, the method employed was identical to that used in the earlier work[2] except in the present case, the evaporated aluminium electrode on one of the surfaces of the polymer acted as an internal standard in order to ascertain an uncertainty in the values of 2θ, where θ is the Bragg angle, not exceeding 0.1°. Figure 1 shows the results of a typical set of diffraction profiles of PVF_2 samples which were poled by corona charging at different values of the surface potentials. For the sake of comparison a diffraction profile of an unpoled sample is also provided in this diagram and it may be stated that the respective 2θ values for different structural planes in this profile are in good agreement with those due to Hasegawa et al[7]. It may be noticed from Figure 1 that the intensities of the peak values for the (100), (020) and (210) of the 'Form 2' decrease with increasing poling field and finally their magnitudes become vanishingly small at fields in excess of $1.6 \times 10^{8} Vm^{-1}$. It may also be observed (Figure 1) that the 'Form 2' (110) peak intensity, on the other hand, first rises with increasing field, not in excess of $3.6\ 10^{8} Vm^{-1}$ beyond which

Figure 1: X-ray diffraction pattern as a function of poling (corona charge) field

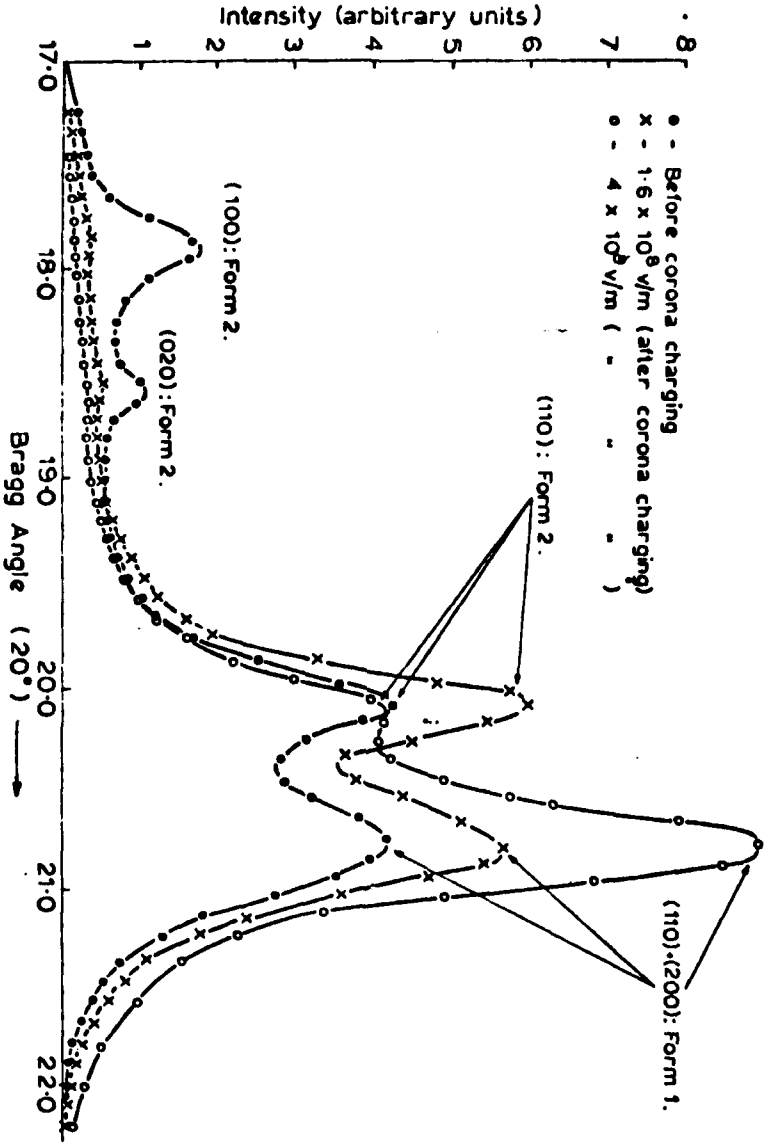

it decreases rapidly. The composite peak (110)+(200) of 'Form 1' was observed to increase continuously as the poling field was increased. It is suggested that initially there is an orientation of both the 'Form 2' and the 'Form 1' crystallites as the poling field is increased, thereby producing increases in the peak heights of their respective (110) and the composite (110)+(200) planes. Furthermore, for fields in excess of a certain magnitude a molecular conformation from 'Form 2' to 'Form 1' occurs in the bulk of PVF_2. It is of interest to note that Kepler[12] also observes an alignment of the 'Form 1' crystallites subsequent to the poling of PVF_2 in a high dc (not corona charging) field of up to $10^8 Vm^{-1}$.

4. Piezoelectric strain coefficient d_{31}

Following the X-ray analysis a second aluminium electrode was evaporated on the other surface of each of the poled samples which was then left for twenty-four hours with the electrodes short circuited. The piezoelectric strain coefficient was then measured by a conventional static method. Figure 2 shows the variation of

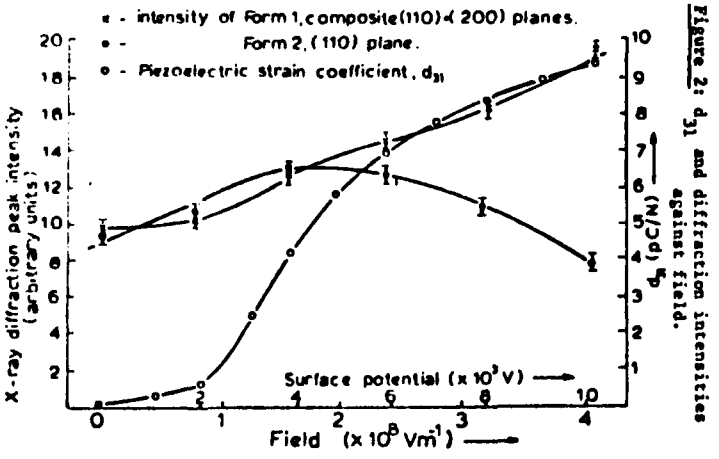

Figure 2: d_{31} and diffraction intensities against field.

d_{31} with the electrical poling stress together with the changes in intensities of the peak values of the X-ray diffraction profiles of 'Form 2' (110) plane and the 'Form 1' composite peak (110)+(200). The d_{31} is observed to be S-shaped and is similar in behaviour to that of the pyroelectric coefficient in PVF_2 due to Southgate[1] after corona charging. It may thus be argued that the piezoelectricity in PVF_2 may be due to an orientation and alignment of the dipole moments of the 'Form 1' crystallites by high external poling stress. Such a phenomenon may also occur in PVF_2 with 'Form 1' crystallites embedded in the amorphous phase of the polymer which has been suggested by Tamura et al[13].

References

1. P.D. Southgate, Appl.Phys.Lett., 28(5), 250 (1976).
2. D.K. Das-Gupta & K. Doughty, Appl.Phys.Lett., 31(9), 585 (1977).
3. K. Okuda, T. Yoshida, M. Sugita & M. Asahina, J. Polym. Sci., B5, 465 (1967).
4. J.B. Lando, H.G. Olf, & A.J. Peterlin, J. Polym. Sc., A1, 4, 941 (1966).
5. K. Nakamura & Y. Wada, J. Polym. Sci., A2, 9, 161 (1971).
6. W.W. Doll & J.B. Lando, J. Macromol. Sci., Phys., B4(2), 309 (1970).
7. R. Hasegawa, Y. Takahashi, Y. Chatani & H. Tadokoro, Polym. J., 3(5), 600 (1972).
8. K. Murayama & K. Kashizumi, J. Polym. Sci., Polym. Phys. Ed., 14, 989 (1976).
9. M. Oshiki & E. Fukada, Jap. J. Appl. Phys., 15(1), 43 (1976).
10. M. Latour, J. Electrostatics, 2, 241 (1977).
11. R.J. Shuford, A.F. Wilde, J.J. Ricca & J.R. Thomas, Polym. Eng. Sci., 16(1), (1976).
12. R.G. Kepler & R.A. Anderson, J. Appl. Phys., 49(1), (1978)
13. M. Tamura, S. Hagiwara, S. Matsumoto & N. Ono, J. Appl. Phys., 48(2), 513 (1977).

ON THE NATURE AND MECHANISM OF PIEZO- AND PYRO-ELECTRICITY IN POLYVINYLIDENE FLUORIDE

D. K. Das-Gupta and K. Doughty

School of Electronic Engineering Science, University College of North Wales, Dean Street, Bangor, Gwynedd, LL57 1UT, G.B.

Polyvinylidene fluoride is a semi-crystalline polymer of the monomer unit (CH_2=CF_2), and it may have simultaneously at least two stable crystalline structures, i.e. a polar Form 1 (β-form) and a non-polar Form 2 (α-form).[1,2] The Form 1 has a nearly planar zig-zag chain conformation with two monomer units per unit cell (figure 1) and a space group CmC2m(C_{2v}^{14}). It has a net dipole moment of 2.1D ($\equiv 7.01\times10^{-30}$ C-m) per monomer unit perpendicular (i.e., b-axis) to the chain axis (i.e., c-axis) which leads to a spontaneous polarization of 0.13C/m^2 for an unpoled single crystal.[3] The Form 2 crystallite belongs to the space group $P2_1(C_{2b}^5)$ in which each molecule has a T-G-T-G' chain conformation. Although each molecule of Form 2 structure has a dipole moment normal to the chain axis, however, the adjacent chains pack in an anti-polar array which results in no net dipole moment along the b-axis (figure 2). Of all the polymers PVF_2 has attracted special attention as a potential transducing material because of the large piezo and pyro-electricity which may be induced in thin films (PVF_2) by suitable poling in a high electrical field. It has been suggested[3] that the piezo- and pyro-electricity in PVF_2 may arise either from the heterogeneity of trapped charges in the bulk or from dipolar orientations. Murayama et al[4] show that for poled films of PVF_2, originally containing a mixture of both Form 1 and Form 2 crystallites, the piezo-electric response increases with increasing Form 1 content. However, Ohigashi[5] has observed considerable piezo-electric responses from poled films of PVF_2, originally containing only Form 2 crystallites. Thus the origin of the piezo- and pyro-electricity in PVF_2 has yet to be established unambiguously.

In a previous report[6] it has been shown that after corona poling of PVF_2 films containing both Form 1 and Form 2 crystallites, at fields not exceeding $\sim2\times10^8$ Vm^{-1}, a conversion of the non-polar Form 2 crystallites into an intermediate polar form occurs in which the T-G-T-G' conformation of the molecular chain is still maintained.[7] This may be accomplished by only a rotation of the alternate molecular chains about the c-axis through 180°. The proposed inter-

mediate polar form is shown in figure 3.[6,8] At fields in excess of 2×10^{8} Vm^{-1} a progressive conversion from the intermediate polar form (figure 3) to Form 1 structure occurs.

The present work is a continuation of the previous structural study[6] in which the changes in X-ray diffraction profiles of corona charged 25μm thick PVF_2 films (Kureha) have been measured up to a Bragg angle (2θ) of 40°. Furthermore, infrared spectral studies of corona charged PVF_2 films have also been made.

The variation of the intensities of the major diffraction peaks with surface potential (corona charging) is shown in figure 4. It may be observed (figure 4) that for a surface potential of ∿5KV the Form 2 (110) peak reaches a maximum whilst the Form 2 (100) becomes vanishingly small. Furthermore, figure 5 shows that the Form 2 (200) also reaches a maximum after corona charging at a surface potential of 5KV. The observed behaviour of Form 2 (110), (200) and (100) is in agreement with the structure of the proposed intermediate polar form (figure 3). However, the observed reduction in the peak heights (Form 2) of (020) (figure 4) and (040)/(210) (see figure 5) may not be explained by the proposed conversion of the non-polar Form 2 into an intermediate polar form (figure 3). By a comparison of the rate of changes in the Form 2 peak values of (100) and (020) due to corona charging at 5KV surface potential (figure 6), it may be observed that in addition to the conversion into an intermediate polar form (figure 3) a further process must also be occurring. The reduction of (020) and (040) peaks may be explained by a process of b-axis orientation by an interaction with the applied field. This has been confirmed by the X-ray transmission diffraction photographs which show the presence of these peaks.[8,9] The result of both these processes will lead to an internal polarization which may account for the significant increases in the piezo- and pyro-electric responses observed for such poling conditions.

It has been shown[10] that the intermediate structure is stable up to a temperature of 90°C and that less than only 10% of the piezo-electricity is lost by cycling the poled specimen up to this temperature. Furthermore, the piezo-electricity was observed to be proportional to the pyro-electricity up to this temperature[10] which suggests that a common origin may be responsible for both the phenomena. It may also be noted that the piezo-electricity due to a thermal expansion against its constraints may be responsible for a significant part of the observed pyro-electricity in this polymer.

Figure 5 shows that the intermediate polar form gets converted in Form 1 structure on poling the specimen with corona charging at a surface potential of 10KV. This corresponds to a change in the chain conformation from a T-G-T-G' to a zig-zag type. This is confirmed (figure 7) by the reduction of infrared absorption peaks of Form 2 structure which are in agreement with Southgate.[11] It may also be observed (figure 7) that the Form 1 absorption peak at 510cm^{-1} increases after poling. This may only be due to a conversion from Form 2 to Form 1 structure because Naegele and Yoon[12] have shown that with conventional poling the absorption at 510cm^{-1} decreases very slightly due to an orientation of CF_2 dipoles along the direction of the poling field.

Figure 1.

Form I PVF_2 viewed along c-axis (along main chains)

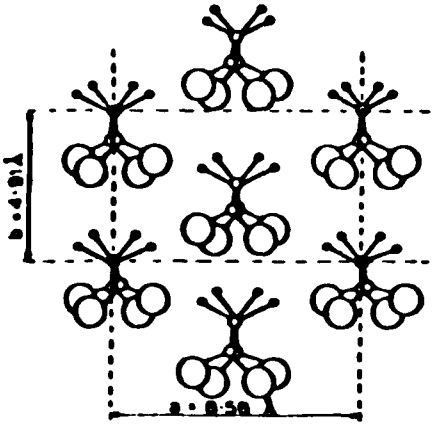

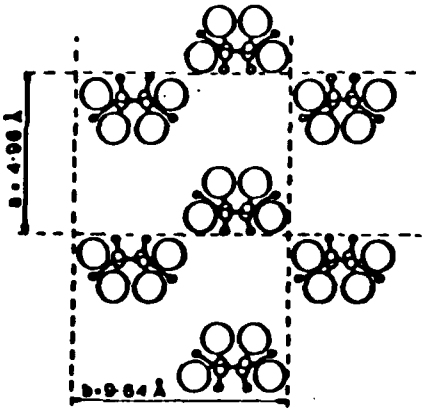

Form II PVF_2 viewed along c-axis (along main chains)

○ = F : ○ = C : ● = H :

Figure 2.

Figure 3.

Suggested intermediate form after corona charging

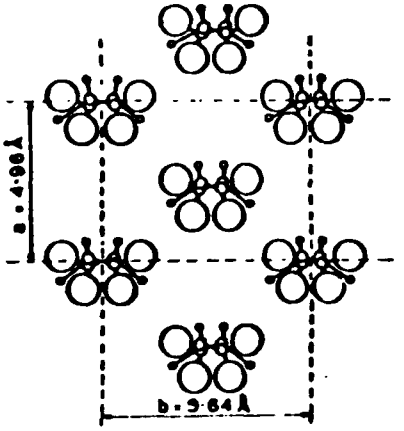

○ = F : ○ = C : ● = H :

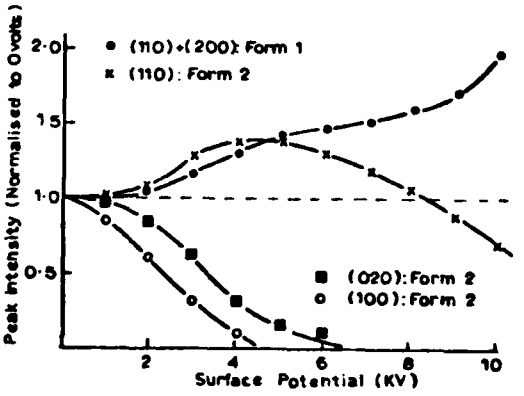

Variation of Intensities of Major Peakes after Corona Charging (25 μm sample)

Figure 4.

Figure 5.
Effect of Increasing Fields on Higher Order Peaks. (25μm sample)

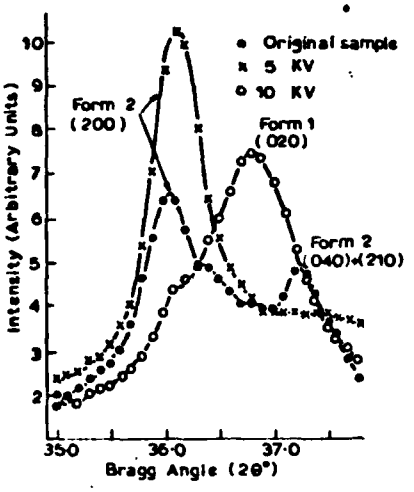

Figure 6.
Variation of Intensities of Form 2 Diffraction Peaks with Time due to Corona Charging (5KV).
(25μm sample)

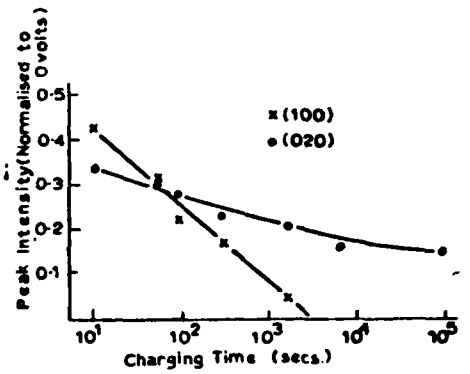

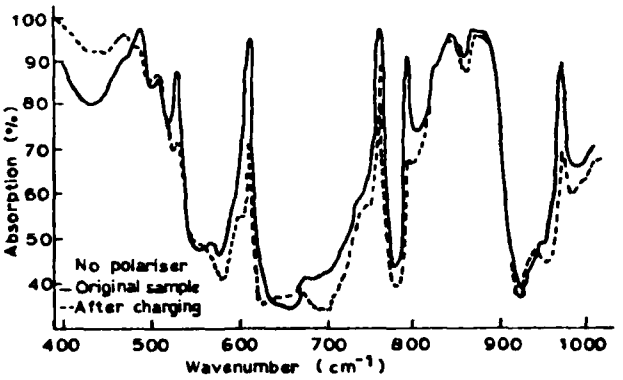

Changes in IR Spectrum after Corona Charging (10KV)
(25μm sample)

Figure 7.

These results demonstrate that the origin of piezo- and pyro-electricity in PVF_2 is dipolar orientation rather than the trapped space charge.

Acknowledgement

This work is supported by a research grant from the US Army. One of the authors (KD) is also grateful to the Science Research Council of Great Britain for a research studentship. The authors express their gratitude to Kureha Chemical Co. Ltd. of Japan for the generous supply of PVF_2 films.

References

1. J.B. Lando, H.G. Olf and A. Peterlin, J. Polym. Sci. A-1, 4, 941 (1966).
2. R. Hasegawa, Y. Takahashi, Y. Chatani and H. Tadokoro, Polym. J. 3(5), 600 (1972).
3. Y. Wada and R. Hayakawa, Jap. J. Appl. Phys., 15(11) 2041 (1976).
4. N. Murayama, T. Oikawa, T. Katto and N. Nakamura, J. Polym. Sci., Polym. Phys. Ed., 13, 1033 (1975).
5. H. Ohigashi, J. Appl. Phys., 47, 949 (1976).
6. D.K. Das-Gupta and K. Doughty, J. Appl. Phys., 49(8), 4601 (1978).
7. R.G. Kepler and R.A. Anderson, J. Appl. Phys., 49(3), 1232 (1978).
8. G.T. Davis, J.E. McKinney, M.G. Broadhurst and S.C. Roth, J. Appl. Phys., (to be published).
9. K. Doughty, Ph.D. Thesis, University of Wales (1978).
10. D.K. Das-Gupta and K. Doughty, J. Phys. D., (to be published).
11. P.D. Southgate, Appl. Phys. Lett., 28, 250 (1976).
12. D. Naegele and D. Y. Yoon, Appl. Phys. Lett., (to be published).